

EPA-450/3-77-003b

January 1977

**IMPROVEMENTS
TO SINGLE-SOURCE MODEL
VOLUME 2:
TESTING AND EVALUATION
OF MODEL IMPROVEMENTS**



**U.S. ENVIRONMENTAL PROTECTION AGENCY
Office of Air and Waste Management
Office of Air Quality Planning and Standards
Research Triangle Park, North Carolina 27711**

**IMPROVEMENTS
TO SINGLE-SOURCE MODEL
VOLUME 2: TESTING AND EVALUATION
OF MODEL IMPROVEMENTS**

by

Michael T. Mills and Roger W. Stern

**GCA Corporation
GCA/Technology Division
Bedford, Massachusetts 01730**

Contract No. 68-02-1376, Task Order 23

EPA Project Officer: Russell F. Lee

Prepared for

**ENVIRONMENTAL PROTECTION AGENCY
Office of Air and Waste Management
Office of Air Quality Planning and Standards
Research Triangle Park, North Carolina 27711**

January 1977

This report is issued by the Environmental Protection Agency to report technical data of interest to a limited number of readers. Copies are available free of charge to Federal employees, current contractors and grantees, and nonprofit organizations - in limited quantities - from the Library Services Office (MD-35). Research Triangle Park, North Carolina 27711; or, for a fee, from the National Technical Information Service, 5285 Port Royal Road, Springfield, Virginia 22161.

This report was furnished to the Environmental Protection Agency by GCA Corporation, GCA/Technology Division, Bedford, Massachusetts 01730, in fulfillment of Contract No. 68-02-1376, Task Order 23. The contents of this report are reproduced herein as received from GCA Corporation. The opinions, findings, and conclusions expressed are those of the author and not necessarily those of the Environmental Protection Agency. Mention of company or product names is not to be considered as an endorsement by the Environmental Protection Agency.

Publication No. EPA-450/3-77-003b

CONTENTS

	<u>Page</u>
List of Figures	iv
List of Tables	x
Acknowledgments	xi
<u>Sections</u>	
I Introduction	1
II Survey of Dispersion Calculation Methods	5
III Site and Data Base Descriptions for Model Improvement Study	44
IV Model Validation Results	54
V Conclusions and Recommendations	89
VI References	91
<u>Appendixes</u>	
A Turner Scheme for Stability Classification	93
B Listings of the Fractional Stability Preprocessor Program and Corresponding Version of the Single Source Model	97
C Concentration Profiles for the Canal and Muskingum Plants for Different Sets of Dispersion Curves	116

LIST OF FIGURES

<u>No.</u>		<u>Page</u>
1	Vertical Dispersion Coefficient as a Function of Distance According to Gifford	7
2	Horizontal Dispersion Coefficient as a Function of Distance According to Gifford	8
3	Vertical Dispersion Coefficient as a Function of Downwind Distance From the Source as Currently Employed in the Single Source Model	10
4	Determination of Hourly Mixing Heights	12
5	Wind Direction Trace Types Used to Determine Atmospheric Stability by the Smith-Singer Method	17
6	Variation of σ_y With Distance for the Smith-Singer Stability Classes	19
7	Variation of σ_z With Distance for Each of the Smith-Singer Stability Classes	20
8	F.B. Smith Scheme for Assignment of Fractional Stability Classes	24
9	Incoming Solar Radiation (mW/cm^2) Measured at Cambridge, England on a Cloudless Day	25
10	Solar Radiation Intensity as a Function of Zenith Angle	27
11	Variation With Distance of the Vertical Dispersion Parameter σ_z (Normalized With Respect to the Neutral Stability Value) for Different Values of P	29
12	Variation of σ_z With Distance for Stability D	30
13	Contours of the Vertical Dispersion Coefficient Correction Factor $F(z_0, x)$	32

LIST OF FIGURES (continued)

<u>No.</u>		<u>Page</u>
14a	Vertical Dispersion Coefficient as a Function of Downwind Distance for Stability Class A According to Briggs, F.B. Smith and Pasquill-Turner	34
14b	Vertical Dispersion Coefficient as a Function of Downwind Distance for Stability Class B According to Briggs, F.B. Smith and Pasquill-Turner	34
14c	Vertical Dispersion Coefficient as a Function of Downwind Distance for Stability Class C According to Briggs, F.B. Smith and Pasquill-Turner	35
14d	Vertical Dispersion Coefficient as a Function of Downwind Distance for Stability Class D According to Briggs, F.B. Smith and Pasquill-Turner	35
14e	Vertical Dispersion Coefficient as a Function of Downwind Distance for Stability Class E According to Briggs, F.B. Smith and Pasquill-Turner	36
14f	Vertical Dispersion Coefficient as a Function of Downwind Distance for Stability Class F According to Briggs, F.B. Smith and Pasquill-Turner	36
15a	Horizontal Dispersion Coefficient as a Function of Downwind Distance for Stability Class A According to Briggs and Pasquill-Turner	37
15b	Horizontal Dispersion Coefficient as a Function of Downwind Distance for Stability Class B According to Briggs and Pasquill-Turner	37
15c	Horizontal Dispersion Coefficient as a Function of Downwind Distance for Stability Class C According to Briggs and Pasquill-Turner	38
15d	Horizontal Dispersion Coefficient as a Function of Downwind Distance for Stability Class D According to Briggs and Pasquill-Turner	38
15e	Horizontal Dispersion Coefficient as a Function of Downwind Distance for Stability Class E According to Briggs and Pasquill-Turner	39
15f	Horizontal Dispersion Coefficient as a Function of Downwind Distance for Stability Class F According to Briggs and Pasquill-Turner	39

LIST OF FIGURES (continued)

<u>No.</u>		<u>Page</u>
16a	Vertical Dispersion Coefficient as a Function of Downwind Distance for Stability Class A and Surface Roughnesses of 10 cm and 100 cm According to F. B. Smith	40
16b	Vertical Dispersion Coefficient as a Function of Downwind Distance for Stability Class B and Surface Roughnesses of 10 cm and 100 cm According to F. B. Smith	40
16c	Vertical Dispersion Coefficient as a Function of Downwind Distance for Stability Class C and Surface Roughnesses of 10 cm and 100 cm According to F. B. Smith	41
16d	Vertical Dispersion Coefficient as a Function of Downwind Distance for Stability Class D and Surface Roughnesses of 10 cm and 100 cm According to F. B. Smith	41
16e	Vertical Dispersion Coefficient as a Function of Downwind Distance for Stability Class E and Surface Roughnesses of 10 cm and 100 cm According to F. B. Smith	42
16f	Vertical Dispersion Coefficient as a Function of Downwind Distance for Stability Class F and Surface Roughnesses of 10 cm and 100 cm According to F. B. Smith	42
17	Map of Eastern Massachusetts and Rhode Island Showing Locations of the Canal Plant	45
18	Sketch of the Canal Plant Area Showing the Locations of the Four Automatic SO ₂ Stations by the Symbol	48
19	Sketch of the Muskingum Plant Area Showing Locations of Four Automatic SO ₂ Monitoring Stations	51
20a	Model Validation Run No. 1	61
20b	Model Validation Run No. 1	61
20c	Model Validation Run No. 2	62
20d	Model Validation Run No. 1	62
20e	Model Validation Run No. 1	63
21a	Model Validation Run No. 2	63
21b	Model Validation Run No. 2	64

LIST OF FIGURES (continued)

<u>No.</u>		<u>Page</u>
21c	Model Validation Run No. 2	64
21d	Model Validation Run No. 2	65
21e	Model Validation Run No. 2	65
22a	Model Validation Run No. 3	66
22b	Model Validation Run No. 3	66
22c	Model Validation Run No. 3	67
22d	Model Validation Run No. 3	67
22e	Model Validation Run No. 3	68
23a	Model Validation Run No. 4	68
23b	Model Validation Run No. 4	69
23c	Model Validation Run No. 4	69
23d	Model Validation Run No. 4	70
23e	Model Validation Run No. 4	70
24a	Model Validation Run No. 5	71
24b	Model Validation Run No. 5	71
24c	Model Validation Run No. 5	72
24d	Model Validation Run No. 5	72
24e	Model Validation Run No. 5	73
25a	Model Validation Run No. 6	73
25b	Model Validation Run No. 6	74
25c	Model Validation Run No. 6	74
25d	Model Validation Run No. 6	75
25e	Model Validation Run No. 6	75

LIST OF FIGURES (continued)

<u>No.</u>		<u>Page</u>
26a	Model Validation Run No. 7	76
26b	Model Validation Run No. 7	76
26c	Model Validation Run No. 7	77
26d	Model Validation Run No. 7	77
26e	Model Validation Run No. 7	78
27a	Model Validation Run No. 8	78
27b	Model Validation Run No. 8	79
27c	Model Validation Run No. 8	79
27d	Model Validation Run No. 8	80
27e	Model Validation Run No. 8	80
28a	Model Validation Run No. 9	81
28b	Model Validation Run No. 9	81
28c	Model Validation Run No. 9	82
28d	Model Validation Run No. 9	82
28e	Model Validation Run No. 9	83
29a	Model Validation Run No. 10	83
29b	Model Validation Run No. 10	84
29c	Model Validation Run No. 10	84
29d	Model Validation Run No. 10	85
29e	Model Validation Run No. 10	85
30a	Model Validation Run No. 11	86
30b	Model Validation Run No. 11	86
30c	Model Validation Run No. 11	87

LIST OF FIGURES (continued)

<u>No.</u>		<u>Page</u>
30d	Model Validation Run No. 11	87
30e	Model Validation Run No. 11	88

LIST OF TABLES

<u>No.</u>		<u>Page</u>
1	Meteorological Categories According to Pasquill ⁹ and Meade ¹⁰	9
2	Wind Profile Exponents (α) for Different Stabilities	13
3	Smith-Singer Power Law Parameters a,b for Horizontal and Vertical Dispersion Parameters $\sigma_{y,z} = ax^b$ Where x is in Meters ¹³	18
4	Variation of σ_y and σ_z with Distance x (Meters) for Rural Areas	22
5	Multiplication Factors for Incoming Solar Radiation Intensity for Different Amounts of Cloud Cover	23
6	Fit Parameters for Dispersion Coefficients	28
7	Coefficients of the Roughness Correction Factor Used in Calculating $\sigma_z(x)$ for Various Roughness Lengths (x is given in Meters)	31
8	Plant Characteristics	46
9	Monthly Percent Sulfur Content of Fuel	47
10	Sulfur Dioxide Monitoring Stations for the Canal and Muskingum Plants	49
11	Description of Model Validation Runs and Results	58
12	Comparison of Pasquill-Turner (P-T) and F. B. Smith (F.B.S.) Stability Assignments for Three Days of Huntington, W. Va. 1973 Surface Meteorological Data	60

ACKNOWLEDGMENTS

The key data used in carrying out this study were made available to GCA/Technology Division by the New England Gas and Electric System and the Ohio Power Company. Project direction and guidance were given by Mr. Russell Lee of the Source-Receptor Analysis Branch, Monitoring and Data Analysis Division, EPA, Durham, North Carolina, who served as project officer.

SECTION I

INTRODUCTION

The purpose of this study is to test a number of suggested improvements to the EPA Single Source Model (CRSTER). In particular three alternate methods for the parameterization of vertical and horizontal dispersion coefficients with distance will be evaluated along with two additional stability class selection algorithms. The predictions of each modified version of the Single Source Model will be compared with actual concentration measurements so that these potential model improvements can be evaluated. Another objective of this study was to determine whether the use of a variable buoyancy flux in the plume rise equation in the model would yield better predictions.

During two previous EPA sponsored projects^{1,2} GCA carried out validation studies for the Single Source 24-Hour Model at four separate power plant sites. Model predictions of 1-hour and 24-hour SO₂ concentration frequency distributions were carried out based upon emission parameters and hourly meteorological data and compared with the corresponding frequency distributions of SO₂ concentration measurements corrected for background contributions.

In the first validation exercise, which was performed for the Canal Power Plant in southeastern Massachusetts, concentration predictions were made for a variety of emissions and meteorological data bases ranging in degree of resolution from monthly average emission rates taken from FPC Form-67 and hourly meteorological data from the nearest weather station to actual hourly emissions and on-site wind speed and direction

data in conjunction with hourly stabilities and mixing heights extracted from the weather station observations. Regardless of the choice of input data sets the model was found to underpredict both 1-hour and 24-hour SO₂ concentrations. With the exception of one receptor location, the ratios of measured minus background to predict second highest yearly SO₂ concentrations fell between 1.0 and 2.0. The corresponding ratios for the 24-hour concentrations, again neglecting one receptor location, ranged from 1.2 to 6.4 with an arithmetic mean of 3.2.

To determine whether the underprediction found for the Canal Plant was due to the coastal location of the plant site or some weakness in the model itself, three power plant sites were chosen in Ohio for additional tests of the model. Source characteristics and emission rates for the J. M. Stuart, Muskingum and Philo power plants were used in conjunction with surface and upper air meteorological data from nearby weather stations to generate model estimates of SO₂ concentrations for the 1-hour and 24-hour averaging times employed in the Canal plant study. With the exception of the Philo plant the predicted 1-hour SO₂ concentrations were in much better agreement with measurements than for the Canal plant study. The average ratio of second highest measured to predicted 1-hour SO₂ concentrations was 1.02 and 1.10 for the Stuart and Muskingum plants respectively. One-hour SO₂ concentrations for the Philo plant were overpredicted by a factor of 2, a circumstance due in large part to the inadequacy of the Single Source Model to handle the dispersion effects associated with complex terrain, particularly for those receptor locations with elevations comparable to that of the stack top. The predicted second highest 24-hour SO₂ concentrations for the J. M. Stuart and Muskingum plants were in better agreement with the measured values than in the case of the Canal plant with the measured to predicted ratios of 1.5 and 2.0 for the J. M. Stuart and Muskingum plants respectively.

Based upon these model validation studies two problems areas could be identified. The first concerned the underprediction of second highest 24-hour concentrations at three of the four plants studied. To a large degree

this tendency to underpredict 24-hour concentrations may be traced to the method by which 24-hour predictions are obtained from 1-hour concentration calculations. For the calculation of 1-hour concentrations the Single Source Model requires that the wind flow vector remain constant for the entire hour so that no mechanism exists for a smooth transition from one hourly flow direction to the next. While this assumption does not seriously affect the quality of the peak 1-hour concentration predictions, the resulting deficiency in low and intermediate concentrations (i.e., large number of zero concentration predictions) may lead to an underestimate in the associated 24-hour concentrations. An alternate method for the estimation of peak 24-hour concentrations is through the application of peak to mean ratio distribution statistics. In each of the model validation studies distributions of peak 1-hour to average 24-hour SO_2 concentration ratios were constructed from actual hourly SO_2 concentration measurements corrected for background. For the four plants studied the geometric means of these distributions ranged from 7.3 to 7.9 and the standard geometric deviations from 1.5 to 1.7. If the second highest predicted 1-hour SO_2 concentration were found to be accurate, then an estimated second highest 24-hour SO_2 concentration obtained by dividing the 1-hour value by the geometric mean of the 1-hour to 24-hour peak to mean ratio should be accurate to at least a factor of 2. Volume I of this study was devoted to a further examination of these ratio distributions to determine their sensitivity to the use of successively higher threshold values of peak 1-hour SO_2 concentrations.

The second area of concern dealt with the theoretical bases for the model predictions, namely, the plume rise formulation, stability class selection procedure and the choice of parameters for the calculation of vertical and horizontal plume dispersion coefficients. The basic question was whether the use of alternate techniques would improve the agreement between predicted and measured 1-hour SO_2 concentrations, particularly at the Canal plant. The Briggs^{3,4,5} plume rise estimates currently incorporated in the Single Source Model represent the best fit to currently existing data. For the Canal plant study, a modification was made to the plume rise

computation in the model to include the effect of stack downwash but this modification did not improve the quality of the predictions to a significant degree. On the other hand, there are a number of techniques different from the Pasquill-Turner method which is currently in use for the classification of stabilities and the calculation of dispersion coefficients. In Section II we shall describe some of these techniques and describe the manner in which they were included in the Single Source Model. Section III will deal with the source and meteorological input data bases to be used in the test of potential model improvements. In Section IV we shall present the model validation results for the alternate dispersion calculation techniques and draw a conclusion as to the adequacy of the existing model formulation. Also, in Section IV we shall investigate the utility of incorporating a variable volume flux in the Single Source Model.

SECTION II

SURVEY OF DISPERSION CALCULATION METHODS

DESCRIPTION OF THE EXISTING MODEL

We shall begin our discussion of dispersion calculation methods with a description of the EPA Single Source Model as it currently exists. The program, which was developed by the EPA Meteorology and Assessment Division, calculates hourly and daily concentrations for an array of receptor locations and maximum hourly and daily pollutant concentrations for a year along with the meteorological conditions which can lead to these maxima. These concentrations are written on magnetic tape for the 252 receptor positions situated at each of 36 directions from the source and seven different distance ranges. The normal version of the model has five distances and 180 receptors. The seven distances and 252 receptors occur only in the special GCA adaptation. The model can handle from 1 to 19 sources but treats all of them as if they were at the same physical location. The expression used for evaluation of 1-hour pollutant concentrations downwind of a point source is the Gaussian plume equation^{6,7} given by

$$\chi(x,y,z) = \frac{Q \exp\left(\frac{-y^2}{2\sigma_y^2(x)}\right)}{2\pi \sigma_y(x) \sigma_z(x) u} \left[\exp\left(-\frac{(z-h(x))^2}{2\sigma_z^2(x)}\right) + \exp\left(-\frac{(z+h(x))^2}{2\sigma_z^2(x)}\right) \right] \quad (1)$$

where

x = distance along plume axis (m)

y = horizontal distance from plume axis (m)

z = distance above surface (m)

$\chi(x,y,z)$ = concentration of pollutant (g/m^3)

Q = effective emission rate of pollutant distance x
(g/sec)

$\sigma_y(x)$, $\sigma_z(x)$ = horizontal and vertical dispersion coefficients for a particular atmospheric stability (A,B,C,D,E,F) and distance x

u = wind speed at source height (m/sec)

h(x) = effective emission height at distance x (m)

The variation of σ_y and σ_z with distance was first parameterized by Gifford⁶ as shown in Figures 1 and 2. These curves represent a fit to a number of concentration field measurements including those made during the Prairie Grass study⁸ conducted during the summer of 1956. Although these plume dispersion estimates were based largely upon ground level releases they are also generally applied to elevated point sources. Criteria for selection of a particular stability class were first suggested by Pasquill⁹ and Meade¹⁰ and are listed in Table 1. The measurements upon which these curves were based were taken within 1 km of the source, the shape of the σ_z curves beyond this distance is somewhat uncertain especially for the A and B stability classes. For the σ_z curves used for the Single Source Model the variation of dispersion with distance for the A and B stabilities is represented by a simple power law beyond 500 m and 700 m, respectively, as shown in Figure 3.⁷ A more detailed stability class assignment algorithm than the one given in Table 1 was suggested by Turner¹¹ and is currently incorporated in the meteorological preprocessor program used in conjunction with the Single Source Model. The details of this method are presented in Appendix A. The Single Source Model makes use of an additional stability class, G, for which the assumption is made that the plume never reaches the ground.

Surface meteorological input to the model consists of hourly surface observations of wind speed (knots), wind direction sector (1-36), temperature ($^{\circ}$ F), and total cloud cover (tenths). The format for these data is that used by the National Climatic Center for WBAN-144 hourly surface observations. These data along with twice daily mixing heights are input into a preprocessor program which in turn writes a tape containing hourly values of stability index, mixing height, temperature, windspeed, flow

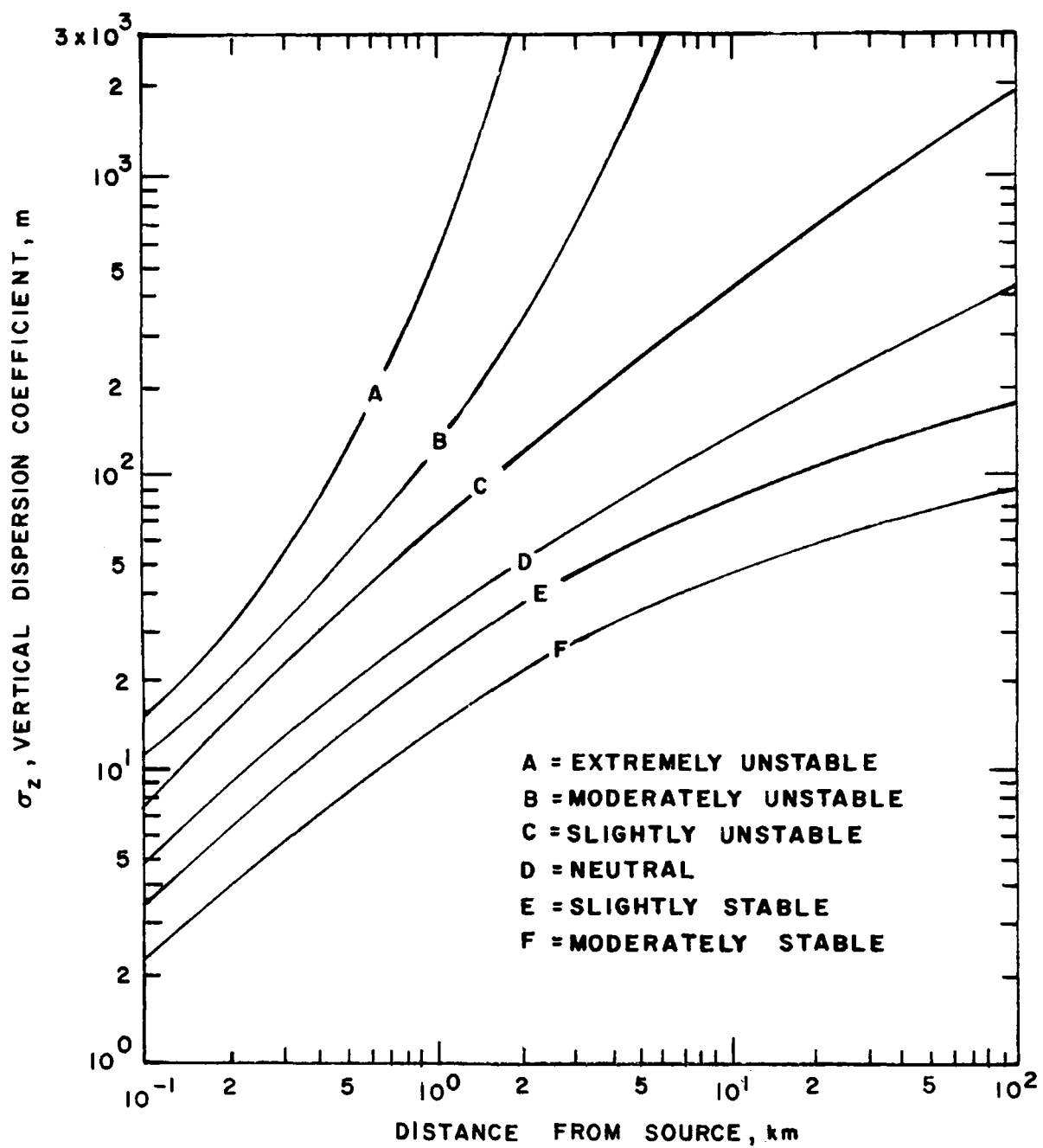


Figure 1. Vertical dispersion coefficient as a function of distance according to Gifford⁶

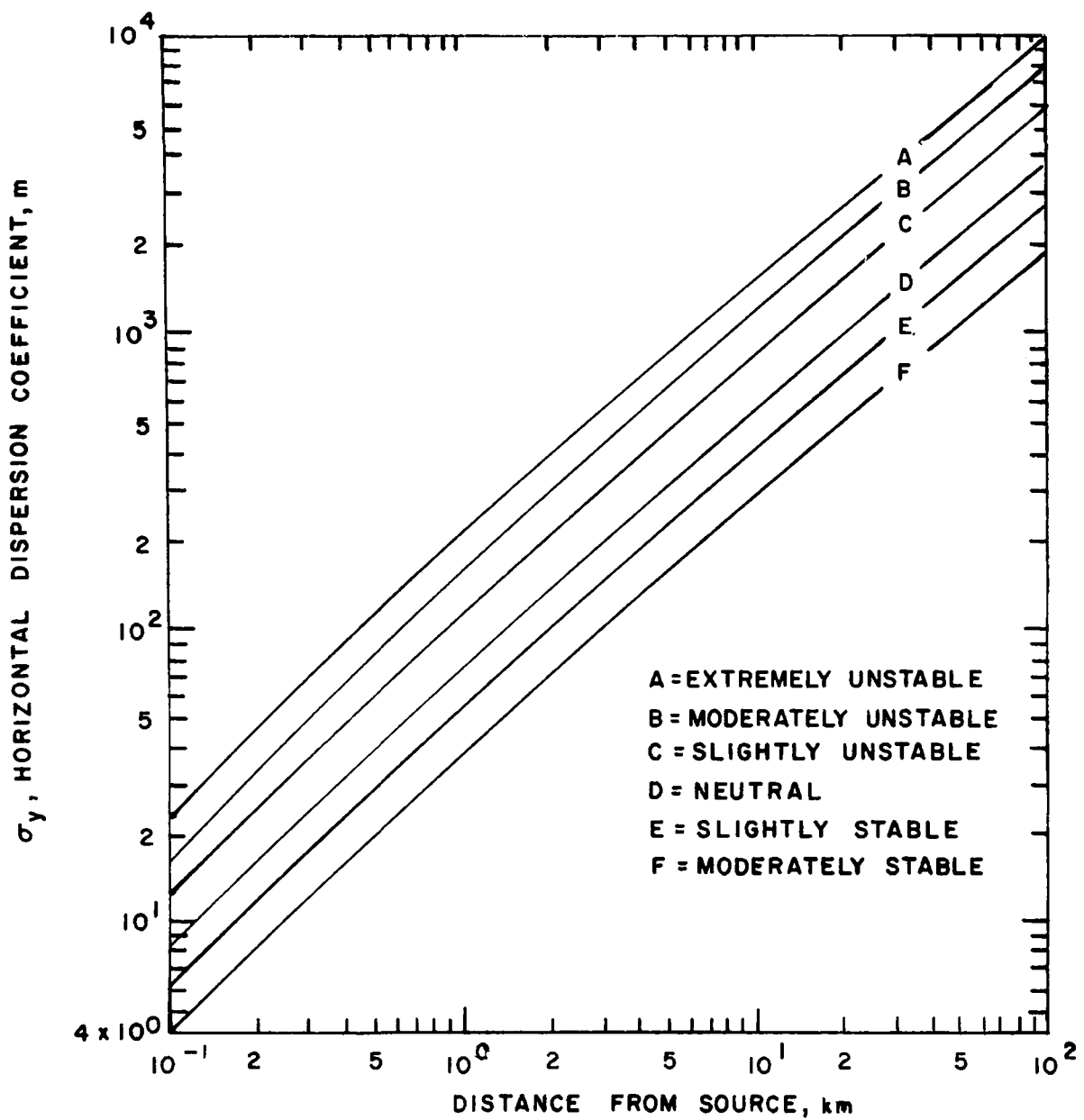


Figure 2. Horizontal dispersion coefficient as a function of distance according to Gifford⁶

Table 1. METEOROLOGICAL CATEGORIES ACCORDING TO
PASQUILL⁹ AND MEADE¹⁰

Surface wind speed, m/sec	Daytime insolation			Thin overcast or $\geq 4/8$ cloudi- ness	$\geq 3/8$ cloudi- ness
	Strong	Moderate	Slight		
< 2	A	A-B	B		
2	A-B	B	C	E	F
4	B	B-C	C	D	E
6	C	C-D	D	D	D
> 6	C	D	D	D	D

A - Extremely unstable conditions

B - Moderately unstable conditions

C - Slightly unstable conditions

D - Neutral conditions (Applicable to heavy overcast,
day or night)

E - Slightly stable conditions

F - Moderately stable conditions

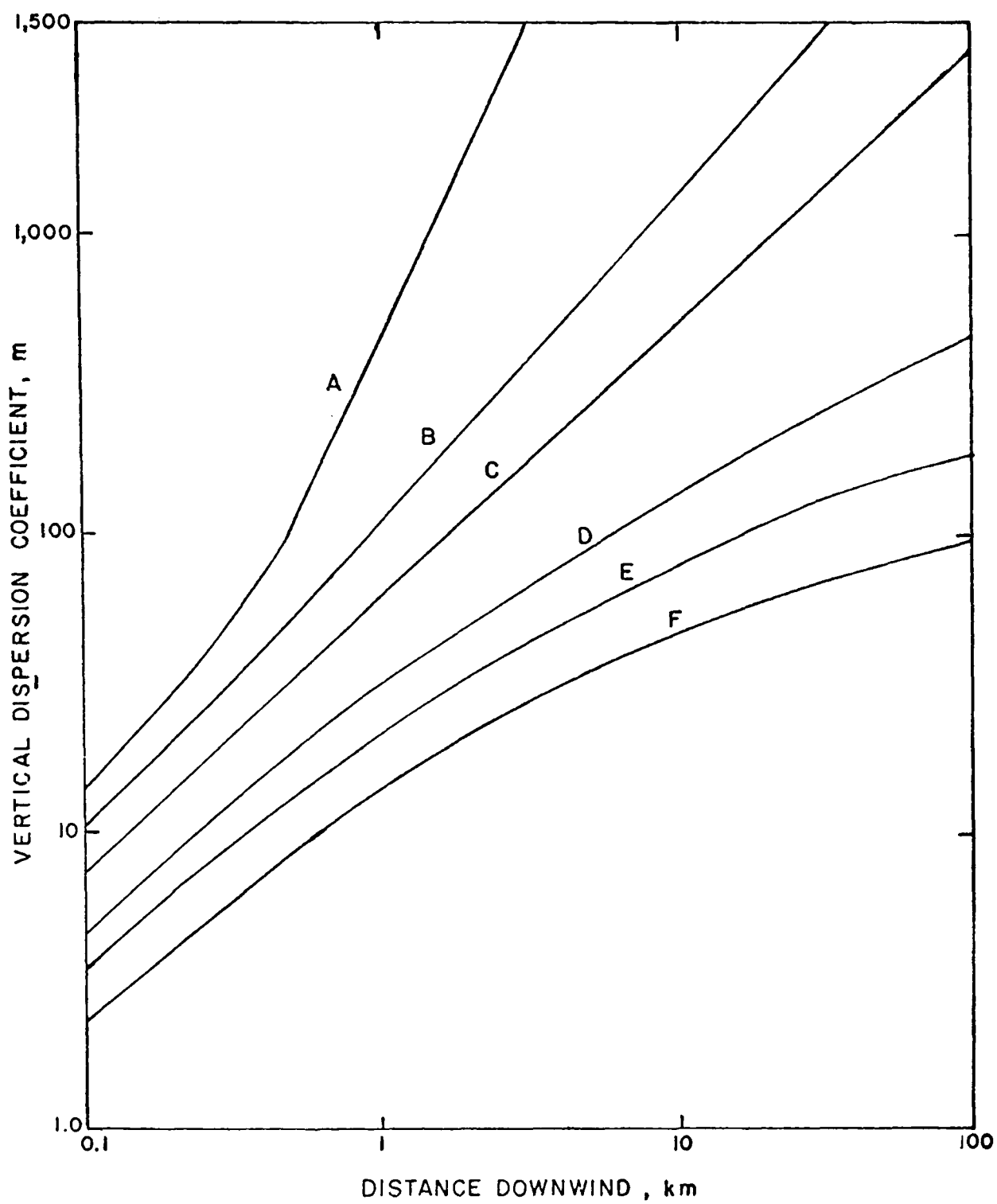


Figure 3. Vertical dispersion coefficient as a function of downwind distance from the source as currently employed in the Single Source Model⁷

vector (wind direction plus 180°), and randomized flow vector. The randomized flow vector is equal to the flow vector minus 4 degrees plus a random number between 0 and 9 degrees. The preprocessor output tape is then read by the Single Source Model which performs the actual concentration calculations. The twice daily mixing height data can be obtained from the National Climatic, Asheville, North Carolina. Missing data were filled in through interpolation.

Two different sets of hourly mixing heights are calculated by the preprocessor. One is for rural surroundings; the other is for urban locations. The way in which hourly mixing heights are determined from maximum mixing heights (MXDP) for yesterday ($i-1$), today (i) and tomorrow ($i+1$) and minimum mixing heights (MNDP) for today (i) and tomorrow ($i+1$) is depicted in Figure 4. For urban mixing height between midnight and sunrise the following procedure is used: if the stability is neutral interpolate between MXDP_{i-1} and MXDP_i (1), if stability is stable use MNDP_i (2). For hours between sunrise and 1400, if the hour before sunrise was neutral, interpolate between MXDP_{i-1} and MXDP_i (3). For sunrise to 1400, if the hour before sunrise was stable, interpolate between MNDP_i and MXDP_i (4). For 1400 to sunset, use MXDP_i (5). For hours between sunset and midnight, if stability is neutral interpolate between MXDP_i and MXDP_{i+1} (6), if stability is stable interpolate between MXDP_i and MNDP_{i+1} (7).

For rural mixing height between midnight and sunrise, interpolate between MXDP_{i-1} and MXDP_i (8). For hours between sunrise and 1400, if the hour before sunrise was neutral interpolate between MXDP_{i-1} and MXDP_i (9). For sunrise to 1400, if the hour before sunrise was stable, interpolate between 0 and MXDP_i (10). For 1400 to sunset, use MXDP_i (11). For sunset to midnight, interpolate between MXDP_i and MXDP_{i-1} (12).

Wind speeds u_0 measured at instrument height h_0 (7 meters is common for weather stations) are adjusted by means of a stability dependent power

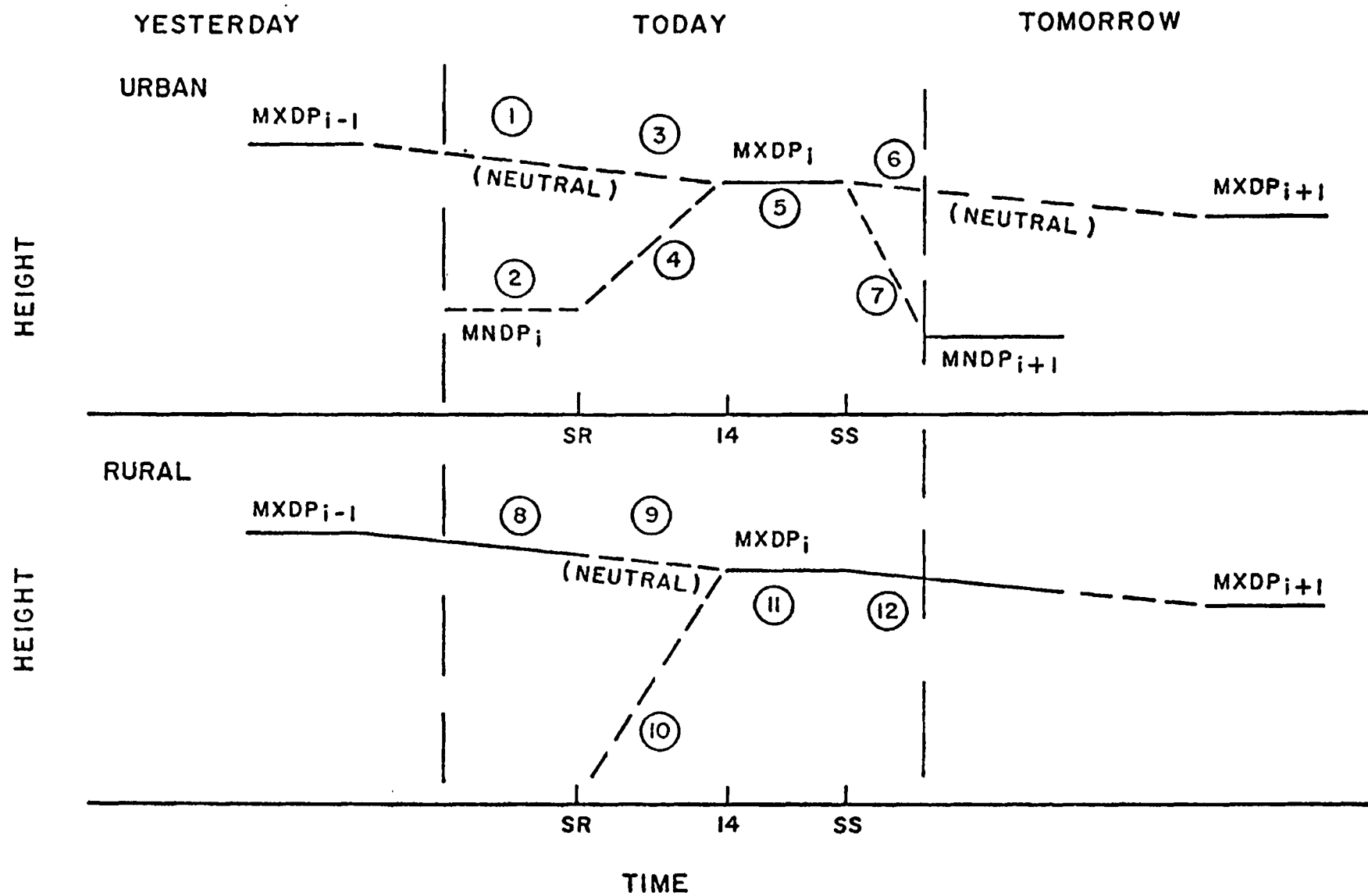


Figure 4. Determination of hourly mixing heights

law ($u = u_0 (h/h_0)^\alpha$) to correspond to values one would expect at the actual stack height h . The variation of the exponent α with stability is shown in Table 2. Plume rise is calculated on an hourly basis using the method of Briggs.³⁻⁵ The effective stack height $h(x)$ will be greater than the actual stack height h_s due to the buoyancy of the plume. The expression for $h(x)$ for stabilities A through D is given by

$$h(x) = h_s + \Delta h \tag{2}$$

where $\Delta h = 1.6F^{1/3} u^{-1} x^{2/3}$ for $x \leq 3.5x^*$
 $\Delta h = 1.6F^{1/3} u^{-1} (3.5x^*)^{2/3}$ for $x > 3.5x^*$
 $x^* = 14F^{5/8}$ when $F < 55 \text{ m}^4/\text{sec}^3$
 $x^* = 34F^{2/5}$ when $F \geq 55 \text{ m}^4/\text{sec}^3$
 $F = gwr^2 \left(\frac{T_s - T_a}{T_s} \right)$
 g = gravitational acceleration (m/sec^2)
 w = stack gas exit velocity (m/sec)
 T_s = stack gas temperature ($^\circ\text{K}$)
 T_a = ambient temperature ($^\circ\text{K}$)

Table 2. WIND PROFILE EXPONENTS (α) FOR DIFFERENT STABILITIES

Stability class	α
A	0.1
B	0.15
C	0.2
D	0.25
E	0.3
F	0.3

For stability classes E and F the plume rise becomes

$$\Delta h = 2.9 \left(\frac{F}{u_s} \right)^{1/3} \quad (3)$$

where $s = \frac{g}{T_e} \frac{d\theta}{dz}$

θ = potential temperature ($^{\circ}\text{K}$)

$$\frac{d\theta}{dz} = 0.02 \text{ } ^{\circ}\text{K/m for stability E}$$

$$\frac{d\theta}{dz} = 0.035 \text{ } ^{\circ}\text{K/m for stability F}$$

If the plume rise calculation indicates that the plume axis will rise above the mixing layer, then a zero concentration contribution is specified. If the final height plume is below the top of the mixing layer, the presence of the mixing boundary is accounted for in the Single Source Model by the incorporation of multiple image sources as was done to satisfy the zero flux condition at ground level. With this assumption Equation (1) is generalized to give

$$\begin{aligned}
\chi(x,y,z) = & \frac{Q \exp\left(\frac{-y^2}{2 \sigma_y^2(x)}\right)}{2\pi \sigma_y(x) \sigma_z(x)} \left\{ \exp\left(-\frac{(z - h(x))^2}{2 \sigma_z^2(x)}\right) \right. \\
& + \exp\left(-\frac{(z + h(x))^2}{2 \sigma_z^2(x)}\right) + \sum_{j=1}^n \exp\left(-\frac{(z - h(x) - 2jL)^2}{2 \sigma_z^2(x)}\right) \\
& + \exp\left(-\frac{(z + h(x) - 2jL)^2}{2 \sigma_z^2(x)}\right) + \exp\left(-\frac{(z - h(x) + 2jL)^2}{2 \sigma_z^2(x)}\right) \\
& \left. + \exp\left(-\frac{(z + h(x) + 2jL)^2}{2 \sigma_z^2(x)}\right) \right\} \quad (4)
\end{aligned}$$

where L = depth of the mixing layer (m)

n = number of images considered

In practice only the first few image terms contribute significantly to the overall ambient concentration. For distances greater than $2 x_L$, where x_L is given by $\sigma_z(x_L) = 1.6$, Equation (5) was approximated by

$$\chi(x,y,z) = \frac{Q \exp\left(\frac{-y^2}{2 \sigma_y^2(x)}\right)}{\sqrt{2\pi} \sigma_y(x) u L} \quad x > 2 x_L \quad (5)$$

Source input to the Single Source Model may possess several degrees of temporal resolution. In the seasonal version of the model an annual average SO_2 source strength is specified along with monthly variation factors. In addition to the seasonal factors, the diurnal version of the model employs hourly emission variation factors for each month of the year. A modification made to the model used in our validation studies allowed actual hourly source strengths to be utilized. A second modification made to the model allowed actual receptor elevations to be accounted for. In Section IV of this report we shall present the results of a validation of a version of the Single Source Model which allows the stack exit velocity to vary with the fuel consumption rate.

DESCRIPTIONS OF OTHER DISPERSION COEFFICIENTS TO BE TESTED

The stability selection algorithm and the dispersion calculation technique currently used within the Single Source Model will henceforth be referred to as the Pasquill-Turner method. During the next three parts of this section we shall discuss three other methods: (1) Smith-Singer, (2) Gifford Briggs and (3) F. B. Smith and the manner in which they were included in modified versions of the Single Source Model.

SMITH SINGER DISPERSION COEFFICIENTS

The Smith-Singer method for determining the horizontal and vertical dispersion coefficients is based upon a series of atmospheric diffusion experiments conducted over a period of 15 years at the Brookhaven National Laboratory. These included oil fog studies for an elevated source, monitoring of reactor emissions by A^{41} and low level uranine dye releases. The choice of a particular stability assignment (A, B2, B1, C or D) for a given hour is related to a subjective estimate of the lateral turbulence intensity determined from analogue wind direction recordings (Figure 5). A more quantitative explanation of the classification scheme shown in Figure 5 is presented below:

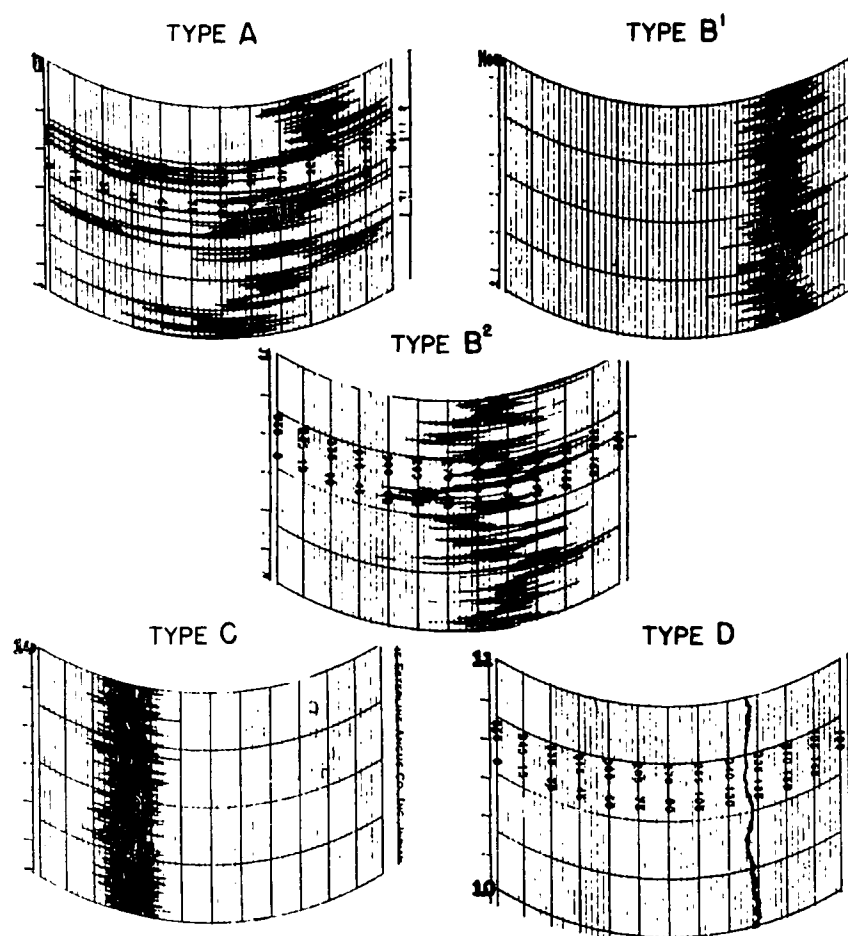


Figure 5. Wind direction trace types used to determine atmospheric stability by the Smith-Singer method¹⁴

- A = fluctuations of the wind direction exceeding 90° ;
- B2 = fluctuations ranging from 40° to 90° ;
- B1 = similar to A and B2, with fluctuations confined to 15° and 45° limits;
- C = distinguished by the unbroken solid core of the trace, through which a straight line can be drawn for the entire hour, without touching "open space"; and
- D = the trace approximates a line - short-term fluctuations do not exceed 15° .

Power law expressions describing the variation of σ_y and σ_z with distance from the source are specified¹² in Table 3 for four of the five "gustiness classes" (B2, B1, C, and D).

Table 3. SMITH-SINGER POWER LAW PARAMETERS a,b FOR HORIZONTAL AND VERTICAL DISPERSION PARAMETERS
 $\sigma_{y,z} = ax^b$ WHERE x IS IN METERS¹³

Stability class							
B2		B1		C		D	
a	b	a	b	a	b	a	b
σ_y 0.40	0.91	0.36	0.86	0.32	0.78	0.31	0.71
σ_z 0.41	0.91	0.33	0.86	0.22	0.78	0.06	0.71

The dispersion curves described by these parameters are shown in Figures 6 and 7.

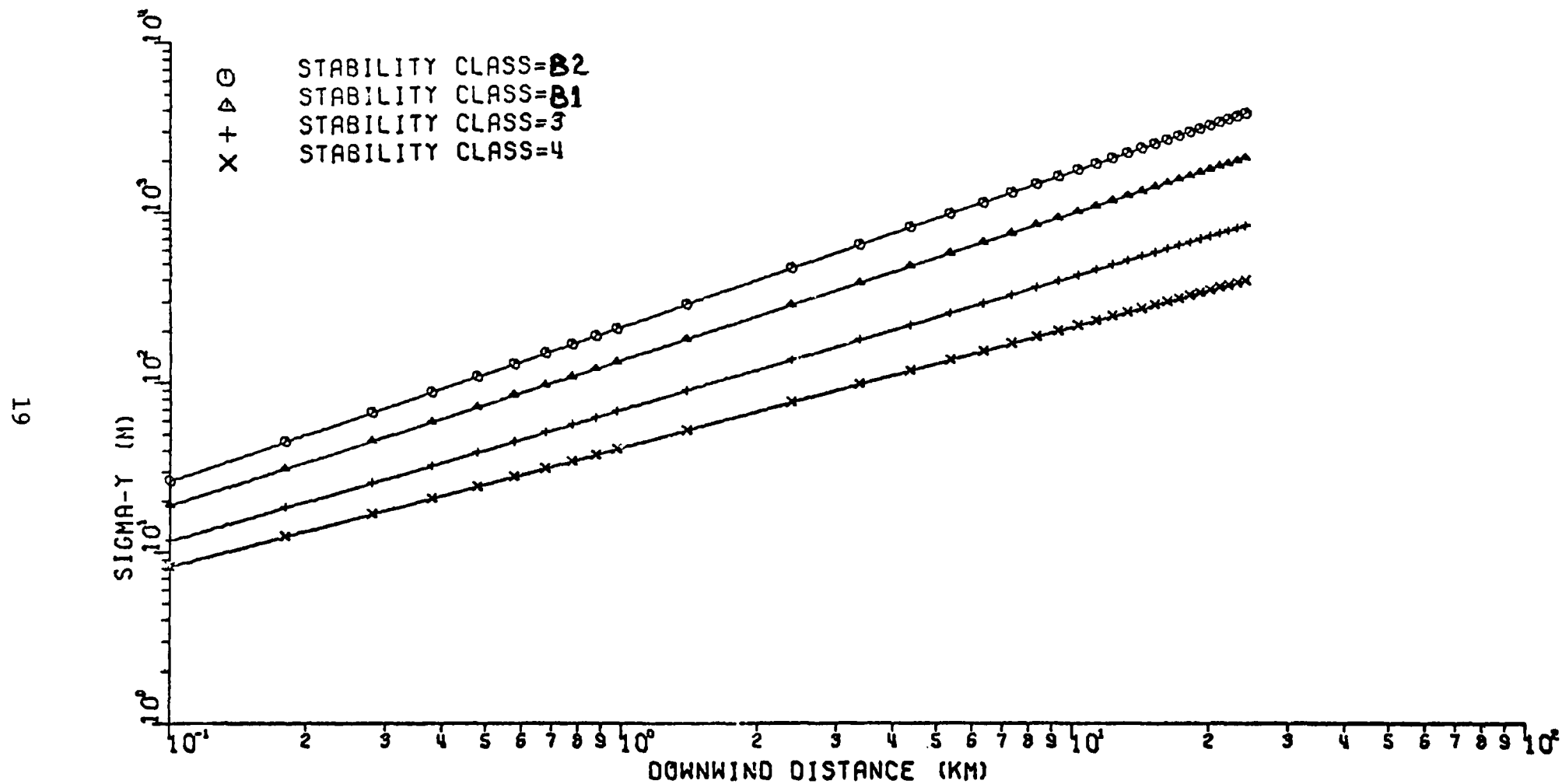


Figure 6. Variation of σ_y with distance for the Smith-Singer stability classes

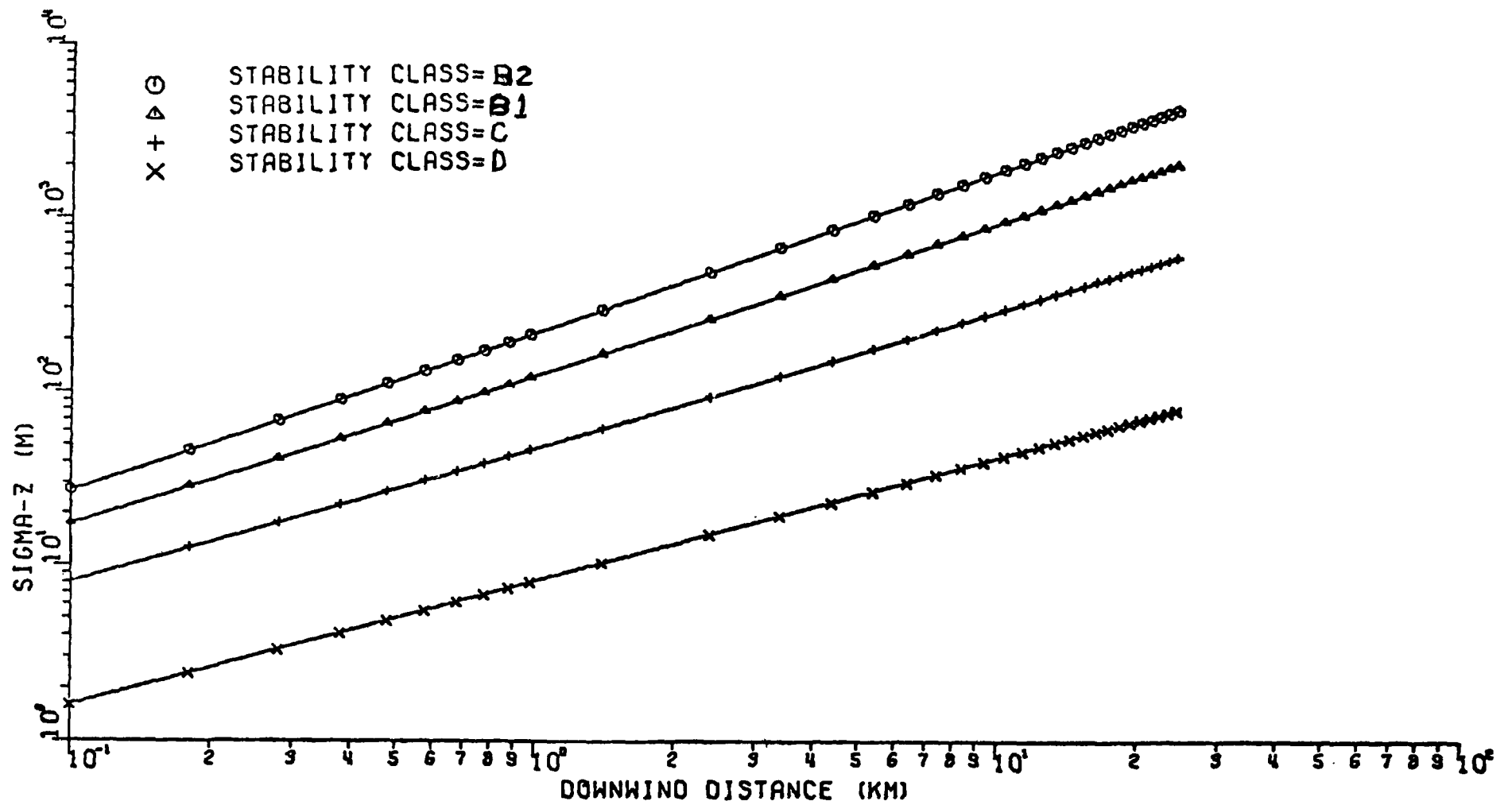


Figure 7. Variation of σ_z with distance for each of the Smith-Singer stability classes

No dispersion parameters are given for stability A since this condition is characterized by no organized horizontal wind flow so that the resultant ground level concentrations may only be described in a qualitative manner. Stability A cases were therefore not included in our validation studies to be described later in this report. As in the case of the Pasquill-Turner scheme the wind speed is assumed to increase with height according to a power law with the exponent α assigned the values 0.16, 0.25, 0.32, and 0.50 for atmospheric stabilities B2 through D.¹³

In the application of these dispersion curves to the prediction of concentrations downwind of large elevated point sources M.E. Smith calculates the effective stack height by use of the following formula presented in the ASME Guide¹⁵ Second Edition, 1973:

$$h = h_s + 7.4 \left(\frac{F^{1/3} h_s^{2/3}}{u} \right) \quad (6)$$

Since we were primarily interested in the comparison of different dispersion calculation methods we continued to employ the Briggs formulae, with Equation (2) used for stabilities B2, B1 and C and Equation (3) used for stability D. For power plant diffusion modeling Smith modifies his estimate of σ_y by adding a term to allow for the presence of directional wind shear:

$$\sigma_y = ax^b + x \tan \phi \quad (7)$$

where ϕ = wind direction change

Since no rule is given for the selection of ϕ as a function of stability or plume height, the term was not included in our analysis. Had the term been included, it would have effectively lowered the predictions of ground level air concentrations especially for the more stable conditions.

GIFFORD-BRIGGS DISPERSION COEFFICIENTS

A method for the determination of plume standard deviations has recently been developed by Briggs¹⁶ using a wide range of experimental data including the TVA and Prairie Grass measurements mentioned earlier. The selection of an appropriate stability class is called out according to the Pasquill-Turner method but the corresponding curves for σ_y and σ_z are chosen to represent a wider range of source elevations and source-receptor distances. Analytical expressions for σ_y and σ_z applicable to rural areas are given in Table 4. The utilization of the Gifford-Briggs method in the Single Source Model required only that the dispersion calculation subroutine be modified. The plume rise and the wind profile equations were left unchanged.

Table 4. VARIATION OF σ_y AND σ_z WITH DISTANCE x (METERS) FOR RURAL AREAS

Stability	σ_y (meters)	σ_z (meters)
A	$0.224 x / \sqrt{1 + 0.0001 x}$	$0.20 x$
B	$0.16 x / \sqrt{1 + 0.0001 x}$	$0.12 x$
C	$0.112 x / \sqrt{1 + 0.0001 x}$	$0.080 x / \sqrt{1 + 0.0002 x}$
D	$0.080 x / \sqrt{1 + 0.0001 x}$	$0.056 x / \sqrt{1 + 0.0015 x}$
E	$0.056 x / \sqrt{1 + 0.0001 x}$	$0.032 x / (1 + 0.0003x)$
F	$0.040 x / \sqrt{1 + 0.0001 x}$	$0.016 x / (1 + 0.0003x)$

F.B. SMITH DISPERSION COEFFICIENTS

Recently the Pasquill-Turner scheme for stability classification for vertical dispersion coefficients has been modified and extended by Pasquill's colleague, F.B. Smith,¹⁷ to include the effect of surface

roughness and provide for the fractional assignment of stability classes. This latter development was especially significant since the variation of ground level air concentration with stability class can be an order of magnitude or more.

The scheme utilizes numerical solutions of the diffusion equation up to 100 km downwind with profiles of wind, $u(z)$, and diffusivity, $(K(z))$, suggested by actual measurements in unstable, neutral and stable conditions. The horizontal dispersion coefficients are chosen to be the same as the Pasquill-Turner. The reason for this is that F. B. Smith does not recommend any specific σ_y curve, but rather advises the use of wind fluctuation data, with an adjustment for downwind distance. At larger distances, this adjustment makes $\sigma_y \propto x^{1/2}$ where x is downwind distance. Since the required wind fluctuation data are not available, the Pasquill-Turner σ_y data were used. It should be pointed out, however, that the Pasquill-Turner curves show σ_y to be approximately proportional to $x^{0.9}$ at all distances, and not $x^{1/2}$. The method for fractional stability assignment is illustrated in Figure 8. F.B. Smith presented Figure 9 as a guide for choosing a value for incoming solar radiation as a function of solar elevation angle. He recommends that this value be multiplied by an appropriate factor to account for the presence of cloud cover (see Table 5).

Table 5. MULTIPLICATION FACTORS FOR INCOMING SOLAR RADIATION INTENSITY FOR DIFFERENT AMOUNTS OF CLOUD COVER

Cloud amount (eighths)	Multiplier
0	1.07
1	0.89
2	0.81
3	0.76
4	0.72
5	0.67
6	0.59
7	0.45
8	0.23

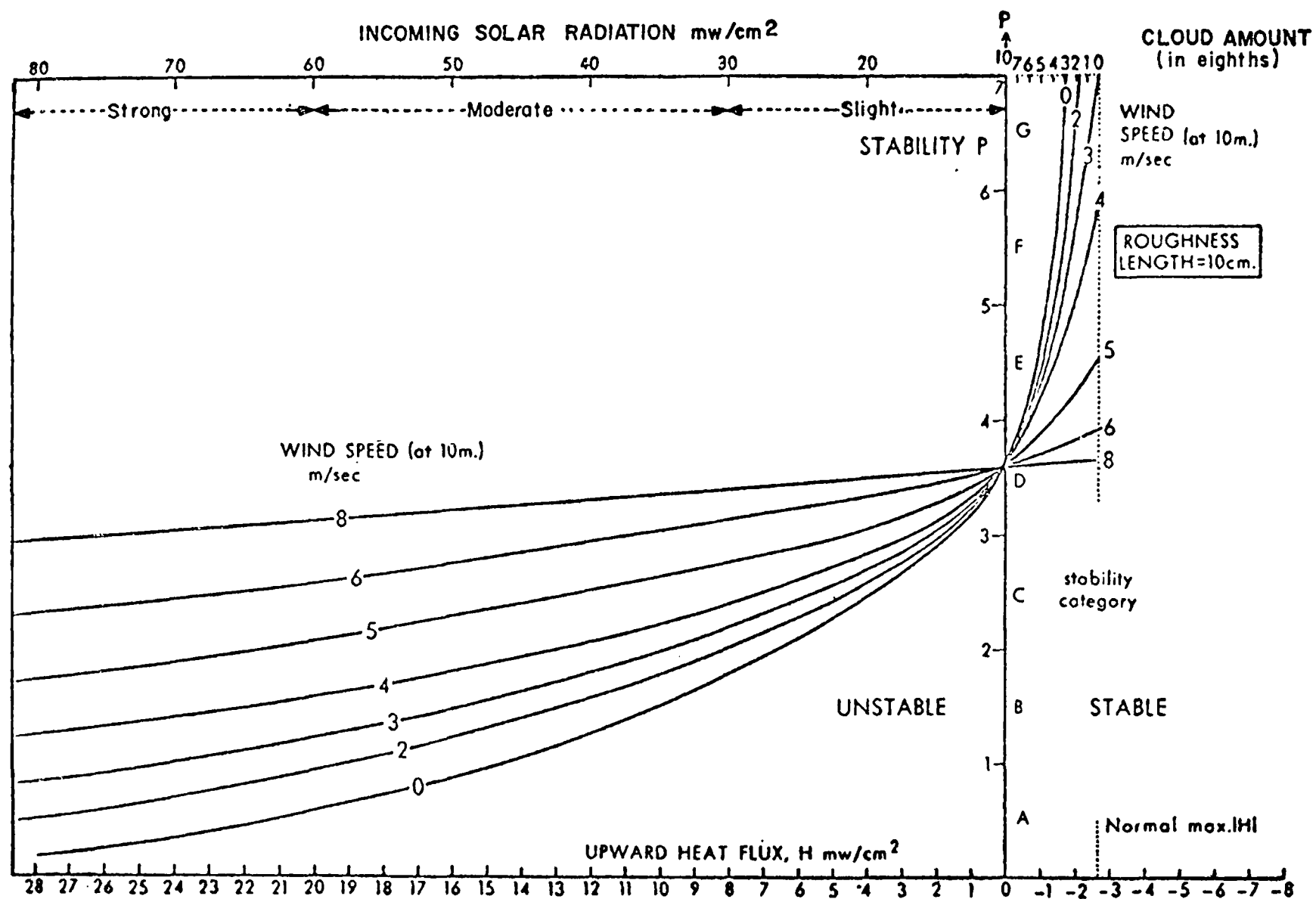


Figure 8. F.B. Smith scheme for assignment of fractional stability classes¹⁷

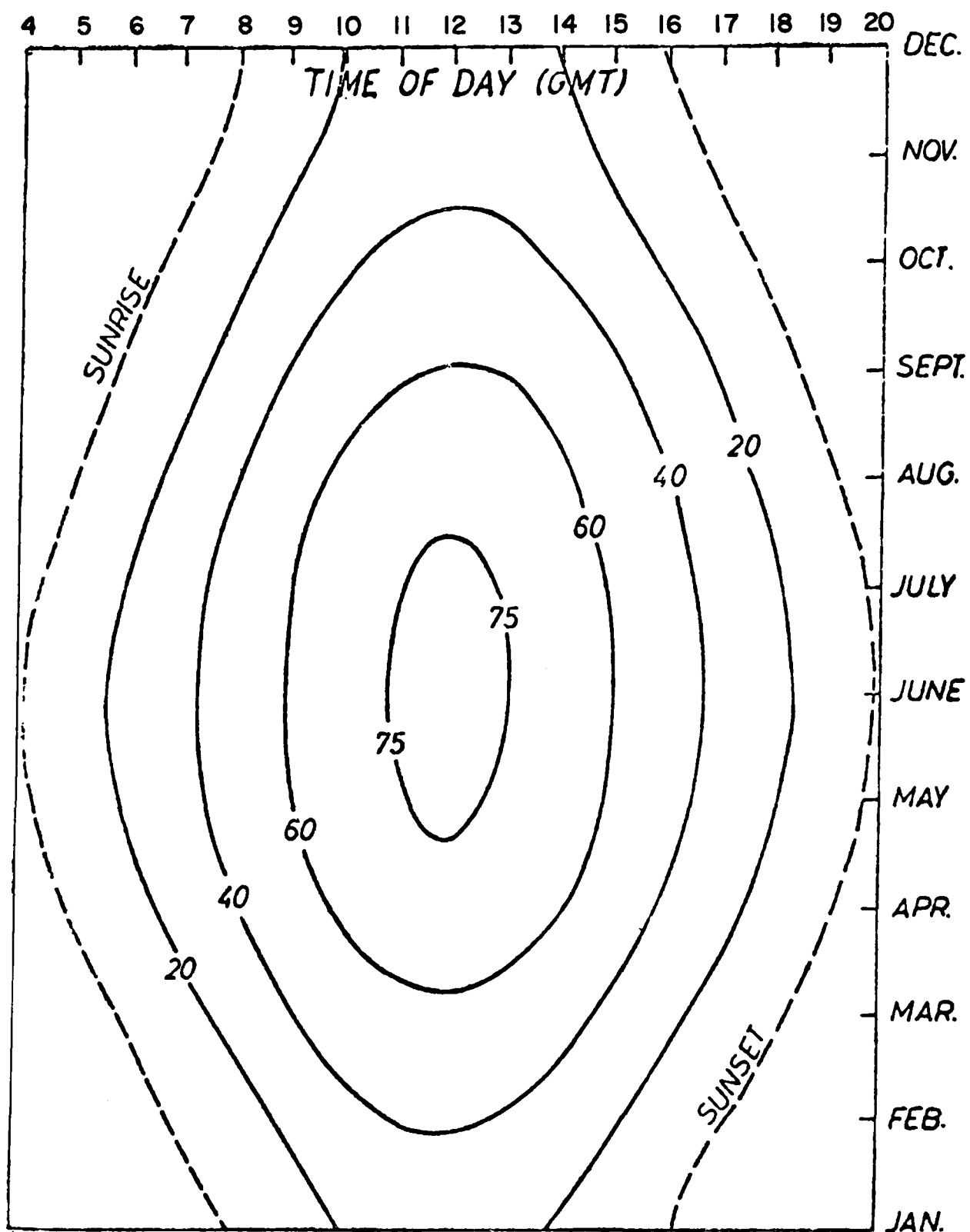


Figure 9. Incoming solar radiation (mW/cm^2) measured at Cambridge, England on a cloudless day¹⁷

To obtain a relationship between solar angle and incident solar radiation, we sought to describe the data presented in Figure 9 for Cambridge, England in terms of the following equation:¹⁸

$$I = \frac{J_o}{r^2} a^{\sec \theta} \cos \theta \quad (8)$$

where I = solar radiation intensity
 $J_o = 135.3$ milliwatts/cm²
 a = transmission factor
 θ = solar zenith angle (90° - solar elevation angle)
 r = "radius vector" of earth's orbit (≈ 1)

For a specific latitude and longitude the angle θ may be determined based upon the time zone classification, hour of the day (standard time) and day of the year. When the data were analyzed it was found that the diurnal and seasonal variation of the radiation intensity, I , could not be reproduced by use of a constant transmission factor a . The best fit was obtained for the following variation of the transmission factor, a , with zenith angle θ .

$$a = 0.57 + 0.0045 \theta \quad (9)$$

where θ is measured in degrees. The fitted solar radiation intensity as a function of zenith angle is shown in Figure 10.

With the relationships given by Equations (8) and (9) the fractional stability index, P , may be determined from the curves shown in Figure 8 once the windspeed and cloud cover have been specified. In his article F. B. Smith identifies a P value of 3.6 with a D stability index (i.e., stability 4) which would have been determined according to the Turner scheme presented in Appendix A. The relationship between the fractional stability P and the Turner stability S_T should then be given by

$$S_T = (P + 0.4) \text{ rounded} \quad (10)$$

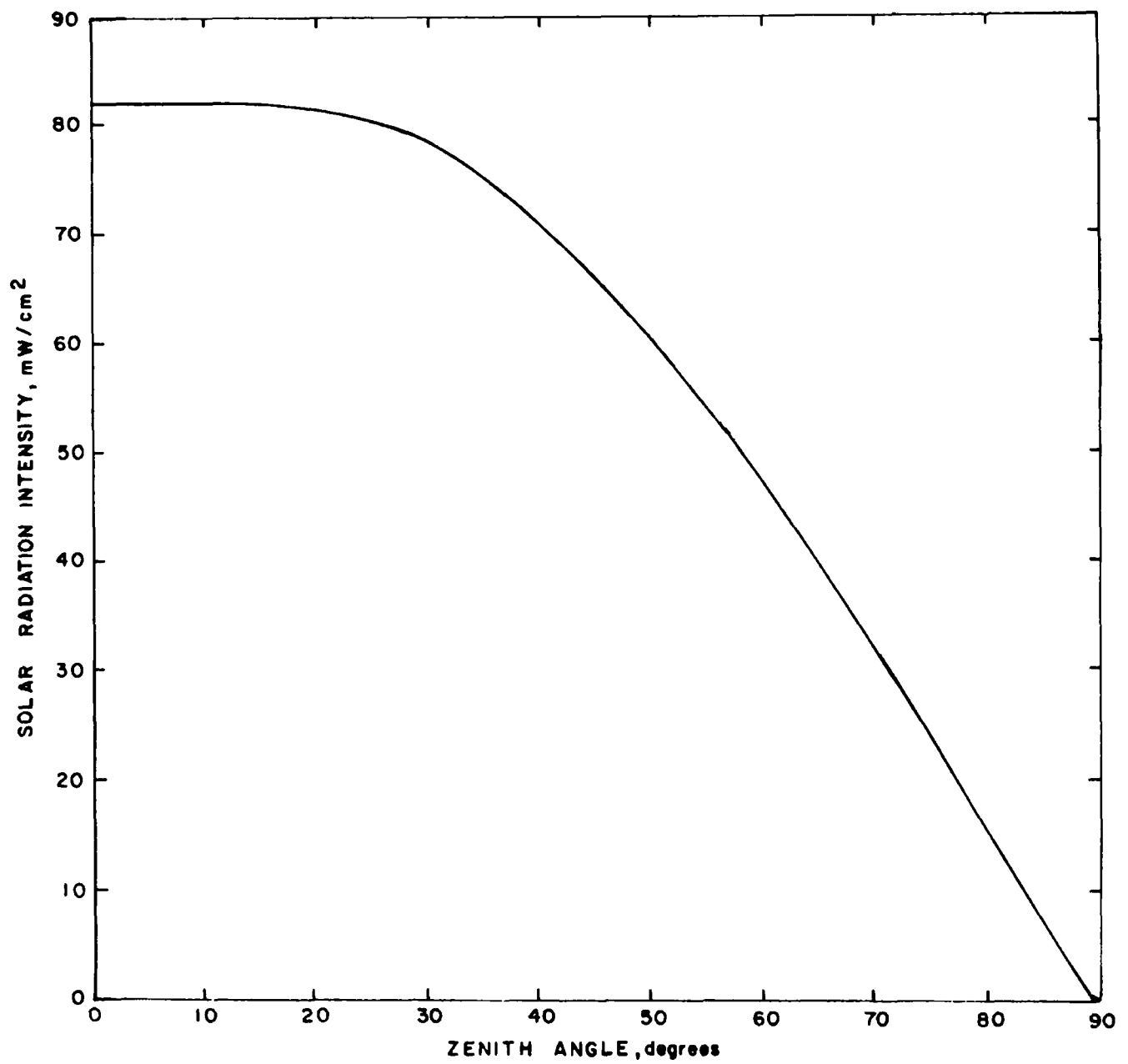


Figure 10. Solar radiation intensity as a function of zenith angle.
Relationship based upon data presented in Figure 9

To determine the validity of this assumption we carried out a polynomial fit to the curves given in Figure 8 so that, based upon the solar elevation angle, cloud cover and wind speed, a comparison between the F. B. Smith and Turner assignment schemes could be made for a wide range of meteorological configurations. Based upon this comparison we found that the Turner stability class assignment was higher during the middle part of the day, especially during the summer months when the difference could be greater than an entire stability class. The polynomial fits used for this comparison formed the basis of the fractional stability of the Single Source Model Preprocessor Program which is presented in Appendix B.

Once the stability parameter P has been selected the corresponding vertical dispersion coefficient σ_z is determined for a particular downwind distance x by use of the curves presented in Figures 11 and 12. These results have been fitted by R. P. Hosker¹⁹ to analytical expressions of the form

$$\sigma_z(x) = \frac{a_1 x^{b_1}}{1 + a_2 x^{b_2}} \tag{11}$$

A list of the numerical values of the parameters used in Equation (11) is given in Table 6.

Table 6. FIT PARAMETERS FOR DISPERSION COEFFICIENTS

Stability category	a_1	b_1	a_2	b_2
A (P = 0.6)	0.112	1.06	5.38×10^{-4}	0.815
B (P = 1.6)	0.130	0.950	6.52×10^{-4}	0.750
C (P = 2.6)	0.112	0.920	9.05×10^{-4}	0.718
D (P = 3.6)	0.098	0.889	1.35×10^{-3}	0.688
E (P = 4.6)	0.0609	0.895	1.96×10^{-3}	0.684
F (P = 5.6)	0.0638	0.783	1.36×10^{-3}	0.672

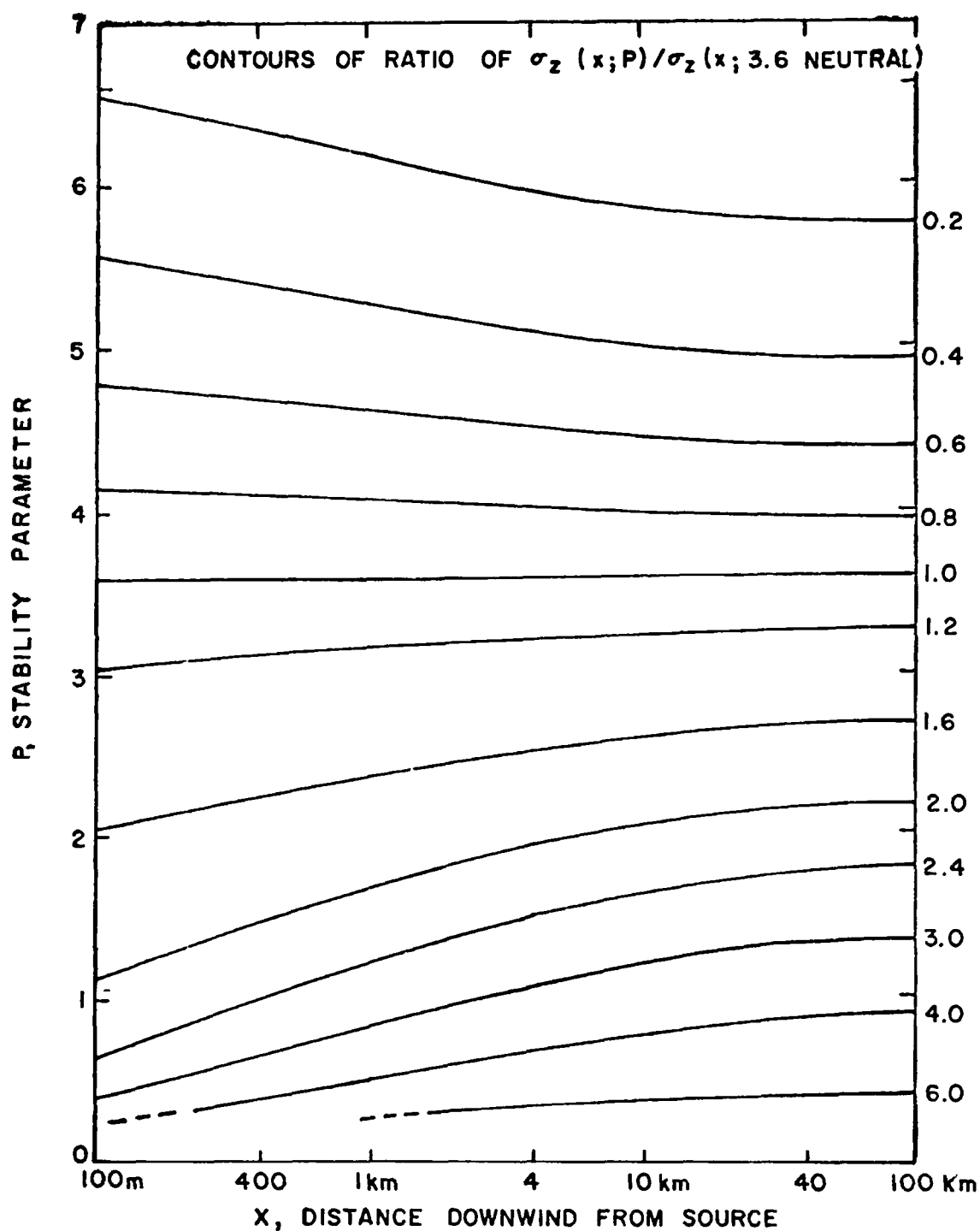


Figure 11. Variation with distance of the vertical dispersion parameter σ_z (normalized with respect to the neutral stability value) for different values of p_{17}

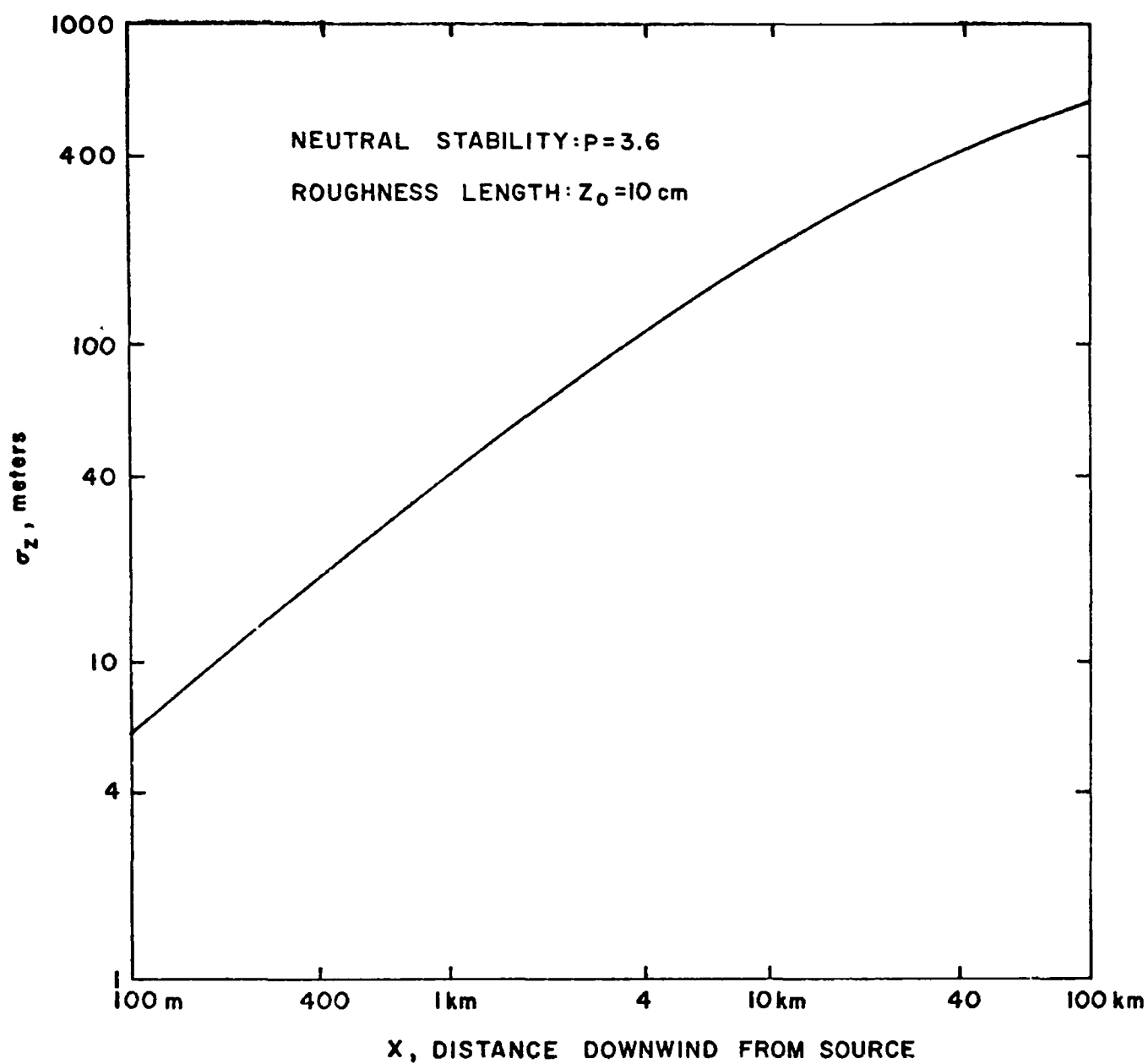


Figure 12. Variation of σ_z with distance for stability D ($P = 3.6$)¹⁷

According to the F.B. Smith method the dispersion curves may be modified to account for the effect of surface roughness z_o . These correction factors are shown in Figure 13. As parameterized by Hosker,¹⁹ this correction factor $F(z_o, x)$ takes the following forms:

$$F(z_o, x) = \ln \left\{ c_1 x^{d_1} \left[1 + \left(c_2 x^{d_2} \right)^{-1} \right] \right\}, \quad z_o > 10 \text{ cm} \quad (12)$$

$$= \ln \left\{ c_1 x^{d_1} \left[1 + c_2 x^{d_2} \right]^{-1} \right\}, \quad z_o < 10 \text{ cm} \quad (13)$$

The corrected dispersion coefficient $\sigma_z(z_o, x)$ may be written as

$$\sigma_z(z_o, x) = F(z_o, x) \sigma(10 \text{ cm}, x) \quad (14)$$

where the $\sigma(10 \text{ cm}, x)$ are the σ_z values given by the curves in Figures 11 and 12. The parameters required to evaluate Equations (12a) and (12b) are presented in Table 7.

Table 7. COEFFICIENTS OF THE ROUGHNESS CORRECTION FACTOR USED IN CALCULATING $\sigma_z(x)$ FOR VARIOUS ROUGHNESS LENGTHS (x IS GIVEN IN METERS)

Roughness length	c_1	d_1	c_2	d_2
1 cm	1.56	0.0480	6.25×10^{-4}	0.45
4 cm	2.02	0.0269	7.76×10^{-4}	0.37
40 cm	5.16	-0.098	18.6	-0.225
100 cm	7.37	-0.0957	4.29×10^3	-0.60
400 cm	11.7	-0.128	4.59×10^4	-0.78

In Section IV of this report we will describe three types of model validation studies based upon the F.B. Smith dispersion coefficients. The first test will combine the Turner stability class assignment scheme with the F.B. Smith dispersion curves for the point stabilities (A, B, C, D, E and F). The second test will involve the calculation and use of fractional

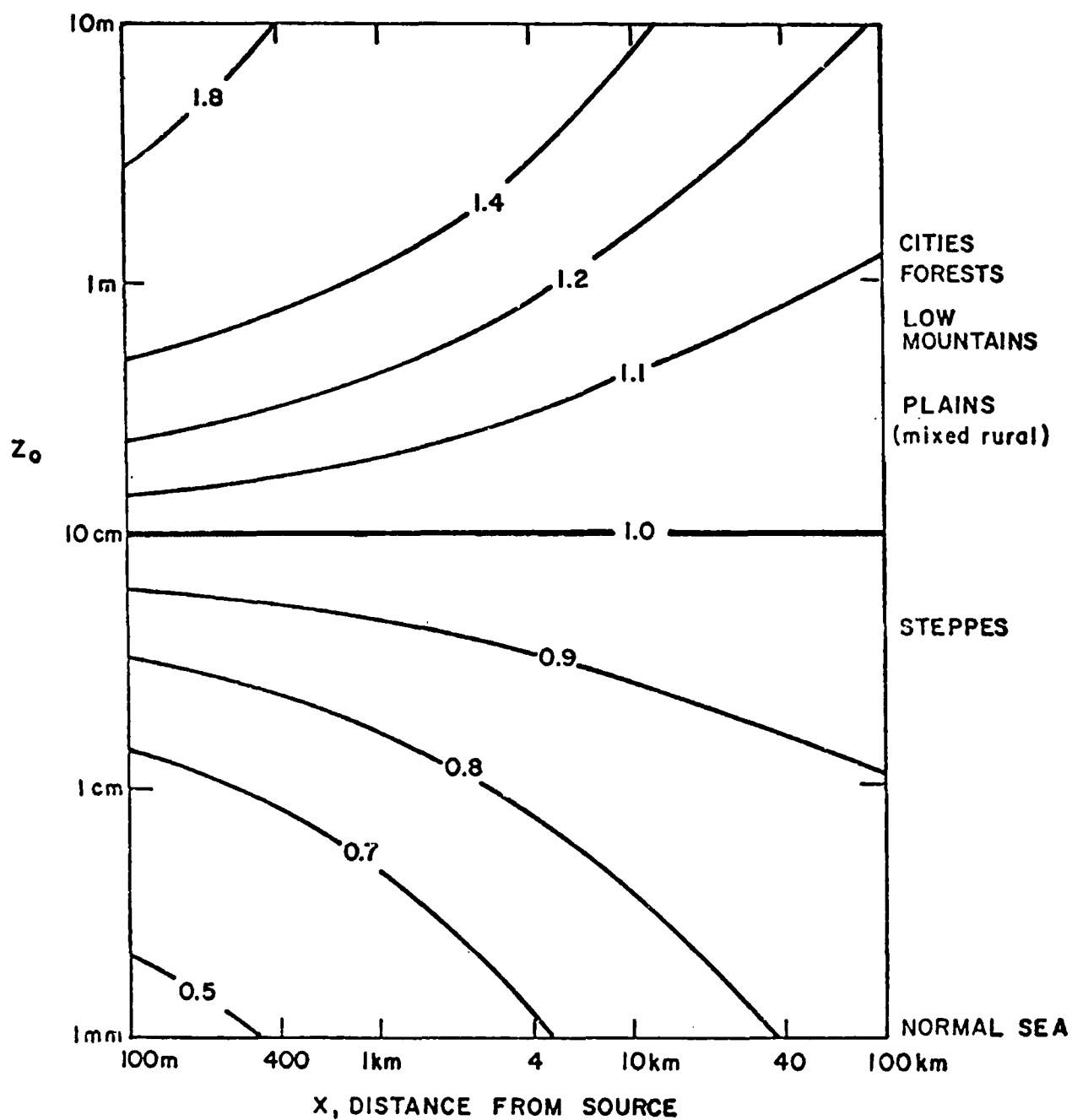


Figure 13. Contours of the vertical dispersion coefficient correction factor $F(z_o, x)$

stabilities. Finally the effect of incorporating surface roughness will be investigated.

COMPARISON OF THE DISPERSION COEFFICIENTS

A comparison of the dispersion curves we have just discussed will prove useful in our analysis of the model validation results which will be presented in Section IV. In Figures 14(a) through (f), vertical dispersion coefficients according to Briggs, F.B. Smith, and Pasquill-Turner are plotted as a function of downwind distance for stabilities A through F. The following observations may be made based upon an examination of these curves:

1. The Briggs and Pasquill-Turner curves are quite close to one another except in the case of stability A.
2. The F.B. Smith vertical dispersion curve falls below the other two curves for stabilities A, B and C and above the other curves for stabilities D, E and F.
3. The worst agreement between all three of the curves is seen for stability A with the best agreement for stabilities D, E and F.

In Figures 15(a) through (f) we have plotted the horizontal dispersion curves according to Briggs and Pasquill-Turner by stability class. The Pasquill-Turner horizontal dispersion curves are used in conjunction with the F.B. Smith vertical dispersion curves, so that no F.B. Smith horizontal curves have been presented. An obvious feature of these plots is that the Briggs and Pasquill curves are virtually identical. The horizontal and vertical dispersion curves according to Smith-Singer were presented in Figures 6 and 7 for the four Smith-Singer stability classes B2, B1, C and D. The most striking feature of these plots is the identical slope for σ_z and σ_y curves for the same stability. Finally the effect of surface roughness upon the F. B. Smith vertical dispersion curves is illustrated in Figures 16(a) through (f).

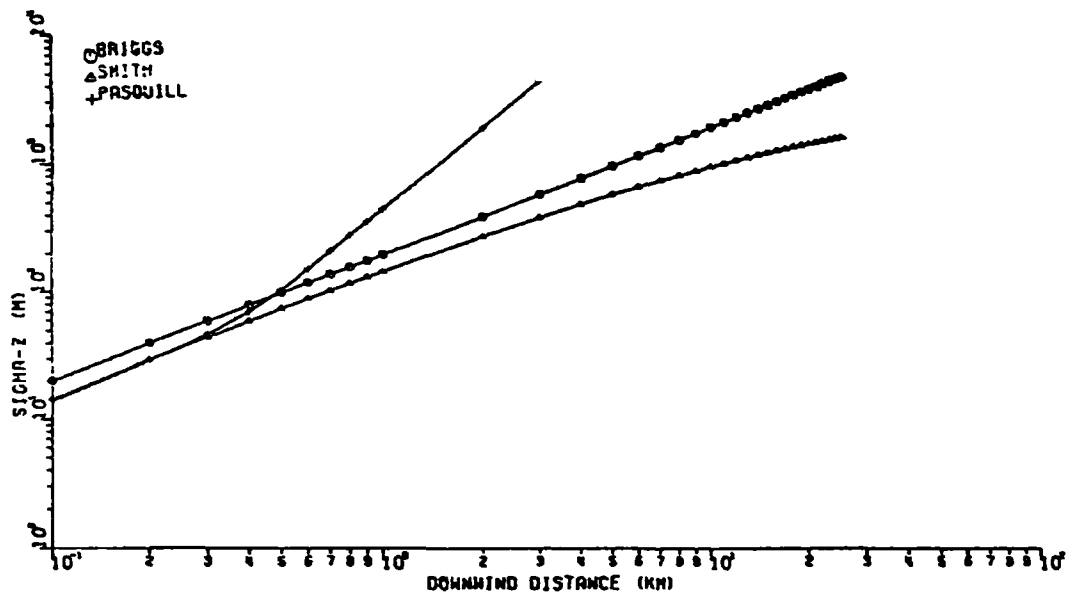


Figure 14a. Vertical dispersion coefficient as a function of downwind distance for Stability Class A according to Briggs, F.B. Smith and Pasquill-Turner

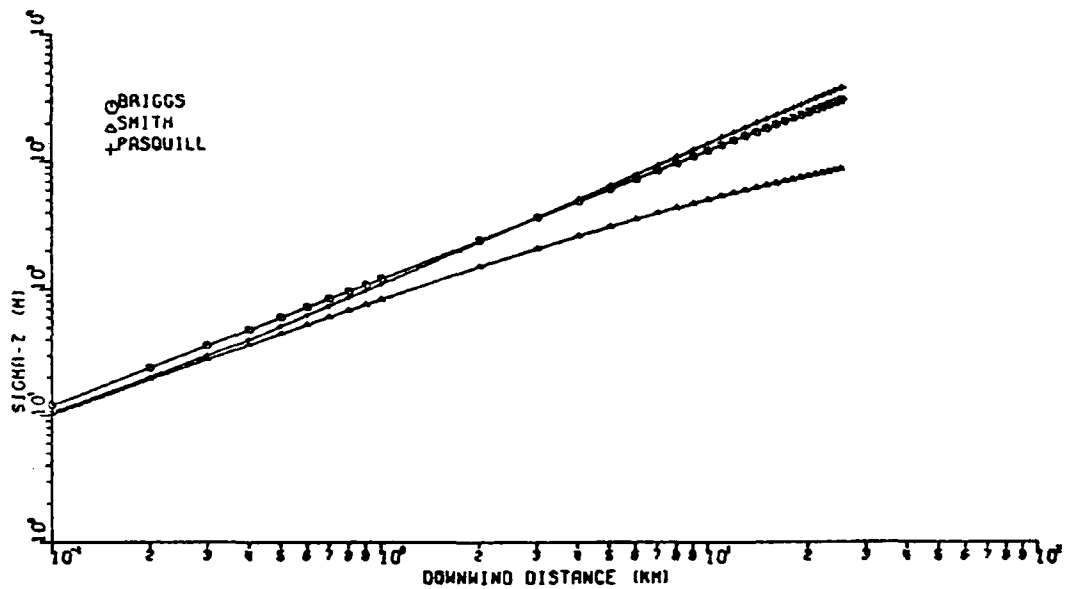


Figure 14b. Vertical dispersion coefficient as a function of downwind distance for Stability Class B according to Briggs, F.B. Smith and Pasquill-Turner

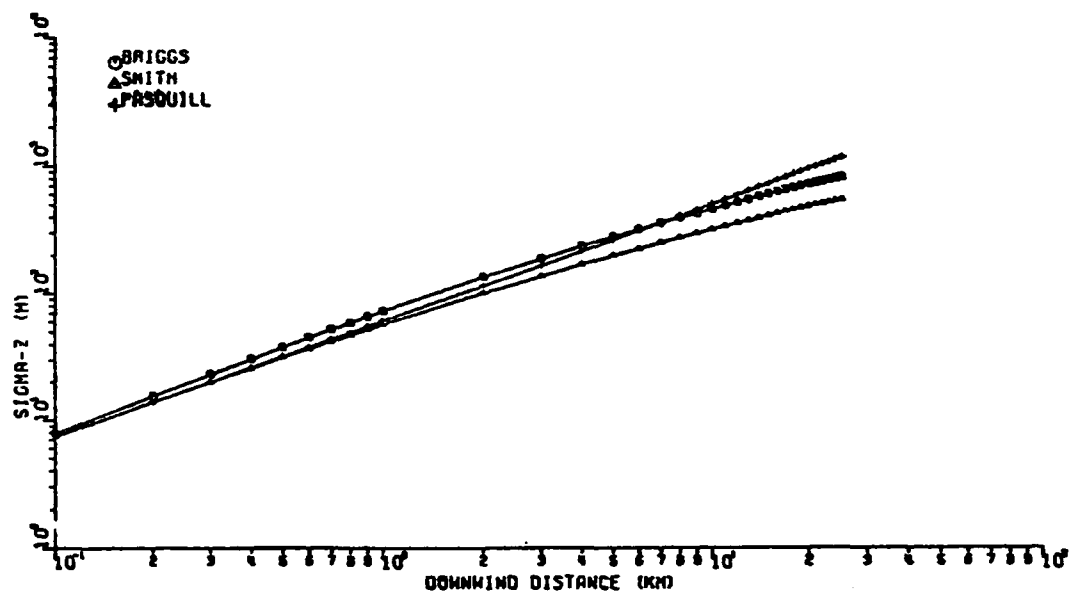


Figure 14c. Vertical dispersion coefficient as a function of downwind distance for Stability Class C according to Briggs, F.B. Smith and Pasquill-Turner

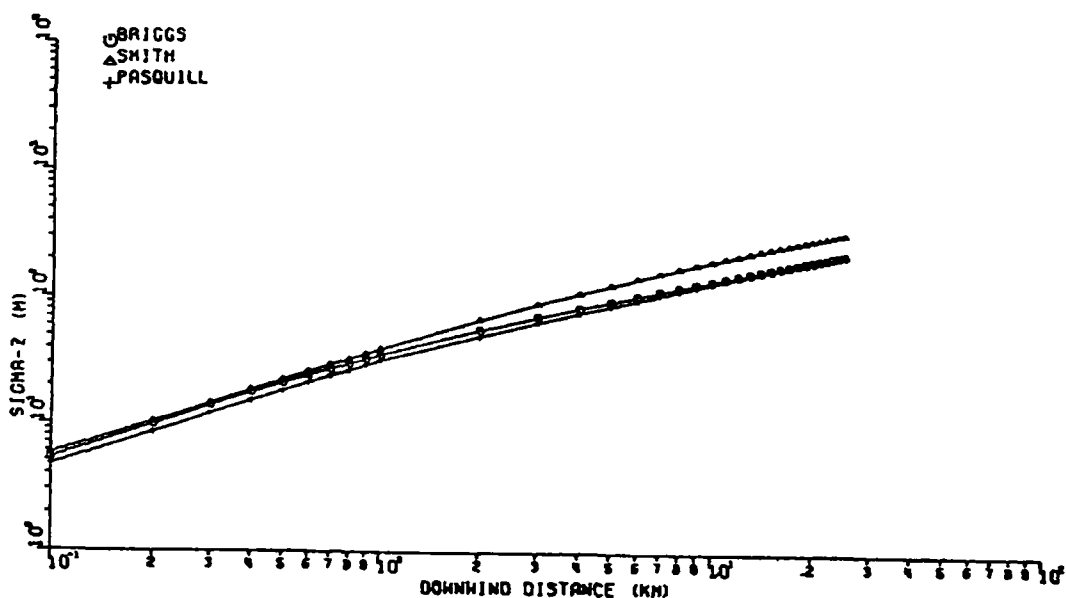


Figure 14d. Vertical dispersion coefficient as a function of downwind distance for Stability Class D according to Briggs, F.B. Smith and Pasquill-Turner

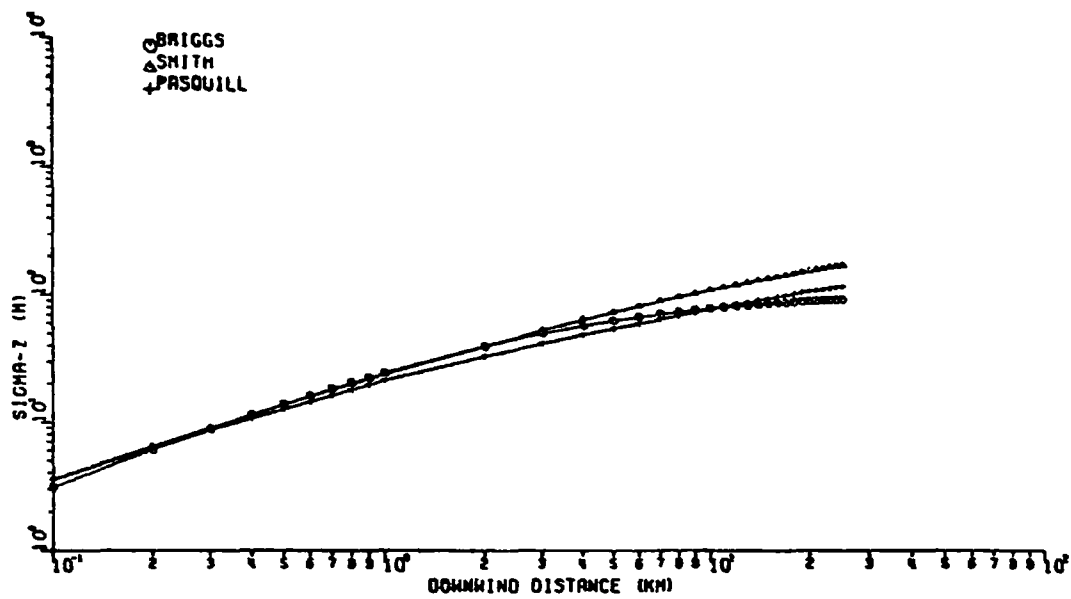


Figure 14e. Vertical dispersion coefficient as a function of downwind distance for Stability Class E according to Briggs, F.B. Smith and Pasquill-Turner

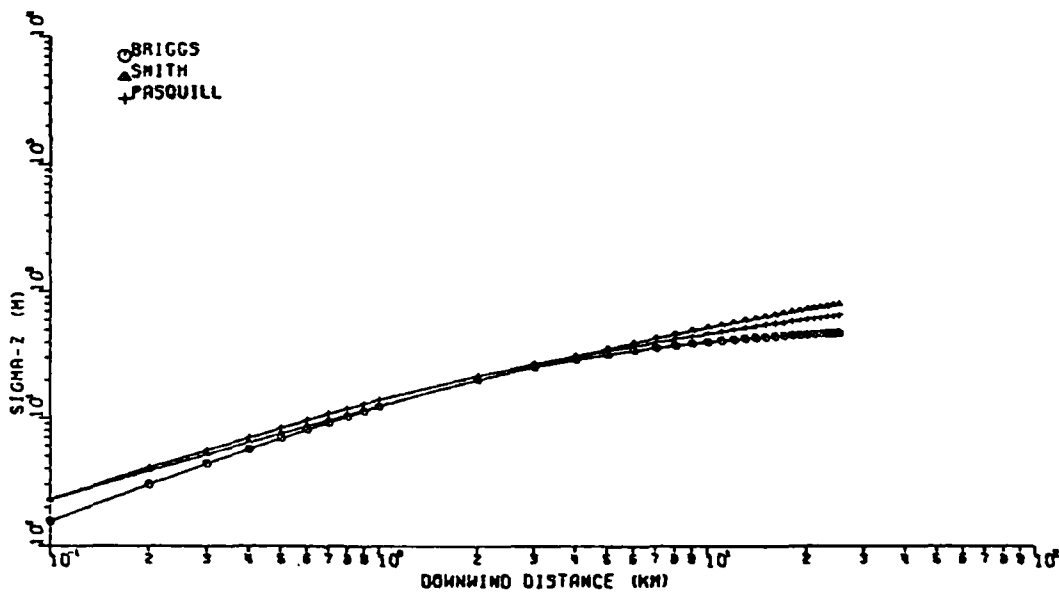


Figure 14f. Vertical dispersion coefficient as a function of downwind distance for Stability Class F according to Briggs, F.B. Smith and Pasquill-Turner

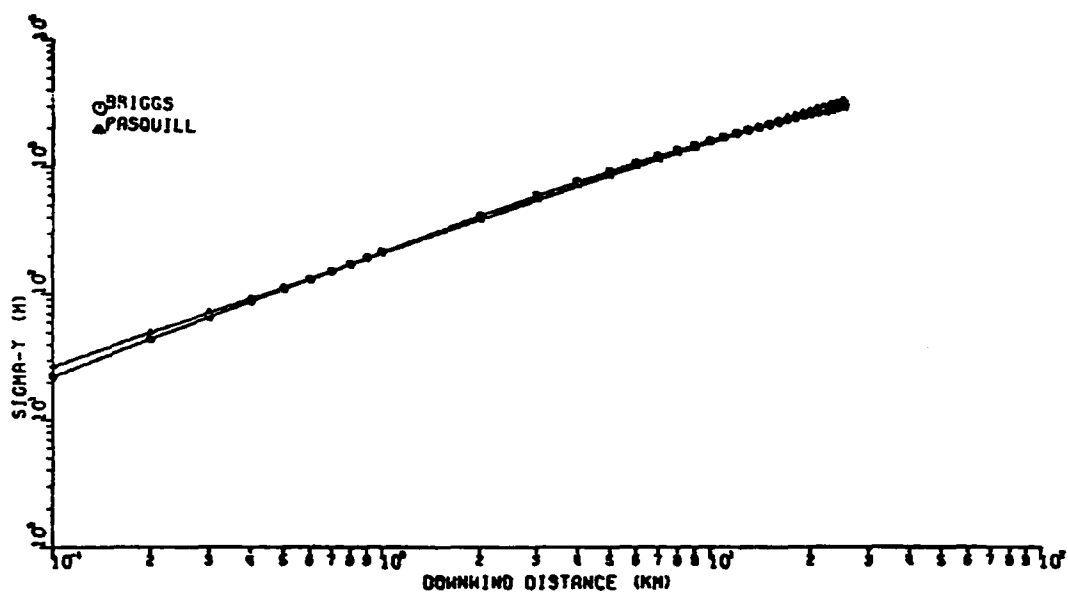


Figure 15a. Horizontal dispersion coefficient as a function of downwind distance for Stability Class A according to Briggs and Pasquill-Turner

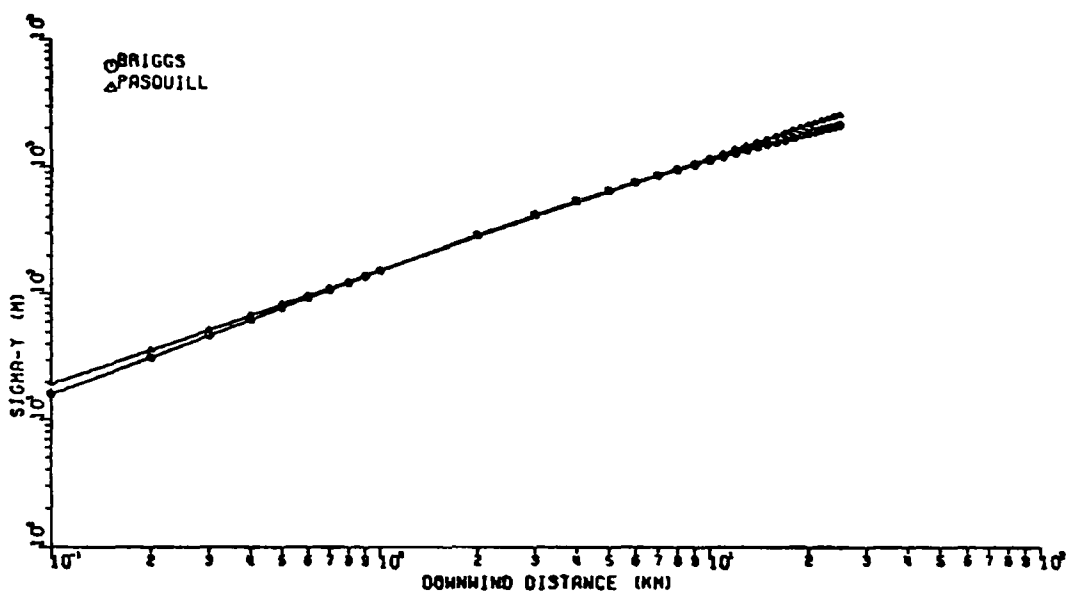


Figure 15b. Horizontal dispersion coefficient as a function of downwind distance for Stability Class B according to Briggs and Pasquill-Turner

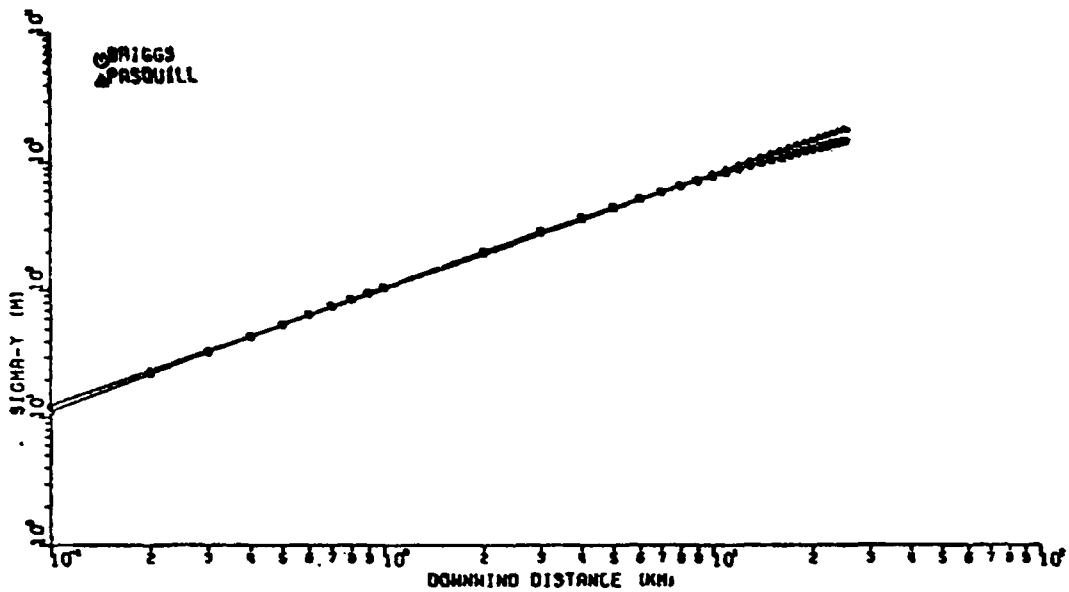


Figure 15c. Horizontal dispersion coefficient as a function of downwind distance for Stability Class C according to Briggs and Pasquill-Turner

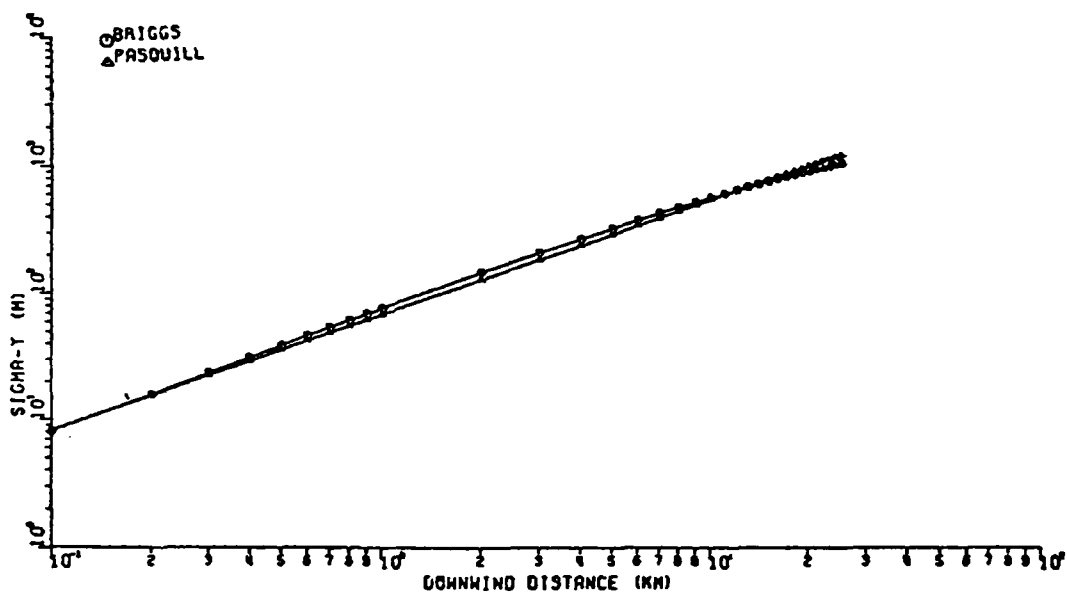


Figure 15d. Horizontal dispersion coefficient as a function of downwind distance for Stability Class D according to Briggs and Pasquill-Turner

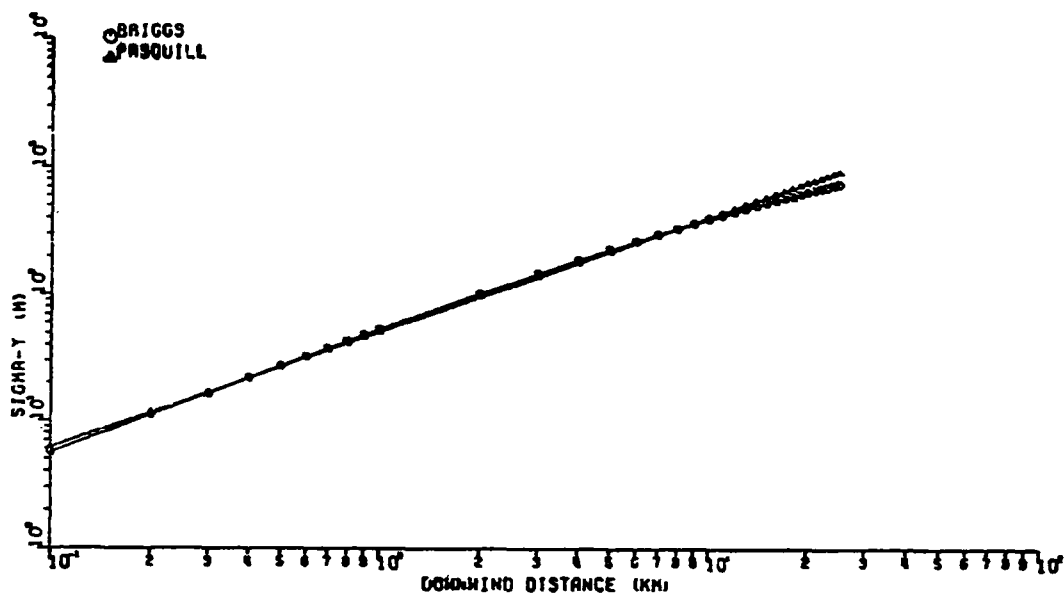


Figure 15e. Horizontal dispersion coefficient as a function of downwind distance for Stability Class E according to Briggs and Pasquill-Turner

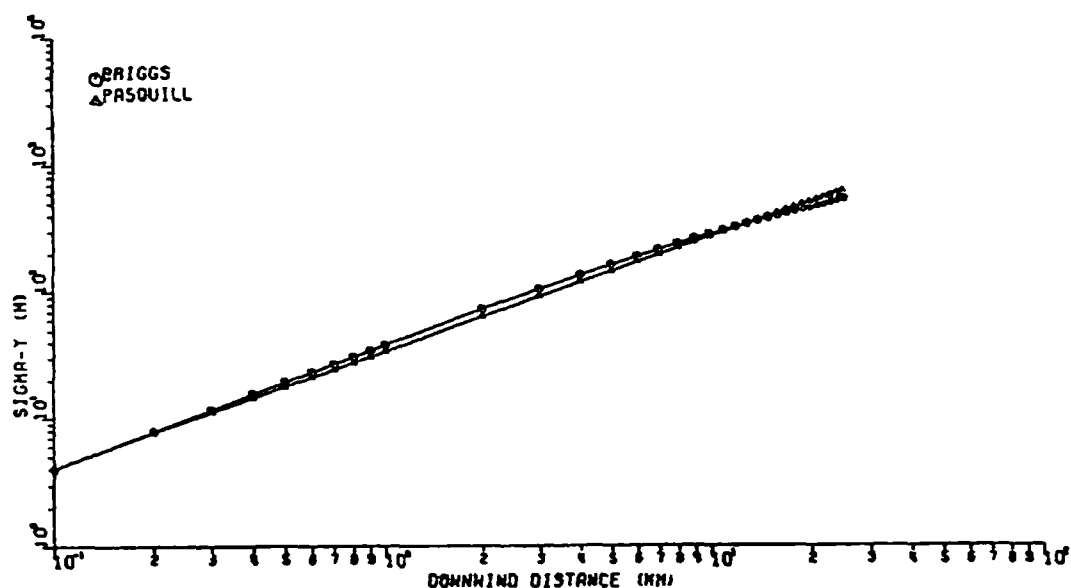


Figure 15f. Horizontal dispersion coefficient as a function of downwind distance for Stability Class F according to Briggs and Pasquill-Turner

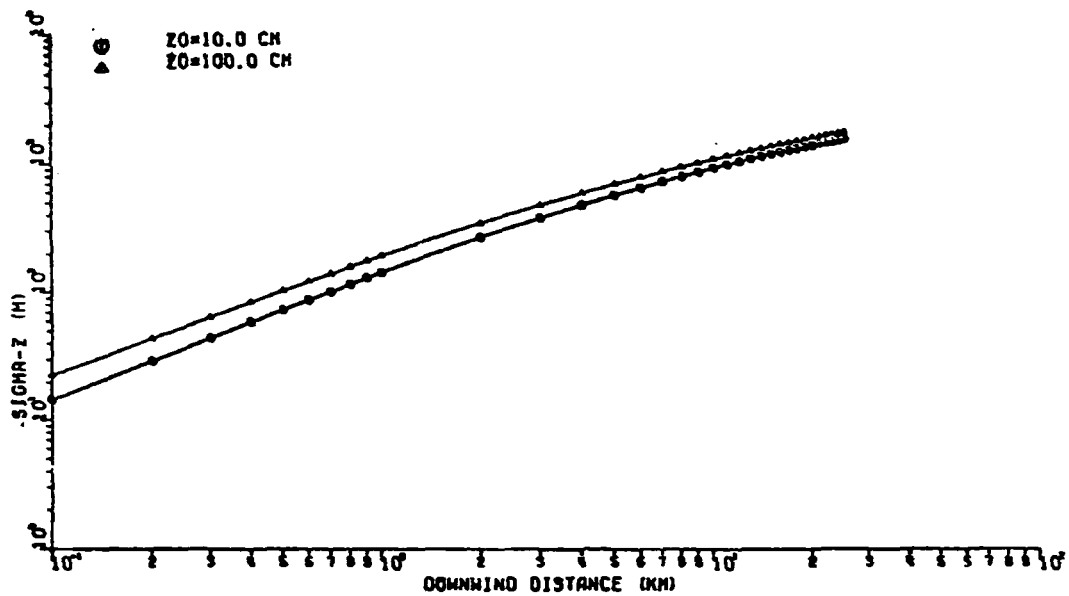


Figure 16a. Vertical dispersion coefficient as a function of downwind distance for Stability Class A and surface roughness of 10 cm and 100 cm according to F.B. Smith

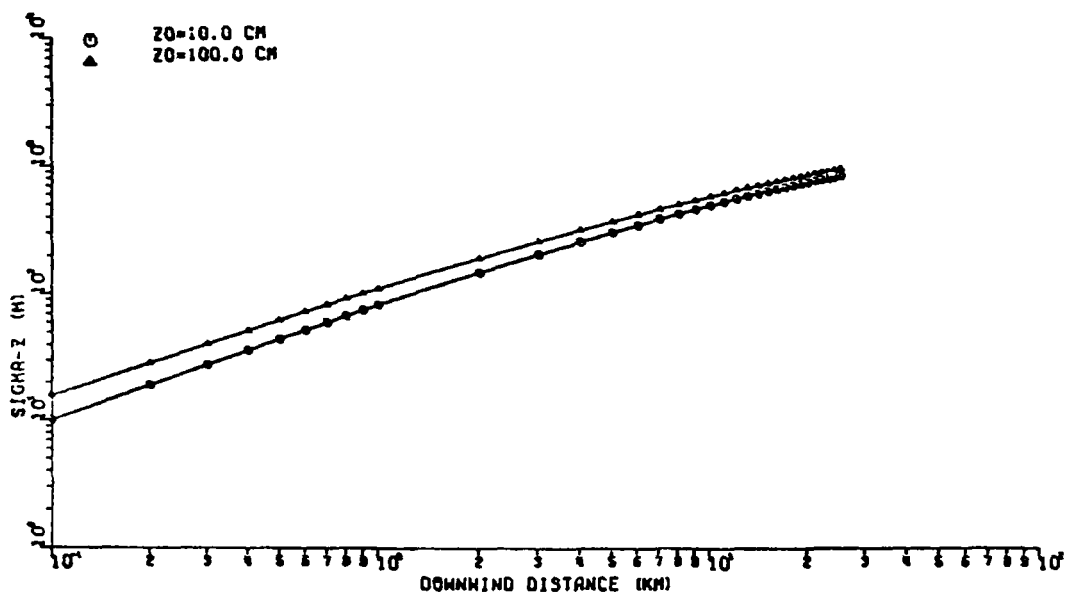


Figure 16b. Vertical dispersion coefficient as a function of downwind distance for Stability Class B and surface roughness of 10 cm and 100 cm according to F.B. Smith

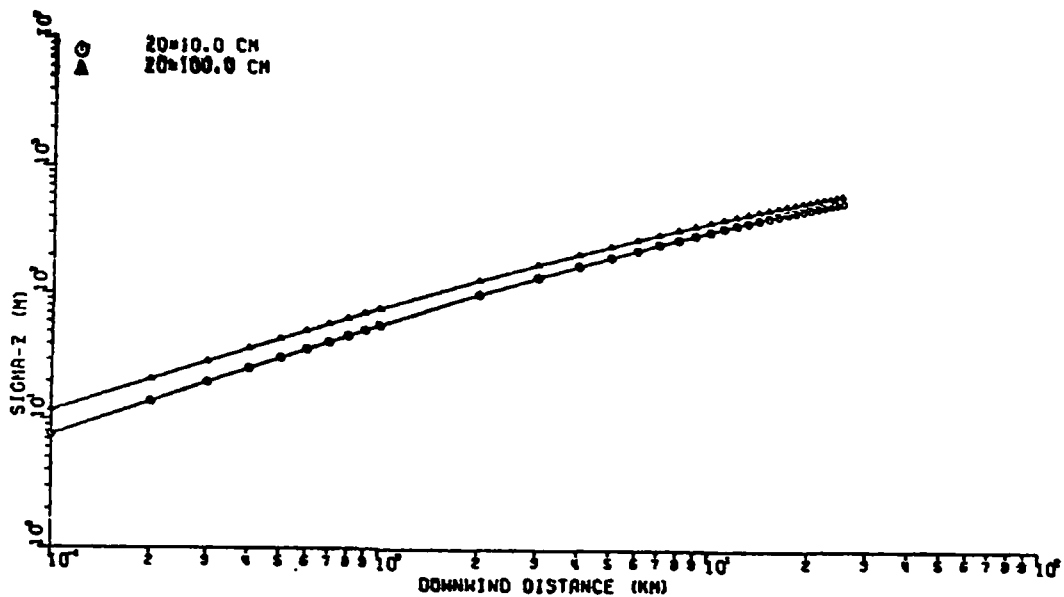


Figure 16c. Vertical dispersion coefficient as a function of downwind distance for Stability Class C and surface roughness of 10 cm and 100 cm according to F.B. Smith

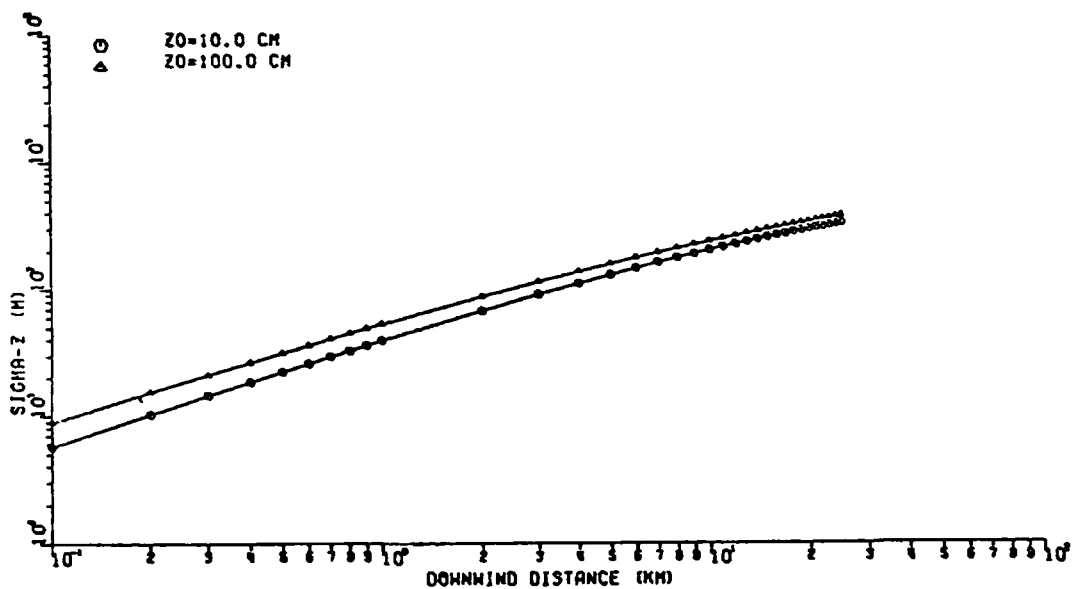


Figure 16d. Vertical dispersion coefficient as a function of downwind distance for Stability Class C and surface roughnesses of 10 cm and 100 cm according to F.B. Smith

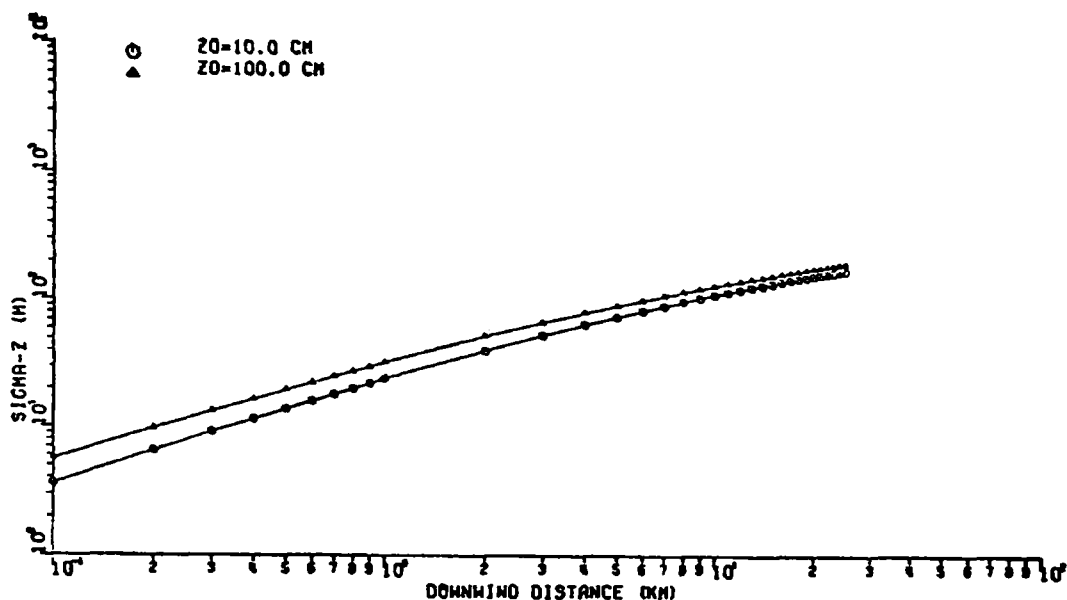


Figure 16e. Vertical dispersion coefficient as a function of downwind distance for Stability Class E and surface roughnesses of 10 cm and 100 cm according to F.B. Smith

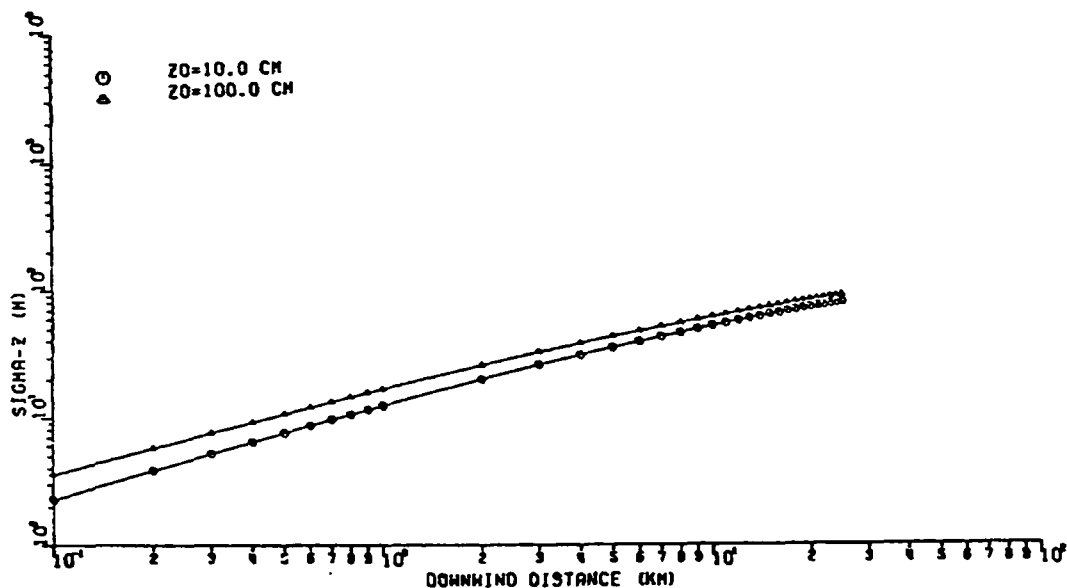


Figure 16f. Vertical dispersion coefficient as a function of downwind distance for Stability Class F and surface roughnesses of 10 cm and 100 cm according to F.B. Smith

DISCUSSION OF THE PROCEDURE FOR VARYING THE PLUME RISE

Another objective of this study was to determine whether the requirement of a constant stack gas exit velocity was adversely affecting the model predictions. To study the effect of a variable stack gas exit velocity, the hourly velocity was calculated according to the following expression:

$$w_h = w_a \frac{f_h}{f_a}$$

where w_a = stack gas exit velocity obtained from form FPC-67

f_h = hourly fuel consumption for all boilers feeding
into the stack

f_a = average hourly fuel consumption for all boilers
feeding into the stack

SECTION III

SITE AND DATA BASE DESCRIPTIONS FOR MODEL IMPROVEMENT STUDY

In this section we shall describe the site characteristics, SO₂ monitoring program and meteorological data base for the two power plants included in the model improvement study. Each topic will be covered on a plant-by-plant basis. Much of this material has already been covered in three previous EPA reports but is presented again for the sake of completeness. Also the description of the meteorological data base is somewhat different for this study since for a large number of cases local wind speed and wind direction data were used for model input as well as for background subtraction.

At the outset of this study we planned to include the J.M. Stuart Plant in our test of the Smith-Singer Dispersion Coefficients, but we subsequently found that the angular resolution of the local wind direction data did not permit a meaningful comparison between measurements and model predictions. The Philo Power Plant was also excluded from our analysis of model improvements due to the complications of terrain mentioned in Section I. The tests of different dispersion calculation methods were, therefore, carried out for the Canal and Muskingum River Plants.

CANAL PLANT

Site Description

The Canal Plant is located on the south side of the Cape Cod Canal about 1.6 kilometers from the entrance on Cape Cod Bay (Figure 17) The

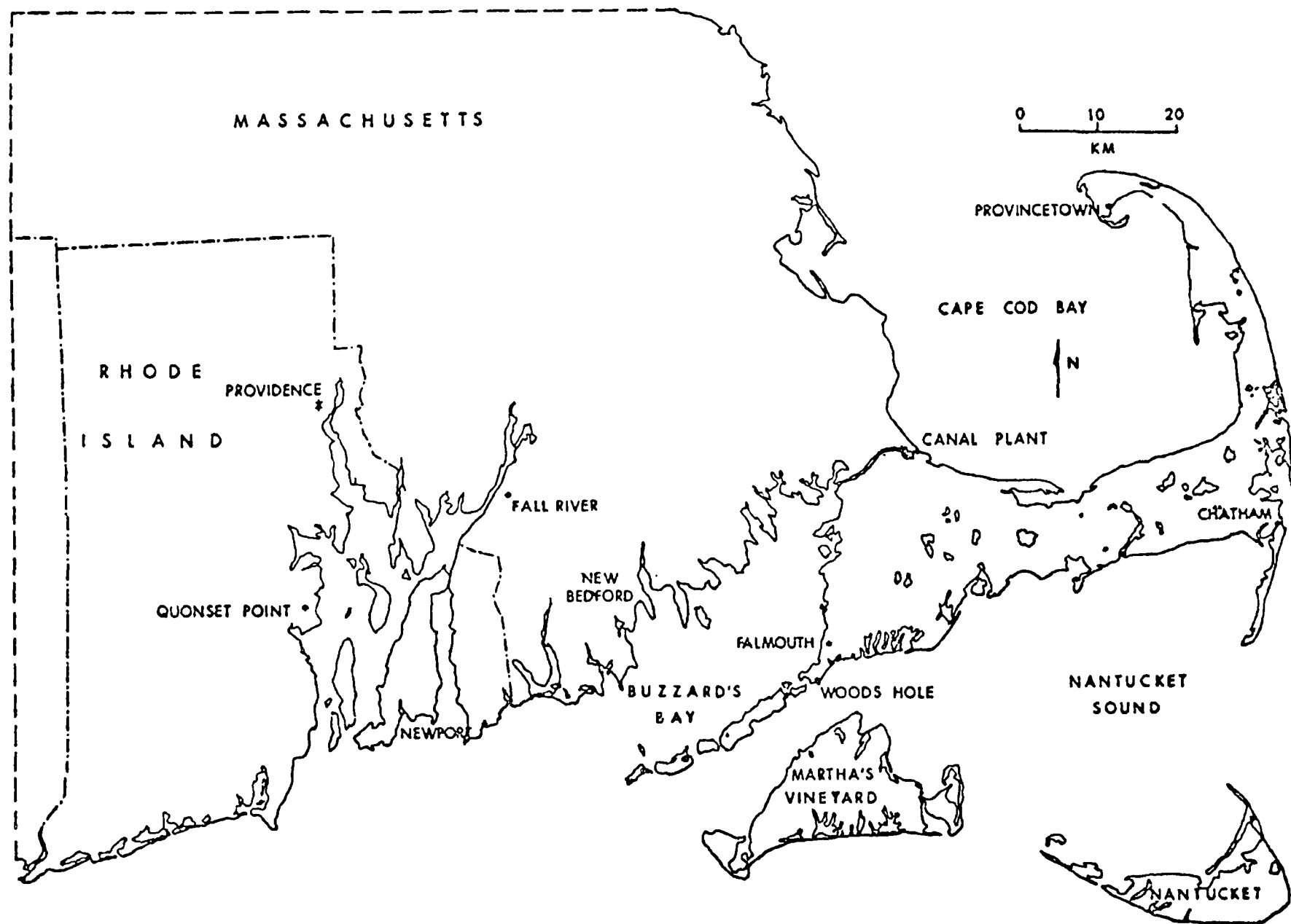


Figure 17. Map of eastern Massachusetts and Rhode Island showing locations of the Canal Plant. Meteorological observations were used from Quonset Point Naval Air Station and Chatham

surrounding terrain is gently rolling with elevations generally below 60 meters above mean sea level. The highest elevations in the area are about 90 meters above sea level in the western end of the Cape. Most of the area is covered with scrub pine forests and low vegetation.

Data for the study were collected in 1971. During that year, the plant consisted of a single oil-fired unit with a generating capacity of 560 megawatts. The top of the stack was about 91 meters above grade and 5.6 meters in diameter. The main power plant structure to the north of the stack totally enclosed the turbine generator and boiler. The roofs of the turbine and boiler rooms were about 30 meters and 59 meters above grade respectively. Stack and boiler data are given in Table 8. The 1971 monthly percent sulfur content of the fuel used at the Canal Plant is given in Table 9.

Table 8. PLANT CHARACTERISTICS

Characteristic	Plant		
	Canal	Muskingum	
	Stack 1	Stack 1	Stack 2
Stack height, m	91	251	251
Diameter, m	5.6	7.6	6.7
Velocity, m/sec	-	28.5	24.8
Temperature, °F	-	430	425
Number of boilers per stack	1	4	1
Maximum generating capacity per stack, MW	560	876	591
Average per stack, MW	-	748	487
Plant total, MW	560	1467	
Plant average, MW	-	1235	

Table 9. MONTHLY PERCENT
SULFUR CONTENT
OF FUEL

Month	Canal	Muskingum
January	2.0	4.9
February	1.9	4.8
March	2.1	4.8
April	1.9	4.5
May	2.1	4.7
June	2.1	5.0
July	2.1	4.7
August	2.0	4.7
September	1.9	4.3
October	0.9	4.6
November	1.0	4.5
December	0.9	4.4

Overview of Canal Plant Monitoring Program

SO₂ concentrations are measured at four locations on a continuous basis with Ultragas SO₂ Analyzers manufactured in Germany by H. Wosthoff. These instruments measure sulfur dioxide by the increase in conductivity of an acidified hydrogen peroxide solution and have a full scale reading of 0.4 ppm. The instruments do not conform to the reference method for sulfur dioxide or to any of the specified equivalent methods. They have, however, been extensively studied and one comparison noted a correlation coefficient of 0.99 with the West-Gaeke method. The instruments used provide a continuous real-time chart trace and a tape printout giving date, time, and average concentration over consecutive 30 minutes. The sensitivity of the instrument in combination with the chart recorder is approximately 0.005 ppm. The locations of the SO₂ monitors with respect to the Canal Plant are given in Figure 18 and Table 10.

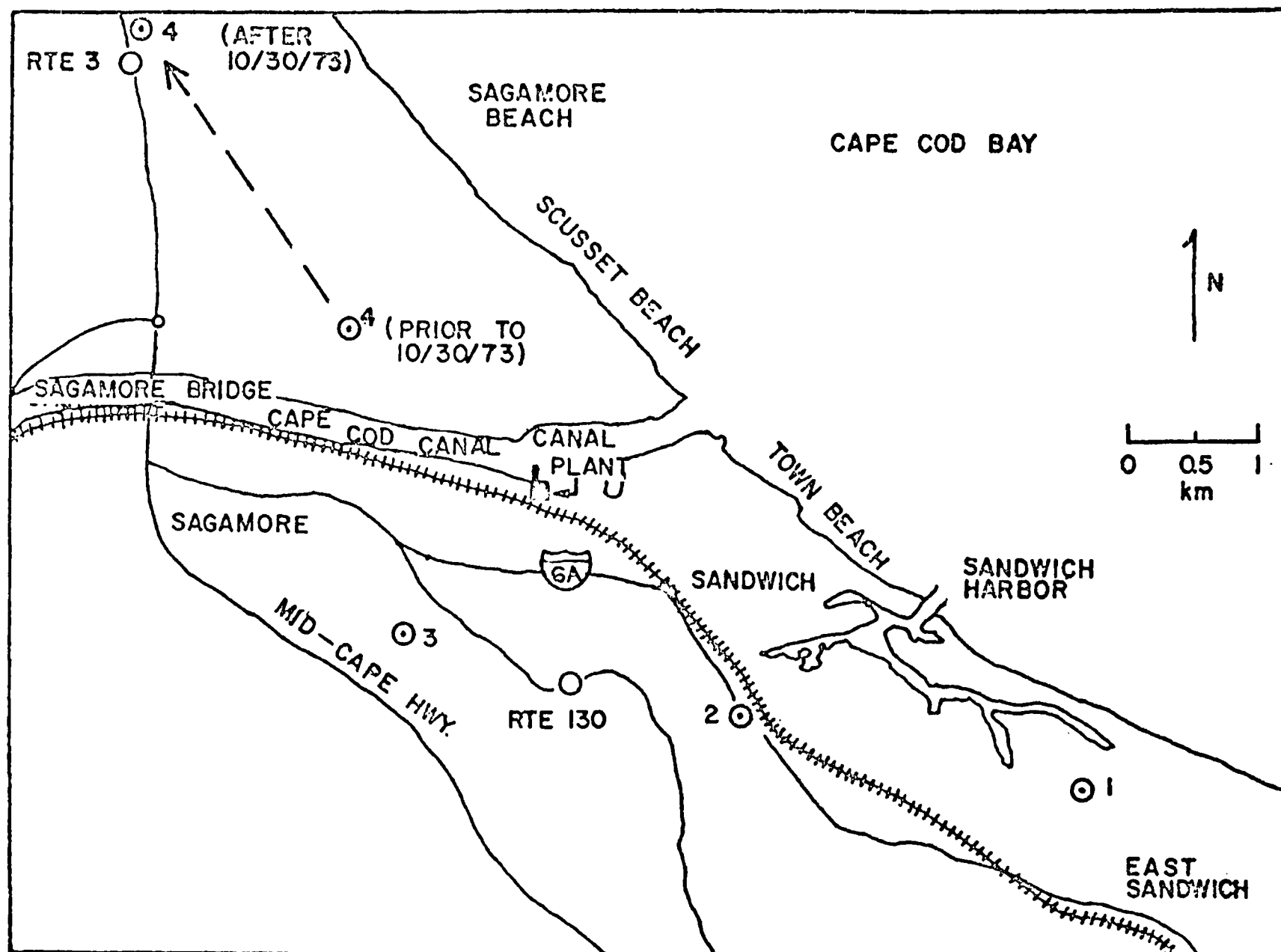


Figure 18. Sketch of the Canal Plant area showing the locations of the four automatic SO_2 stations by the symbol \odot

Table 10. SULFUR DIOXIDE MONITORING STATIONS FOR THE CANAL AND MUSKINGUM PLANTS

Plant	Station		Distance, km	Heading, degrees	Elevation above stack base, m
	No.	Name			
Canal	1		4.7	119	10
	2		2.3	138	4
	3		1.4	224	40
	4		2.0	312	20
Muskingum	1	Beverly	5.3	140	64
	2	Hackney	4.3	40	82
	3	Rich Valley	8.3	35	101
	4	Caldwell	19.6	35	128
	-	Top of stacks	-	-	251

Meteorological Data for Canal Plant

Bendix-Friez Aerovanes are used to provide local wind speed and direction data. Through July 1971, the principal source of wind data was the Aerovane mounted on a 12.2 meter mast located on the 58.8 meter boiler-room roof. Since July 1971, wind data are obtained from a second Aerovane installed on a 44 meter tower near the top of Telegraph Hill approximately 5 kilometers south-southeast of the Canal Plant. This hourly wind data was used to define upwind receptor locations for calculation of hourly background concentrations. A station was considered to be a background receptor if it were located outside the boundaries of a 90 degree sector centered about the wind flow vector. The concentrations for these background stations are then averaged and subtracted from the hourly concentrations at all stations. Any resultant negative concentrations were set equal to zero. The on-site wind speed, wind direction and ambient temperature data were also input to the Single Source Model after proper conversion to a wind measurement height of 7 meters. These stability dependent wind speed corrections, which were discussed in Section II, were based upon hourly atmospheric stabilities derived from a Single

Source Model Preprocessor run using surface meteorological data for 1971 collected at Quonset Point Naval Air Station. Hourly mixing heights for 1971 were based upon surface data from Quonset Point, Rhode Island and upper air observations taken at Chatham, Massachusetts. In this way a "hybrid" Preprocessor output file was generated containing on-site wind speed, wind direction and temperature measurements and nonlocal stability and mixing height assignments.

MUSKINGUM PLANT

Site Description

The Muskingum Plant is located in southeastern Ohio on the Muskingum River about 6 kilometers northwest of the town of Beverly. Figure 19 indicates the location of the plant, the SO₂ monitoring sites, and the surrounding towns. The plant is in the river valley about 500 meters from the valley walls which rise about 75 meters above the valley floor. The two 251 meter stacks are 640 meters apart and extend about 185 meters above the surrounding terrain. During 1973 the plant consisted of five coal-fired units with a total capacity of 1467 megawatts (Table 8). Percent sulfur content of the fuel for 1973 is given in Table 9.

Overview of the Muskingum Monitoring Program

Four sulfur dioxide monitoring stations make up the monitoring network (Figure 19 and Table 10). Data were available from all stations for January 1 to November 21, 1973. During the entire year of 1973, Station 1 missed 57 days and the other three stations missed approximately 41 days. Instruments at Muskingum were Leeds & Northrup Company, Catalog No. 7860-SW, Aeroscan Air Quality Monitors. The sample was obtained by passing ambient air taken from 5 feet above ground level, through an absorption column along with an absorption solution. The sample analysis method was by electrolytic conductivity. Data were taken continuously and listed every hour. Each instrument was automatically zeroed once a day

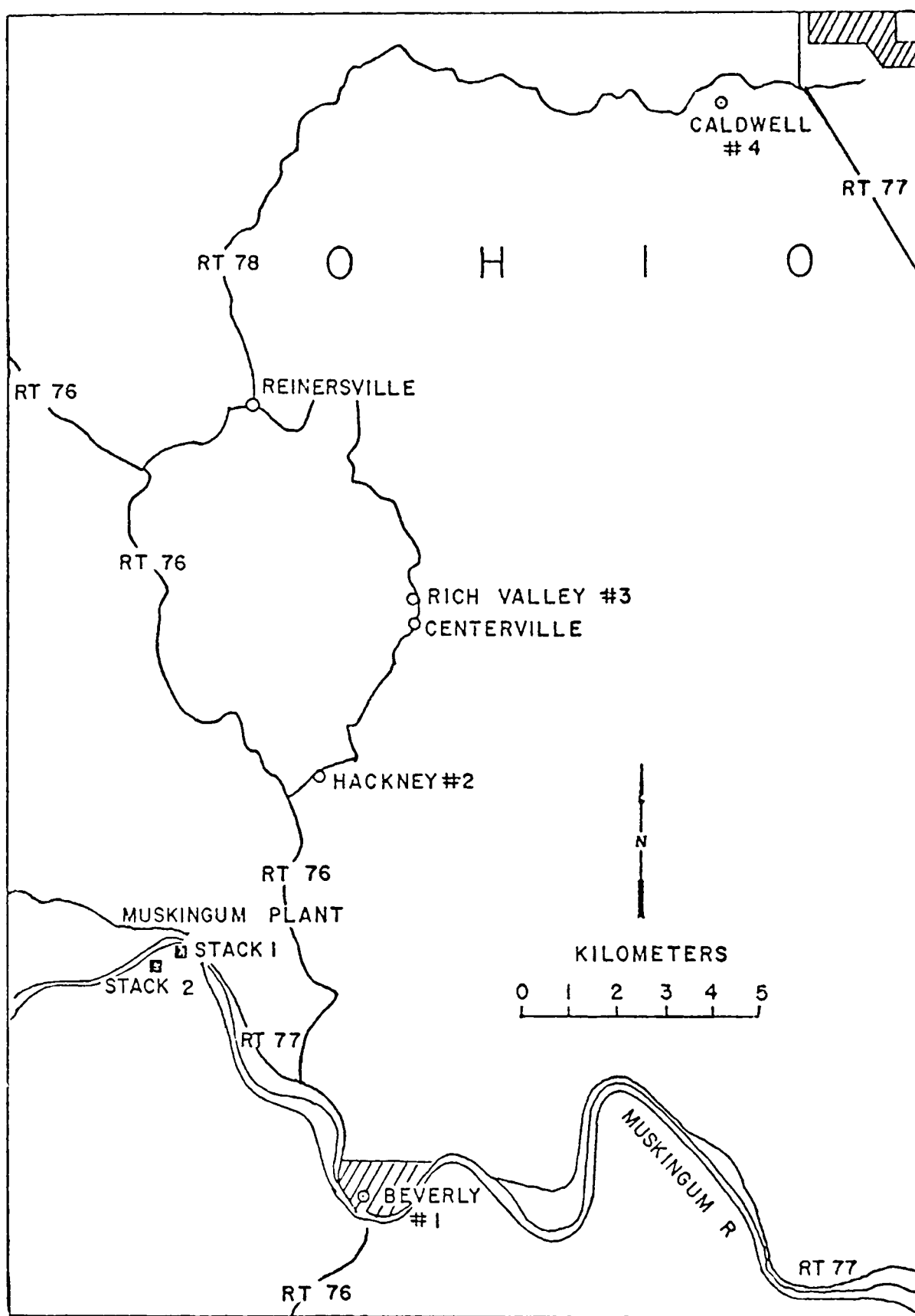


Figure 19. Sketch of the Muskingum Plant area showing locations of four automatic SO₂ monitoring stations

The manufacturer's performance accuracy specifications for this instrument are as follows. In a typical ambient atmosphere which includes the normal interfering gases, this instrument has:

- Zero drift = 2 percent of full scale per week
- Sensitivity drift < 1 percent of full scale per week
- Reproducibility < 1 percent of full scale
- Sensitivity = 0.01 ppm
- Recorder error < 0.5 percent of full scale
- Range = approximately 0 - 1 ppm

Meteorological Data for Muskingum Plant

There were two wind monitoring stations at the Muskingum Plant consisting of Bendix-Friez Aerovane wind speed and direction devices. One station was located 24 meters above ground at Beverly, and the other at the Hackney SO₂ monitoring station, where the wind monitors were also located 24 meters above ground. The data from Hackney was used in this study, as it was higher and common to more stations, but Beverly data was used when the Hackney system was not recording. On-site hourly wind direction data were used for the assignment of upwind receptor locations whose concentrations were then used in a background subtraction procedure identical to the one described for the Canal plant. Wind speeds at these two meteorological stations were adjusted to the 7 meter height by means of the stability dependent power law currently used in the Single Source Model and hourly stabilities based upon Huntington, West Virginia surface observations for 1973. A hybrid Preprocessor output file was then constructed using local wind direction and adjusted windspeed data in conjunction with ambient temperature and stability assignments from Huntington. Hourly mixing heights were based upon surface and upper air data both collected at Huntington. This particular combination of on-site and nonlocal meteorological data were used to test the Pasquill-Turner, Gifford-Briggs and F. B. Smith dispersion parameters at the Muskingum Plant. In our test of the F. B. Smith fractional stabilities, the Preprocessor program was modified to include a two-digit stability class.

For the test of the Smith-Singer dispersion coefficients, local values for wind direction, wind speed (uncorrected) and Smith-Singer stability class (1 - 4) were used with nonlocal values for ambient temperature and mixing height as input to the Single Source Model modified to include Smith-Singer dispersion coefficients and wind speed profile parameters.

SECTION IV

MODEL VALIDATION RESULTS

Our test of the different sets of dispersion coefficients described in Section II was based upon a comparison of cumulative frequency distributions of measured and predicted 1-hour SO_2 concentrations at the Canal and Muskingum Power Plants. The combinations of power plant sites, stability assignment algorithms, dispersion coefficients and meteorological data bases are presented in Table 11 along with the results of each model validation test and the numbers of the figures illustrating each test. The results of the variable plume rise test are also included in Table 11.

The overall conclusion which may be reached based upon the examination of results presented in Table 11 is that the Pasquill-Turner dispersion coefficients and stability assignment algorithm yield the best agreement of the methods tested with the possible exception of the Gifford-Briggs dispersion coefficients. Although in the case of the Canal Plant the Gifford-Briggs coefficients gave slightly better agreement with measurements than the Pasquill-Turner curves, the two schemes worked equally well for the Muskingum Plant. This outcome is reasonable in light of the close agreement between the σ_z curves, except for stability A, for the two different methods (see Figures 15a through 15f).

The most surprising result of the study was the failure of the Smith-Singer dispersion coefficients and stability assignment scheme to predict the upper percentile or even the shape of the 1-hour concentration frequency distribution (see Figures 24a through 24e). One would expect these

coefficients to be better suited to the prediction of short-term SO_2 levels in the vicinity of power plants since they were based upon experiments involving the release of tracers from elevated sources. Since the criteria for selection of a given curve is somewhat qualitative, this may be a factor in their not giving a proper frequency distribution shape.

Since a major portion of our validation efforts involved the testing of the fractional stability scheme of F.B. Smith, we shall examine a number of reasons behind the resulting poor agreement with measured 1-hour SO_2 concentrations. Our first test of the F.B. Smith method involved point stability assignments according to Pasquill-Turner and the corresponding F.B. Smith Dispersion curves for stabilities A through F. Again it should be pointed out that only the F.B. Smith σ_z estimates were used in this model validation test. The Pasquill-Turner σ_y curves (see Figure 2), were used in conjunction with the F.B. Smith σ_z 's. The results of this first validation exercise (Run Nos. 6 and 8) indicated a strong tendency for the F.B. Smith point stability dispersion curves to underpredict 1-hour SO_2 concentrations both for the Canal and Muskingum Plants. The only exception to this finding was the result for Muskingum Station 4 which showed slightly improved agreement over the Pasquill-Turner results (Run No. 2). The reason that this station did not follow the trend toward underprediction may have been its location 19.6 km from the plant. At this distance the largest concentrations should be observed during the more stable conditions (D, E and F). For these stability classes the F.B. Smith σ_z curves do not differ radically from the Pasquill-Turner curves (see Figures 14c through 14e). When a surface roughness of 100 cm, rather than the standard value of 10 cm, was used for calculation of the F.B. Smith σ_z curves the agreement between predicted and measured 1-hour SO_2 concentrations was somewhat better for the Canal Plant (Run No. 7), although the assumption of 100 cm surface roughness for this site is clearly unrealistic.

To determine whether the F. B. Smith vertical dispersion curves would yield better results when used in conjunction with the F. B. Smith stabilities described in Section II, we rewrote the Single Source Model

Preprocessor Program to include the fractional stability calculation techniques discussed in Section II. Minor modifications to the Single Source Model itself were made to provide for the interpolation of σ_y and σ_z values based upon the fractional stability assignment. A comparison of the Pasquill-Turner and F. B. Smith stabilities for three days in 1973 based upon Huntington, West Virginia surface meteorological data is presented in Table 12. Local windspeed and wind direction data for the Muskingum River Plant were not used in this calculation since the windspeed measurements were obtained at 24.2 m above the ground and not the 10 m height required for use in the F. B. Smith calculation. A stability dependent power law correction could have been used to convert the windspeed to the 10 m height except that the purpose of the exercise was to actually determine the fractional stability. Although the 7 m measurement height assumed for Huntington, W. Va. was not equal to the required 10 m height, the resulting error is negligible.

When the fractional stability versions of the Preprocessor Program and the Single Source Model were run for the Muskingum Plant, an overprediction occurred for stations 2, 3 and 4, compared to the substantial underprediction which resulted when the F. B. Smith dispersion coefficients were used in conjunction with the Pasquill-Turner point stability assignments. The generally lower stability index assignments based upon the F. B. Smith method have overcompensated for the smaller F. B. Smith σ_z values for the A, B and C stability classes. An example of the generally lower stability indices calculated by the F. B. Smith method is shown in Table 12. For the midday hours during the summer months the F. B. Smith stability indices can be more than one stability class lower than the corresponding Pasquill-Turner values.

The final objective of the model improvement study was to determine whether the incorporation of an hourly variation of a stack gas exit velocity, which is directly proportional to the fuel consumption rate, would improve model agreement with measured 1-hour SO_2 concentrations. The procedure for calculating hourly exit velocities was described in

Section II. Although the tests for the Canal and Muskingum River Plants showed no such improvement, the inclusion of a variable buoyancy flux in the model still may be desirable in the case of highly variable fuel consumption.

Table 11. DESCRIPTION OF MODEL VALIDATION RUNS AND RESULTS

Run number	Site	Stability assignment method	Dispersion calculation method	Meteorological data base	Special modifications	Validation results	Figure numbers
1	Canal	Pasquill-Turner	Pasquill-Turner	Local wind speed, wind direction and ambient temperature. Stabilities based upon surface data from Quonset Point, R.I. mixing heights from Chatham, Mass.		All stations underpredicted for the entire distribution, especially stations 2 and 4. Closest agreement for station 3, which had the highest elevation above the stack base. Except for station 3, the calculated distribution shapes are also in error.	20
2	Muskingum	Pasquill-Turner	Pasquill-Turner	Local wind speed and wind direction. Ambient temperature and stability from Huntington, W. Va. surface data. Mixing heights from Huntington, W. Va.		Good agreement for the higher end of the distributions except for station 2 which is overpredicted.	21
3	Canal	Pasquill-Turner	Gifford-Briggs	Same as Run No. 1		In comparison with Run No. 1 slightly better agreement for all stations was obtained, but the entire frequency distribution is still underpredicted.	22
4	Muskingum	Pasquill-Turner	Gifford-Briggs	Same as Run No. 2		Slightly better agreement for stations 2 and 4 when compared with Run No. 1.	23
5	Muskingum	Smith-Singer	Smith-Singer	Local wind speed, wind direction and atmospheric stability. Ambient temperature and mixing height from Huntington, W. Va.	Smith-Singer windspeed profile incorporated. For stabilities B2, B1 and C, plume rise is calculated according to Equation (2) in Section II. For stability D, Equation (3) is used.	Considerable overprediction for stations 1, 2 and 3 even at the lower end of the distributions. Calculated distribution shapes are unrealistic.	24
6	Canal	Pasquill-Turner	F. B. Smith	Same as Run No. 1	Surface roughness of 10 cm.	All stations underpredicted for the entire distribution. For stations 2, 3 and 4 agreement considerably worse than for Run No. 1.	25
7	Canal	Pasquill-Turner	F. B. Smith	Same as Run No. 1	Surface roughness of 100 cm.	Improved agreement over Run No. 6.	26

Table 11 (continued). DESCRIPTION OF MODEL VALIDATION RUNS AND RESULTS

Run number	Site	Stability assignment method	Dispersion calculation method	Meteorological data base	Special modifications	Validation results	Figure numbers
8	Muskingum	Pasquill-Turner	F. B. Smith	Same as Run No. 2		Only station 4 at 19.6 km from the plant showed better agreement than for Run No. 2. All other stations were considerably underpredicted for the entire distribution.	27
9	Muskingum	F. B. Smith (fractional stabilities)	F. B. Smith (values for σ_y and σ_z interpolated based upon fractional stability assignment).	1973 Huntington, W. Va. surface and upper air data.	Preprocessor and single Source Model modified to include a two-digit stability index and provide for the interpolation of dispersion coefficients.	All stations except 1 were overpredicted at the high end of the distributions.	28
10	Muskingum	Same as Run No. 2	Same as Run No. 2	Same as Run No. 2	Variable buoyancy flux.	No improvement over Run No. 2.	29
11	Canal	Same as Run No. 1	Same as Run No. 1	Same as Run No. 1	Variable buoyancy flux.	No improvement over Run No. 2	30

Table 12. COMPARISON OF PASQUILL-TURNER
(P-T) AND F. B. SMITH (F.B.S.)
STABILITY ASSIGNMENTS FOR THREE
DAYS OF HUNTINGTON, W. VA. 1973
SURFACE METEOROLOGICAL DATA^a

Day No. 64		Day No. 134		Day No. 323	
P-T	F.B.S.	P-T	F.B.S.	P-T	F.B.S.
6	4.1	4	4.1	4	4.1
5	4.1	4	4.1	4	4.0
5	4.1	7	4.1	4	4.1
6	4.1	4	4.1	4	4.1
5	4.1	4	4.1	4	4.1
5	4.1	6	4.8	4	4.1
6	4.1	4	4.1	5	4.5
4	4.1	3	3.1	4	4.1
4	4.1	3	2.2	4	4.1
4	3.8	2	1.7	4	4.1
3	2.6	2	1.4	4	3.6
3	2.8	3	1.5	4	3.4
4	3.4	3	1.8	4	3.4
4	2.4	4	2.7	4	3.3
4	2.4	4	2.9	4	3.4
4	2.5	4	2.4	4	3.8
4	2.6	3	3.0	4	4.3
3	3.3	3	2.5	3	7.0
4	6.2	3	3.3	6	6.9
5	5.0	4	7.0	6	7.0
7	7.0	6	7.0	7	7.0
7	7.0	6	7.0	7	7.0
7	7.0	6	7.0	6	7.0
7	7.0	4	4.3	7	7.0

^aA value of 0.4 has been added to the F.B. Smith stabilities so that they could be compared with the Pasquill-Turner values.

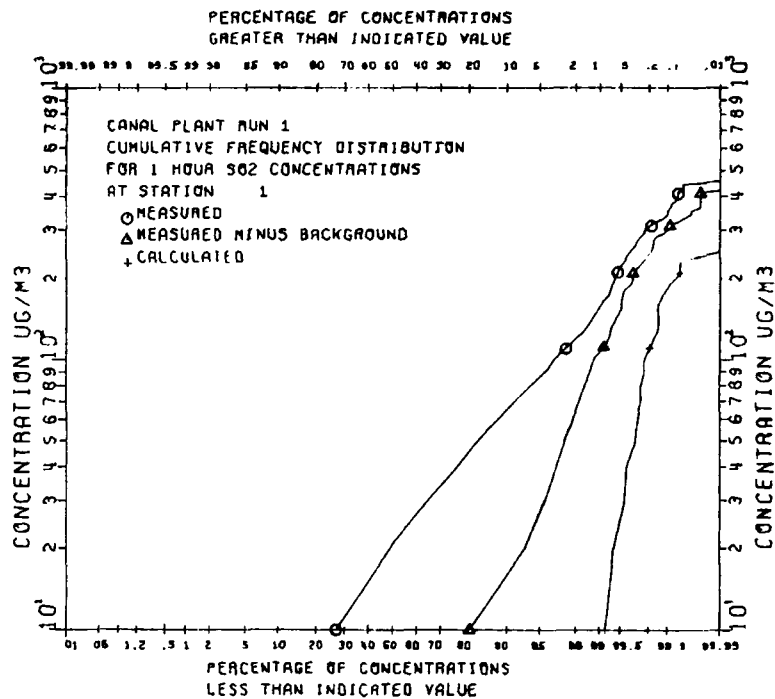


Figure 20a. Model validation Run No. 1. Pasquill-Turner stability assignment and dispersion calculation method. Measured and predicted cumulative frequency distributions of 1-hour SO₂ concentrations for Canal Plant Station 1

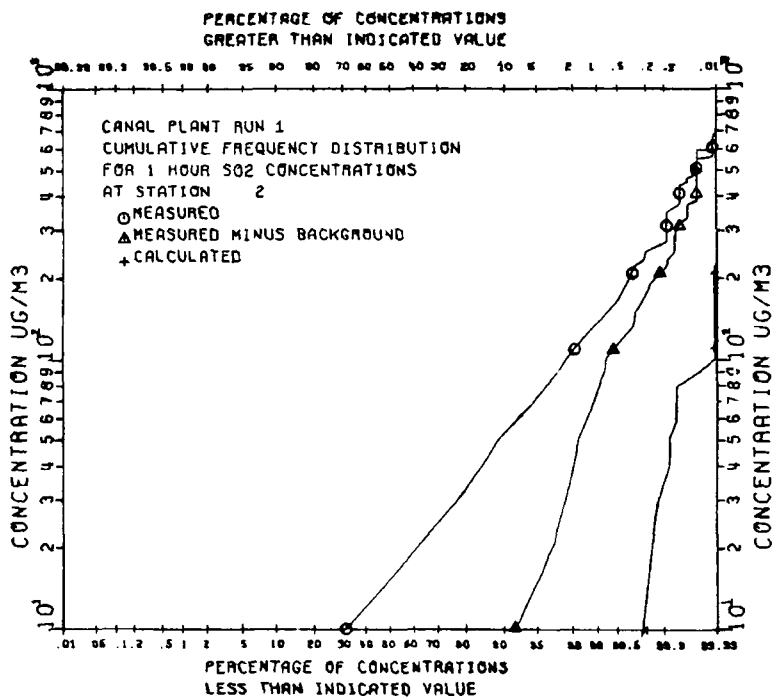


Figure 20b. Model validation Run No. 1. Pasquill-Turner stability assignment and dispersion calculation method. Measured and predicted cumulative frequency distributions of hourly SO₂ concentrations for Canal Plant Station 2

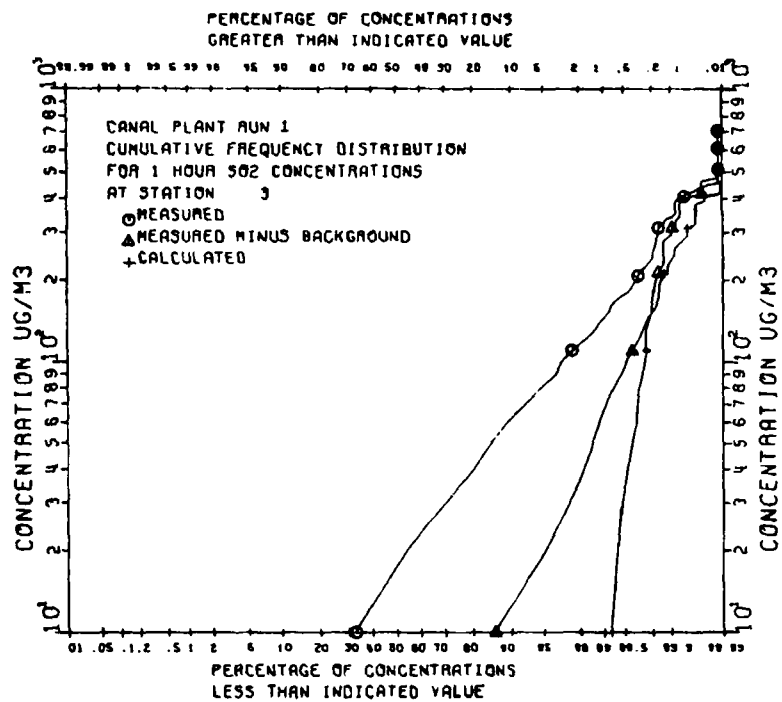


Figure 20c. Model validation Run No. 2. Pasquill-Turner stability assignment and dispersion calculation method. Measured and predicted cumulative frequency distributions of 1-hour SO₂ concentrations for Canal Plant Station 3

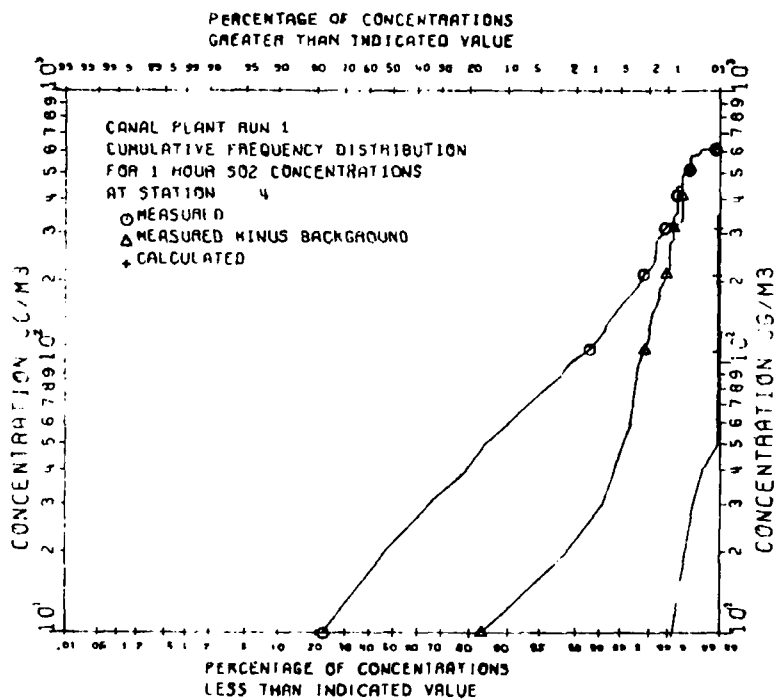


Figure 20d. Model validation Run No. 1. Pasquill-Turner stability assignment and dispersion calculation method. Measured and predicted cumulative frequency distributions of 1-hour SO₂ concentrations for Canal Plant Station 4

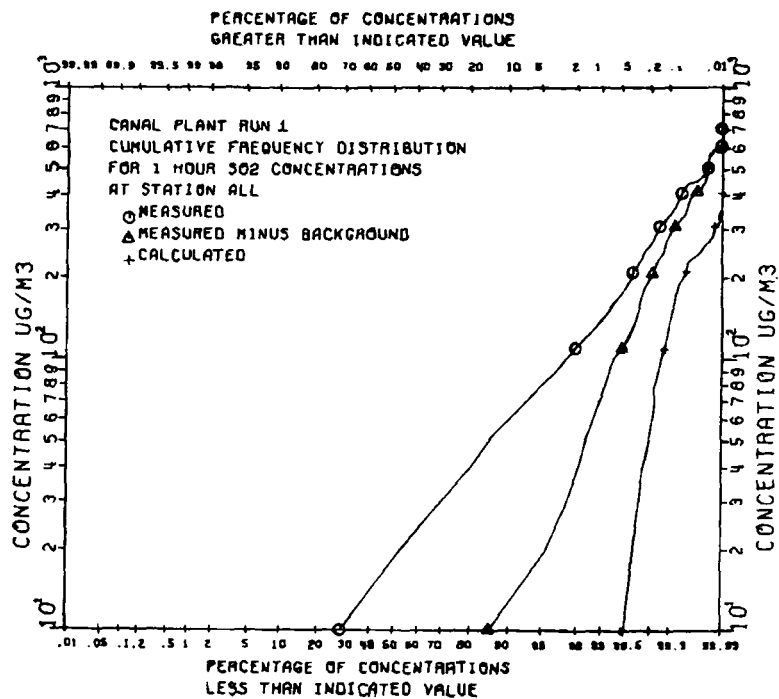


Figure 20e. Model validation Run No. 1. Pasquill-Turner stability assignment and dispersion calculation method. Measured and predicted cumulative frequency distributions of 1-hour SO₂ concentrations for Canal Plant for all stations

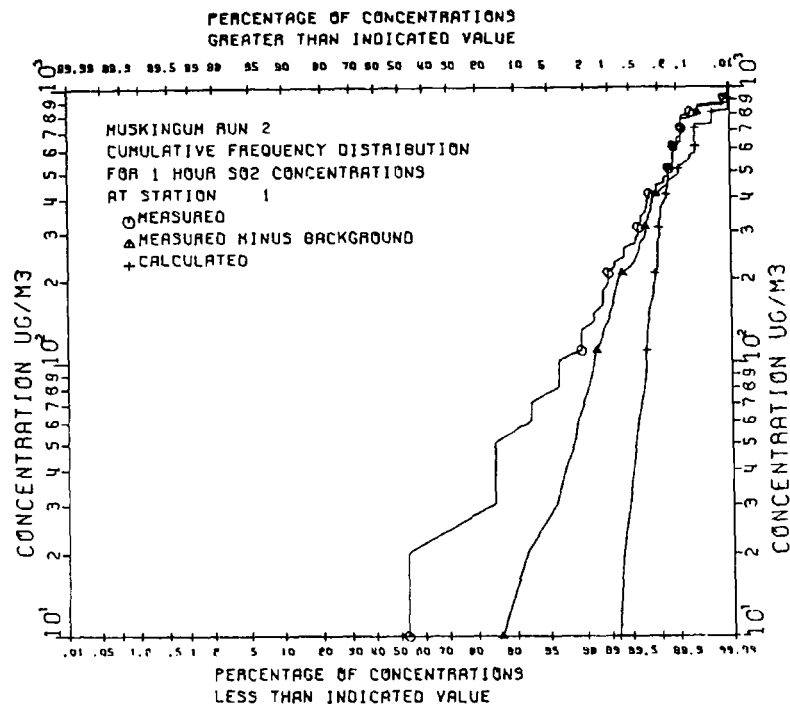


Figure 21a. Model validation Run No. 2. Pasquill-Turner stability assignment and dispersion calculation method. Measured and predicted cumulative frequency distributions of 1-hour SO₂ concentrations for Muskingum Plant Station 1

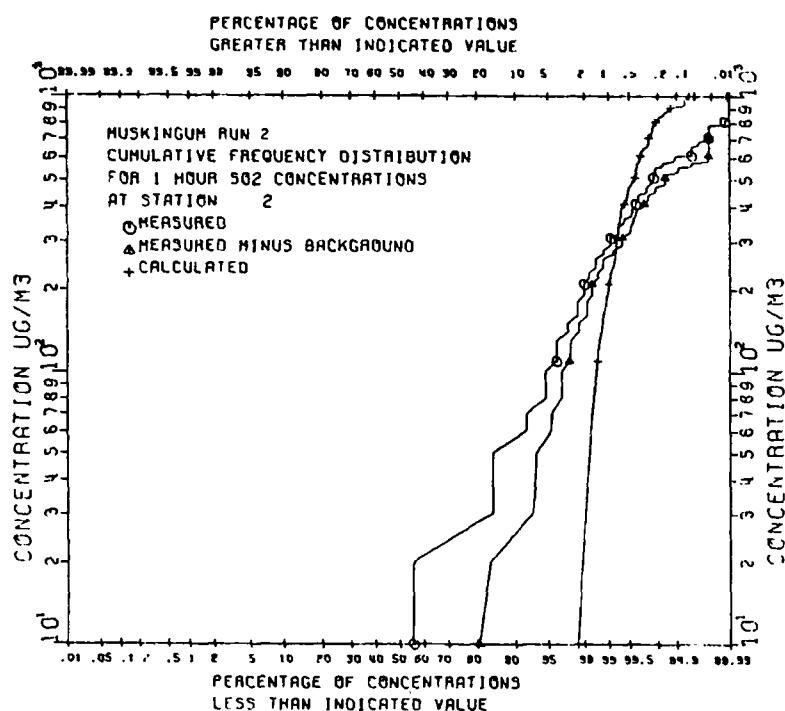


Figure 21b. Model validation Run No. 2. Pasquill-Turner stability assignment and dispersion calculation method. Measured and predicted cumulative frequency distributions of 1-hour SO₂ concentrations for Muskingum Plant Station 3

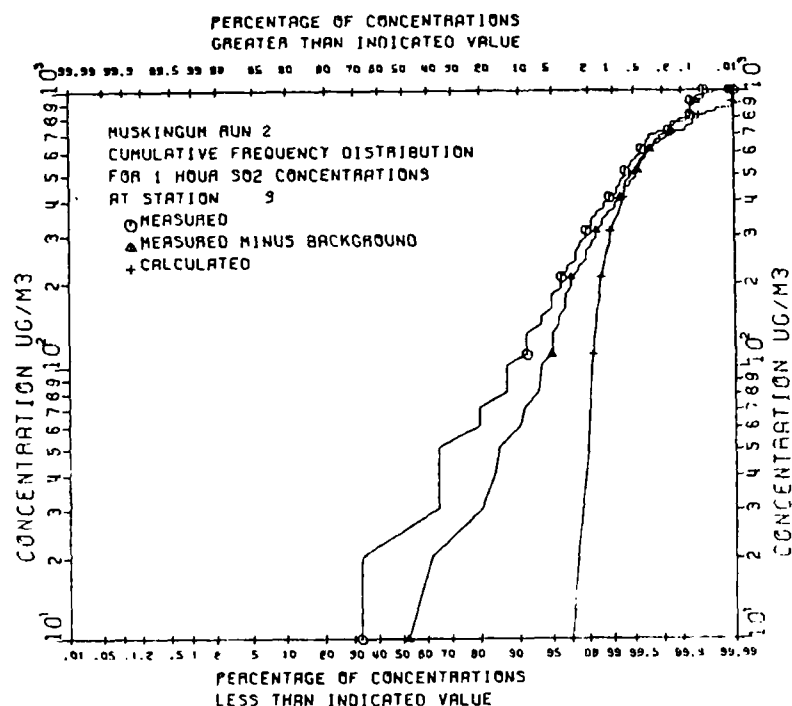


Figure 21c. Model validation Run No. 2. Pasquill-Turner stability assignment and dispersion calculation method. Measured and predicted cumulative frequency distributions of 1-hour SO₂ concentrations for Muskingum Plant Station 2

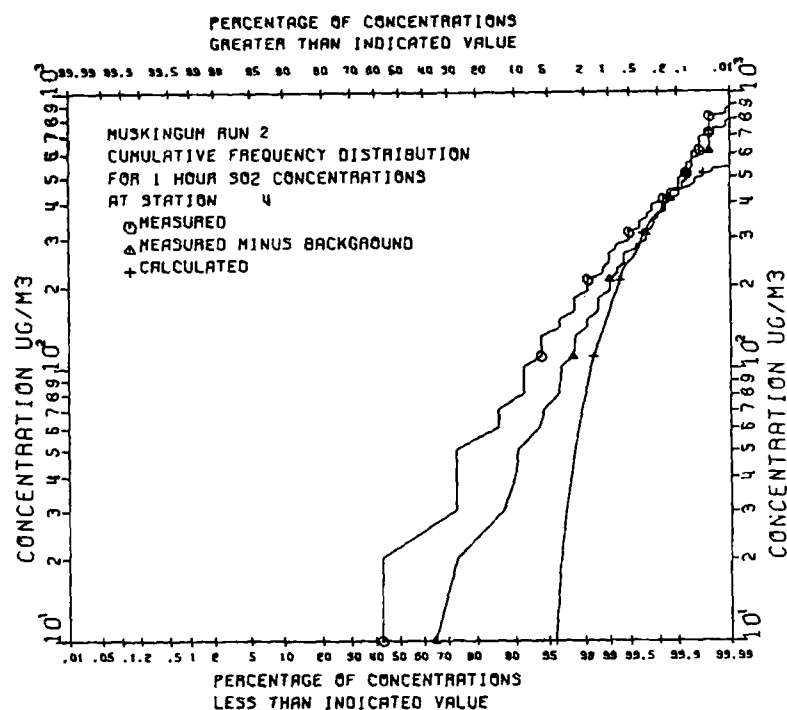


Figure 21d. Model validation Run No. 2. Pasquill-Turner stability assignment and dispersion calculation method. Measured and predicted cumulative frequency distributions of 1-hour SO₂ concentrations for Muskingum Plant Station 4

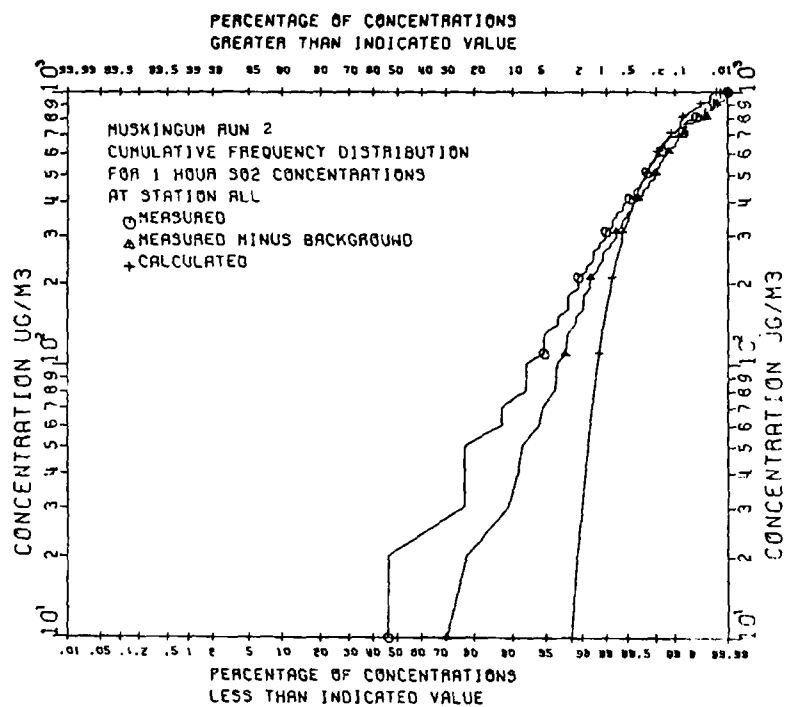


Figure 21e. Model validation Run No. 2. Pasquill-Turner stability assignment and dispersion calculation method. Measured and predicted cumulative frequency distributions of 1-hour SO₂ concentrations for Muskingum Plant for all stations

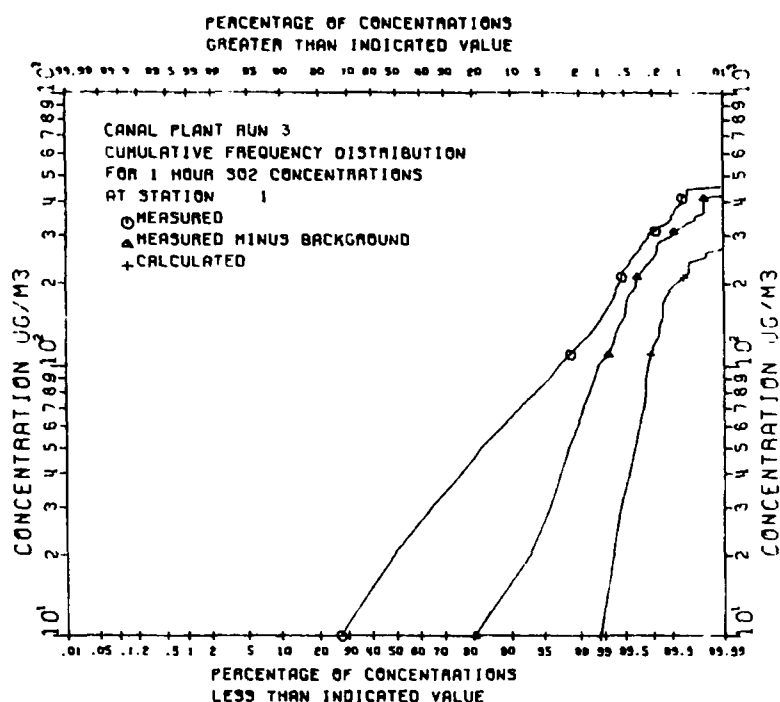


Figure 22a. Model validation Run No. 3. Pasquill-Turner stability assignment method and Gifford-Briggs dispersion calculation method. Measured and predicted cumulative frequency distributions of 1-hour SO₂ concentrations for Canal Plant Station 1

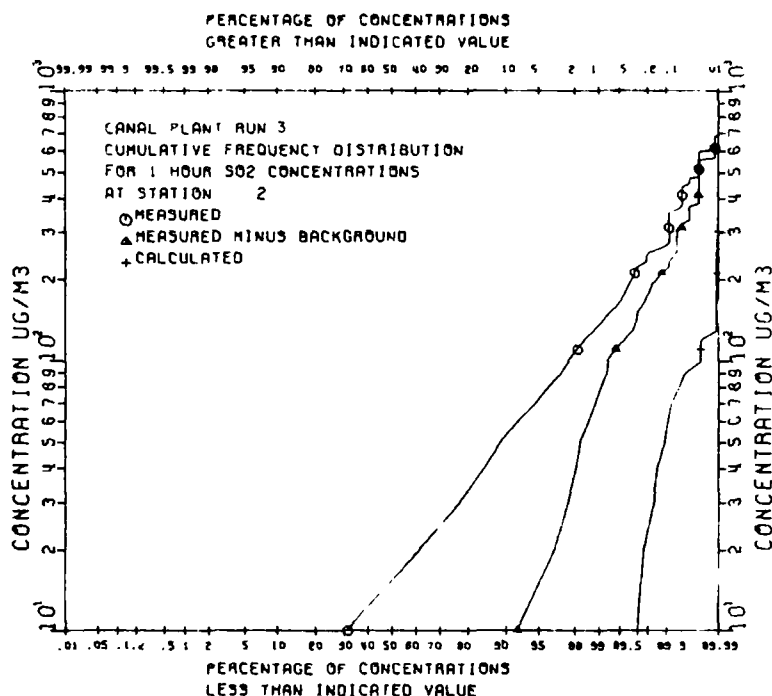


Figure 22b. Model validation Run No. 3. Pasquill-Turner stability assignment method and Gifford-Briggs dispersion calculation method. Measured and predicted cumulative frequency distributions of 1-hour SO₂ concentrations for Canal Plant Station 2

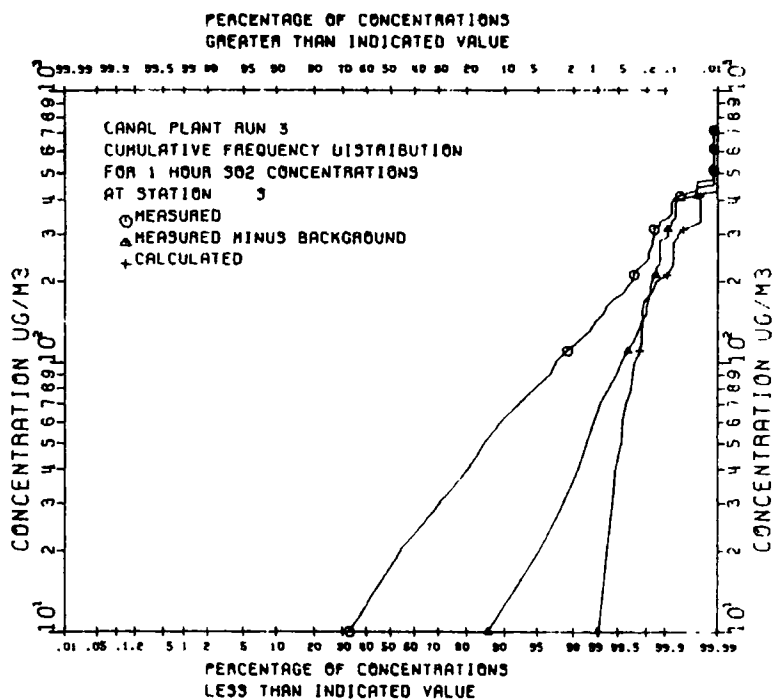


Figure 22c. Model validation Run No. 3. Pasquill-Turner stability assignment method and Gifford-Briggs dispersion calculation method. Measured and predicted cumulative frequency distributions of 1-hour SO₂ concentrations for Canal Plant Station 3

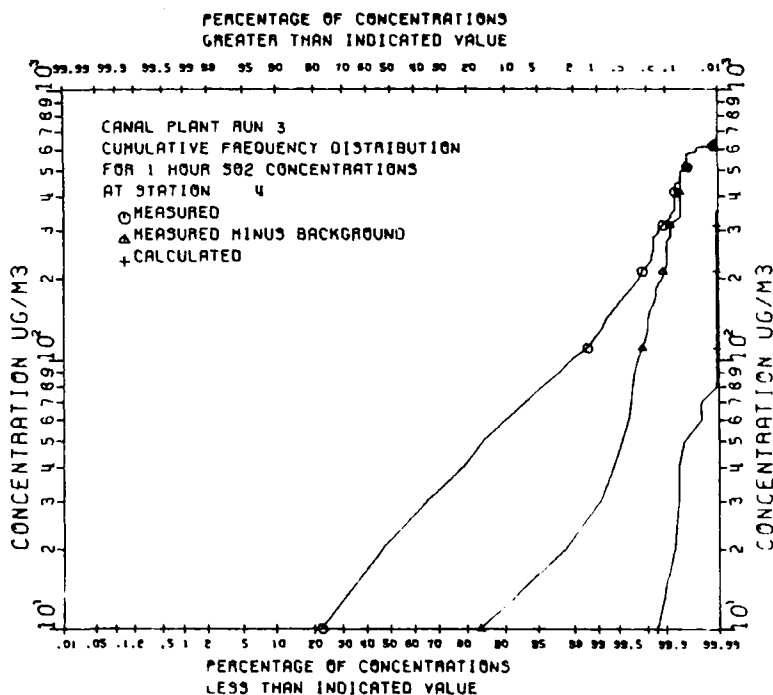


Figure 22d. Model validation Run No. 3. Pasquill-Turner stability assignment method and Gifford-Briggs dispersion calculation method. Measured and predicted cumulative frequency distributions of 1-hour SO₂ concentrations for Canal Plant Station 4

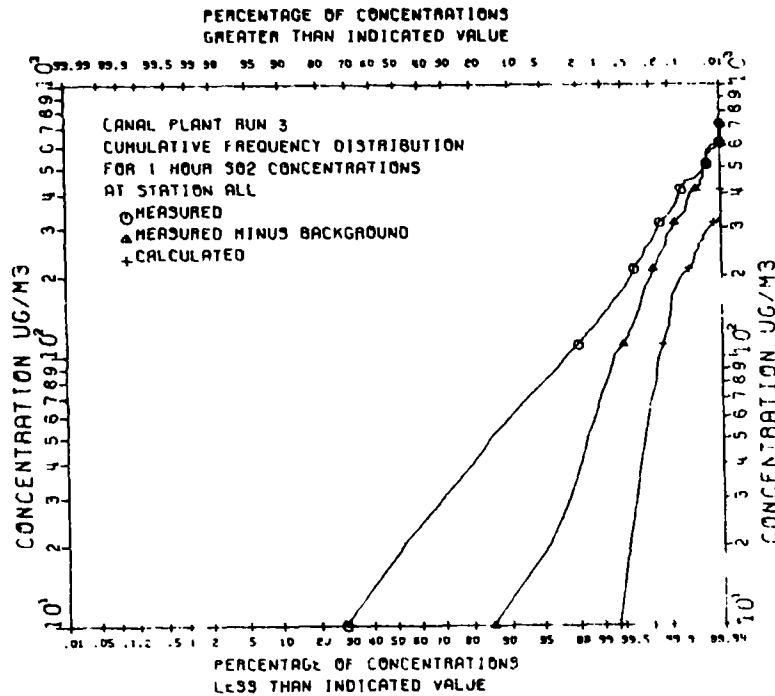


Figure 22e. Model validation Run No. 3. Pasquill-Turner stability assignment method and Gifford-Briggs dispersion calculation method. Measured and predicted cumulative frequency distributions of 1-hour SO₂ concentrations for Canal Plant for all stations

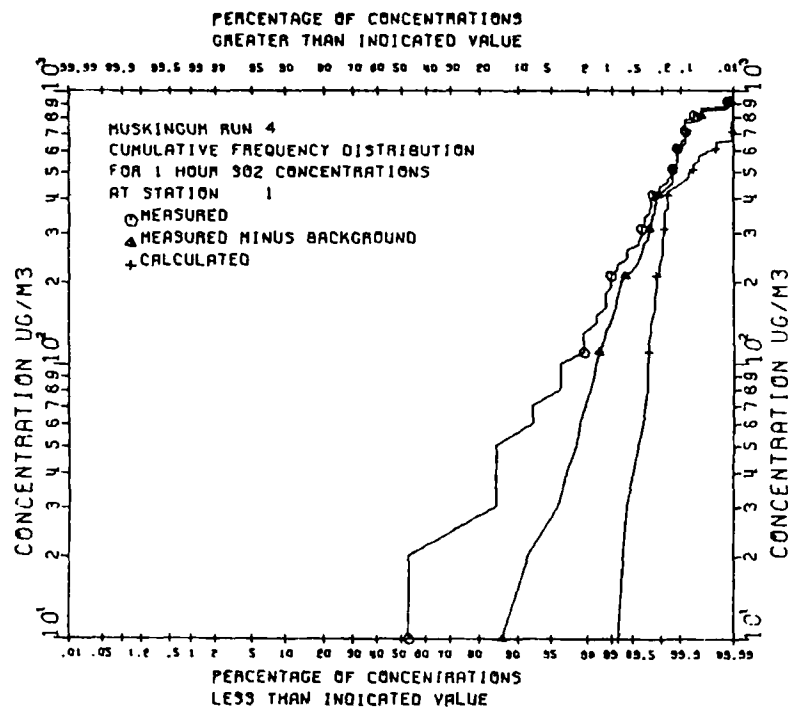


Figure 23a. Model validation Run No. 4. Pasquill-Turner stability assignment method and Gifford-Briggs dispersion calculation method. Measured and predicted cumulative frequency distributions of 1-hour SO₂ concentrations for Muskingum Plant Station 1

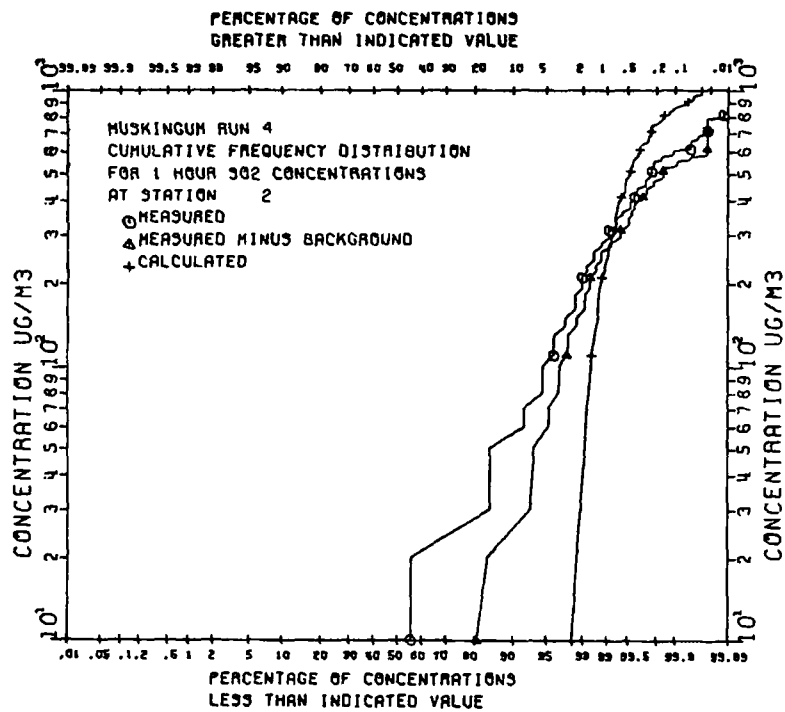


Figure 23b. Model validation Run No. 4. Pasquill-Turner stability assignment method and Gifford-Briggs dispersion calculation method. Measured and predicted cumulative frequency distributions of 1-hour SO₂ concentrations for Muskingum Plant Station 2

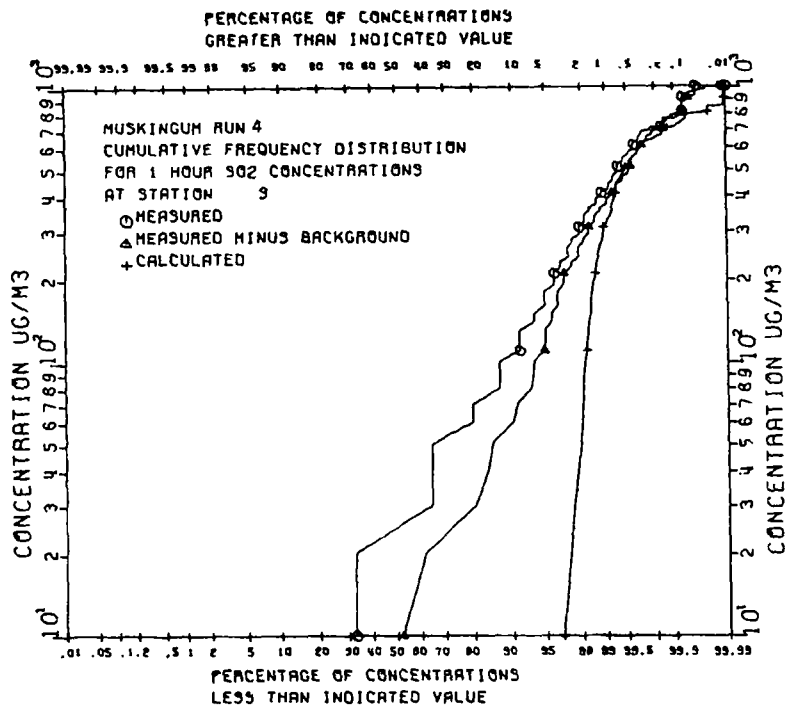


Figure 23c. Model validation Run No. 4. Pasquill-Turner stability assignment method and Gifford-Briggs dispersion calculation method. Measured and predicted cumulative frequency distributions of 1-hour SO₂ concentrations for Muskingum Plant Station 3

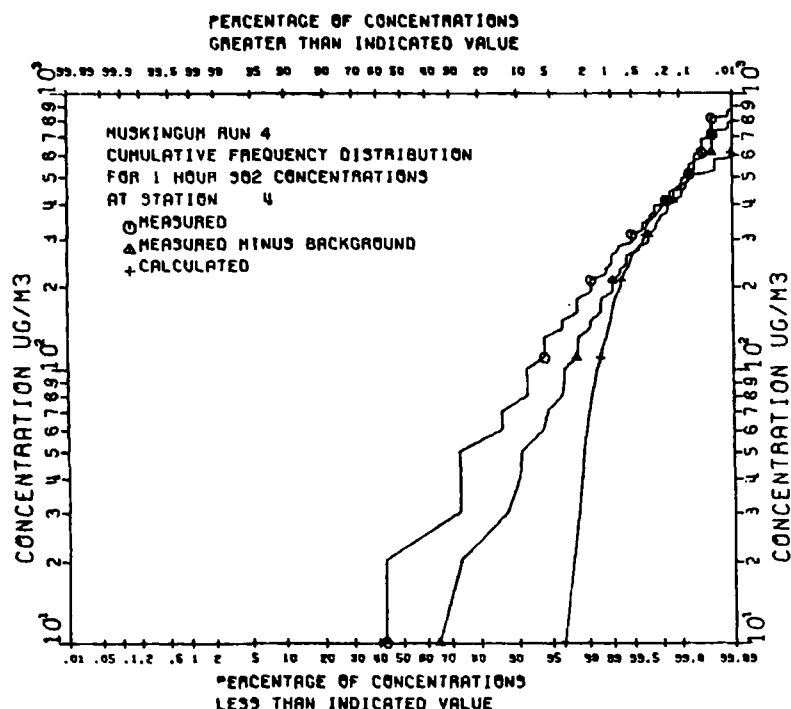


Figure 23d. Model validation Run No. 4. Pasquill-Turner stability assignment method and Gifford-Briggs dispersion calculation method. Measured and predicted cumulative frequency distributions of 1-hour SO₂ concentrations for Muskingum Plant Station 4

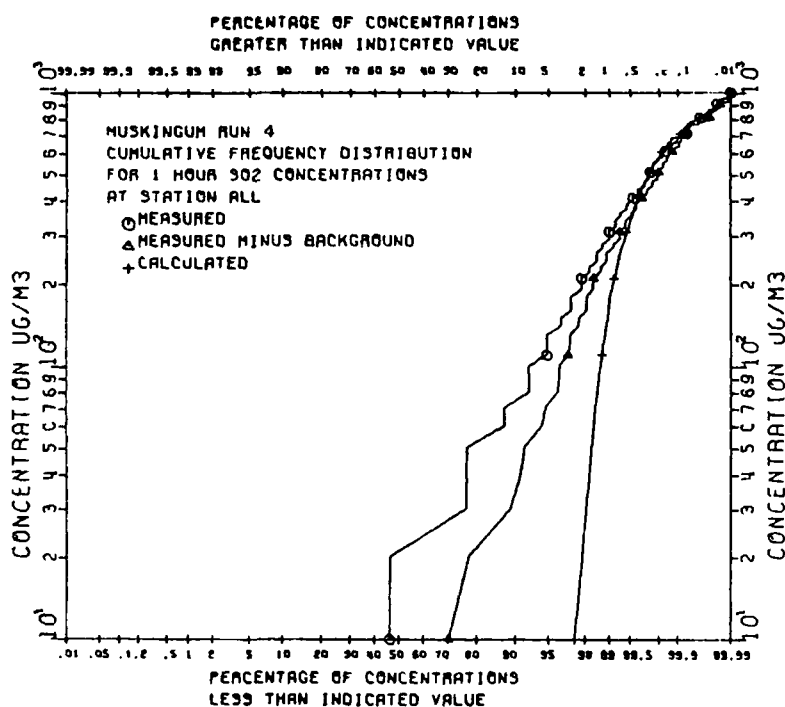


Figure 23e. Model validation Run No. 4. Pasquill-Turner stability assignment method and Gifford-Briggs dispersion calculation method. Measured and predicted cumulative frequency distributions of 1-hour SO₂ concentrations for Muskingum Plant for all stations

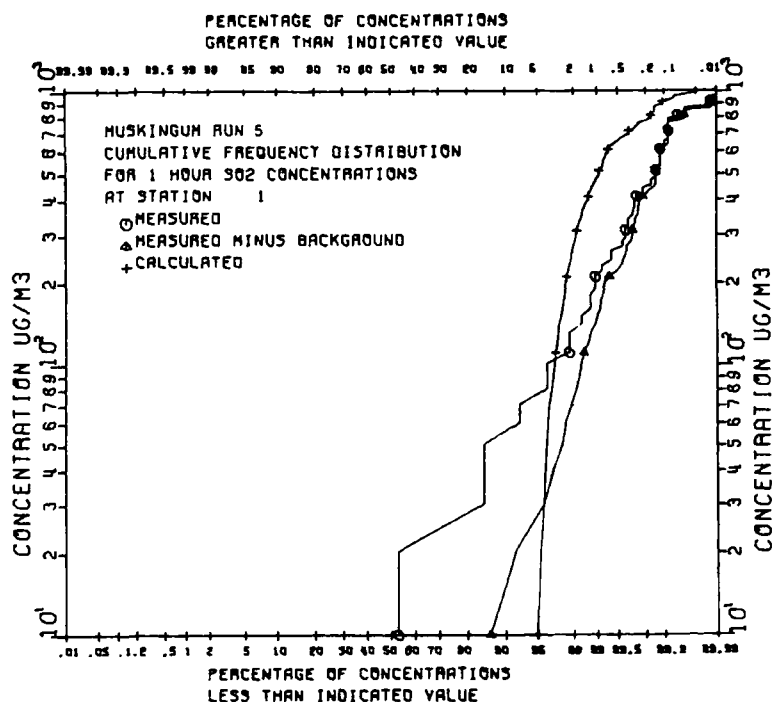


Figure 24a. Model validation Run No. 5. Smith-Singer stability assignment and dispersion calculation method. Measured and predicted cumulative frequency distributions of 1-hour SO₂ concentrations for Muskingum Plant Station 1

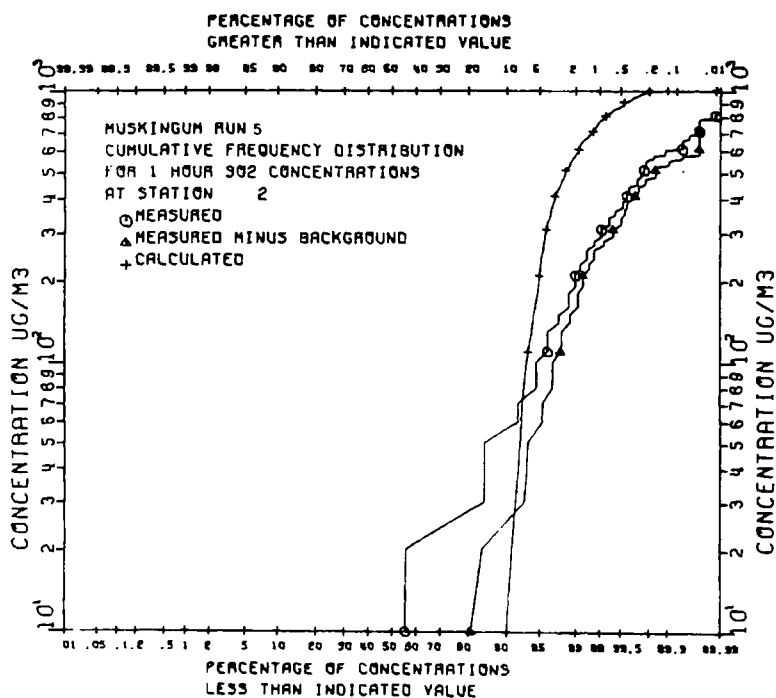


Figure 24b. Model validation Run No. 5. Smith-Singer stability assignment and dispersion calculation method. Measured and predicted cumulative frequency distributions of 1-hour SO₂ concentrations for Muskingum Plant Station 2

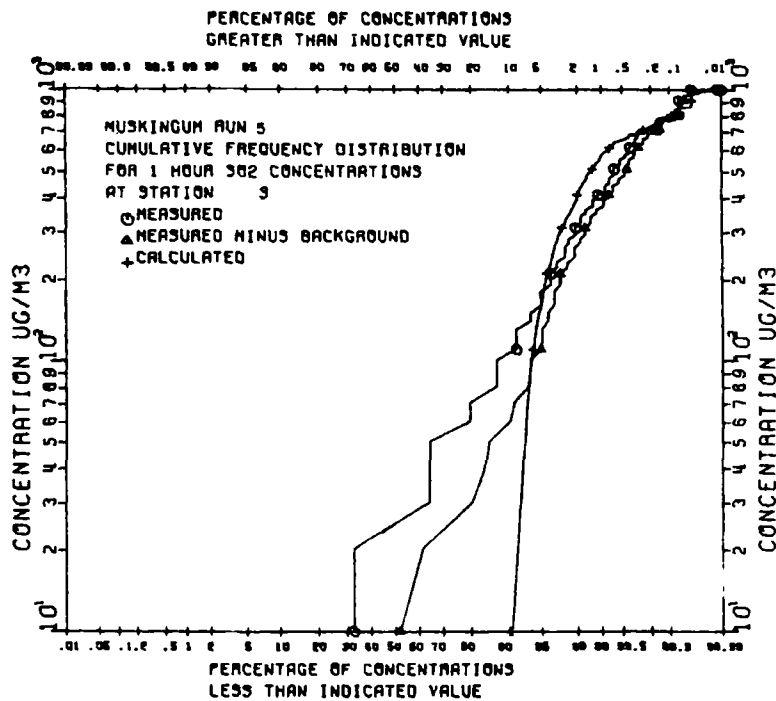


Figure 24c. Model validation Run No. 5. Smith-Singer stability assignment and dispersion calculation method. Measured and predicted cumulative frequency distributions of 1-hour SO₂ concentrations for Muskingum Plant Station 3

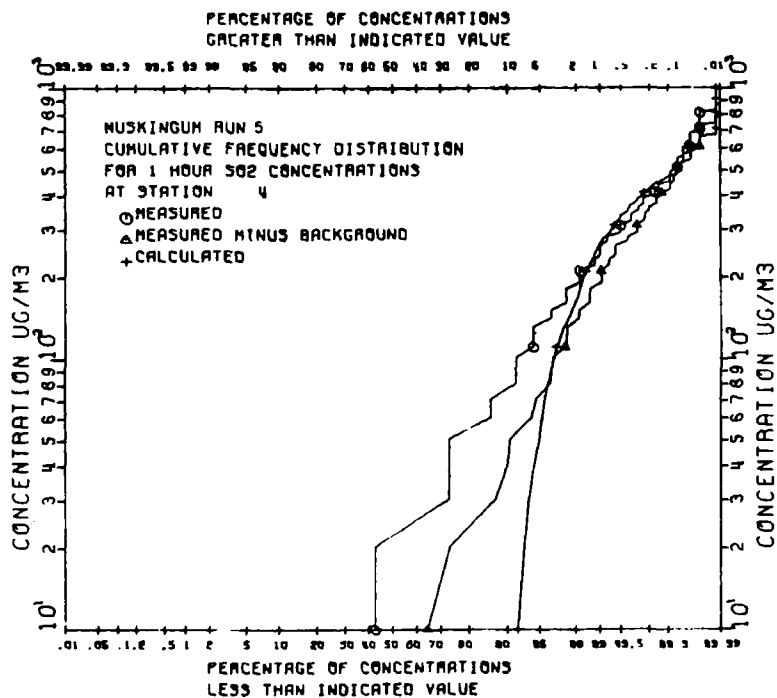


Figure 24d. Model validation Run No. 5. Smith-Singer stability assignment and dispersion calculation method. Measured and predicted cumulative frequency distributions of 1-hour SO₂ concentrations for Muskingum Plant Station 4

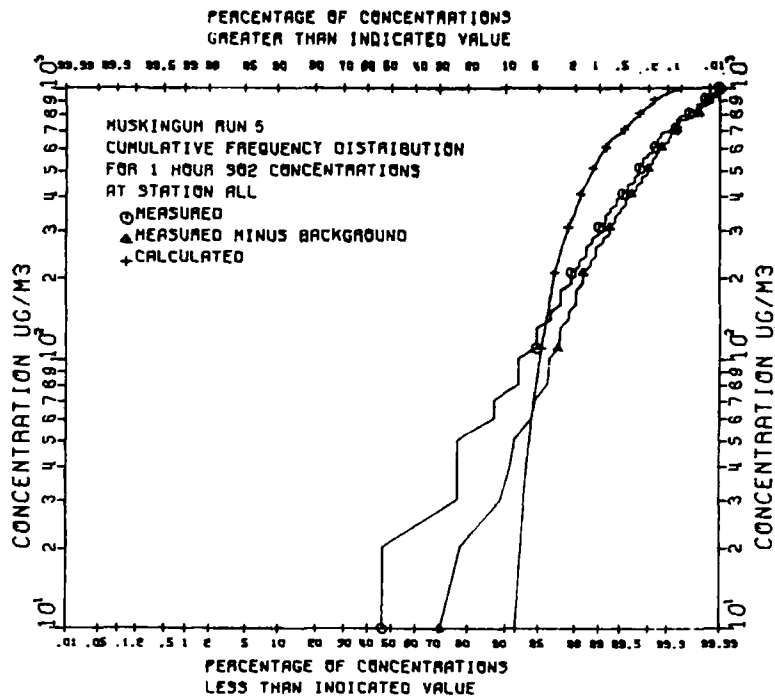


Figure 24e. Model validation Run No. 5. Smith-Singer stability assignment and dispersion calculation method. Measured and predicted cumulative frequency distributions of 1-hour SO₂ concentrations for Muskingum Plant for all stations

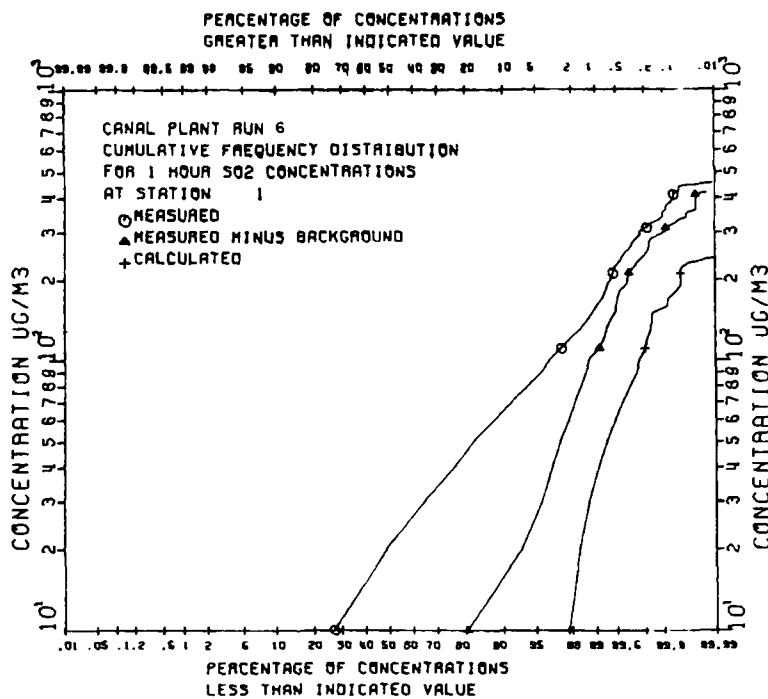


Figure 25a. Model validation Run No. 6. Pasquill-Turner stability assignment method and F.B. Smith dispersion calculation method. Surface roughness equal to 10 cm. Measured and predicted cumulative frequency distributions of 1-hour SO₂ concentrations for Canal Plant Station 1

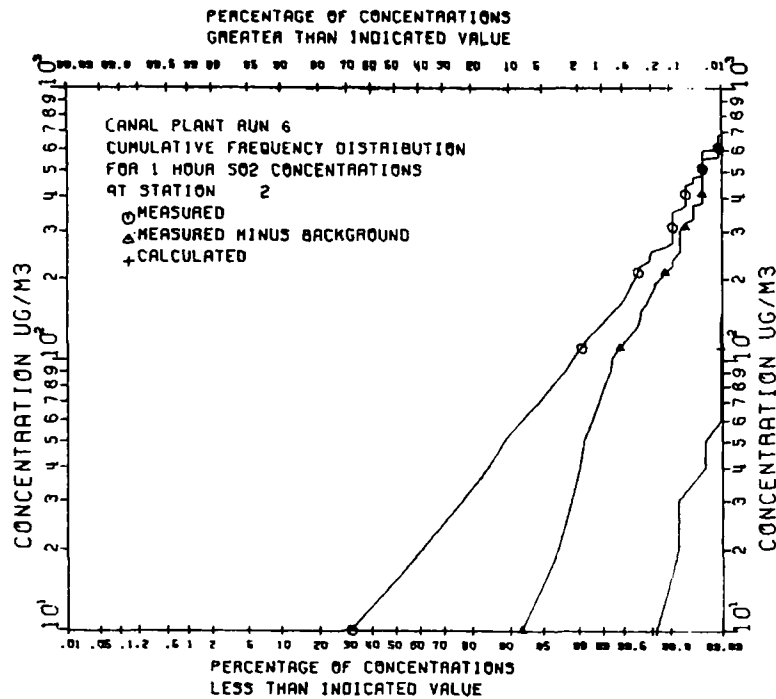


Figure 25b. Model validation Run No. 6. Pasquill-Turner stability assignment method and F.B. Smith dispersion calculation method. Surface roughness equal to 10 cm. Measured and predicted cumulative frequency distributions of 1-hour SO₂ concentrations for Canal Plant Station 2

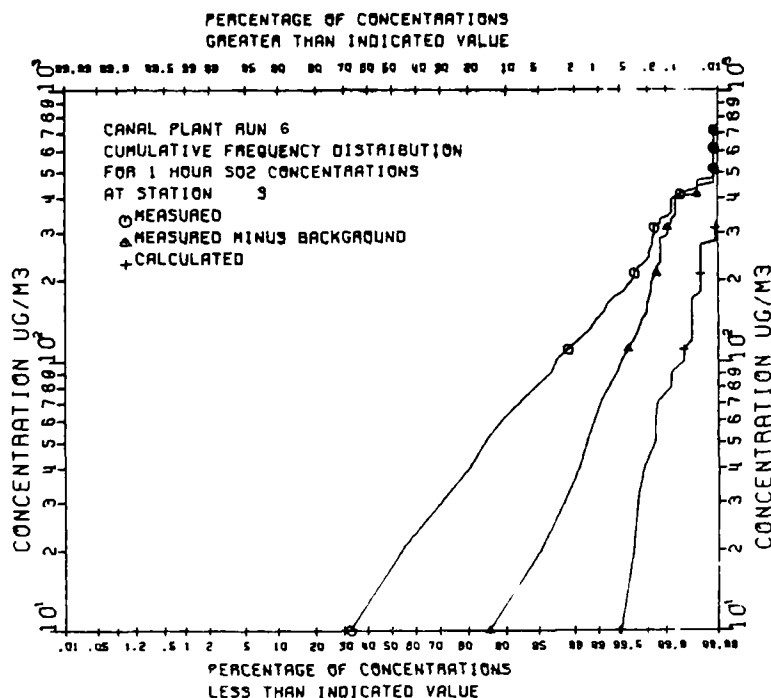


Figure 25c. Model validation Run No. 6. Pasquill-Turner stability assignment method and F.B. Smith dispersion calculation method. Surface roughness equal to 10 cm. Measured and predicted cumulative frequency distributions of 1-hour SO₂ concentrations for Canal Plant Station 3

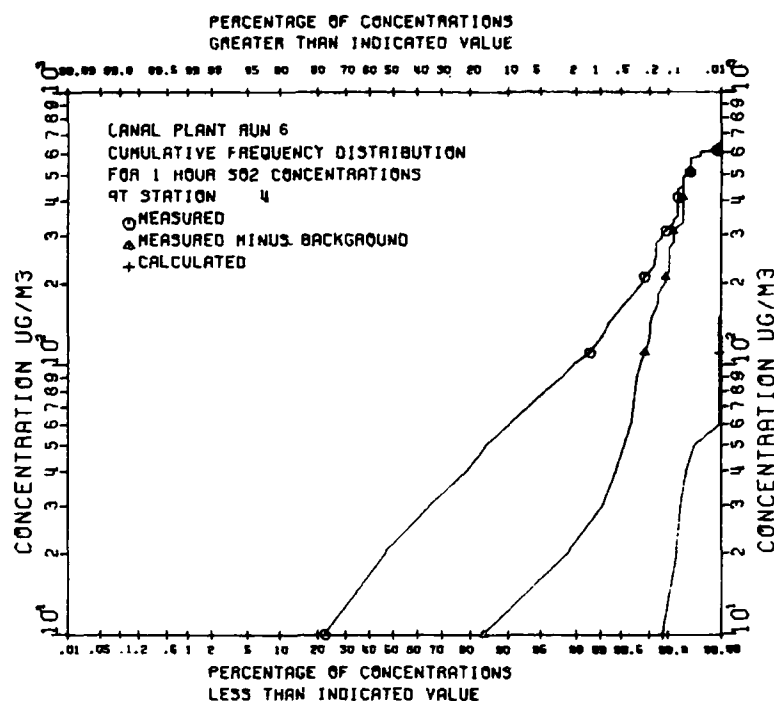


Figure 25d. Model validation Run No. 6. Pasquill-Turner stability assignment method and F.B. Smith dispersion calculation method. Surface roughness equal to 10 cm. Measured and predicted cumulative frequency distributions of 1-hour SO₂ concentrations for Canal Plant Station 4

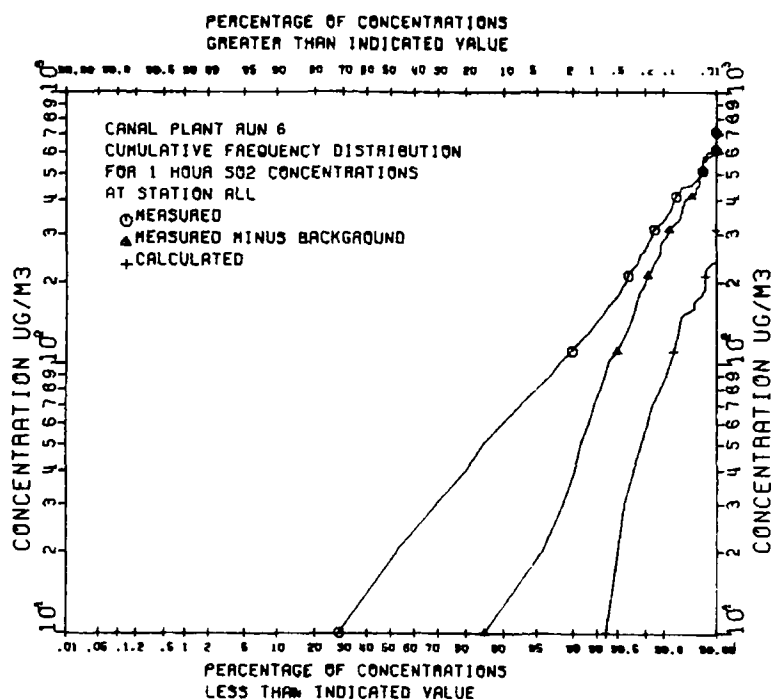


Figure 25e. Model validation Run No. 6. Pasquill-Turner stability assignment method and F.B. Smith dispersion calculation method. Surface roughness equal to 10 cm. Measured and predicted cumulative frequency distributions of 1-hour SO₂ concentrations for Canal Plant for all stations

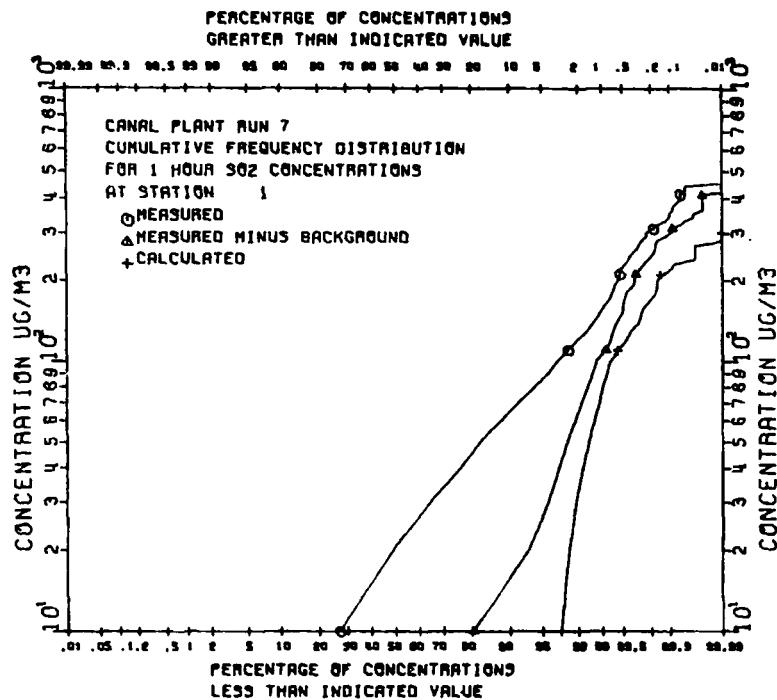


Figure 26a. Model validation Run No. 7. Pasquill-Turner stability assignment method and F.B. Smith dispersion calculation method. Surface roughness equal to 100 cm. Measured and predicted cumulative frequency distributions of 1-hour SO₂ concentrations for Canal Plant Station 1

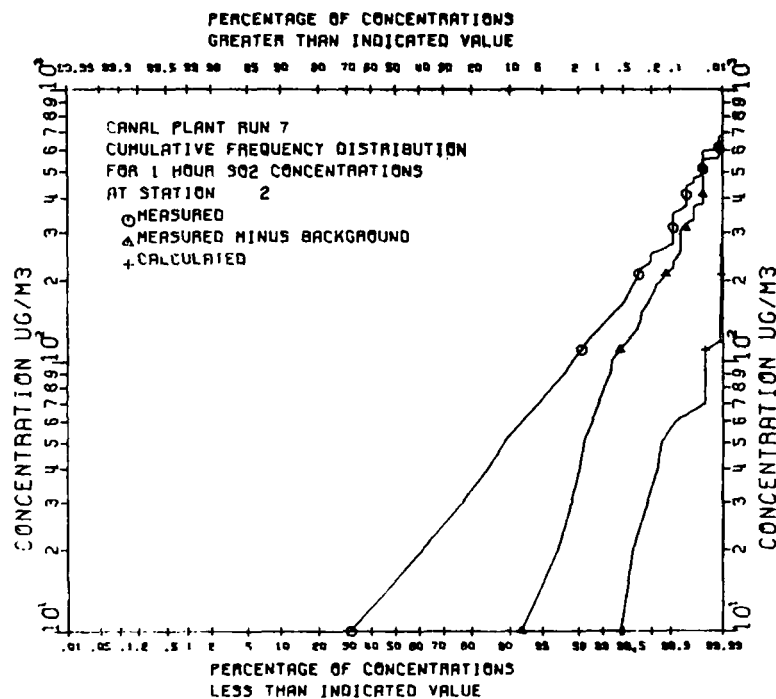


Figure 26b. Model validation Run No. 7. Pasquill-Turner stability assignment method and F.B. Smith dispersion calculation method. Surface roughness equal to 100 cm. Measured and predicted cumulative frequency distributions of 1-hour SO₂ concentrations for Canal Plant Station 2

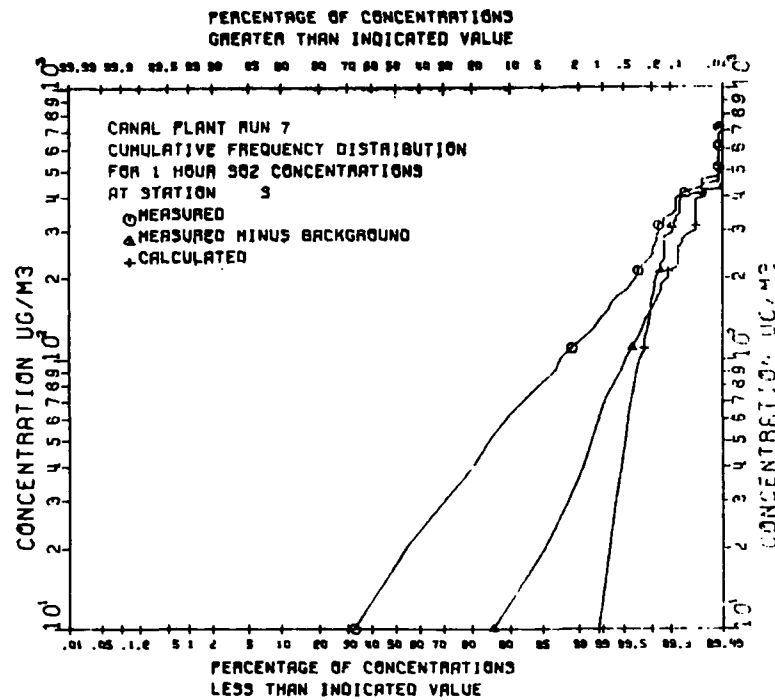


Figure 26c. Model validation Run No. 7. Pasquill-Turner stability assignment method and F.B. Smith dispersion calculation method. Surface roughness equal to 100 cm. Measured and predicted cumulative frequency distributions of 1-hour SO₂ concentrations for Canal Plant Station 3

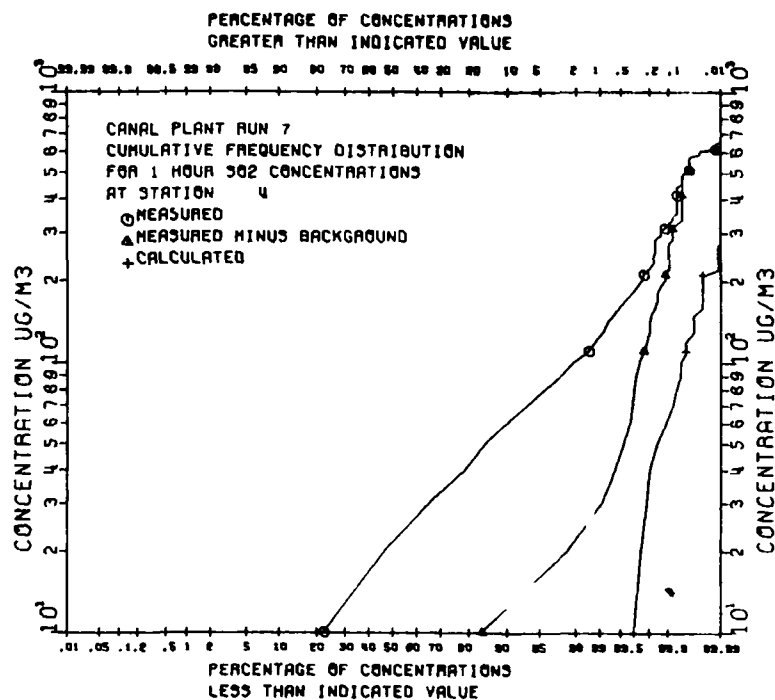


Figure 26d. Model validation Run No. 7. Pasquill-Turner stability assignment method and F.B. Smith dispersion calculation method. Surface roughness equal to 100 cm. Measured and predicted cumulative frequency distributions of 1-hour SO₂ concentrations for Canal Plant Station 4

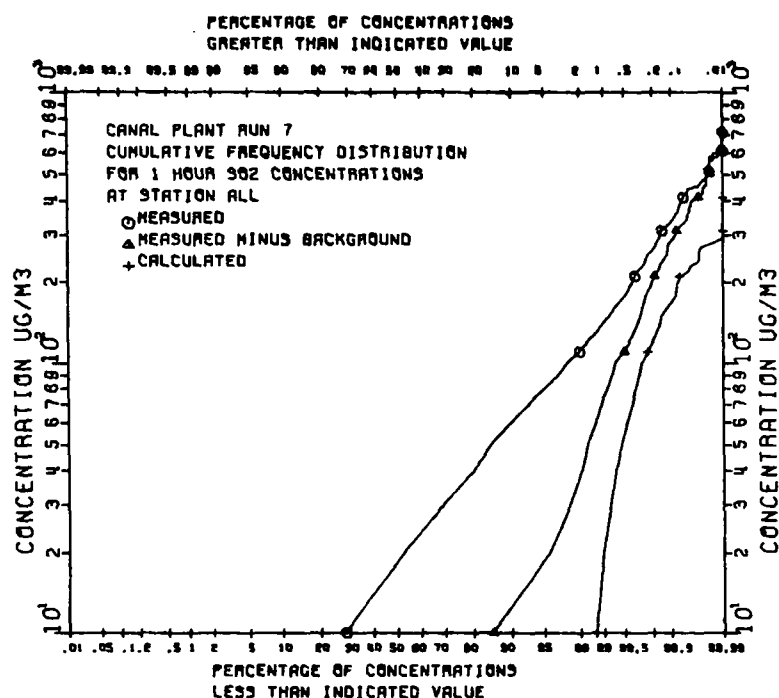


Figure 26e. Model validation Run No. 7. Pasquill-Turner stability assignment method and F.B. Smith dispersion calculation method. Surface roughness equal to 100 cm. Measured and predicted cumulative frequency distributions of 1-hour SO₂ concentrations for Canal Plant for all stations

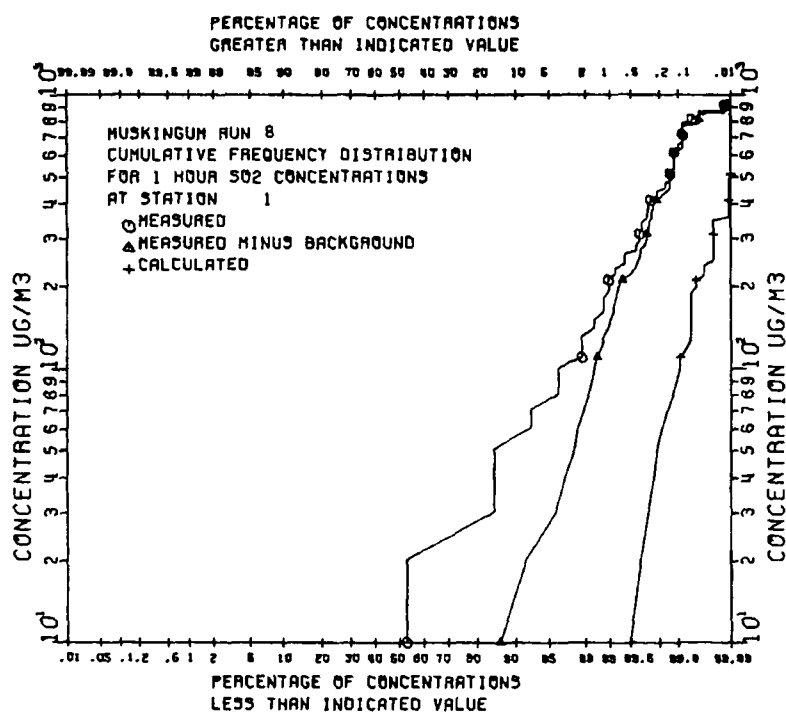


Figure 27a. Model validation Run No. 8. Pasquill-Turner stability assignment method and F.B. Smith dispersion calculation method. Measured and predicted cumulative frequency distributions of 1-hour SO₂ concentrations for Muskingum Plant Station 1

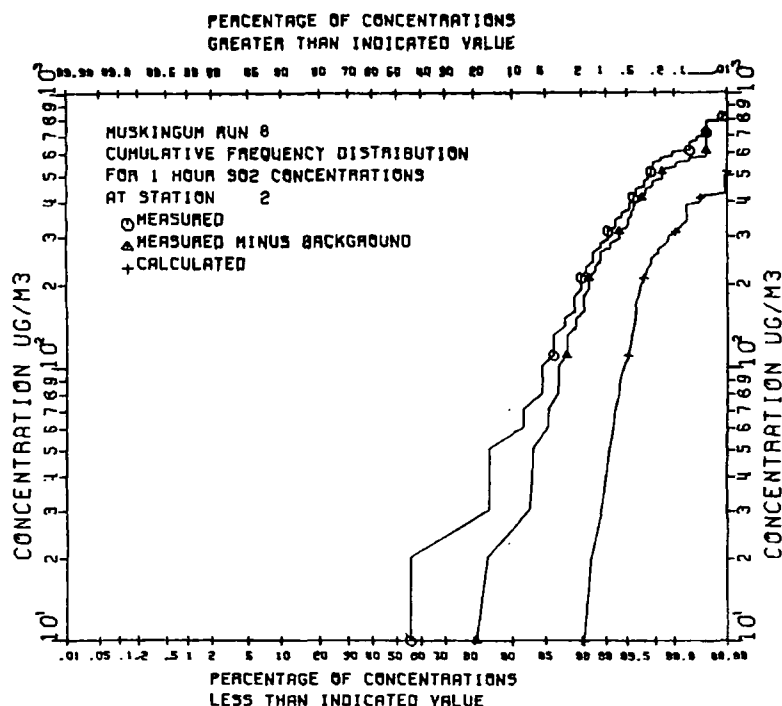


Figure 27b. Model validation Run No. 8. Pasquill-Turner stability assignment method and F.B. Smith dispersion calculation method. Measured and predicted cumulative frequency distributions of 1-hour SO₂ concentrations for Muskingum Plant Station 2

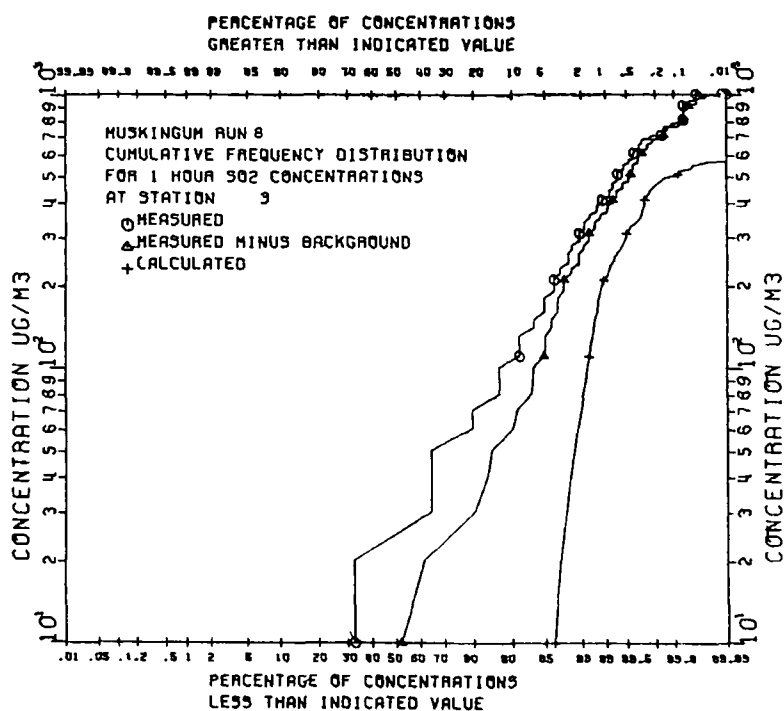


Figure 27c. Model validation Run No. 8. Pasquill-Turner stability assignment method and F.B. Smith dispersion calculation method. Measured and predicted cumulative frequency distributions of 1-hour SO₂ concentrations for Muskingum Plant Station 3

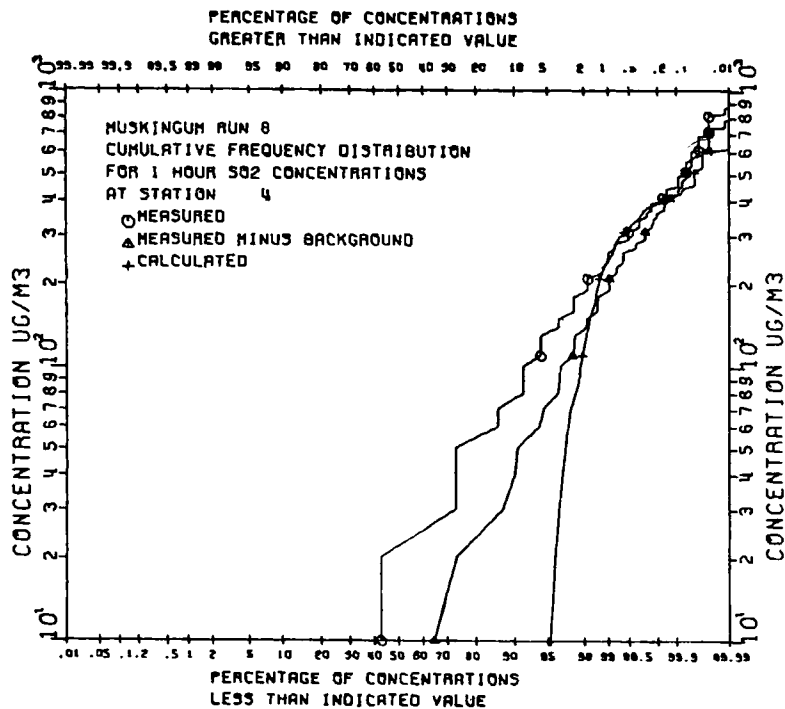


Figure 27d. Model validation Run No. 8. Pasquill-Turner stability assignment method and F.B. Smith dispersion calculation method. Measured and predicted cumulative frequency distributions of 1-hour SO₂ concentrations for Muskingum Plant Station 4

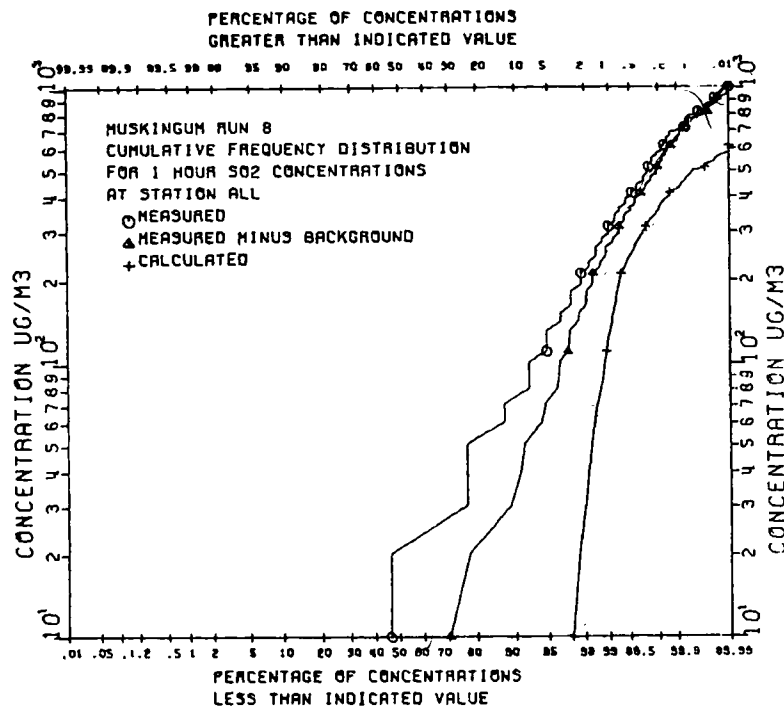


Figure 27e. Model validation Run No. 8. Pasquill-Turner stability assignment method and F.B. Smith dispersion calculation method. Measured and predicted cumulative frequency distributions of 1-hour SO₂ concentrations for Muskingum Plant for all stations

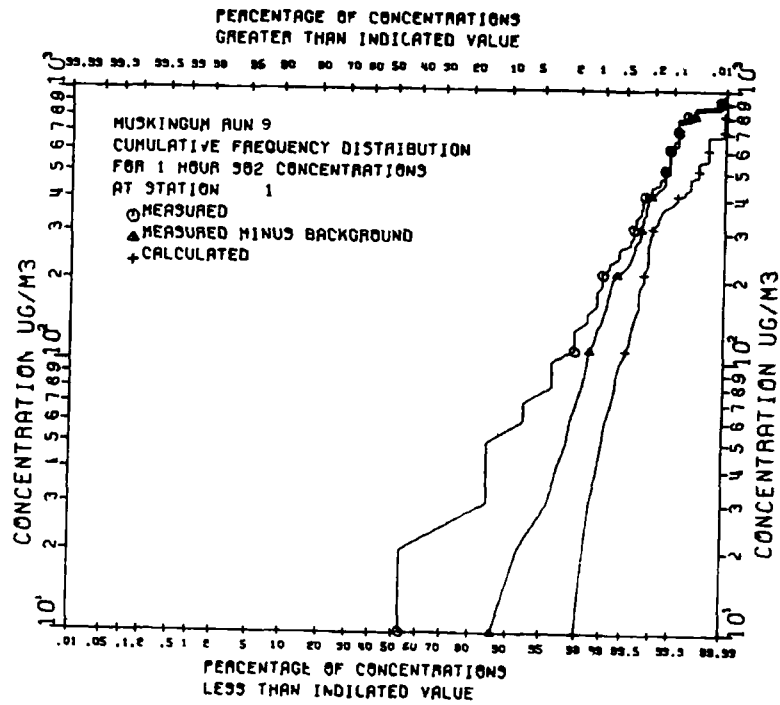


Figure 28a. Model validation Run No. 9. F.B. Smith stability assignment and dispersion calculation method. Measured and predicted cumulative frequency distributions of 1-hour SO₂ concentrations for Muskingum Plant Station 1

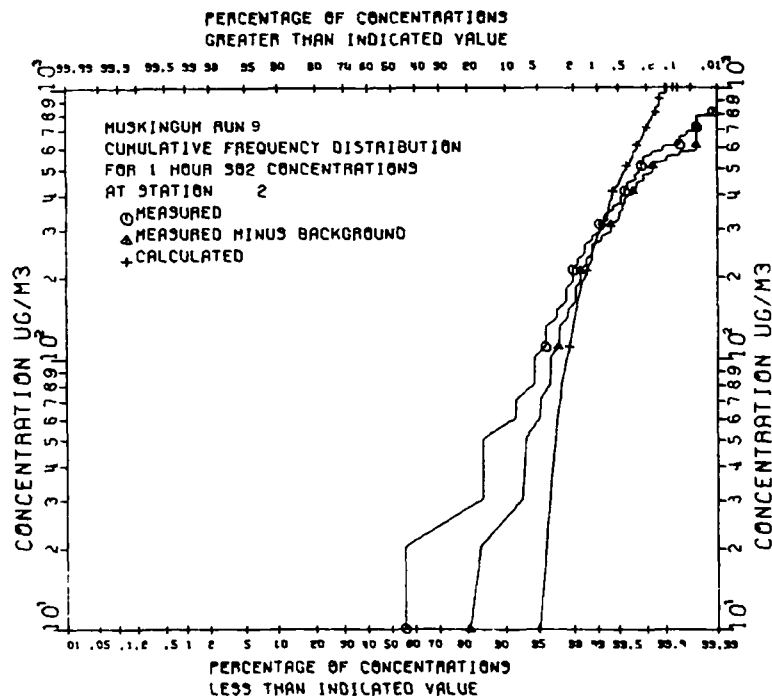


Figure 28b. Model validation Run No. 9. F.B. Smith stability assignment and dispersion calculation method. Measured and predicted cumulative frequency distributions of 1-hour SO₂ concentrations for Muskingum Plant Station 2

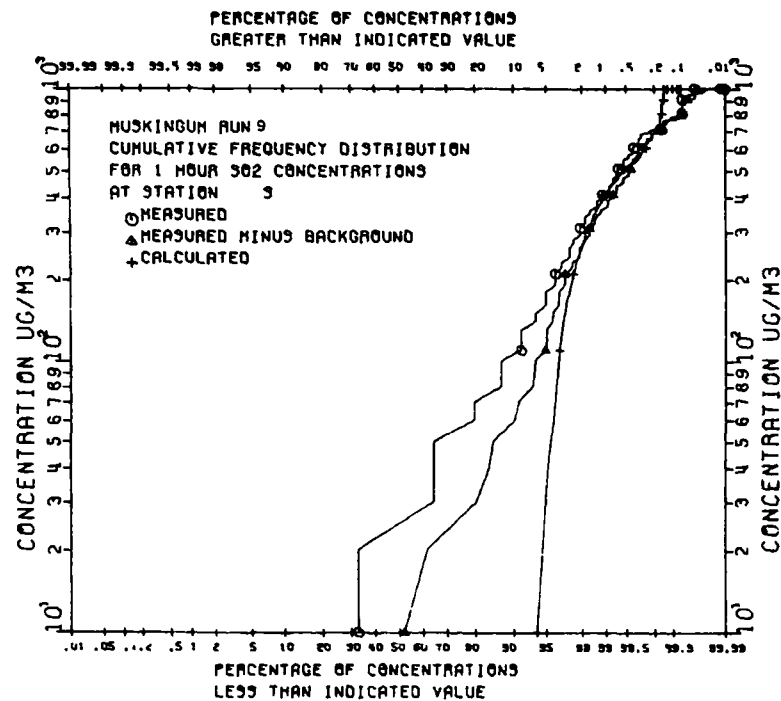


Figure 28c. Model validation Run No. 9. F.B. Smith stability assignment and dispersion calculation method. Measured and predicted cumulative frequency distributions of 1-hour SO₂ concentrations for Muskingum Plant Station 3

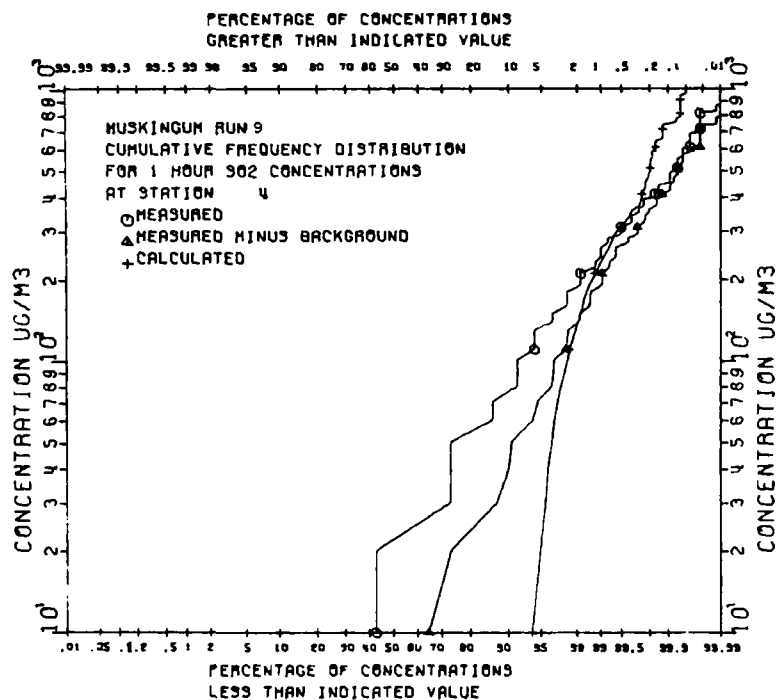


Figure 28d. Model validation Run No. 9. F.B. Smith stability assignment and dispersion calculation method. Measured and predicted cumulative frequency distributions of 1-hour SO₂ concentrations for Muskingum Plant Station 4

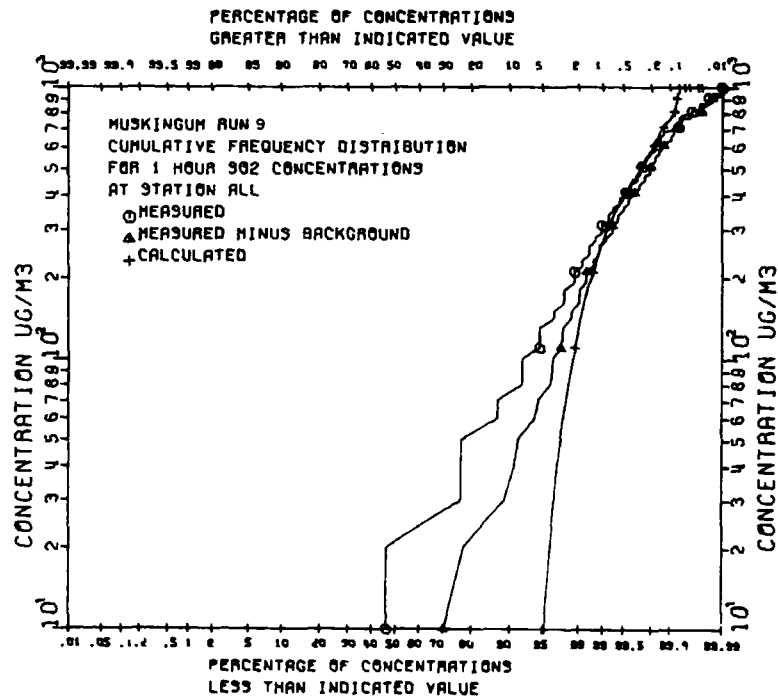


Figure 28e. Model validation Run No. 9. F.B. Smith stability assignment and dispersion calculation method. Measured and predicted cumulative frequency distributions of 1-hour SO₂ concentrations for Muskingum Plant for all stations

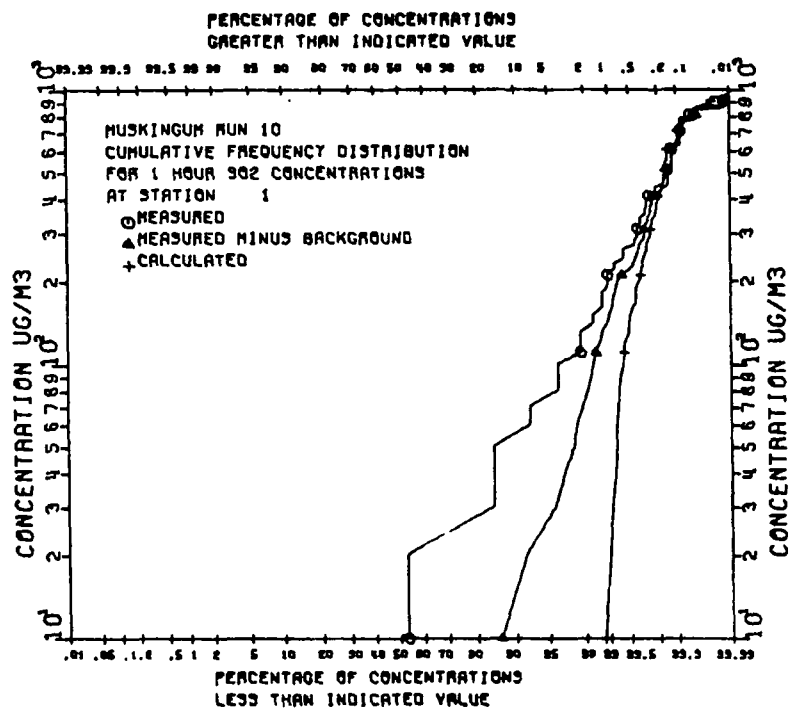


Figure 29a. Model validation Run No. 10. Variable buoyancy flux. Measured and predicted cumulative frequency distributions of 1-hour SO₂ concentrations for Muskingum Plant Station 1

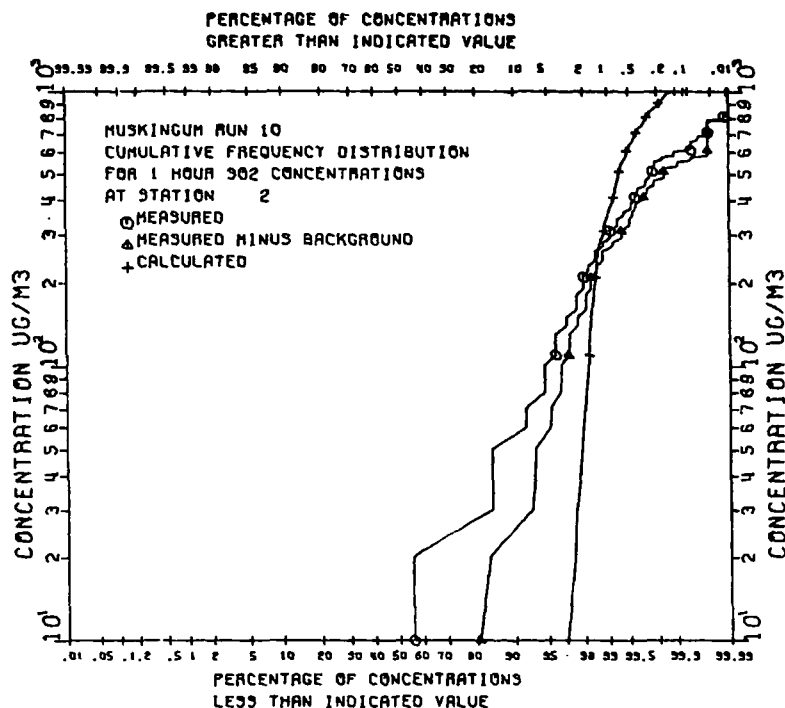


Figure 29b. Model validation Run No. 10. Variable buoyancy flux. Measured and predicted cumulative frequency distributions of 1-hour SO₂ concentrations for Muskingum Plant Station 2

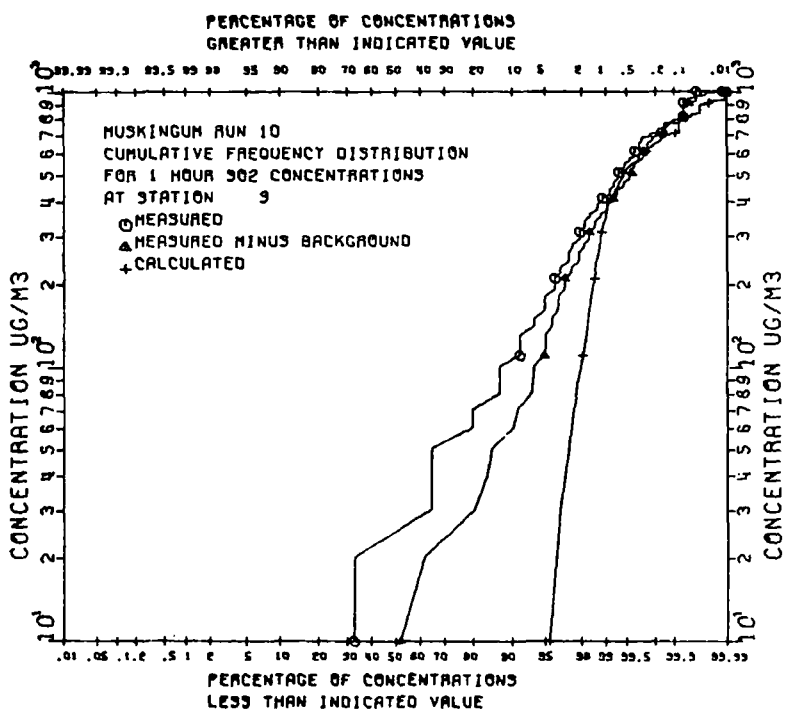


Figure 29c. Model validation Run No. 10. Variable buoyancy flux. Measured and predicted cumulative frequency distributions of 1-hour SO₂ concentrations for Muskingum Plant Station 3

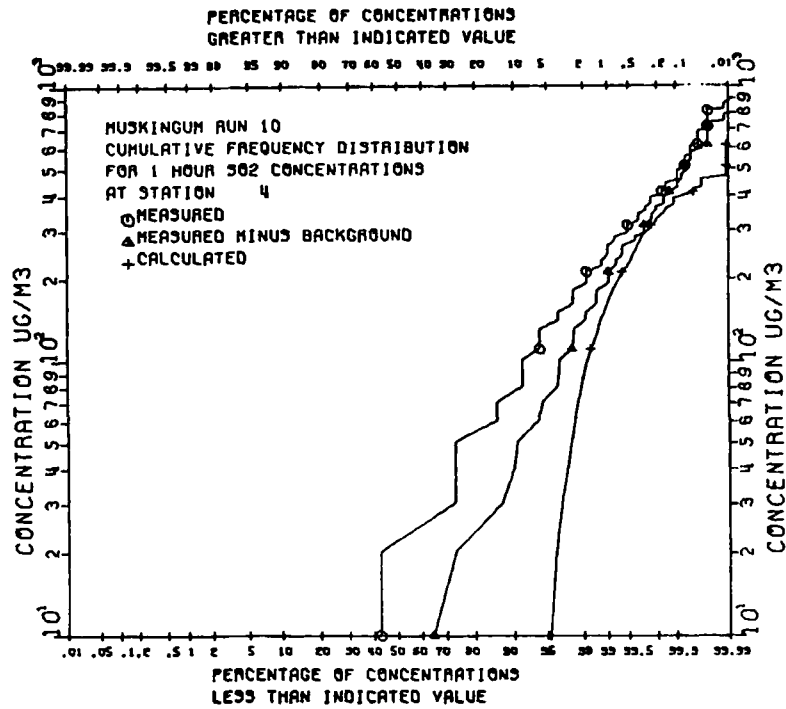


Figure 29d. Model validation Run No. 10. Variable buoyancy flux. Measured and predicted cumulative frequency distributions of 1-hour SO_2 concentrations for Muskingum Plant Station 4

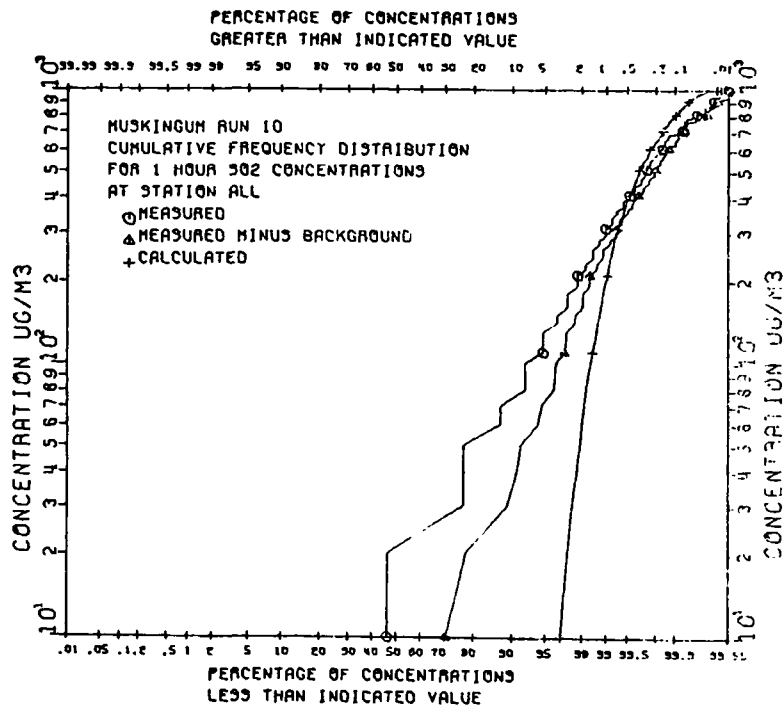


Figure 29e. Model validation Run No. 10. Variable buoyancy flux. Measured and predicted cumulative frequency distributions of 1-hour SO_2 concentrations for Muskingum Plant for all stations

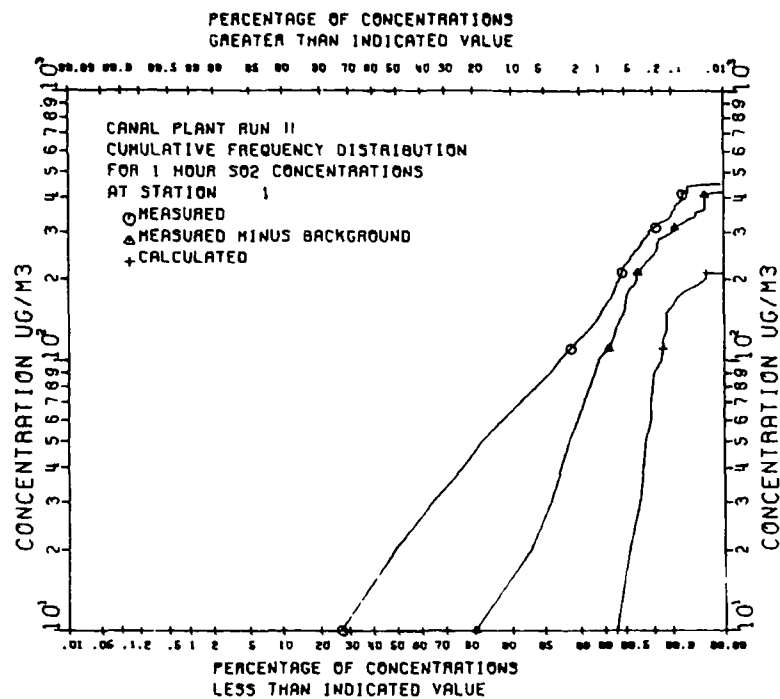


Figure 30a. Model validation Run No. 11. Variable buoyancy flux. Measured and predicted cumulative frequency distributions of 1-hour SO₂ concentrations for Canal Plant Station 1

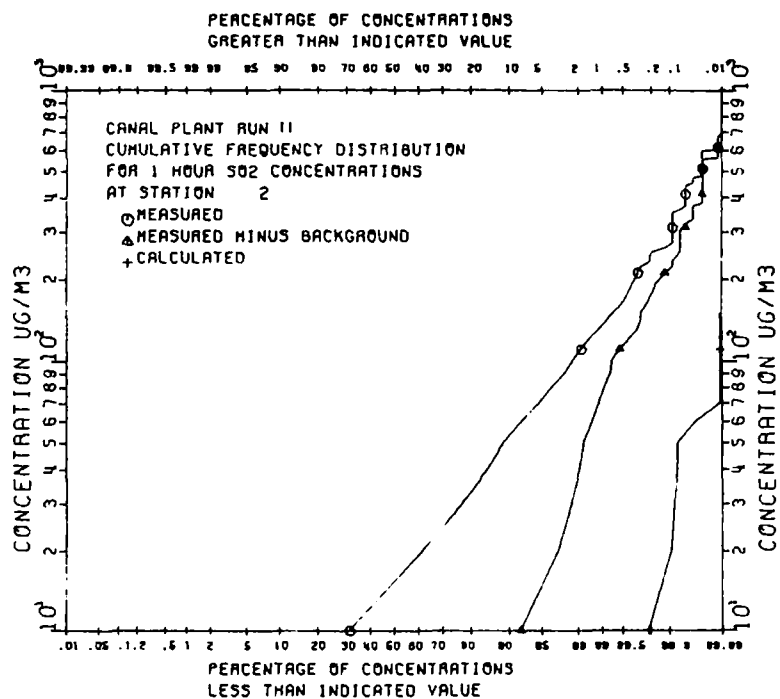


Figure 30b. Model validation Run No. 11. Variable buoyancy flux. Measured and predicted cumulative frequency distributions of 1-hour SO₂ concentrations for Canal Plant Station 2

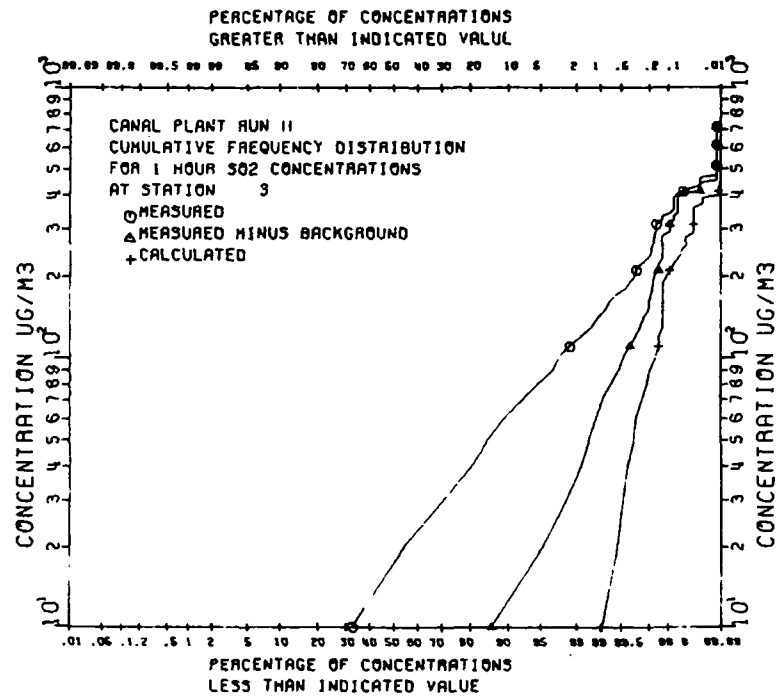


Figure 30c. Model validation Run No. 11. Variable buoyancy flux. Measured and predicted cumulative frequency distributions of 1-hour SO₂ concentrations for Canal Plant Station 3

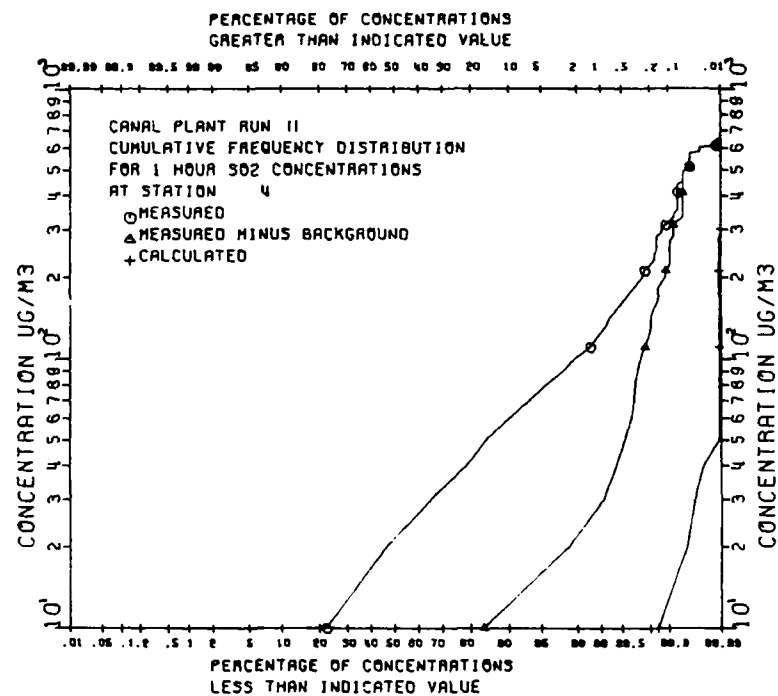


Figure 30d. Model validation Run No. 11. Variable buoyancy flux. Measured and predicted cumulative frequency distributions of 1-hour SO₂ concentrations for Canal Plant Station 4

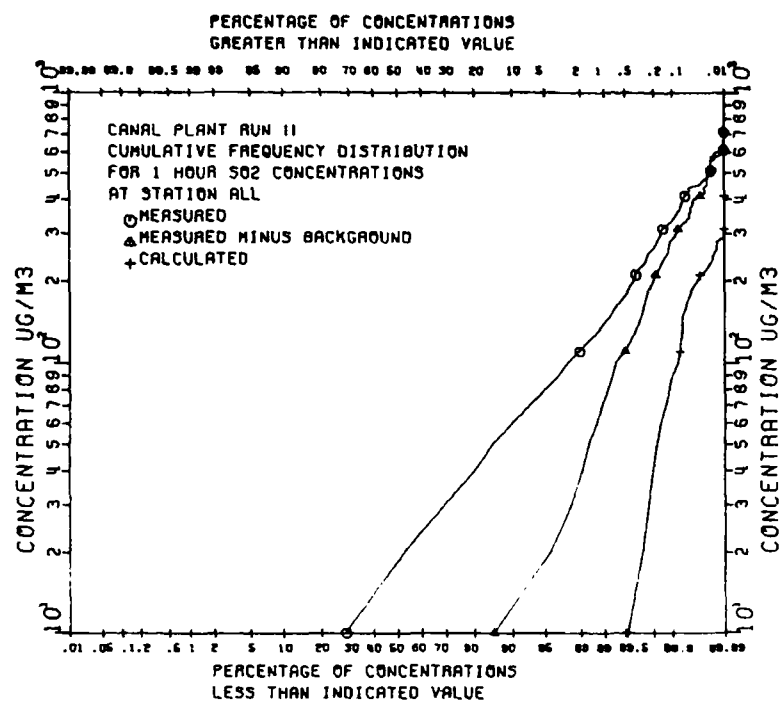


Figure 30e. Model validation Run No. 11. Variable buoyancy flux. Measured and predicted cumulative frequency distributions of 1-hour SO₂ concentrations for Canal Plant for all stations

SECTION V

CONCLUSIONS AND RECOMMENDATIONS

Based upon the results of this study we would recommend that the methods currently used for the calculation of dispersion coefficients and the selection of stability classes not be replaced by alternate techniques, at least until further model validation studies are conducted. Since data from only two power plants were used in this study the results could hardly be called definitive. Nevertheless, even from these limited results, we may draw a number of conclusions:

1. The similarity between the Pasquill-Turner and Gifford-Briggs dispersion coefficients (except for stability A) will require that a large number of model validation exercises be carried to determine which method is more accurate.
2. The use of the Smith-Singer stability assignment and dispersion calculation methods in the Single Source Model may yield unrealistic frequency distributions of 1-hour concentrations. This observation must be qualified, however, by the fact that the validation was carried out only for the Muskingum Plant. Since the rather subjective stability assignment scheme may have been carried out differently at the Muskingum Plant, the Smith-Singer version of the Single Source Model may give better agreement with measured concentrations if applied elsewhere.
3. Due to the strong variation of calculated concentrations as a function of stability, the use of fractional stability assignments should, in principle, lead to more accurate model predictions. The F.B. Smith stability classification method did not, however, provide better agreement between measured and calculated concentration frequency distributions, primarily because of its tendency to underestimate the stability class.

4. The use of a variable buoyancy flux in the Single Source Model did little to improve the agreement between measured and calculated concentration frequency distributions. This conclusion is similar to others reached when more detailed or applicable emissions or meteorological data has been used in model validation exercises. The success or failure of the model in any given application is much more a function of the assumptions regarding plume rise, dispersion, and terrain effects that form the theoretical basis for the model.

SECTION VI

REFERENCES

1. Mills, M. T. and F. A. Record. Comprehensive Analysis of Time Concentration Relationships and the Validation of a Single Source Dispersion Model. Publication Number EPA-450/3-75-083. Prepared by GCA/Technology Division for the U.S. Environmental Protection Agency, Research Triangle Park, North Carolina. March 1975.
2. Mills, M. T. and R. W. Stern. Model Validation and Time-Concentration Analysis of Three Power Plants. Publication Number EPA-450/3-76-002. Prepared by GCA/Technology Division for the U.S. Environmental Protection Agency, Research Triangle Park, North Carolina. December 1975.
3. Briggs, G. A. Plume Rise USAEC Critical Review Series TID-25075, National Technical Information Service, Springfield, Va. 22151. 1969.
4. Briggs, G. A. Some Recent Analyses of Plume Rise Observation, pp. 1029-1032, in Proceedings of the Second International Clean Air Congress, edited by H. M. Englund and W. T. Berry. Academic Press, New York. 1971.
5. Briggs, G. A. Discussion on Chimney Plumes in Neutral and Stable Surroundings. Atmos. Environ. 6, 507-510. July 1972.
6. Gifford, F. A. Atmospheric Dispersion Calculation Using the Generalized Gaussian Plume Model. Nucl Saf. 1(3). 1960.
7. Turner, D. B. Workbook of Atmospheric Dispersion Estimates. U.S. Environmental Protection Agency, Office of Air Programs. Publication Number AP-26.
8. Cramer, H. E. A Practical Method for Estimating the Dispersal of Atmospheric Contaminants. In: Proceedings of the First National Conference on Applied Meteorology. Hartford, Connecticut, American Meteorological Society. p. C-33 - C-55. October 1957.
9. Pasquill, F. The Estimation of the Dispersion of Windborne Material. Meteorol Mag. 90:33-49. 1961.

10. Mead, P. J. Meteorological Aspects of the Peaceful Uses of Atomic Energy. WMO Tech Note. 3, Part I. 1960.
11. Turner, D. B. A Diffusion Model for an Urban Area. J Appl Meteor. 3:83-91. February 1969.
12. Smith, M. E. and I. A. Singer. An Improved Method of Estimating Concentrations and Related Phenomena From a Point Source Emission. J Appl Meteor. 5(5):631-639. October 1966.
13. Smith, M. E. and T. T. Frankenberg. Improvement of Ambient Sulfur Dioxide Concentrations by Conversion From Low to High Stacks. J Air Pollu Control Assoc. 25(6):595-601. June 1975.
14. Singer, I. A. and M. E. Smith. Atmospheric Dispersion at Brookhaven National Laboratory. Air and Water Pollution International Journal. Pergamon Press 1966. Vol. 10, pp. 125-135.
15. Smith, M. E. (ed.). Recommended Guide for the Prediction of the Dispersion of Airborne Effluent. Am Soc Mech Eng. Second Edition. 1973.
16. Briggs, G. A. Diffusion Estimation for Small Emissions. U.S. Department of Commerce. NOAA-ERL-ARATDL Contribution Number 79. Oak Ridge, Tennessee. May 1973.
17. Smith, F. B. A Scheme for Estimating the Vertical Dispersion of a Plume From a Source Near Ground Level, Chapter XVII. In: Proceeding, N.A.T.O. Committee on the Challenge of Modern Society, Paris, France, October 2-3, 1972. (Proceedings Number 14, Air Pollution Technical Information Center, U.S. Environmental Protection Agency, Research Triangle Park, North Carolina. 1973).
18. List, R. J. Smithsonian Meteorological Tables. Sixth Revised Edition. Published by the Smithsonian Institute, Washington, D.C. 1951.
19. Hosker, R. P. Jr. Estimates of Dry Deposition and Plume Depletion Over Forests and Grassland. (Presented at the IAEA Symposium on the Physical Behavior of Radioactive Contaminants in the Atmosphere. Vienna, Austria. November 12-16, 1973.)

APPENDIX A

TURNER SCHEME FOR STABILITY CLASSIFICATION

The following scheme for stability classification was described by D. Bruce Turner in the February 1964 edition of the Journal of Applied Meteorology:

This system of classifying stability on an hourly basis for research in air pollution is based upon work accomplished by Dr. F. Pasquill of the British Meteorological Office. Stability near the ground is dependent primarily upon net radiation and wind speed. Without the influence of clouds, insolation (incoming radiation) during the day is dependent upon solar altitude, which is a function of time of day and time of year. When clouds exist their cover and thickness decrease incoming and outgoing radiation. In this system insolation is estimated by solar altitude and modified for existing conditions of total cloud cover and cloud ceiling height. At night estimates of outgoing radiation are made by considering cloud cover. This stability classification system has been made completely objective so that an electronic computer can be used to compute stability classes. The stability classes are as follows: (1) Extremely unstable; (2) unstable; (3) slightly unstable; (4) neutral; (5) slightly stable; (6) stable; (7) extremely stable. Table A-1 gives the stability class as a function of wind speed and net radiation. The net radiation index ranges from 4, highest positive net radiation (directed toward the ground), to -2, highest negative net radiation (directed away from the earth). Instability occurs with high positive net radiation and low wind speed, stability with high negative net radiation and light winds, and neutral conditions with cloudy skies or high wind speeds.

Table A-1. STABILITY CLASS AS A FUNCTION OF NET RADIATION AND WIND SPEED

Wind speed, knots	Net radiation index						
	4	3	2	1	0	-1	-2
0,1	1	1	2	3	4	6	7
2,3	1	2	2	3	4	6	7
4,5	1	2	3	4	4	5	6
6	2	2	3	4	4	5	6
7	2	2	3	4	4	4	5
8,9	2	3	3	4	4	4	5
10	3	3	4	4	4	4	5
11	3	3	4	4	4	4	4
<u>>12</u>	3	4	4	4	4	4	4

The net radiation index used with wind speed to obtain stability class is determined by the following procedure:

1. If the total cloud cover is 10/10 and the ceiling is less than 7000 feet, use net radiation index equal to 0 (whether day or night).
2. For night-time (between sunset and sunrise):
 - a. If total cloud cover $\leq 4/10$, use net radiation index equal to -2.
 - b. If total cloud cover $> 4/10$, use net radiation index equal to -1.
3. For daytime:
 - a. Determine the insolation class number as a function of solar altitude from Table A-2.
 - b. If total cloud cover $\leq 5/10$, use the net radiation index in Table A-1 corresponding to the insolation class number.
 - c. If cloud cover $> 5/10$, modify the insolation class number by following these six steps.
 - (1) Ceiling $< 7,000$ ft, subtract 2.

Table A-2. INSOLATION AS A FUNCTION OF SOLAR ALTITUDE

Solar altitude (a)	Insolation	Insolation class number
$60^\circ < a$	Strong	4
$35^\circ < a \leq 60^\circ$	Moderate	3
$15^\circ < a \leq 35^\circ$	Slight	2
$a \leq 15^\circ$	Weak	1

- (2) Ceiling ≥ 7000 ft but $< 16,000$ ft, subtract 1.
- (3) Total cloud cover equal 10/10, subtract 1.
(This will only apply to ceilings ≥ 7000 ft since cases with 10/10 coverage below 7000 ft are considered in item 1 above.)
- (4) If insolation class number has not been modified by steps (1), (2), or (3) above, assume modified class number equal to insolation class number.
- (5) If modified insolation class number is less than 1, let it equal 1.
- (6) Use the net radiation index in Table A-1 corresponding to the modified insolation class number.

The Pasquill-Turner technique for stability class assignment is the one currently employed in the Single Source Model Preprocessor program except that Table A-1 has been expanded to provide a greater resolution according to wind speed (see Table A-3).

Table A-3. ADAPTATION OF TABLE A-1 FOR USE IN THE SINGLE SOURCE
MODEL PREPROCESSOR PROGRAM

Wind speed, knots	Net radiation index						
	4	3	2	1	0	-1	-2
1	1	1	2	3	4	7	7
2	1	2	2	3	4	7	7
3	1	2	2	3	4	6	7
4	1	2	3	4	4	5	7
5	1	2	3	4	4	5	6
6	2	2	3	4	4	5	6
7	2	2	3	4	4	4	5
8	2	3	3	4	4	4	5
9	2	3	3	4	4	4	5
10	3	3	4	4	4	4	5
11	3	3	4	4	4	4	4
<u>>12</u>	3	4	4	4	4	4	4

APPENDIX B

LISTINGS OF THE FRACTIONAL STABILITY PREPROCESSOR
PROGRAM AND CORRESPONDING VERSION OF THE
SINGLE SOURCE MODEL

PREP: PROCEDURE OPTIONS(MAIN);

STMT	LEVEL	NEST	CODE
1			PREP: PROCEDURE OPTIONS(MAIN); /* OCTOBER 1972 VERSION */
2	1		DECLARE ASHV FILE RECORD;
3	1		DECLARE MET FILE RECORD OUTPUT;
4	1		DECLARE IDC FIXED DECIMAL(5,0), (YRC,LWD,XHR) FIXED DECIMAL(2,0), (IND,ISKY,IROOF,IRADX,IREF INITIAL(1),I,J,IDY,IHR,KHR,IY, IX INITIAL(65549),IMO INITIAL(1), ICN,KSTSP,ZONE,KST(24) INITIAL((24) 0)) FIXED BIN(31), (IDFAC(12) INITIAL(0,31,59,90,120,151,181,212,243,273,304,334), ANGL(3) INITIAL(60., 35., 15.), FV,XDIR) FIXED DECIMAL(3,0), IFVR FIXED DECIMAL(1,0), (YFL,DAYNO,TDAYNO,SIND,COSD,SINTD,COSTD,SIGMA,DSIN,DCOS, SINLAT,COSLAT,ALAT,ALONG,HCOS,H2,H1,CONST INITIAL(57.29578), ALF,ALFSN,AMM,TSR,TSS) FLOAT DECIMAL, (S,XAF,XAFPI,XAFMI,XMN,XMNP1,XMNM1) FIXED DECIMAL(8,3);
5	1		DECLARE HSKIP INITIAL(0) FIXED BIN(31);
6	1		DECLARE (COEF(4,14) INITIAL(.3696429E+01,.3877143E+01, .4148571E+01,.4479286E+01,.462E+01,.4755E+01,.4932857E+01, .3649495E+01,.3913232E+01,.4554444E+01,.5839798E+01, .7017677E+01,.9922898E+01,.1471869E+02, -.9542929E-02,-.3097042E-01,-.6534488E-01,-.103329,-.1196898, -.135526,-.1548445,-.8374218E-02,-.5276575E-01,-.1726251, -.4260185,-.7639839,-.2155727E+01,-.4151976E+01, -.1655844E-04,.2341991E-03,.7816017E-03,.1350649E-02, .1526299E-02,.1738961E-02,.1946537E-02,.1219336E-02, .3607504E-02,.1104257E-01,.245202E-01,.5354618E-01, .2839127,.5724983, .2020202E-06,-.1161616E-05,-.4343434E-05, -.7121212E-05,-.7853535E-05,-.8939394E-05, -.9520202E-05,-.1178451E-03,-.2356902E-03, -.5387205E-03,-.7744108E-03,-.1380471E-02, -.1416177E-01,-.284291E-01), CLOUD(9) INITIAL(8.,7.,6.,5.,4.,3.,2.,1.,0.), CMULT(9) INITIAL (.23,.45,.59,.67,.72,.76,.81,.89,1.07),WIND(7) INITIAL (8.,6.,5.,4.,3.,2.,0.),XMULT,WATTS,WATTS1,FKST(24) INITIAL((24) 0.),P1,P2,CLD,Z,ZALF,A0) FLOAT DECIMAL;
7	1		DECLARE 1 INDATA, 2 ID PICTURE '99999', 2 IYEAR PICTURE '99', 2 IMONTH PICTURE '99', 2 IDAY PICTURE '99', 2 IHOURL PICTURE '99', 2 ICEIL CHAR(3), 2 IDUM1 CHAR(22), 2 IDIR PICTURE '99', 2 ISPEED PICTURE '99', 2 IDUM2 CHAR(4), 2 ITEMP PICTURE '999', 2 IDUM3 CHAR(29), 2 ICOVER CHAR(1), 2 IDUM4 CHAR(1), 1 OUTDATA, 2 YR PICTURE '99', 2 MONTH PICTURE '99', 2 DAY1 PICTURE '999',

PREP: PROCEDURE OPTIONS(MAIN);

STMT LEVEL NEST

```

2 KKST(0:23) PICTURE '99',
2 SPEED(0:23) PICTURE '999V99',
2 TEMP(0:23) PICTURE '999V9',
2 AFV(0:23) PICTURE '999',
2 FVR(0:23) PICTURE '999',
2 HLH(2,0:23) PICTURE '99999V999';

8 1 DECLARE TITLEA CHAR(8);
9 1 DECLARE TITLEB CHAR(8);
10 1 F1: FORMAT(COL(14),F(4,0),COL(25),F(4,0));
11 1 ON ENDFILE(SYSIN)GO TO FINISH;
/* READ CARD TO INITIALIZE MET TAPE ID, YEAR & LAST WIND DIRECTION*/
13 1 AGAIN: GET FILE(SYSIN) DATA (IDC,YRC,LWD,ALAT,ALONG,ZONE,TITLEA,
TITLEB);
14 1 IREC=1; IMO=1; IX=65549;
17 1 OPEN FILE(ASHV) RECORD TITLE(TITLEA);
18 1 OPEN FILE(MET) RECORD OUTPUT TITLE(TITLEB);
19 1 ON ERROR PUT FILE(SYSPRINT) EDIT
/*RECORD # AT TIME OF ERROR CONDITION=',IREC) (A(36),F(4,0));
21 1 ON ENDFILE(ASHV) GO TO LAST;
/* READ A CARD WITH FIRST HOUR'S DATA */
23 1 READ FILE(ASHV) INTO(INDATA);
/* READ PRIOR DAY'S MIXING HEIGHT VALUES */
24 1 GET FILE(SYSIN) EDIT (XMNMI,XAFMI) (R(F1));
/* READ PRESENT DAY'S MIXING HEIGHT VALUES */
25 1 GET FILE(SYSIN) EDIT (XMN,XAF) (R(F1));
/* ENTER DAY LOOP TO READ NEXT DAY'S MIXING HEIGHT VALUES */
26 1 DO IDY=1 TO 365;
27 1 1 GET FILE(SYSIN) EDIT (XMNP1,XAFP1) (R(F1));
/* CALCULATE THE DAYNO AND THE TIME OF SUNRISE AND SUNSET */
28 1 1 DAY1=IDAY+IDFAC*IMONTH;
/* CONSTANT 20926.82528=365.242*57.29578 */
29 1 1 DAYNO=(DAY1-1.0)*360./20926.82528 ;
30 1 1 TDAYNO=2.*DAYNO ;
31 1 1 SIND=SIN(DAYNO) ;
32 1 1 COSD=COS(DAYNO) ;
33 1 1 SINTD=SIN(TDAYNO) ;
34 1 1 COSTD=COS(TDAYNO) ;
35 1 1 SIGMA=279.9348+(DAYNO*CONST)+1.914827*SIND-0.079525*COSD+
0.019938*SINTD-0.00162*COSTD ;
/* CONSTANT .4091720193=23.44383/57.29578 */
36 1 1 DSIN=SIN(.4091720193)*SIN(SIGMA/CONST);
37 1 1 DCOS=SQRT(1.0-DSIN*DSIN) ;
38 1 1 AMM=12.0+0.12357*SIND-0.004289*COSD+0.153809*SINTD+0.060783*COSTD;
39 1 1 SINLAT=SIN(ALAT/CONST) ;
40 1 1 COSLAT=COS(ALAT/CONST) ;
41 1 1 HCOS=(-SINLAT*DSIN)/(COSLAT*DCOS) ;
42 1 1 H2=ATAND(SQRT(1.-HCOS*HCOS),HCOS)/15.0;
43 1 1 TSR=(ALONG/15.0+AMM-H2)-ZONE ;
44 1 1 TSS=(ALONG/15.0+AMM+H2)-ZONE ;
45 1 1 DO KHR=0 TO 23;
/*CHECK DATA FOR CORRECTNESS & CONTINUITY */
46 1 2 CHECK: IF ID=IDC THEN DO;
48 1 3 PUT SKIP FILE(SYSPRINT) EDIT
('ID DOES NOT MATCH IN RECORD # ',IREC,' ID IS ',ID)
(A(30),F(4,0),A(9),F(5,0));

```

PREP: PROCEDURE OPTIONS(MAIN);

STMT	LEVEL	NEST	CODE
49	1	3	GO TO NEWREC;
50	1	3	END;
51	1	2	IF IYEAR = YRC THEN DO; PUT SKIP FILE(SYSPRINT) EDIT ('YEAR IS ', IYEAR, ' INSTEAD OF ', YRC, ' IREC=', IREC) (A(8), F(2,0), A(12), F(2,0), A(6), F(4,0));
54	1	3	GO TO NEWREC; END;
56	1	2	OUTDATA.YR=IYEAR;
57	1	2	IF IMONTH=IMO THEN IF IMONTH=IMO+1 THEN DO;
60	1	3	PUT SKIP FILE(SYSPRINT) EDIT ('MONTH ', IMONTH, ' DOES NOT AGREE WITH LOOP ', IMO, ' IREC=', IREC) (A(6), F(2,0), A(26), F(2,0), A(6), F(4,0));
61	1	3	GO TO FINISH; END;
63	1	2	ELSE IMO=IMONTH;
64	1	2	OUTDATA.MONTH=IMONTH;
65	1	2	IF DAY1=IDY THEN DO; PUT SKIP FILE(SYSPRINT) EDIT ('DAY ', DAY1, ' DOES NOT AGREE WITH LOOP ', IDY, ' IREC=', IREC) (A(4), F(2,0), A(26), F(2,0), A(6), F(4,0));
68	1	3	GO TO DLOOP; END;
70	1	2	IF IHOURL=KHR THEN DO; PUT SKIP FILE(SYSPRINT) EDIT ('HOURL ', IHOURL, ' DOES NOT AGREE WITH LOOP ', KHR, ' IREC=', IREC) (A(5), F(2,0), A(26), F(2,0), A(6), F(4,0));
73	1	3	HSKIP=1;
74	1	3	END;
			/* CONVERSION OF ISKY & IROOF */
75	1	2	IF ICEIL='---' THEN IROOF=998;
77	1	2	ELSE IROOF=ICEIL;
78	1	2	IF ICOVER='--' THEN ISKY=10;
80	1	2	ELSE ISKY=ICOVER;
			/* CONVERT TEMPERATURE FROM FAHRENHEIT TO KELVIN */
81	1	2	OUTDATA.TEMP(KHR)=0.5556*(ITEMP-32.)*273.15 ;
			/* CONVERT WIND SPEED FROM KNOTS TO METERS/SECOND */
82	1	2	S=ISPEED*0.51444 ;
83	1	2	IF S<1.0 THEN S=1.0 ;
85	1	2	OUTDATA.SPEED(KHR)=S ;
86	1	2	CLD=ISKY*.8;
			/* CHECK FOR CALMS */
87	1	2	IF IDIR=0. THEN IDIR=LWD;
89	1	2	ELSE LWD=IDIR;
90	1	2	XDIR=IDIR*10.;
			/* CALCULATE FLOW VECTOR AND RANDOM FLOW VECTOR */
91	1	2	IF XDIR>180. THEN FV=XDIR-180.;
93	1	2	ELSE FV=XDIR+180.;
94	1	2	OUTDATA.AFV(KHR)=FV;
95	1	2	(NOFIXEDOVERFLOW):B1:BEGIN;
96	2	2	IY=IX*65539 ;
97	2	2	IF IY<0 THEN IY=IY+2147433647+1 ;
99	2	2	YFL=IY ;
100	2	2	YFL=YFL*.4656613E-09 ;
101	2	2	IX=IY ;
102	2	2	END;
103	1	2	IFVR=YFL*10000;
104	1	2	OUTDATA.FVR(KHR)=FV+IFVR-4.0 ;
105	1	2	IF OUTDATA.FVR(KHR)>360. THEN
106	1	2	OUTDATA.FVR(KHR)=OUTDATA.FVR(KHR)-360.;
			/* DETERMINE STABILITY */

PREP: PROCEDURE OPTIONS(MAIN);

STMT	LEVEL	NEST	CODE
107	1	2	IF S>8. THEN GO TO BB;
109	1	2	IF IHOURLTSR THEN GO TO C;
111	1	2	IF IHOURLTSS THEN GO TO C;
113	1	2	/* DETERMINE THE ANGLE OF ELEVATION */
114	1	2	DAYTIME: H1=(15.0*((KHR+ZONE)-AMM)-ALONG)/CONST;
115	1	2	ALFSN=SINLAT*DSIN+DCOS*COSLAT*COS(H1);
116	1	2	ALF=ATAND(ALFSN,SQRT(1.-ALFSN*ALFSN));
117	1	2	ZALF=90.-ALF;
118	1	2	AO=.57+.0045*ZALF;
119	1	2	ZALF=ZALF/CONST;
120	1	2	WATTS1=135.3*AO**2*(1./COS(ZALF))*COS(ZALF);
121	1	3	/* INTERPOLATE INCOMING SOLAR RADIATION FACTOR */
122	1	3	DO I=2 TO 9;
123	1	3	IF CLD>=CLOUD(I) & CLD<=CLOUD(I-1) THEN GO TO A;
124	1	2	END;
125	1	2	K=I-1;
126	1	2	XMULT=CMULT(K)-((CLOUD(K)-CLD)*(CMULT(K)-CMULT(I))/(CLOUD(K)-CLOUD(I)));
127	1	2	WATTS=WATTS1*XMULT;
128	1	2	IF WATTS<10. THEN GO TO C;
129	1	2	/* FIND STABILITY USING RADIATION, WIND, AND CLOUD COVER */
130	1	3	DO J=2 TO 7;
131	1	3	IF S>=WIND(J) & S<=WIND(J-1) THEN GO TO B;
132	1	3	END;
133	1	2	B: M=J-1;
134	1	2	P1=COEF(1,M)+COEF(2,M)*WATTS+COEF(3,M)*WATTS**2+COEF(4,M)*WATTS**3;
135	1	2	P2=COEF(1,J)+COEF(2,J)*WATTS+COEF(3,J)*WATTS**2+COEF(4,J)*WATTS**3;
136	1	2	FKST(KHR)=P1-((WIND(M)-S)*(P1-P2)/(WIND(M)-WIND(J)));
137	1	2	GO TO D;
138	1	2	BB: FKST=3.6;
139	1	2	GO TO D;
140	1	2	/* CALCULATE STABILITY USING CLOUD COVER AND WINDSPEED */
141	1	3	DO J=2 TO 7;
142	1	3	IF S>=WIND(J) & S<=WIND(J-1) THEN GO TO CC;
143	1	3	END;
144	1	2	CC: M=J+6;
145	1	2	MM=J+7;
146	1	2	K=J-1;
147	1	2	P1=COEF(1,M)+COEF(2,M)*CLD+COEF(3,M)*CLD**2+COEF(4,M)*CLD**3;
148	1	2	P2=COEF(1,MM)+COEF(2,MM)*CLD+COEF(3,MM)*CLD**2+COEF(4,MM)*CLD**3;
149	1	2	FKST(KHR)=P1-((WIND(K)-S)*(P1-P2)/(WIND(K)-WIND(J)));
150	1	2	D: KST(KHR)=FKST(KHR)+0.9;
151	1	2	ITEST=10.*(FKST(KHR)+0.4);
152	1	2	OUTDATA.KKST(KHR)=ITEST
153	1	2	IF ITEST>70 THEN OUTDATA.KKST(KHR)=70;
154	1	2	/* CALCULATE MIXING HEIGHT */
155	1	2	IHR=KHR+1;
156	1	2	XHR=IHR;
157	1	2	IF IHR>14 THEN IF XHR<=TSS THEN DO:
160	1	3	HLH(1,KHR)=XAF;
161	1	3	HLH(2,KHR)=XAF;
162	1	3	GO TO NEWREC; END;

PREP: PROCEDURE OPTIONS(MAIN);

STMT	LEVEL	NEST	CODE
164	1	2	IND=2;
165	1	2	IF XHR>TSS THEN DO;
167	1	3	IF KST(KHR)=4 THEN DO;
169	1	4	HLH(2,KHR)=XAF+(XMNP1-XAF)*((XHR-TSS)/(24.-TSS));
170	1	4	IND=1; END;
172	1	3	HLH(IND,KHR)=XAF+(XAF1-XAF)*((XHR-TSS)/(38.-TSS));
173	1	3	IF IND=2 THEN HLH(1,KHR)=HLH(2,KHR);
175	1	3	GO TO NEWREC; END;
177	1	2	IF XHR<=TSR THEN DO;
179	1	3	KSTSP=KST(KHR);
180	1	3	IF KST(KHR)=4 THEN DO;
182	1	4	HLH(2,KHR)=XMN;
183	1	4	IND=1; END;
185	1	3	HLH(IND,KHR)=XAFM1+(XAF-XAFM1)*((24.-TSS+XHR)/(24.-TSS+14.));
186	1	3	IF IND=2 THEN HLH(1,KHR)=HLH(2,KHR);
188	1	3	GO TO NEWREC; END;
190	1	2	IF KSTSP=4 THEN DO;
192	1	3	HLH(2,KHR)=XMN+(XAF-XMN)*((XHR-TSR)/(14.-TSR));
193	1	3	HLH(1,KHR)=XAF*(XHR-TSR)/(14.-TSR);
194	1	3	END;
195	1	2	ELSE DO;
196	1	3	HLH(1,KHR)=XAFM1+(XAF-XAFM1)*((24.-TSS+XHR)/(24.-TSS+14.));
197	1	3	HLH(2,KHR)=HLH(1,KHR);
198	1	3	END;
199	1	2	/* READ NEXT HOUR'S MET DATA */
201	1	3	NEWREC: IF HSKIP=0 THEN DO;
202	1	3	READ FILE(ASHV) INTO(INDATA);
203	1	3	IREC=I: EC+1;
204	1	2	END;
205	1	2	ELSE HSKIP=0;
206	1	1	HLOOP: END;
207	1	1	/* UPDATE MIXING HEIGHTS */
208	1	1	XMNM1=XMN;
209	1	1	XAFM1=XAF;
210	1	1	XMN=XMNP1;
211	1	1	XAF=XAF1;
212	1	1	/* WRITE A DAY'S CALCULATIONS ON TO TAPE */
213	1	1	WRITE FILE(MET) FROM(OUTDATA);
214	1	1	DLOOP: END;
215	1	1	LAST: WRITE FILE(MET) FROM(OUTDATA);
216	1	1	CLOSE FILE(ASHV),FILE(MET);
217	1	1	PUT SKIP FILE(SYSPRINT) EDIT
218	1	1	(' ALL RECORDS HAVE BEEN PROCESSED ') (A(33));
219	1	1	GO TO AGAIN;
220	1	1	FINISH: END PREP;

```

C*** PROGRAM JMHCRS1 (KLUG VALIDATION) 00001800
C*** THIS PROGRAM CALCULATES HOURLY AND 24-HOURLY CONCENTRATIONS FOR 00001900
C*** A YEAR ABOUT A SINGLE SOURCE. 00002000
C*** OCTOBER 1972 VERSION *** 00002100
C*** DESCRIPTION OF ARRAYS *** 00002200
C*** DHRS(L)=RECEPTOR ELEVATION MINUS SOURCE ELEVATION(METERS) 00002300
C*** QHOUR(IHOUR)=HOURLY SOURCE STRENGTH OF SO2(GM/SEC) 00002400
C*** HMAX(RECEPTOR,3) 1=HOURLY CONCENTRATION, 2=DAY, 3=HOUR 00002500
C*** DMAX(RECEPTOR,2) 1=24-HOUR CONCENTRATION, 2=DAY 00002600
C*** HMAXYR(5) 1=MAX HOUR CONCENTRATION, 2=DIRECTION, 3=DISTANCE, 00002700
C*** 4=DAY, 5=HOUR 00002800
C*** JMAXYR(4) 1=MAX 24-HOUR CONCENTRATION, 2=DIRECTION, 3=DISTANCE, 4= 00002900
C*** CHI(RECEPTOR,26) 1-24=HOURLY CONCENTRATIONS, 25=24-HOUR CONCENTRAT 00003000
C*** 25=ANNUAL CONCENTRATION 00003100
C*** IUR IS INDICATOR FOR 1=RURAL, 2=URBAN MIXING HEIGHTS 00003200
C*** 00003300
C*** NSTA=NUMBER OF STATIONS UP TO 7 00003400
C*** NMOD=NUMBER OF MODEL STATIONS =NSTA*36 00003500
0001 DIMENSION RNG(7),DTH(11),IHC(4),SYD(7,60),SZD(7,60),P(6),WS(20),
*HE(20),HMAX(252,3),CHI(252,26),DMAX(252,2),LOOP(6,2), 00003700
*HMAXYR(5),DMAXYR(4),Q(20),HP(20),TS(20),VF(20),ISTAB(24),AWS(24), 00003800
*TEMP(24),AFV(24),AFVR(24),HLH(2,24),TITLE(20),SOURCE(20), 00003900
*IDENT(5),ISTABP(24)
0002 DIMENSION DHRS(7),QHOUR(20,24),IDSOR(3) 00004100
0003 DATA IHC/6,13,18,24/, P/0.1,0.15,0.2,0.25,0.3,0.3/, 00004200
* DTH/-50., -40., -30., -20., -10., 0., 10., 20., 30., 40., 50./ 00004300
0004 DATA HMAXYR/5*0.0/, DMAXYR/4*0.0/ 00004400
0005 DATA LOOP/1, 1, 2, 3, 4, 4, 11, 11, 10, 9, 8, 8/ 00004500
0006 IE=4 00004600
0007 IN=5 00004700
0008 IO=6 00004800
0009 IP=7 00004900
0010 READ(IN,5501) TITLE 00005000
0011 5501 FORMAT(20A4) 00005100
0012 WRITE(IO,5502) TITLE 00005200
0013 5502 FORMAT('1',20A4//1X) 00005300
C*** READ CARD TO INITIALIZE STABILITY AND TO DETERMINE RURAL OR URBAN 00005400
C*** MIXING HEIGHTS 00005500
0014 READ(IN,5502) KSTL,IUR,IDENT,NSTA 00005600
0015 KSTLP=10*KSTL
0016 5502 FORMAT(I11,I1,I17,I1,T20,5A4,T45,I1) 00005700
0017 IF(NSTA.LT.1.OR.NSTA.GT.7) NSTA=7 00005800
0018 READ(IN,603) (DHRS(L),L=1,NSTA) 00005900
0019 603 FORMAT(7F10.2) 00006000
0020 WRITE(IO,604) (DHRS(L),L=1,NSTA) 00006100
0021 604 FORMAT(/,1X,'ELEVATION DIFFERENCES BETWEEN RECEPTOR AND SOURCE LOC 00006200
ATIONS=',7E10.2,/) 00006300
0022 WRITE(IO,5504) IUR 00006400

```

0023	5504	FORMAT(1X,'IUR=',I2,/,)	00006500
	C***	INITIALIZATIONS	00006600
0024		NMOD=NSTA*36	00006700
0025		JDAY=0	00006800
0026		NS=0	00006900
0027		DO 4 I=1,NMOD	00007000
0028		CHI(I,26)=0.0	00007100
0029		DO 3 J=1,3	00007200
0030	3	HMAX(I,J)=0.0	00007300
0031		DO 6 J=1,2	00007400
0032	6	DMAX(I,J)=0.0	00007500
0033	4	CONTINUE	00007600
	C***		00007700
	C***	INPUT RECEPTOR RANGES	00007800
0034		READ(IN,605) RNG	00007900
0035		605 FORMAT(7F10.3)	00008000
	C***	CALCULATE AND STORE SIGMAS FOR 6 STAR. & NSTA DIST.	00008100
	C***	DISTANCE IS ASSUMED TO BE IN KILOMETERS***	00008200
	C***		00008300
0036		DO 7 J=1,NSTA	00008400
0037		X=RNG(J)	00008500
0038		DO 7 KSTP=10,60	
0039		CALL SIGMA(X,X,KSTP,SY,SZ)	
0040		SYD(J,KSTP)=SY	
0041		SZD(J,KSTP)=SZ	
0042	7	CONTINUE	00009000
	C***		00009100
	C***	INPUT SOURCES TO BE CONSIDERED	00009200
0043	2	NS=NS+1	00009300
0044		READ(IN,5501) SOURCE	00009400
0045		READ(IN,2001) HP(NS),TS(NS),VS,D	00009500
0046	200	FORMAT(10,F6.2,8X,3F8.2)	00009600
0047		VF(NS) = 0.785398*VS*D*D	00009700
0048		IF(HP(NS).LE.0.001) GO TO 5	00009800
0049		WRITE(IO,5555) SOURCE	00009900
0050	5555	FORMAT(1X,20A4)	00010000
0051		WRITE(IO,201) NS,HP(NS),TS(NS),VS,D,VF(NS)	00010100
0052	201	FORMAT(1X,'NS=',I2,' HP=',F7.2,' TS=',F5.0,' VS=',	00010200
		*F7.2,' D=',F6.2,' VF=',F8.2//1X)	00010300
0053		GO TO 2	00010400
0054	5	NS=NS-1	00010500
0055		WRITE(IO,203) (RNG(J),J=1,NSTA)	00010600
0056	203	FORMAT(' RANGE(KM)=',7F7.2,/,)	00010700
	C***		00010800
	C***		00010900
	C***	BEGIN LOOP ON DAYS***	00011000
0057		DO 90 IDY=1,365	00011100
	C***	RE-INITIALIZE DAILY AVERAGE AT BEGINNING OF EACH DAY***	00011200

0058	VPS=0.0	00011400
0059	UPS=0.0	00011500
0060	WSS=0.0	00011600
0061	DO 33 IR=1,NMOD	00011700
0062	DO 33 IHR=1,25	00011800
0063	33 CHI(IR,IHR)=1.0E-50	00011900
0064	HMAXT=0.0	00012000
0065	MIH=0	00012100
0066	MJH=0	00012200
	C***	00012300
	C***INPUT INFORMATION FROM MET FILE***	00012400
	C***	00012500
0067	JDAY=JDAY	00012600
0068	READ(9,400) JYR,IMO,JDAY,ISTABP,AWS,TEMP,AFV,AFVR,	
	*((HLH(I,J),J=1,24),I=1,2)	00012800
0069	400 FORMAT(2I2,I3,24I2,24F5.2,24F4.1,24F3.0,24F3.0,48F8.3)	00012900
0070	DO 399 LL=1,24	
0071	IF(ISTABP(LL).LT.10) ISTABP(LL)=10	
0072	IF(ISTABP(LL).GT.70) ISTABP(LL)=70	
0073	ISTAB(LL)=FLOAT(ISTABP(LL))/10.+0.5	
0074	399 CONTINUE	
	C* CHANGE	00013000
	C IF(IDY.GT.10.AND.(JDAY.EQ.(JDAY+1).OR.JDAY.EQ.1)) GO TO 6404	00013100
0075	IF(JDAY.NE.(JDAY+1).AND.JDAY.NE.1) WRITE(IE,6403)	00013200
0076	6403 FORMAT(' MET DATA INPUT ERROR')	00013300
0077	WRITE(IO,6400) JYR,IMO,JDAY	00013400
0078	6400 FORMAT(' JYR=',I2,' IMO=',I2,' JDAY=',I3)	00013500
0079	WRITE(IO,6401) ISTABP	
0080	6401 FORMAT(' ISTAB= ',24(I2,3X))	
0081	WRITE(IO,6402) AWS,TEMP,AFV,AFVR,((HLH(I,J),J=1,24),I=1,2)	00013800
0082	6402 FORMAT(' AWS= ',24(F4.1,1X))/' TEMP=',24(F4.0,1X))/' AFV= ',	00013900
	*24(F4.0,1X))/' AFVR=',24(F4.0,1X))/' HLH1=',12(F5.0,1X))/'	00014000
	*12(F5.0,1X))/' HLH2=',12(F5.0,1X))/'	00014100
	C* CHANGES	00014200
0083	6404 CONTINUE	00014300
0084	IOSOR=IOSOR(3)	00014400
0085	DO 610 IH=1,NS	00014500
0086	DO 610 LOOP3=1,3	00014600
0087	ITHIRD=(LOOP3-1)*8	00014700
0088	READ(10,606) (IOSOR,((QHOUR(IH,IHOUR+ITHIRD)),IHOUR=1,8))	00014800
0089	606 FORMAT(A4,2I2,8E9.3)	00014900
0090	IF(LOOP3.EQ.1) IOID=IOSOR(1)	00015000
0091	IF((LOOP3.GT.1.AND.IOID.NE.IOSOR(1)).OR.(IOSOR(3).NE.(IOSOR+1)	00015100
	6.AND.IOSOR(3).NE.1)) WRITE(IE,607) IOSOR	00015200
0092	607 FORMAT(' ERROR IN SQ2 INPUT ',A4,2(I2,1X))	00015300
	C IF(IDY.LT.10) WRITE(6,608)IOSOR,(QHOUR(IH,IHOUR+ITHIRD),IHOUR=1,8)	00015400
0093	WRITE(6,608)IOSOR,(QHOUR(IH,IHOUR+ITHIRD),IHOUR=1,8)	00015500
0094	608 FORMAT(1X,A4,2(1X,I2),8(2X,E10.3))	00015600

0095	610 CONTINUE	00015700
	C***LOOP ON HOURS	00015800
0096	DO 80 IHR=1,24	00015900
0097	XWS=AWS(IHR)	00016000
0098	FV=AFV(IHR)	00016100
0099	FVR=AFVR(IHR)	00016200
0100	XMH=HLH(IUR,IHR)	00016300
0101	T=TEMP(IHR)	00016400
	C***SUM WIND PERSISTENCE DATA	00016500
0102	FVRAD=FV/57.29578	00016600
0103	UP=XWS*SIN(FVRAD)	00016700
0104	VP=XWS*COS(FVRAD)	00016800
0105	UPS=UPS+UP	00016900
0106	VPS=VPS+VP	00017000
0107	WSS=WSS+XWS	00017100
	C***	00017200
	C***DO NOT ALLOW STABILITY TO VARY RAPIDLY	00017300
	C***	00017400
0108	IF((ISTAB(IHR)-KSTL).GT.1) GO TO 12	00017500
0109	GO TO 13	00017600
0110	12 ISTAB(IHR)=KSTL+1	00017700
0111	ISTABP(IHR)=KSTLP+10	
0112	GO TO 10	00017800
0113	13 IF((KSTL-ISTAB(IHR)).GT.1) ISTAB(IHR)=KSTL-1	00017900
0114	IF((KSTL-ISTAB(IHR)).GT.1) ISTABP(IHR)=KSTKP-10	
0115	10 IF(IUR.NE.2) GO TO 11	00018000
0116	IF(ISTAB(IHR).GT.4) ISTAB(IHR)=4	00018100
0117	IF(ISTAB(IHR).GT.4) ISTABP(IHR)=40	
0118	11 KST=ISTAB(IHR)	00018200
0119	KSTP=ISTABP(IHR)	
0120	KSTL=KST	00018300
0121	KSTLP=KSTP	
	C*** IF STABILITY=7 THE PLUME DOES NOT GET TO THE GROUND***	00018400
0122	IF(ISTABP(IHR).GE.60) GO TO 80	
0123	ILOW=LOOP(KST,1)	00018600
0124	ITOP=LOOP(KST,2)	00018700
	C***	00018800
	C***DETERMINE WIND SPEED AT TOP OF STACK AND PLUME RISE FOR EACH SOURCE	00018900
	C***	00019000
0125	DO 79 IS=1,NS	00019100
0126	WS(IS)=XWS*((HP(IS)/7.)**P(KST))	00019200
0127	F = 3.12139*VF(IS)*(TS(IS)-T)/TS(IS)	00019300
0128	GO TO(71,71,71,71,75,76),KST	00019400
0129	71 IF(F<.55.) 72,73,73	00019500
0130	72 XST=14.*F**.625	00019600
0131	GO TO 74	00019700
0132	73 XST=34.*F**.4	00019800
0133	74 DISTF=3.5*XST	00019900

0134		DHA=1.6*F**0.333333*DISTF**0.666667/WS(IS)	00020000
0135		GO TO 78	00020100
0136	75	DTHDZ = 0.02	00020200
0137		GO TO 77	00020300
0138	76	DTHDZ = 0.035	00020400
0139	77	S = 9.80616*DTHDZ/T	00020500
0140		DHA = 2.9*(F/(WS(IS)*S))**0.333333	00020600
0141	78	HE(IS)=HP(IS)+DHA	00020700
0142	79	CONTINUE	00020800
		C***	00020900
		C***LOOP ON DIRECTIONS***	00021000
		C***	00021100
0143		DO 25 IDT=ILOW,ITOP	00021200
0144		DIR=FV+DTH(IDT)	00021300
0145		IDIR=DIR/10.	00021400
0146		IF(IDIR.LE.0) GO TO 18	00021500
0147		IF(IDIR.LE.36) GO TO 19	00021600
0148		IDIR=IDIR-36	00021700
0149		GO TO 19	00021800
0150	18	IDIR=IDIR+36	00021900
0151	19	ANG=(FVR-DIR)/757.29578	00022000
		C***	00022100
		C***CALCULATE YD AND CONCENTRATIONS FOR EACH DISTANCE***	00022200
		C***YD IS IN METERS	00022300
		C***	00022400
0152		DO 25 J=1,NSTA	00022500
0153		IR=IDIR+36*(J-1)	00022600
0154		YD=RNG(J)*ANG*1000.	00022700
0155		SY=SYD(J,KSTP)	
0156		SZ=SZD(J,KSTP)	
		C***LOOP ON SOURCES***	00023000
0157		DO 310 IH=1,NS	00023100
0158		U=US(IH)	00023200
0159		H=HE(IH)-DHRS(J)	00023300
0160		AN=0.	00023400
		C***IF THE SOURCE IS ABOVE THE LID, NO CONCENTRATION IS ADDED	00023500
0161		IF(H-XMH)40,40,310	00023600
0162	40	C1=0.5*(YD/SY)*(YD/SY)	00023700
0163		IF(C1-50.)50,310,310	00023800
0164	50	CHEK=SZ/XMH	00023900
0165		IF(CHEK.GE.1.6) GO TO 251	00024000
0166		A1=1./(6.28318*U*SY*SZ*EXP(C1))	00024100
0167		IF(A1.LT.1.0E-30) GO TO 310	00024200
0168		C2=2.*SZ*SZ	00024300
0169		C3=H*H/C2	00024400
0170		IF(C3-50.)60,70,70	00024500
0171	60	A2=2./EXP(C3)	00024600
0172		GO TO 110	00024700

0173	70	A2=0.	00024800
0174	110	SUM=0.	00024900
0175		THL=2.*XMH	00025000
0176	120	AN=AN+1.	00025100
0177		C5=AN*THL	00025200
0178		CC=H-C5	00025300
0179		CE=H+C5	00025400
0180		C6=CC*CC/C2	00025500
0181		C8=CE*CE/C2	00025600
0182		IF(C6-50.) 130,140,140	00025700
0183	130	A4=2./EXP(C6)	00025800
0184		GO TO 180	00025900
0185	140	A4=0.	00026000
0186	180	IF(C8-50.) 190,194,194	00026100
0187	190	A6=2./EXP(C8)	00026200
0188		GO TO 240	00026300
0189	194	A6=0.	00026400
0190	240	TOT=A4+A6	00026500
0191		SUM=SUM+TOT	00026600
0192		IF(TOT-0.01) 250,260,260	00026700
0193	260	IF(AN-45.) 120,270,270	00026800
0194	270	WRITE(10,9) RNG(J),YD,H,TOT,SUM	00026900
0195	9	FORMAT(1X,'N GREATER THAN 45',/,6X,'X= ',F7.0,5X,'YD= ',F7.0,5X, *H= ',F5.1,5X,'TOT = ',F7.3,5X,'SUM = ',F7.3)	00027000
0196	250	RC=A1*(A2+SUM)	00027200
0197		GO TO 252	00027300
0198	251	RC=1./(2.5066*SY*XMH*U*EXP(C1))	00027400
0199		IHR=IDY*24+IHR-IDY	00027500
0200	252	CHI(IR,IHR)=CHI(IR,IHR)+QHOUR(IH,IHR)*RC	00027600
0201	310	CONTINUE	00027700
		C***SAVE MAX 1-HOUR CONC FOR THIS 24-HOUR PERIOD	00027800
		C***SPECIFY RECEPTOR WHERE MAX OCCURRED	00027900
0202		IF(CHI(IR,IHR).LE.HMAXT) GO TO 31	00028000
0203		HMAXT=CHI(IR,IHR)	00028100
0204		MIH=IDIR	00028200
0205		MJH=J	00028300
0206		MHH=IHR	00028400
		C***ACCUMULATE 24-HOUR CONCENTRATIONS FOR EACH RECEPTOR	00028500
0207	31	CHI(IR,25)=CHI(IR,25)+CHI(IR,IHR)	00028600
		C***	00028700
		C***CHECK THIS DAY'S MAX 1 HOUR CONC AGAINST MAX FROM PREVIOUS DAYS	00028800
		C*** AT THE SAME RECEPTOR.	00028900
		C***FINAL VALUE IS MAX 1-HOUR CONC FOR EACH RECEPTOR	00029000
0208		IF(CHI(IR,IHR).LE.HMAX(IR,1)) GO TO 25	00029100
0209		HMAX(IR,1)=CHI(IR,IHR)	00029200
0210		HMAX(IR,2)=IDY+.05	00029300
0211		HMAX(IR,3)=IHR+.05	00029400
		C***END OF RANGES AND AZIMUTHS	00029500

0212	25	CONTINUE	00029600
		C***END OF 24 HOUR PERIOD	00029700
0213	80	CONTINUE	00029800
		C***	00029900
		C***OUTPUT HOURLY CONCENTRATIONS FOR THIS DAY	00030000
		C***24 RECORDS OF NMOD HOURLY CONCENTRATIONS***	00030100
		C***	00030200
0214		DO 36 J=1,24	00030300
0215		WRITE(8) (CHI(IR,J),IR=1,NMOD)	00030400
0216	36	CONTINUE	00030500
		C***	00030600
		C***CALCULATE 24-HOUR AVERAGES FOR EACH RECEPTOR	00030700
0217		DMAXT=0.0	00030800
0218		DO 35 I=1,36	00030900
0219		DO 35 J=1,NSTA	00031000
0220		IR=I+36*(J-1)	00031100
0221		CHI(IR,25)=CHI(IR,25)/24.	00031200
0222		IF(CHI(IR,25).LE.DMAXT) GO TO 34	00031300
0223		DMAXT=CHI(IR,25)	00031400
0224		MID=I	00031500
0225		MJD=J	00031600
		C***	00031700
		C***SAVE DAILY AVERAGES***	00031800
		C***	00031900
		C***CHECK THIS DAY'S MAX CONC AGAINST PREVIOUS 24-HOUR MAX.	00032000
		C***FINAL VALUE IS MAX 24 HOUR CONC FOR EACH RECEPTOR	00032100
		C***	00032200
0226	34	IF(CHI(IR,25).LE.DMAX(IR,1)) GO TO 35	00032300
0227		DMAX(IR,1)=CHI(IR,25)	00032400
0228		DMAX(IR,2)=IDY+.05	00032500
		C***	00032600
		C***SUM DAILY AVERAGES FOR CALCULATION OF ANNUAL MEAN	00032700
		C***	00032800
0229	35	CHI(IR,26)=CHI(IR,26)+CHI(IR,25)	00032900
		C***COMPUTE WIND PERSISTANCE	00033000
0230		RSP=SQRT(UPS*UPS+VPS*VPS)/24.	00033100
0231		PERST=RSP/(WSS/24.)	00033200
0232		RATIO=HMAXT/DMAXT	00033300
		C***	00033400
		C***OUTPUT DAILY CONCENTRATIONS	00033500
		C***1 RECORD OF NMOD 24-HOUR CONCENTRATIONS***	00033600
		C***	00033700
0233		WRITE(8) (CHI(IR,25),IR=1,NMOD)	00033800
		C***	00033900
		C***OUTPUT MAX 1-HOUR CONC AND HIGHEST 24-HOUR CONC AT ANY RECEPTOR	00034000
		C WRITE(IP,601) IDY,DMAXT,MID,RNG(MJD),MHM,HMAXT,MIH,RNG(MJH),	00034100
		C *RATIO,PERST,IDENT	00034200
0234	601	FORMAT(I3,1PE11.4,I3,0PF5.1,I3,1PE11.4,I3,0PF5.1,0P2F7.3,I61,5A4)	00034300

0235		WRITE(IO,600) IDY,HMAXT,MIH,RNG(MJH),MHH,DMAXT,MID,RNG(MJD)	00034400
0236	600	FORMAT(' DAY= ',I3,' MAX HOURLY CONC=',1PE13.6,' DIRECTION=',	00034500
		*I2,' DISTANCE=',OPF7.1,' KM HOUR=',I2/Ix,T11,	00034600
		*MAX 24-HOUR CONC=',1PE13.6,' DIRECTION=',I2,' DISTANCE='.	00034700
		*OPF7.1,' KM')	00034800
0237		WRITE(IO,7000) RATIO,PERST	00034900
0238	7000	FORMAT(' RATIO=',F9.3,' PERSIST=',F9.3//IX)	00035000
0239		IF(HMAXT.LE.HMAXYR(1)) GO TO 85	00035100
0240		HMAXYR(1)=HMAXT	00035200
0241		HMAXYR(2)=MIH	00035300
0242		HMAXYR(3)=RNG(MJH)	00035400
0243		HMAXYR(4)=IDY	00035500
0244		HMAXYR(5)=MHH	00035600
0245	85	IF(DMAXT.LE.DMAXYR(1)) GO TO 90	00035700
0246		DMAXYR(1)=DMAXT	00035800
0247		DMAXYR(2)=MID	00035900
0248		DMAXYR(3)=RNG(MJD)	00036000
0249		DMAXYR(4)=IDY	00036100
		C***END DAILY LOOP***	00036200
0250	90	CONTINUE	00036300
		C***	00036400
		C***CALCULATE ANNUAL MEANS AND DETERMINE THE MAXIMUM	00036500
		C***	00036600
0251		AMMAX=0.0	00036700
0252		MAXI=0	00036800
0253		MAXJ=0	00036900
0254		DO 91 I=1,36	00037000
0255		DO 91 J=1,NSTA	00037100
0256		IR=I+36*(J-1)	00037200
0257		CHI(IR,26)=CHI(IR,26)/365.	00037300
0258		IF(CHI(IR,26).LE.AMMAX) GO TO 91	00037400
0259		AMMAX=CHI(IR,26)	00037500
0260		MAXI=I	00037600
0261		MAXJ=J	00037700
0262	91	CONTINUE	00037800
		C***	00037900
		C***OUTPUT ANNUAL MEAN AT EACH RECEPTOR AND PRINT RECEPTOR WITH HIGHEST	00038000
		C*** ANNUAL MEAN CONCENTRATION	00038100
		C***1 RECORD OF NMOD MEAN ANNUAL CONCENTRATIONS***	00038200
		C***	00038300
0263		WRITE(8) (CHI(IR,26),IR=1,NMOD)	00038400
		C***PUNCH HMAXYR,DMAXYR & AMMAX, HOURLY,DAILY & YEARLY MAXIMA FOR THE YE	00038500
		C WRITE(IP,710) HMAXYR,IDENT	00038600
0264	710	FORMAT(' MAX HOURLY ',1PE11.4,OPF4.0,OPF5.1,OPF5.0,OPF4.0,T61,5A4)	00038700
		C WRITE(IP,720) DMAXYR,IDENT	00038800
0265	720	FORMAT(' MAX DAILY ',1PE11.4,OPF4.0,OPF5.1,OPF5.0,T61,5A4)	00038900
		C WRITE(IP,730) AMMAX,MAXI,RNG(MAXJ),IDENT	00039000
0266	730	FORMAT(' MAX ANNUAL ',1PE11.4,I3,OPF5.1,T61,5A4)	00039100

```

C      DO 740 I=1,36
C      WRITE(IP,703) I,(CHI((I+36*(J-1)),26),J=1,5),IDENT
0267 703 FORMAT(I3,1P5E11.4,T61,5A4)
C      IF(NSTA.GT.5) WRITE(IP,704) (CHI((I+36*(J-1)),26),J=6,7)
0268 704 FORMAT(I3,1P2E11.4)
0269 740 CONTINUE
C***WRITE MAX ANNUAL MEAN***
0270 WRITE(IO,5500) TITLE
0271 WRITE(IO,700) AMMAX,MAXI,RNG(MAXJ)
0272 700 FORMAT(1X,T4,' MAXIMUM MEAN CONC=',1PE12.4,' DIRECTION=',
*13,' DISTANCE=',0PF5.1,' KM'//1X)
C***
C*** PRINT ANNUAL MEANS***
C***
0273 WRITE(IO,900) (RNG(IDUM),IDUM=1,NSTA)
0274 900 FORMAT(1X, /1X,T21,'ANNUAL MEAN CONCENTRATION AT EACH RECEPTOR'
*OR'/1X,T7,'RANGE',2X,7(F5.1,' KM',7X)/1X,T2,'DIR')
0275 DO 420 I=1,36
0276 WRITE(IO,800) I,(CHI((I+36*(J-1)),26),J=1,NSTA)
0277 800 FORMAT(1X,T3,I2,T10,1P7E15.5)
0278 420 CONTINUE
C***
C*** PRINT HIGHEST 24-HOUR CONCENTRATION FOR THE YEAR AT EACH RECEPTOR
0279 WRITE(IO,5500) TITLE
0280 WRITE(IO,705) DMXYR
0281 705 FORMAT(1X,'YEARLY MAXIMUM 24-HOUR CONC=',1PE12.4,' DIRECTION=',
*0PF4.0,' DISTANCE=',0PF5.1,' KM', ' DAY=',0PF5.0//1X)
0282 WRITE(IO,910) (RNG(IDUM),IDUM=1,NSTA)
0283 910 FORMAT(1X, /1X,T17,'HIGHEST 24-HOUR CONCENTRATION AT EACH RECEPTOR'
*CEPTOR'/1X,T4,'RANGE',7(F5.1,' KM',7X)/1X,T2,'DIR')
0284 DO 421 I=1,36
0285 WRITE(IO,801) I,(DMAX((I+36*(J-1)),1),J=1,NSTA)
0286 801 FORMAT(1X,T3,I2,T6,7(1PE15.5))
0287 WRITE(IO,803) I,(DMAX((I+36*(J-1)),2),J=1,NSTA)
0288 803 FORMAT(1X,'(I,12,')',7(9X,'(,0PF4.0,')'))
0289 421 CONTINUE
C***
C*** PRINT HIGHEST 1-HOUR CONCENTRATIONS FOR THE YEAR AT EACH RECEPTOR
0290 WRITE(IO,5500) TITLE
0291 WRITE(IO,701) HMAXYR
0292 701 FORMAT(1X,'YEARLY MAXIMUM 1-HOUR CONC=',1PE12.4,' DIRECTION=',
*0PF4.0,' DISTANCE=',0PF5.1,' KM', ' DAY=',0PF5.0,' HOUR=',
*0PF4.0//1X)
0293 WRITE(IO,920) (RNG(IDUM),IDUM=1,NSTA)
0294 920 FORMAT(1X, /1X,T17,'HIGHEST 1-HOUR CONCENTRATION AT EACH RECEPTOR'
*EPTOR'/1X,T4,'RANGE',7(F5.1,' KM',7X)/1X,T2,'DIR')
0295 DO 422 I=1,36
0296 WRITE(IO,802) I,(HMAX((I+36*(J-1)),1),J=1,NSTA)

```

0297	502	FORMAT(1X,T3,I2,T6,7(1PE15.5))	00044000
0298		WRITE(10,804) I,((HMAX((I+36*(J-1)),L),L=2,3),J=1,NSTA)	00044100
0299	804	FORMAT(1X,'(',I2,')',7(5X,'(',OP2F4.0,')'))	00044200
0300	422	CONTINUE	00044300
0301		CALL EXIT	00044400
0302		END	00044500

```

0001      SUBROUTINE SIGMA1 (X,XY,KST,SY,SZ)
      C SUBROUTINE TO CALCULATE SIGMA Y AND SIGM Z USING F.B.SMITH'S METHOD.
      C (SMITH-SIGMA Z,PASQUILL-SIGMA Y)
0002      GO TO (10,20,30,40,50,60),KST
      C STABILITY A(10)
0003      10 TH = (24.167 - 2.5334*ALOG(XY))/57.2958
0004      SZ=.112*(X*1000.)**.06/(1.+.000538*(X*1000.)**.815)
0005      GO TO 71
      C STABILITY B(20)
0006      20 TH = (18.333 - 1.8096*ALOG(XY))/57.2958
0007      SZ=.130*(X*1000.)**.950/(1.+.000652*(X*1000.)**.750)
0008      GO TO 71
      C STABILITY C(30)
0009      30 TH = (12.5 - 1.0857*ALOG(XY))/57.2958
0010      SZ=.112*(X*1000.)**.9207/(1.+.000903*(X*1000.)**.718)
0011      GO TO 71
      C STABILITY D(40)
0012      40 TH = (9.3333-0.72382*ALOG(XY))/57.2958
0013      SZ=.098*(X*1000.)**.889/(1.+.00135*(X*1000.)**.698)
0014      GO TO 71
      C STABILITY E(50)
0015      50 TH = (6.25 - 0.54287*ALOG(XY))/57.2958
0016      SZ=.0609*(X*1000.)**.895/(1.+.00196*(X*1000.)**.684)
0017      GO TO 71
      C STABILITY F(60)
0018      60 TH = (4.1667 - 0.36191*ALOG(XY))/57.2958
0019      SZ=.0638*(X*1000.)**.7837/(1.+.00136*(X*1000.)**.672)
0020      71 SY = 1000. * XY * SIN(TH)/(2.15 * COS(TH))
0021      RETURN
0022      END

```

```
0001 SUBROUTINE SIGMA(X,XY,KST,SY,SZ)
0002 FKST=FLOAT(KST)/10.
0003 KST1=FKST
0004 KST2=KST1+1
0005 IF(KST1.LT.1) KST1=1
0006 IF(KST2.GT.6) KST2=6
0007 CALL SIGMA1(X,XY,KST1,SY1,SZ1)
0008 CALL SIGMA1(X,XY,KST2,SY2,SZ2)
0009 DY=SY2-SY1
0010 DZ=SZ2-SZ1
0011 DK=FKST-KST1
0012 SY=SY1+DK*DY
0013 SZ=SZ1+DK*DZ
0014 RETURN
0015 END
```

ELEVATION DIFFERENCES BETWEEN RECEPTOR AND SOURCE LOCATIONS= 0.64E+02 0.82E+02 0.10E+03 0.13E+03
IUR= 1

MUSKINGUM RIVER POWER PLANT STACK 1 BOILERS 1-4 00062500
NS= 1 HP= 251.00 TS= 430. VS= 28.50 D= 7.60 VF= 1292.89

MUSKINGUM RIVER POWER PLANT STACK 2 BOILER 5 00062700
NS= 2 HP= 251.00 TS= 425. VS= 24.80 D= 6.70 VF= 874.36

RANGE(KM)= 5.27 4.28 8.26 19.63

JYR=73 IMO= 1 JDAY= 1
ISTAB= 70 70 70 70 60 70 70 45 70 36 35 29 34 32 34 34 34 47 67 63 59 63 70 70
AWS= 2.6 2.6 2.1 3.1 4.1 2.1 2.6 5.6 3.1 5.1 6.2 5.1 7.2 6.2 6.7 6.2 4.6 5.1 3.1 3.6 3.6 3.1 2.6 3.1
TEMP=277. 277. 276. 275. 275. 275. 274. 274. 274. 274. 275. 277. 278. 279. 280. 280. 281. 279. 278. 276. 276. 275. 274. 274.
AFV= 20. 20. 20. 20. 20. 20. 20. 50. 20. 60. 60. 80. 60. 60. 60. 50. 50. 70. 80. 80. 90. 110. 120. 110.
AFVR= 20. 22. 21. 19. 16. 22. 18. 50. 18. 60. 64. 83. 65. 57. 62. 50. 46. 70. 85. 79. 94. 112. 118. 115.
HLH1=1002. 1002. 1002. 1002. 1002. 1002. 1002. 21. 195. 348. 512. 675.
839. 1002. 1002. 1002. 1002. 996. 988. 980. 972. 965. 957. 949.
HLH2= 958. 958. 958. 958. 958. 958. 958. 959. 966. 973. 980. 988.
995. 1002. 1002. 1002. 1002. 984. 959. 935. 911. 887. 863. 839.
MUS4 1 1 0.426E+04 0.426E+04 0.423E+04 0.424E+04 0.424E+04 0.424E+04 0.435E+04 0.432E+04
MUS4 1 1 0.426E+04 0.439E+04 0.439E+04 0.444E+04 0.440E+04 0.434E+04 0.426E+04 0.426E+04
MUS4 1 1 0.442E+04 0.441E+04 0.463E+04 0.517E+04 0.512E+04 0.461E+04 0.442E+04 0.437E+04
MUS5 1 1 0.147E+04 0.147E+04 0.142E+04 0.143E+04 0.143E+04 0.142E+04 0.143E+04 0.142E+04
MUS5 1 1 0.142E+04 0.144E+04 0.142E+04 0.143E+04 0.145E+04 0.144E+04 0.134E+04 0.139E+04
MUS5 1 1 0.152E+04 0.147E+04 0.151E+04 0.186E+04 0.167E+04 0.142E+04 0.142E+04 0.146E+04
DAY= 1 MAX HOURLY CONC= 6.336607E-04 DIRECTION= 6 DISTANCE= 8.3 KM HOUR=10
MAX 24-HOUR CONC= 6.656564E-05 DIRECTION= 6 DISTANCE= 8.3 KM
RATIO= 9.519 PERSIST= 0.898

JYR=73 IMO= 1 JDAY= 2
ISTAB= 70 70 70 70 57 54 53 56 48 38 27 25 22 21 21 25 35 65 46 46 48 48 46 45
AWS= 3.1 3.1 2.1 2.6 2.6 2.1 2.6 1.5 1.0 1.0 1.0 3.1 2.6 2.1 2.1 2.1 1.5 1.0 1.0 1.0 1.0 1.0 1.0 1.5
TEMP=273. 273. 272. 271. 271. 271. 271. 270. 270. 270. 271. 272. 273. 274. 275. 276. 276. 275. 274. 274. 273. 271. 271. 271.
AFV= 110. 100. 40. 40. 60. 120. 160. 130. 130. 130. 130. 50. 80. 360. 170. 20. 200. 200. 200. 200. 200. 200. 280.
AFVR= 113. 101. 41. 39. 64. 117. 158. 129. 126. 129. 130. 53. 81. 2. 172. 23. 205. 202. 198. 204. 199. 205. 201. 279.
HLH1= 941. 933. 925. 918. 910. 902. 894. 18. 155. 292. 428. 565.
702. 839. 839. 839. 839. 817. 788. 760. 731. 702. 673. 644.
HLH2= 839.
839. 839. 839. 839. 839. 772. 583. 595. 506. 418. 329. 241.
MUS4 1 2 0.460E+04 0.464E+04 0.460E+04 0.469E+04 0.471E+04 0.511E+04 0.584E+04 0.621E+04
MUS4 1 2 0.758E+04 0.838E+04 0.843E+04 0.940E+04 0.842E+04 0.848E+04 0.852E+04 0.869E+04
MUS4 1 2 0.840E+04 0.829E+04 0.841E+04 0.830E+04 0.840E+04 0.850E+04 0.734E+04 0.599E+04
MUS5 1 2 0.169E+04 0.174E+04 0.174E+04 0.174E+04 0.175E+04 0.175E+04 0.174E+04 0.177E+04
MUS5 1 2 0.227E+04 0.235E+04 0.211E+04 0.227E+04 0.225E+04 0.225E+04 0.228E+04 0.229E+04
MUS5 1 2 0.199E+04 0.202E+04 0.225E+04 0.223E+04 0.224E+04 0.224E+04 0.191E+04 0.154E+04
DAY= 2 MAX HOURLY CONC= 1.101867E-03 DIRECTION=20 DISTANCE= 19.6 KM HOUR=23
MAX 24-HOUR CONC= 1.917259E-04 DIRECTION=20 DISTANCE= 19.6 KM
RATIO= 5.747 PERSIST= 0.459

JYR=73 IMO= 1 JDAY= 3
ISTAB= 42 52 43 41 41 41 41 41 41 41 39 36 34 34 35 38 40 40 40 40 40 40 41 41
AWS= 3.6 3.1 2.1 3.6 2.6 3.1 1.5 3.6 3.6 3.1 2.6 2.1 2.6 2.1 2.1 2.1 4.1 4.6 5.1 5.2 5.6 5.6 3.6 3.6
TEMP=271. 272. 272. 272. 272. 273. 273. 273. 273. 274. 274. 275. 275. 275. 275. 275. 277. 279. 280. 281. 283. 283. 283. 283.
AFV= 240. 200. 240. 250. 240. 220. 200. 270. 240. 240. 300. 280. 300. 280. 240. 260. 290. 300. 310. 320. 320. 360. 340. 10.

APPENDIX C .

CONCENTRATION PROFILES FOR THE CANAL AND MUSKINGUM
PLANTS FOR DIFFERENT SETS OF DISPERSION CURVES

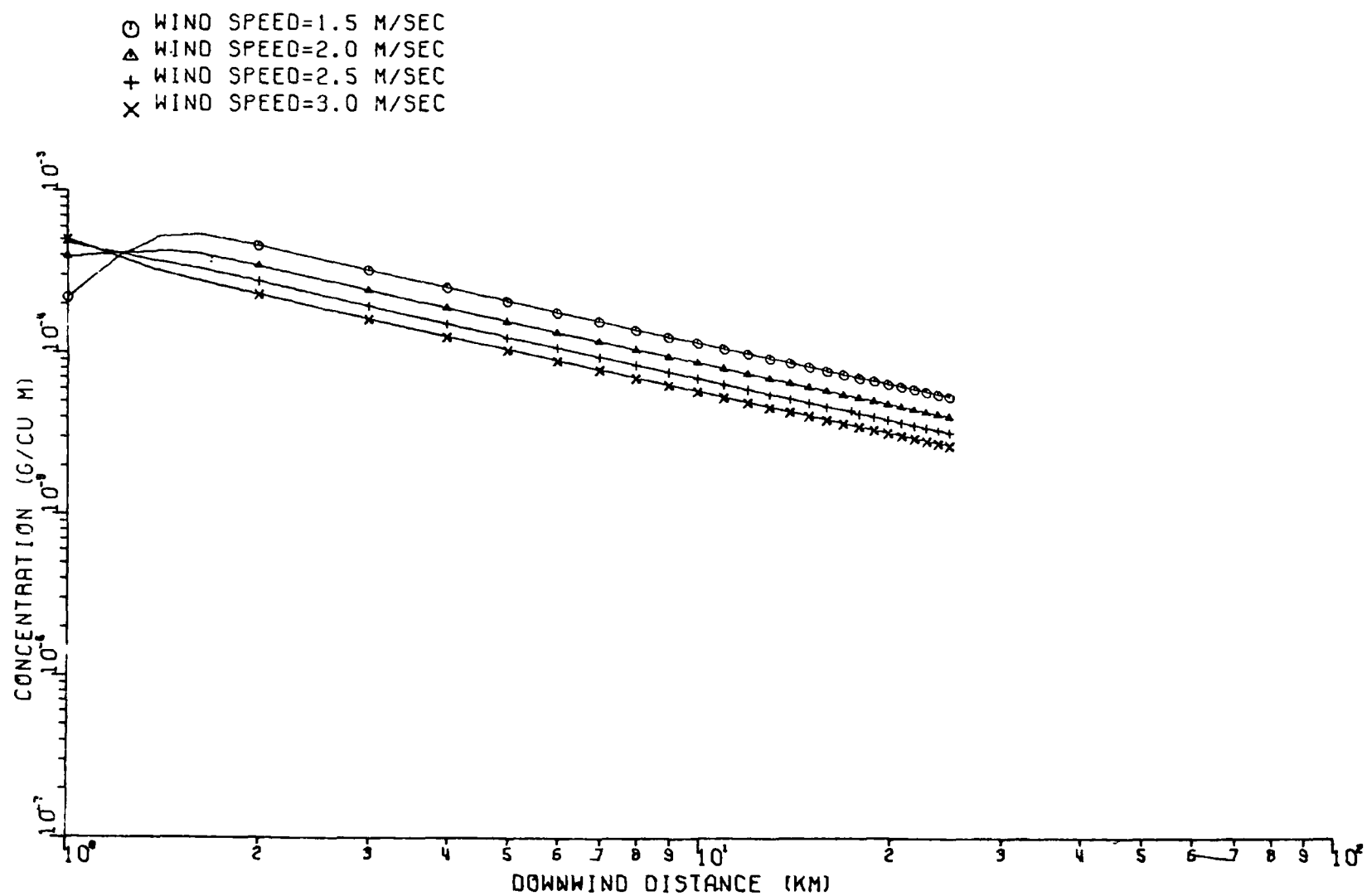


Figure C-1a. Plume centerline concentration versus downwind distance for stability Class A at the Canal Plant. Pasquill-Turner dispersion curves used. Flat terrain assumed. Wind speeds are at stack top

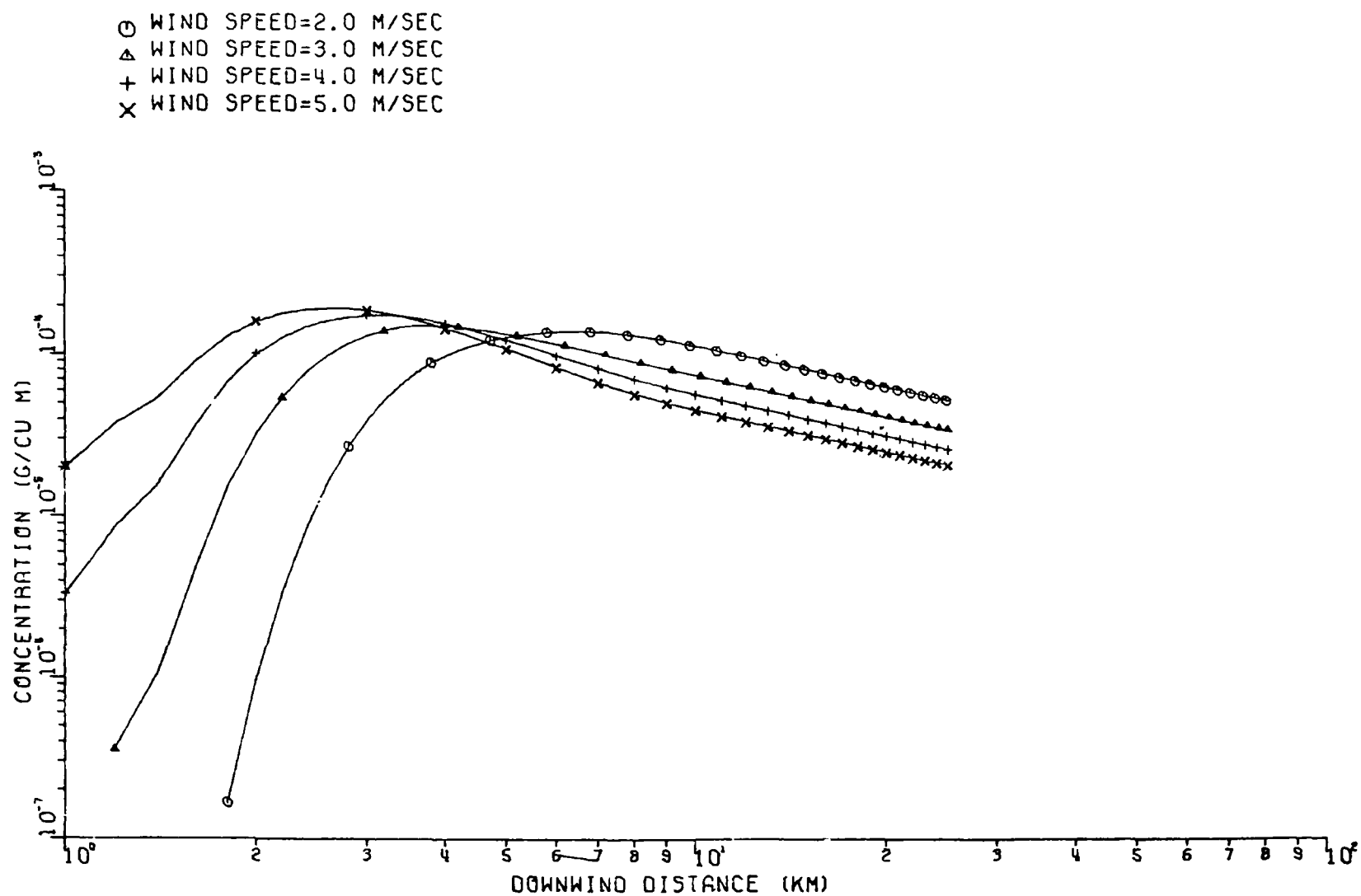


Figure C-1b. Plume centerline concentration versus downwind distance for stability Class B at the Canal Plant. Pasquill-Turner dispersion curves used. Flat terrain assumed. Wind speeds are at stack top

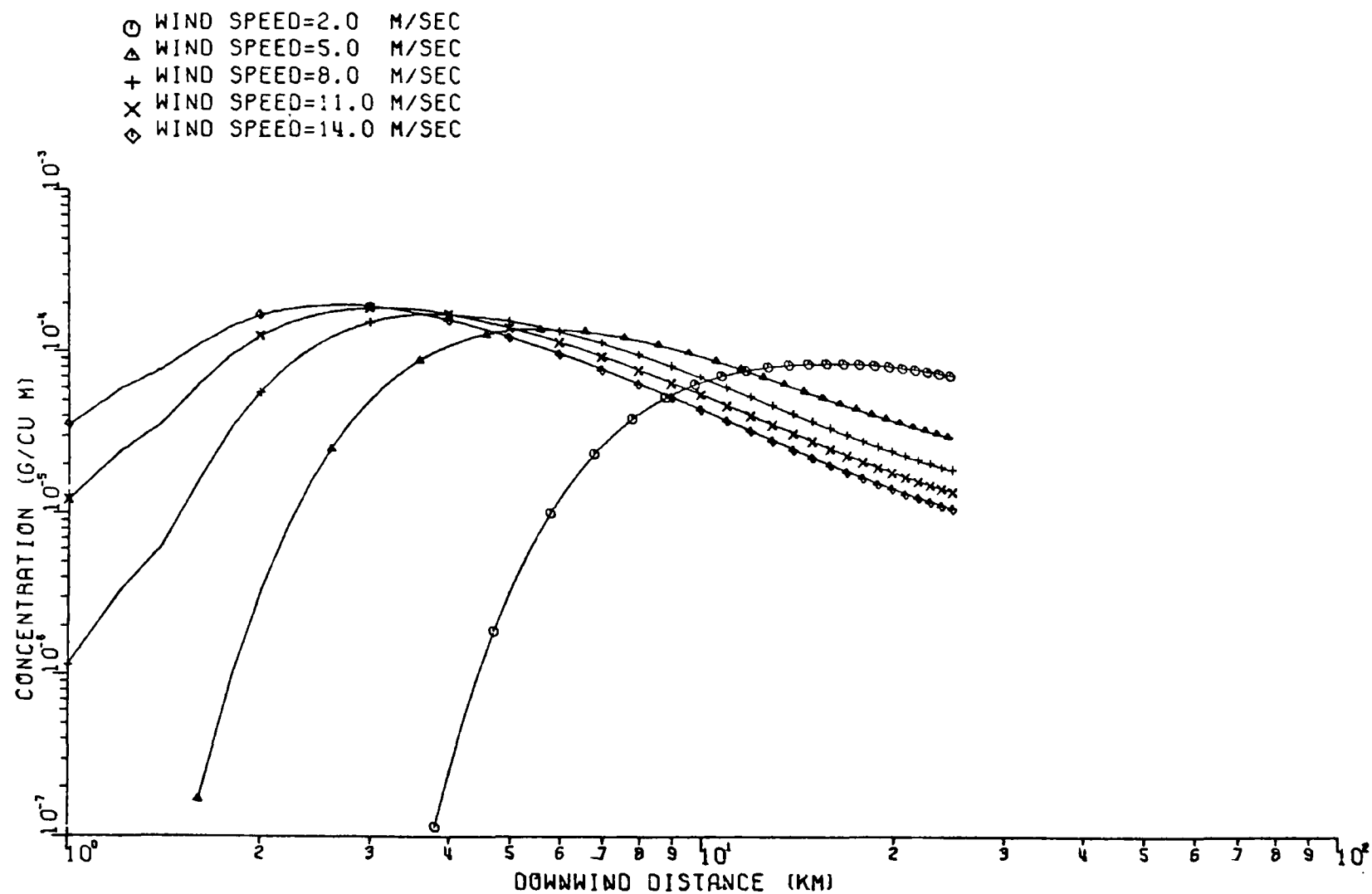


Figure C-1c. Plume centerline concentration versus downwind distance for stability Class C at the Canal Plant. Pasquill-Turner dispersion curves used. Flat terrain assumed. Wind speeds are at stack top

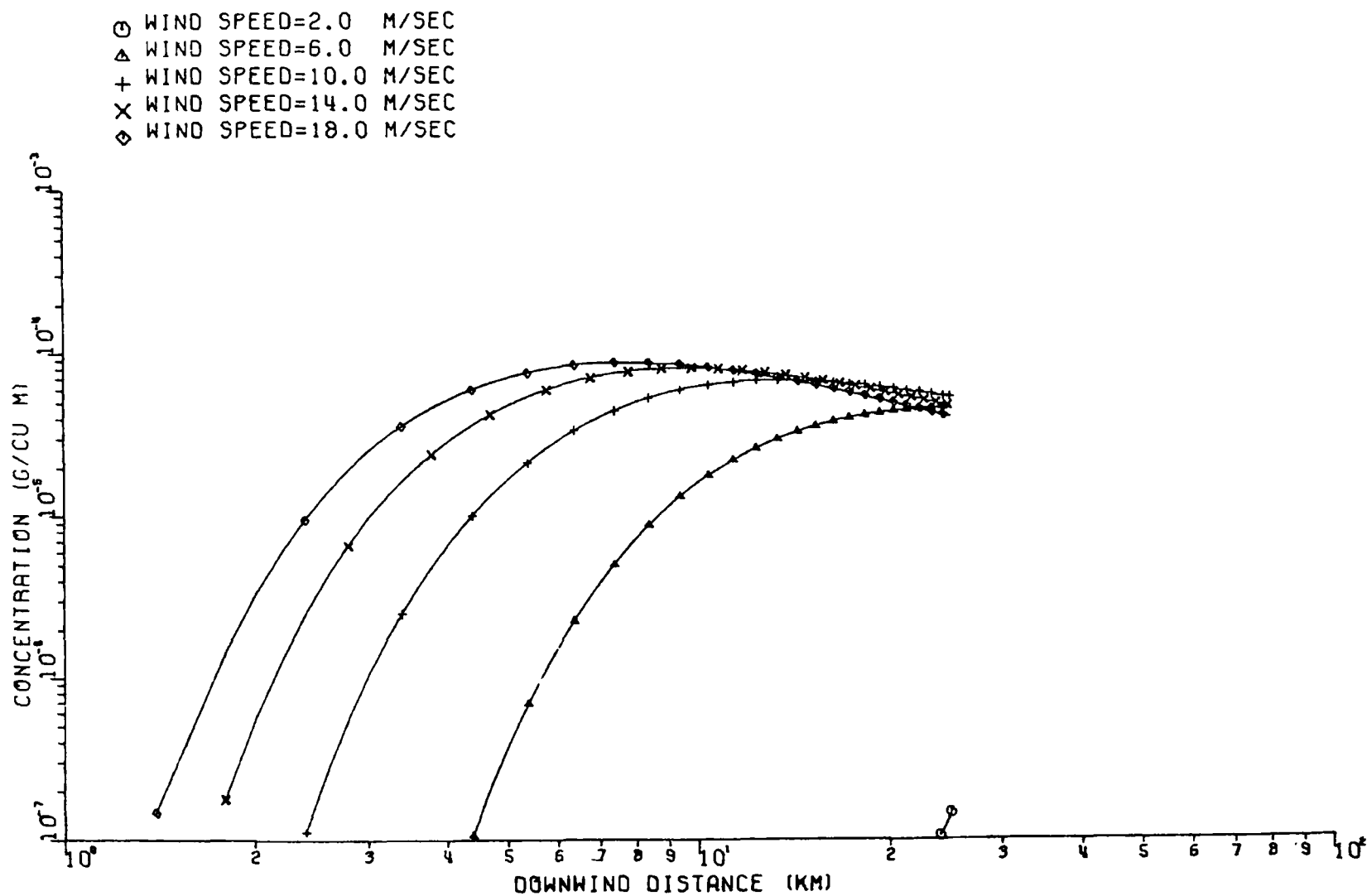


Figure C-1d. Plume centerline concentration versus downwind distance for stability Class D at the Canal Plant. Pasquill-Turner dispersion curves used. Flat terrain assumed. Wind speeds are at stack top

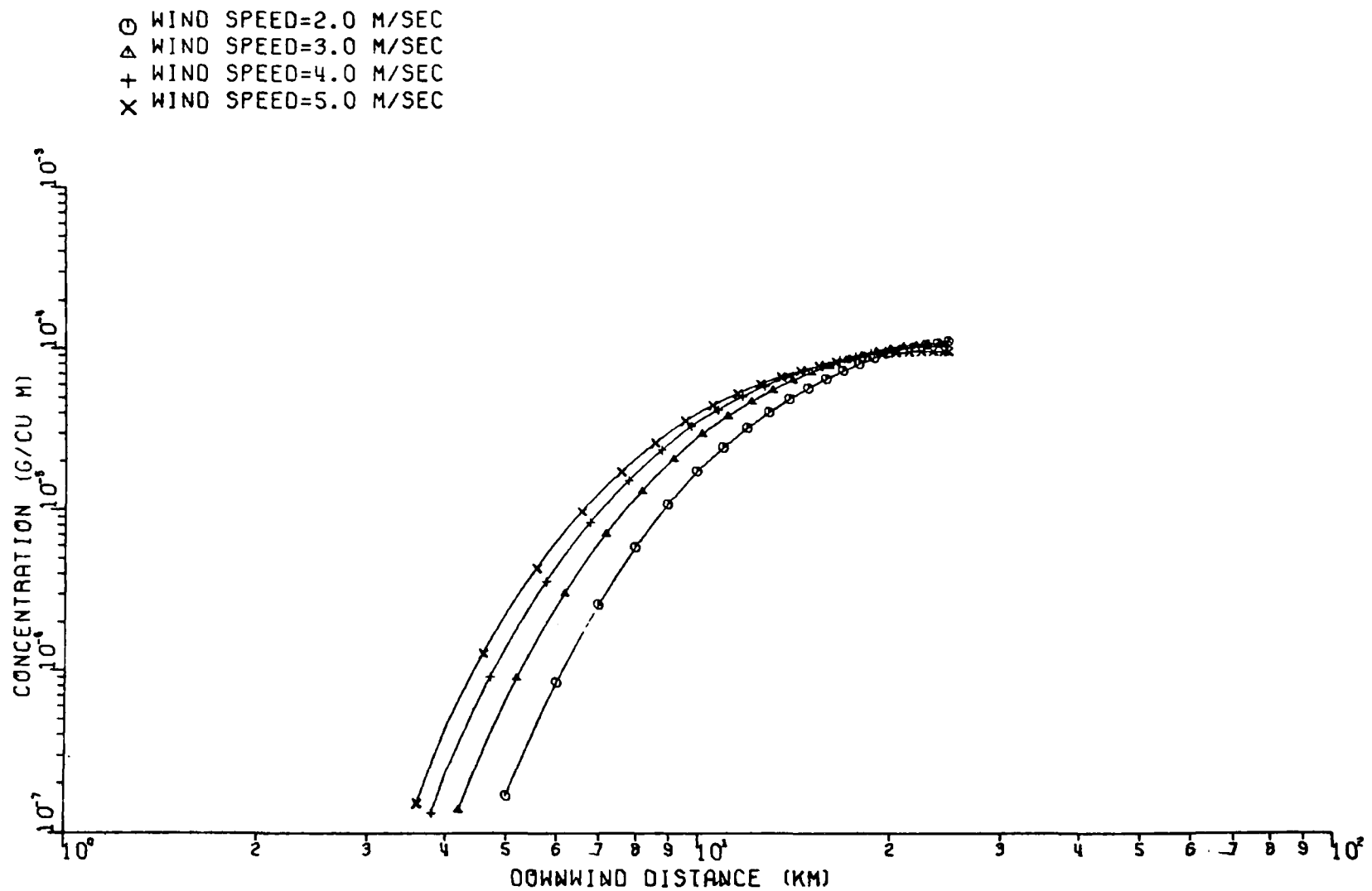


Figure C-1e. Plume centerline concentration versus downwind distance for stability Class E at the Canal Plant. Pasquill-Turner dispersion curves used. Flat terrain assumed. Wind speeds are at stack top

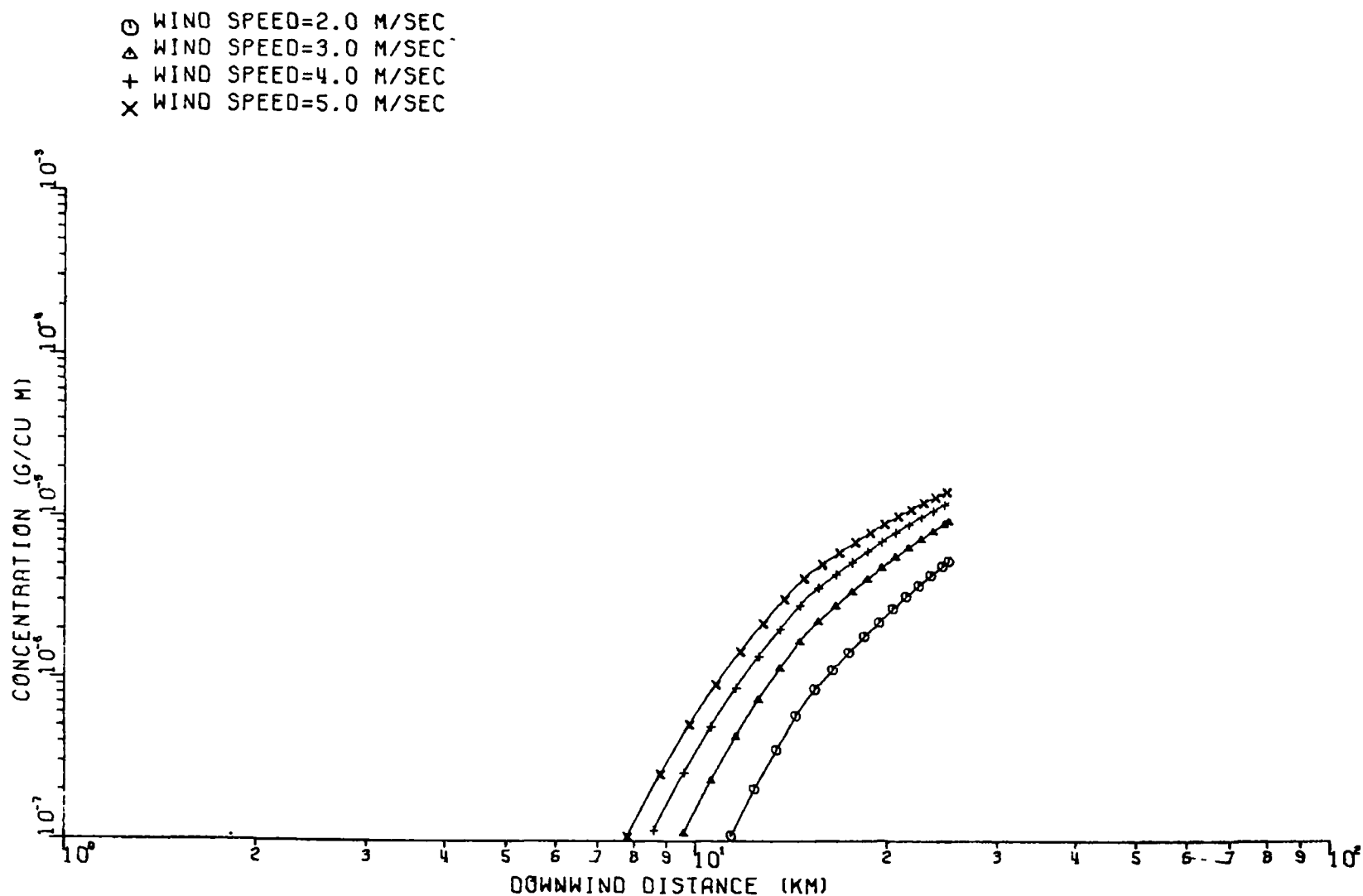


Figure C-1f. Plume centerline concentration versus downwind distance for stability Class F at the Canal Plant. Pasquill-Turner dispersion curves used. Flat terrain assumed. Wind speeds are at stack top

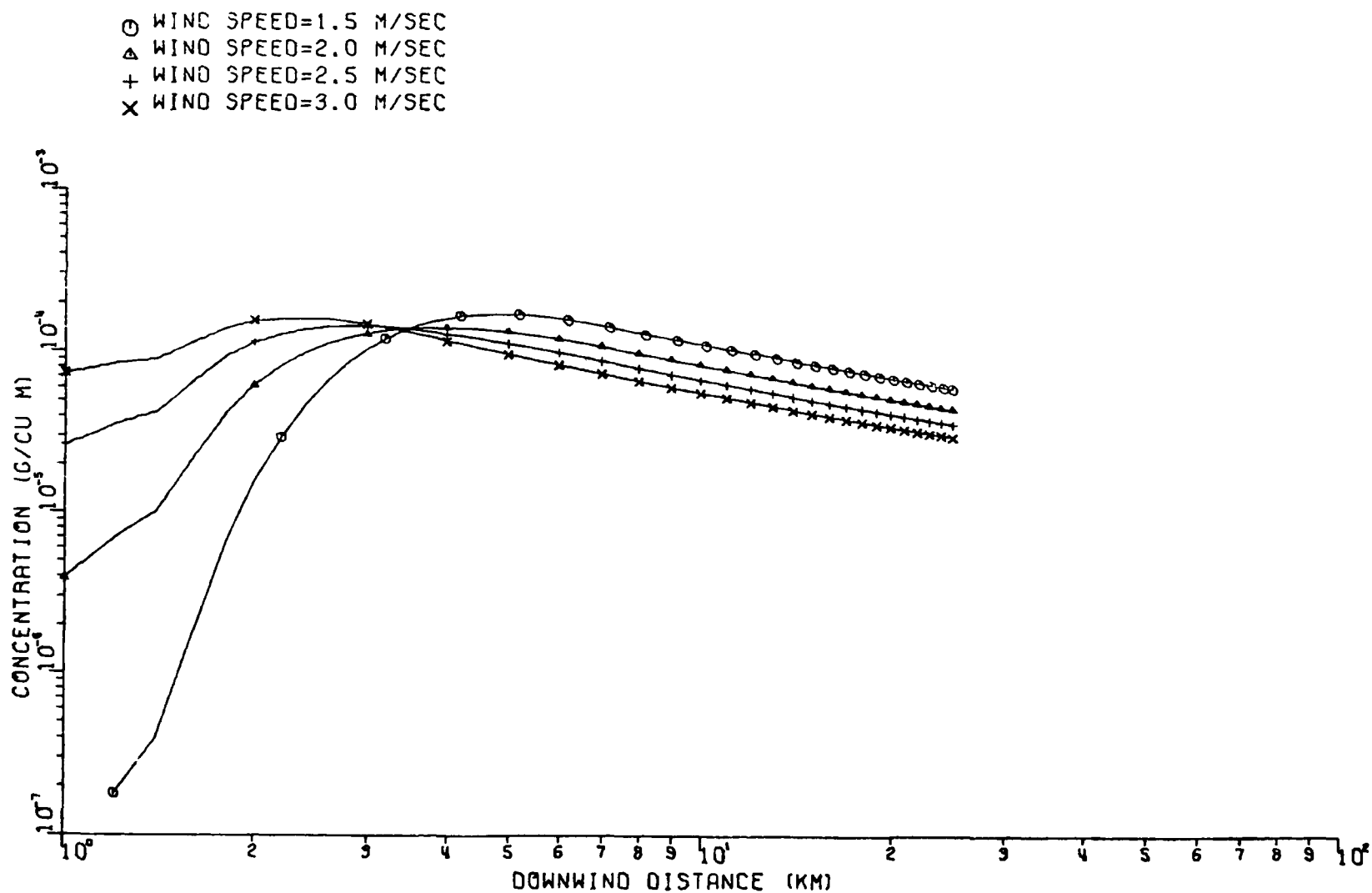


Figure C-2a. Plume centerline concentration versus downwind distance for stability Class A at the Canal Plant. Gifford-Briggs dispersion curves used. Flat terrain assumed. Wind speeds are at stack top

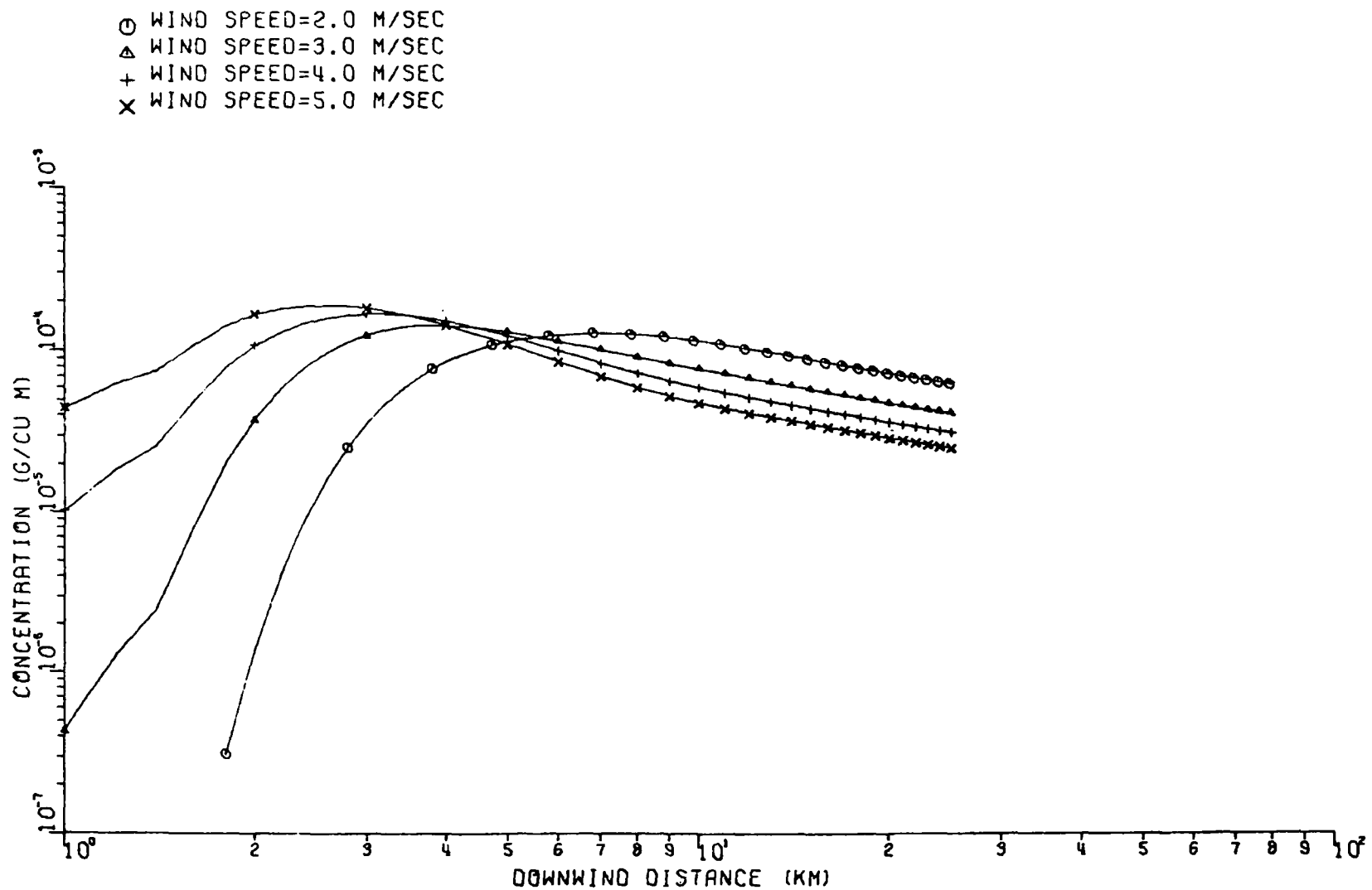


Figure C-2b. Plume centerline concentration versus downwind distance for stability Class B at the Canal Plant. Gifford-Briggs dispersion curves used. Flat terrain assumed. Wind speeds are at stack top

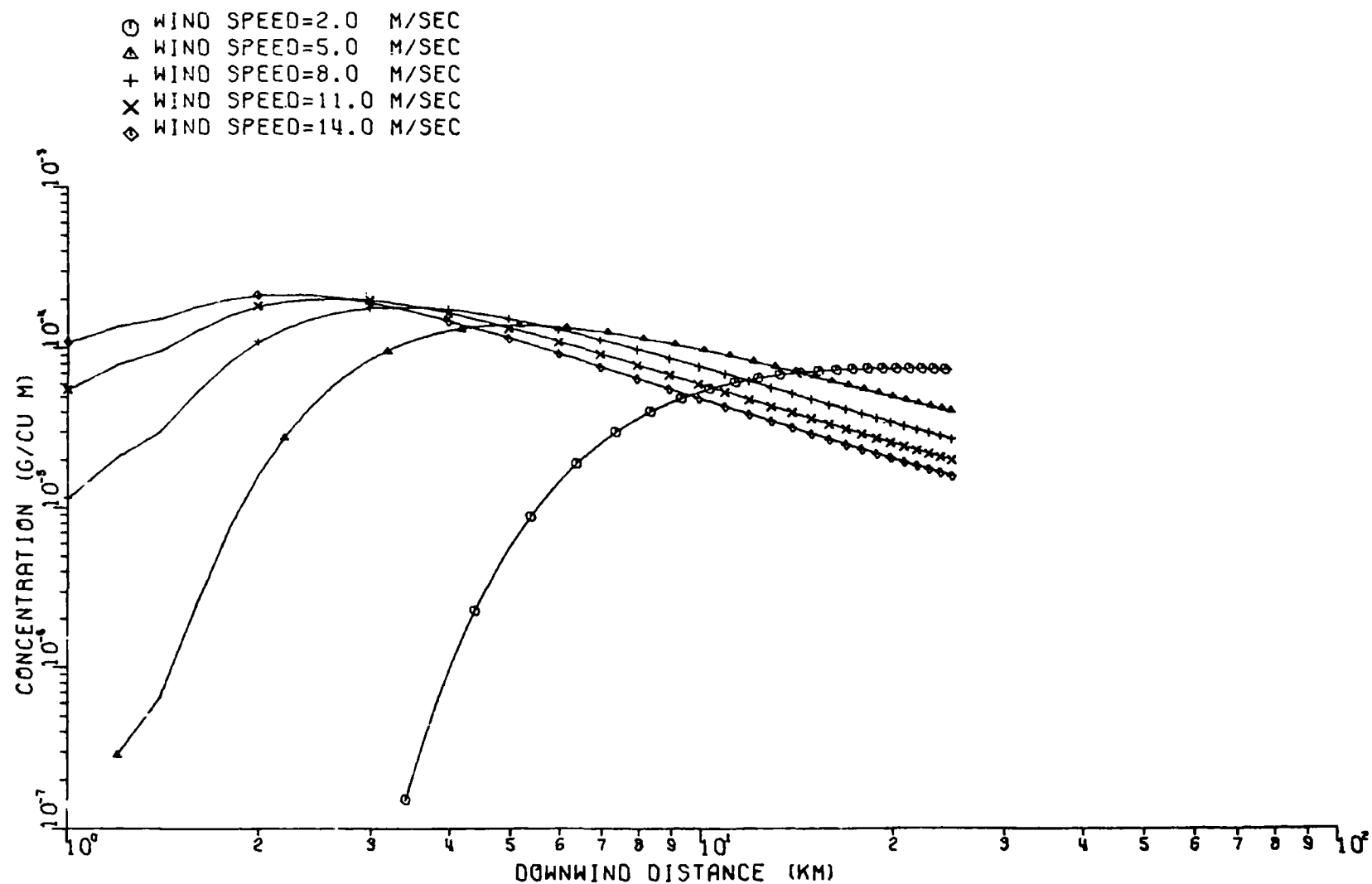


Figure C-2c. Plume centerline concentration versus downwind distance for stability Class C at the Canal Plant. Gifford-Briggs dispersion curves used. Flat terrain assumed. Wind speeds are at stack top

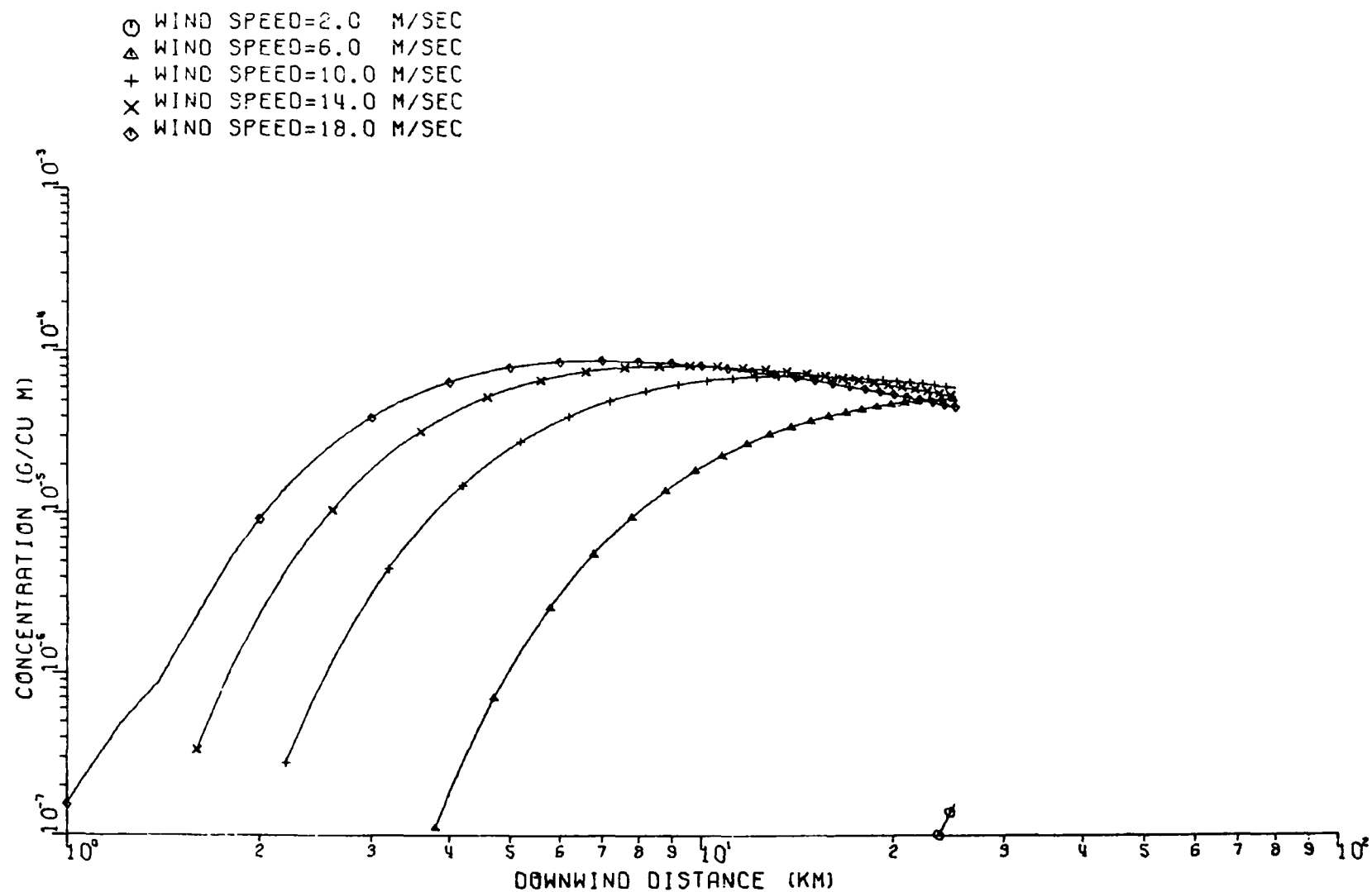


Figure C-2d. Plume centerline concentration versus downwind distance for stability Class D at the Canal Plant. Gifford-Briggs dispersion curves used. Flat terrain assumed. Wind speeds are at stack top

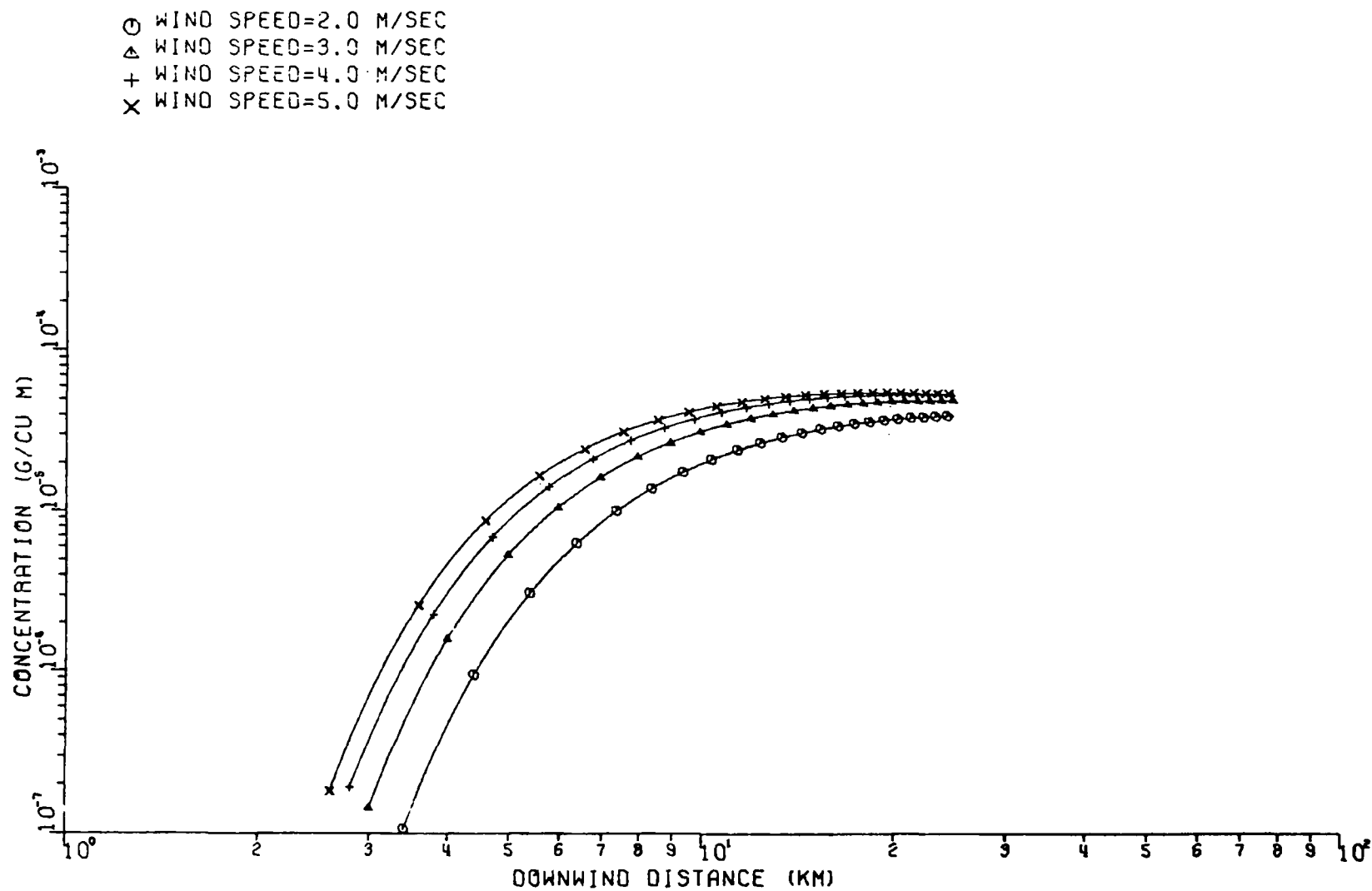


Figure C-2e. Plume centerline concentration versus downwind distance for stability Class E at the Canal Plant. Gifford-Briggs dispersion curves used. Flat terrain assumed. Wind speeds are at stack top

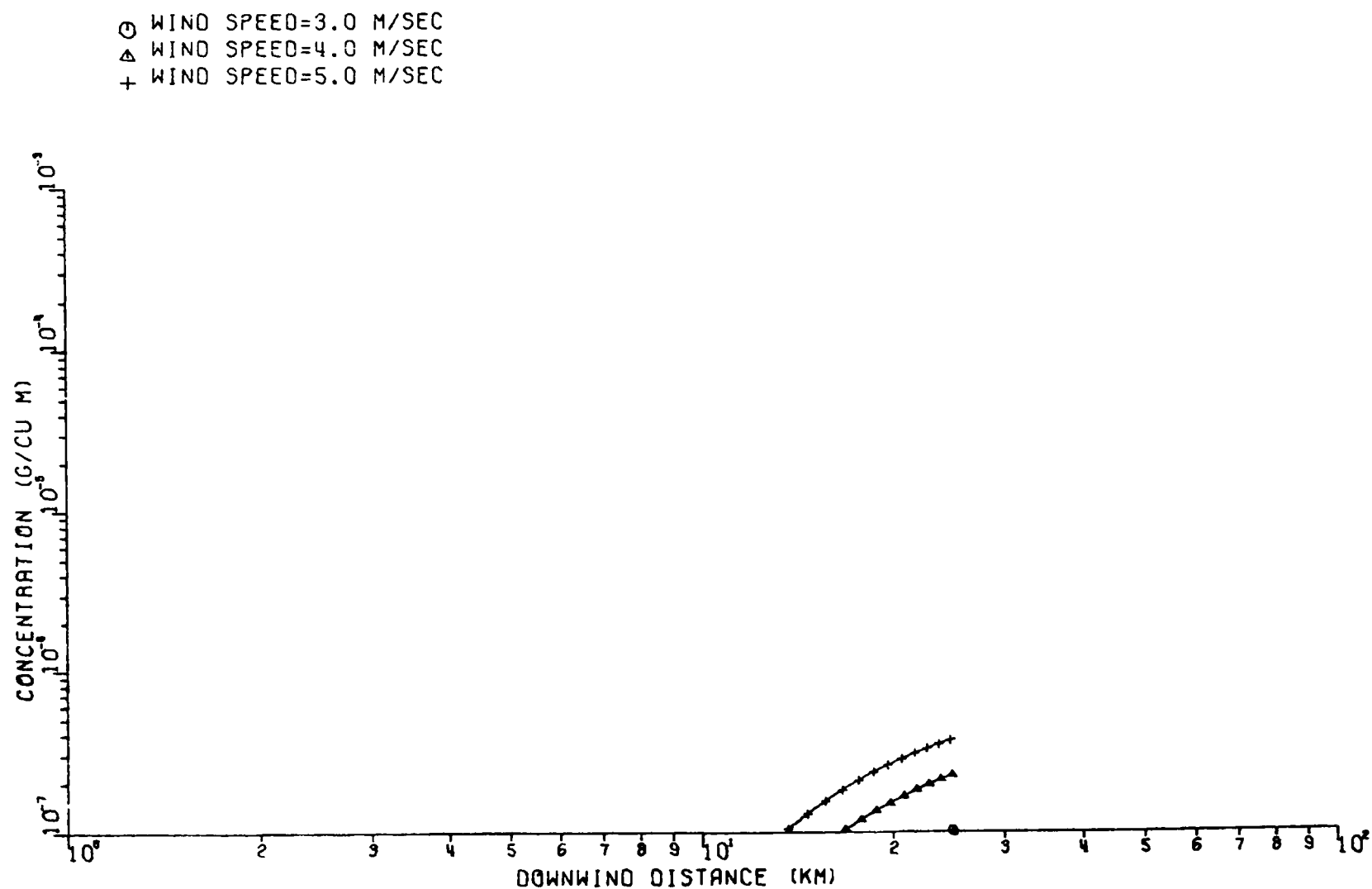


Figure C-2f. Plume centerline concentration versus downwind distance for stability Class F at the Canal Plant. Gifford-Briggs dispersion curves used. Flat terrain assumed. Wind speeds are at stack top

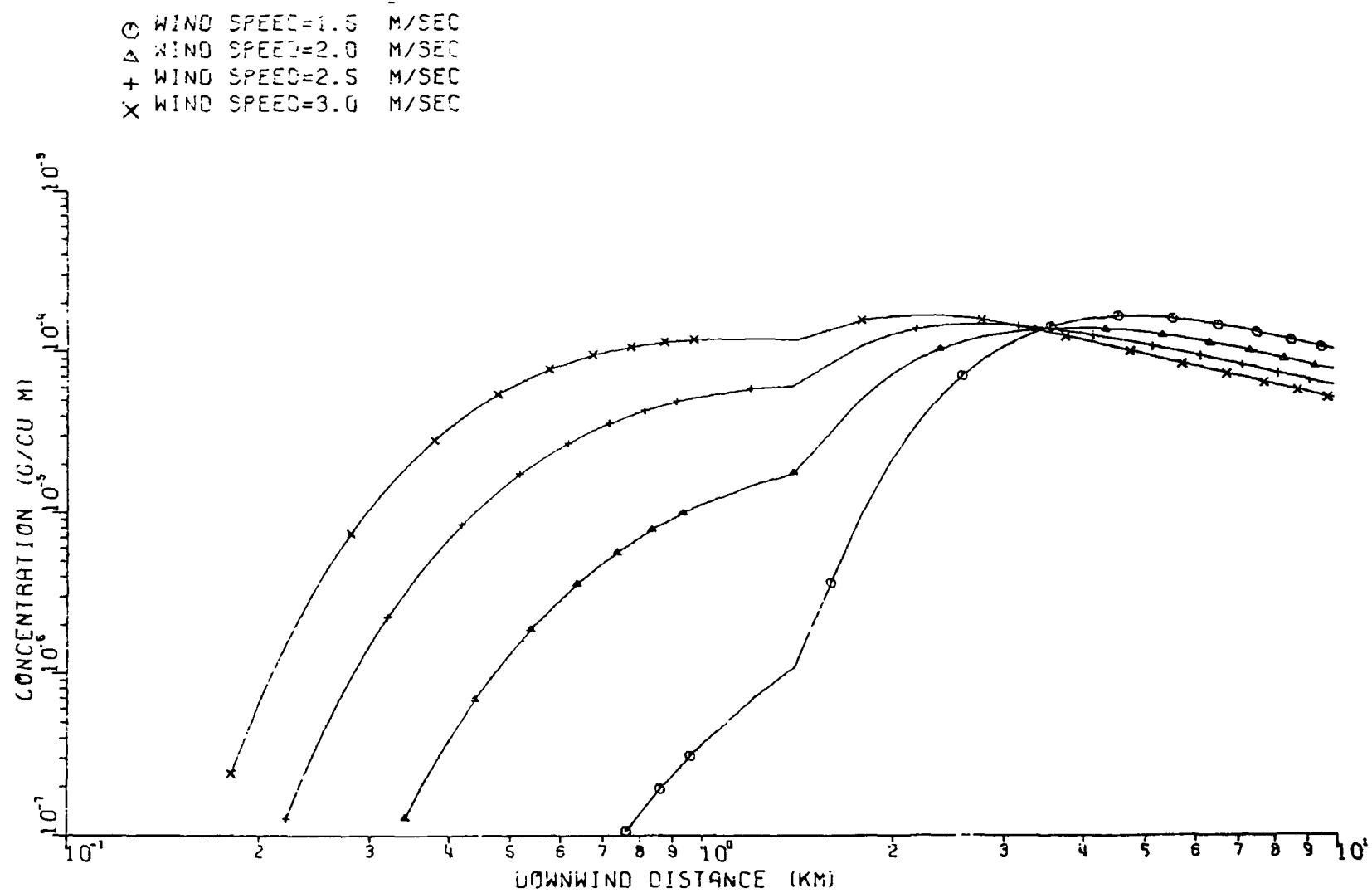


Figure C-3a. Plume centerline concentration versus downwind distance for stability Class B2 at the Canal Plant. Smith-Singer dispersion curves used. Flat terrain assumed. Wind speeds are at stack top

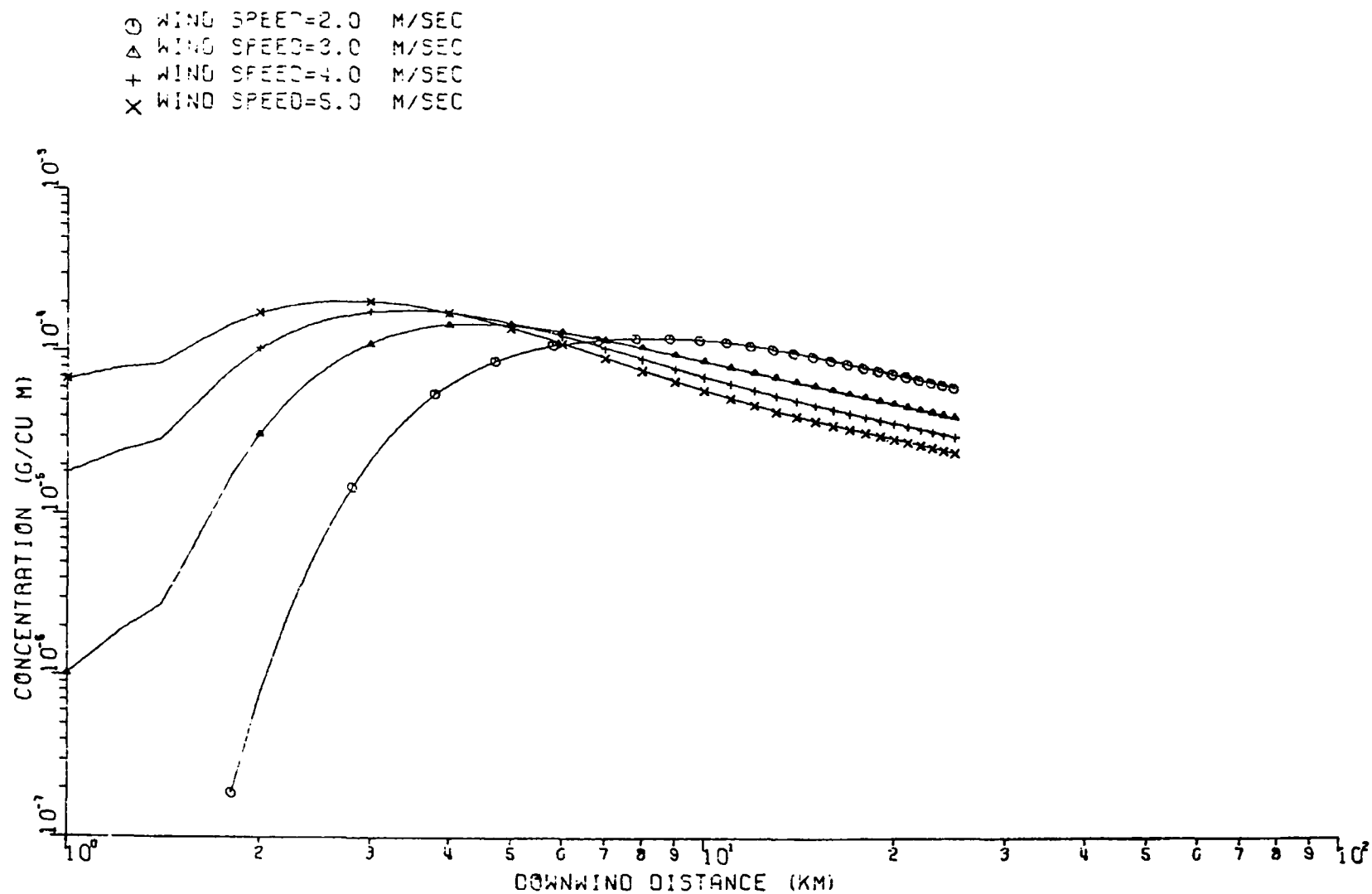


Figure C-3h. Plume centerline concentration versus downwind distance for stability Class B1 at the Canal Plant. Smith-Singer dispersion curves used. Flat terrain assumed. Wind speeds are at stack top

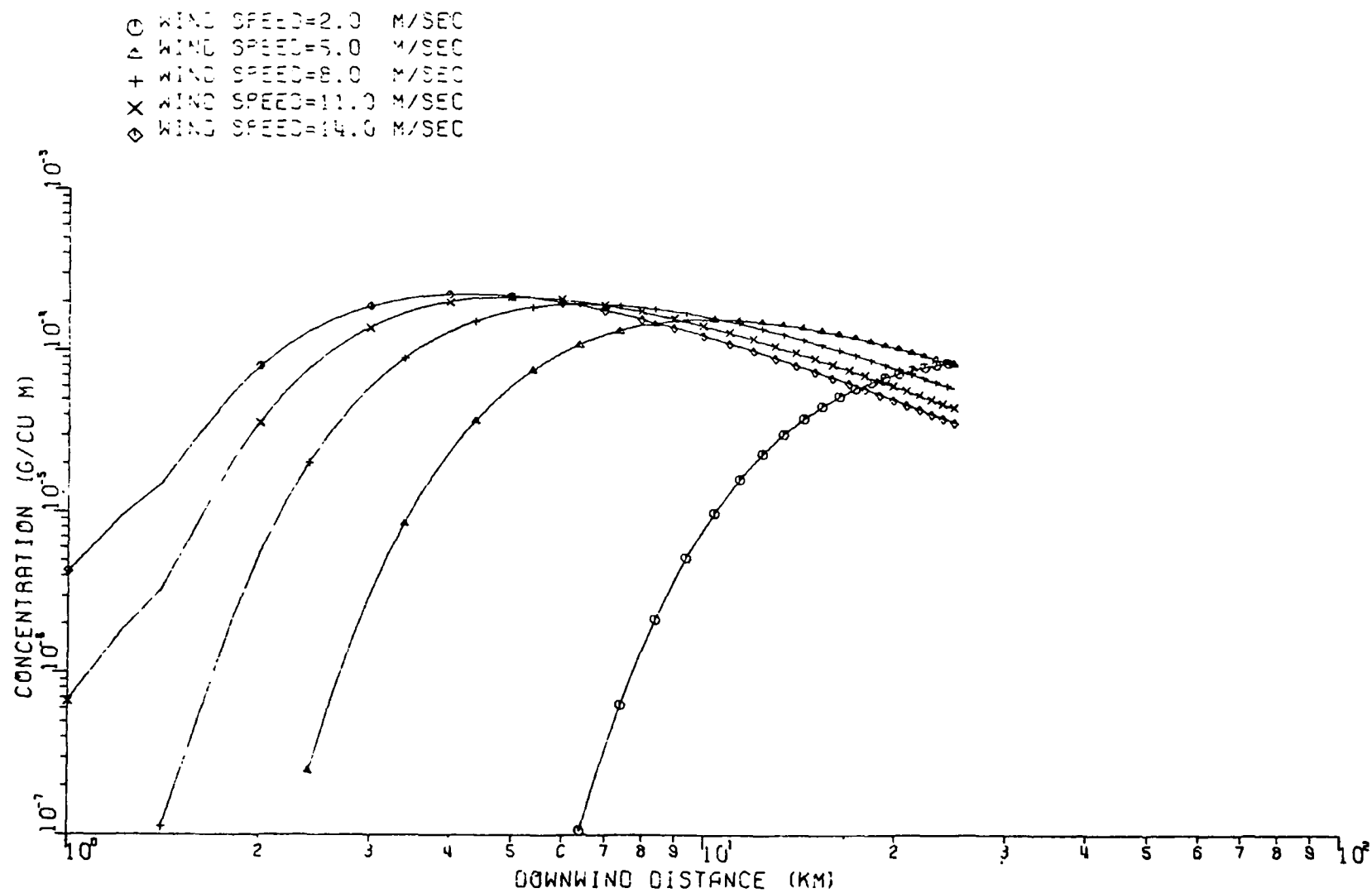


Figure C-3c. Plume centerline concentration versus downwind distance for stability Class C at the Canal Plant. Smith-Singer dispersion curves used. Flat terrain assumed. Wind speeds are at stack top

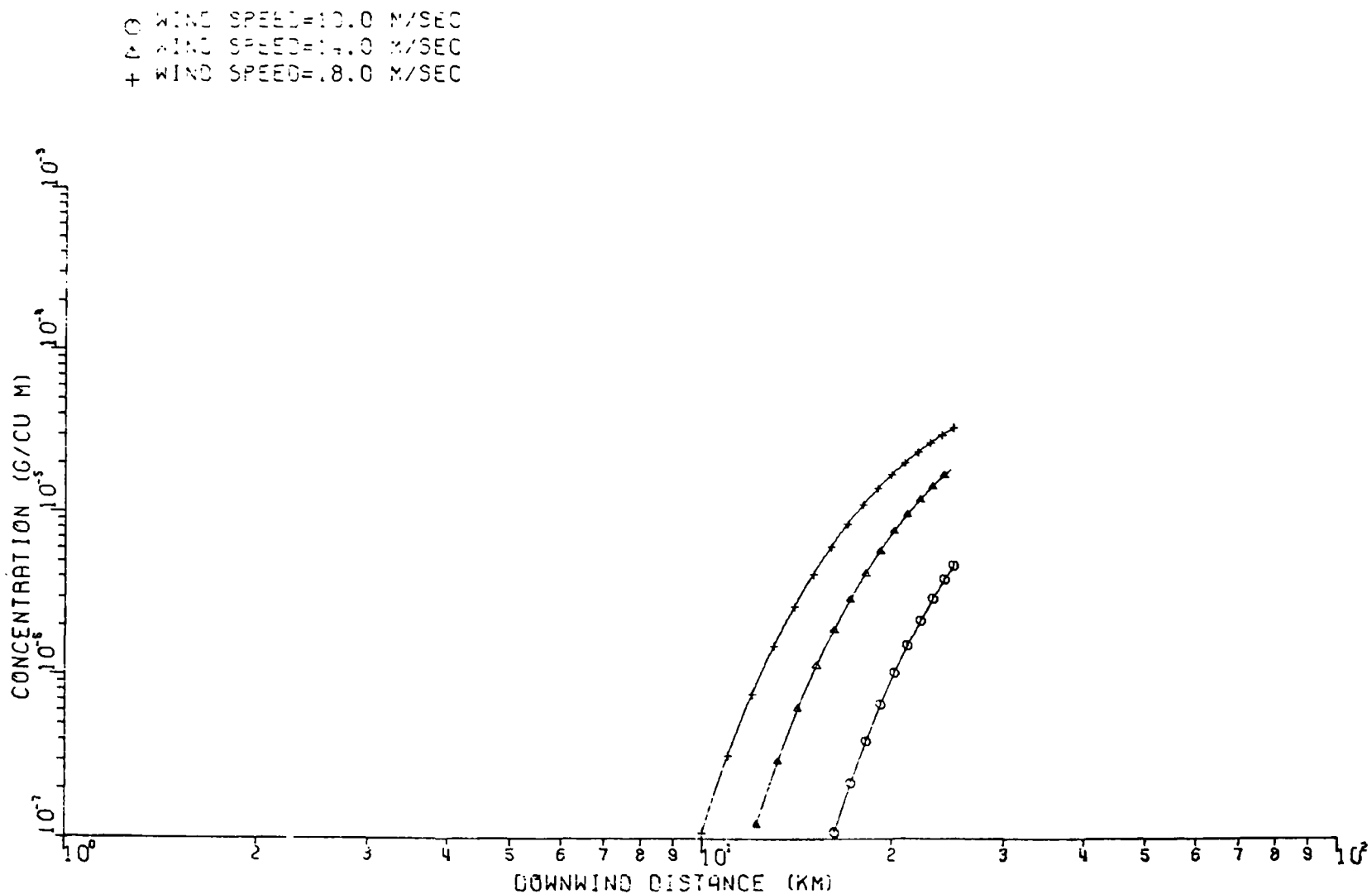


Figure C-3d. Plume centerline concentration versus downwind distance for stability Class D at the Canal Plant. Smith-Singer dispersion curves used. Flat terrain assumed. Wind speeds are at stack top

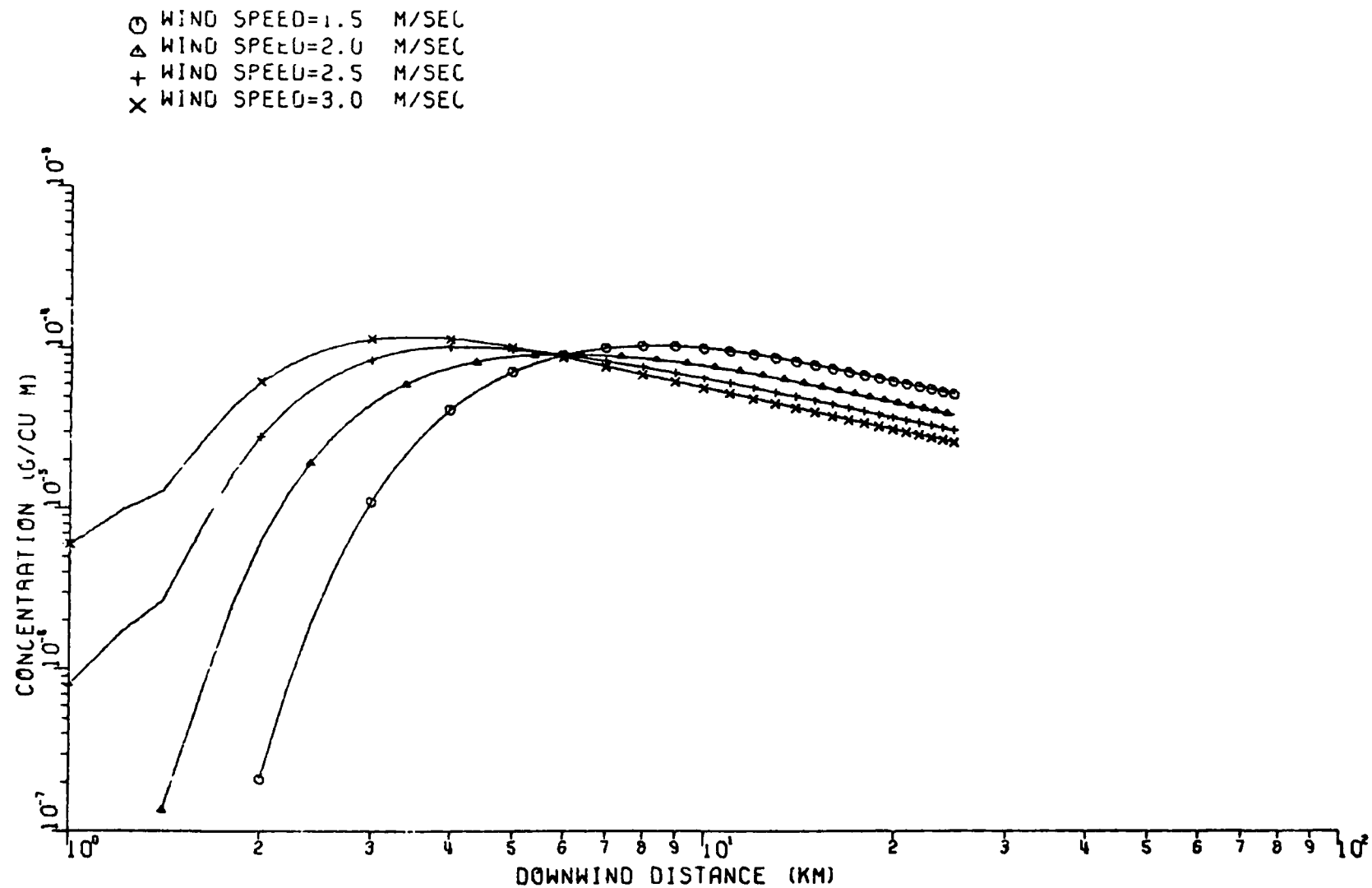


Figure C-4a. Plume centerline concentration versus downwind distance for stability Class A at the Canal Plant. F. B. Smith σ_z and Pasquill-Turner σ_y dispersion curves used. Flat terrain assumed. Wind speeds are at stack top

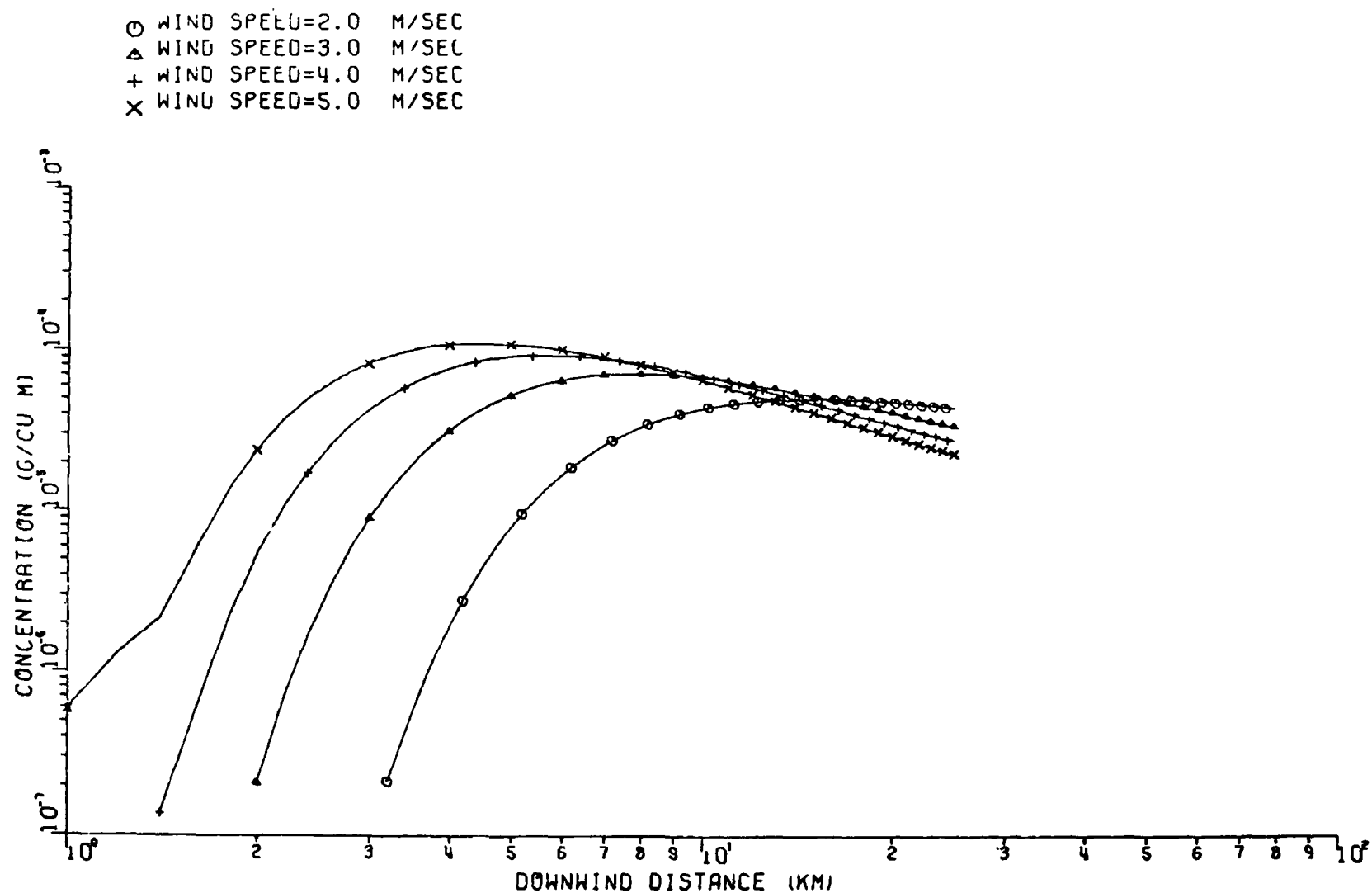


Figure C-4b. Plume centerline concentration versus downwind distance for stability Class B at the Canal Plant. F. B. Smith σ_z and Pasquill-Turner σ_y dispersion curves used. Flat terrain assumed. Wind speeds are at stack top

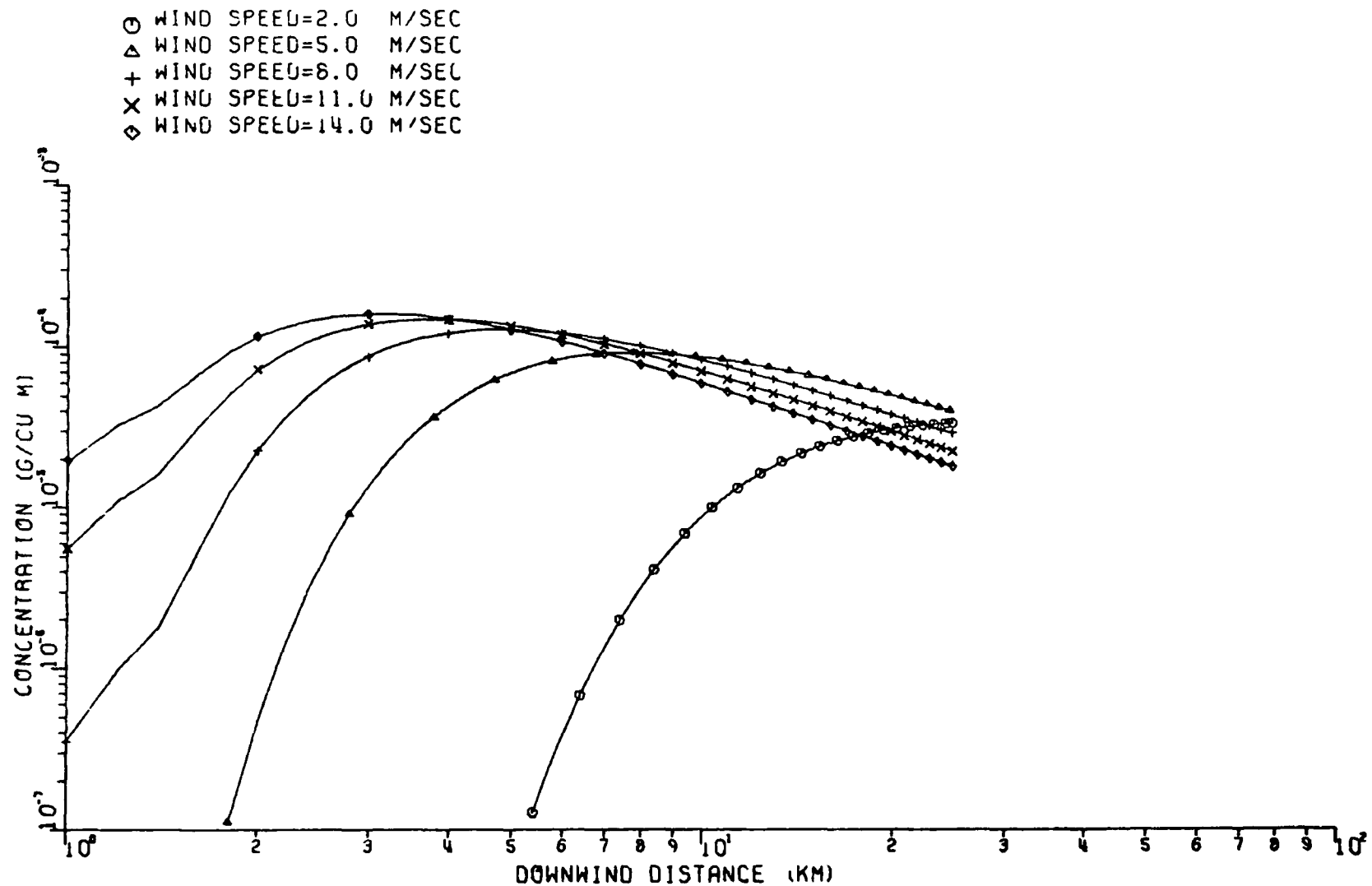


Figure C-4c. Plume centerline concentration versus downwind distance for stability Class C at the Canal Plant. F. B. Smith σ_z and Pasquill-Turner σ_y dispersion curves used. Flat terrain assumed. Wind speeds are at stack top

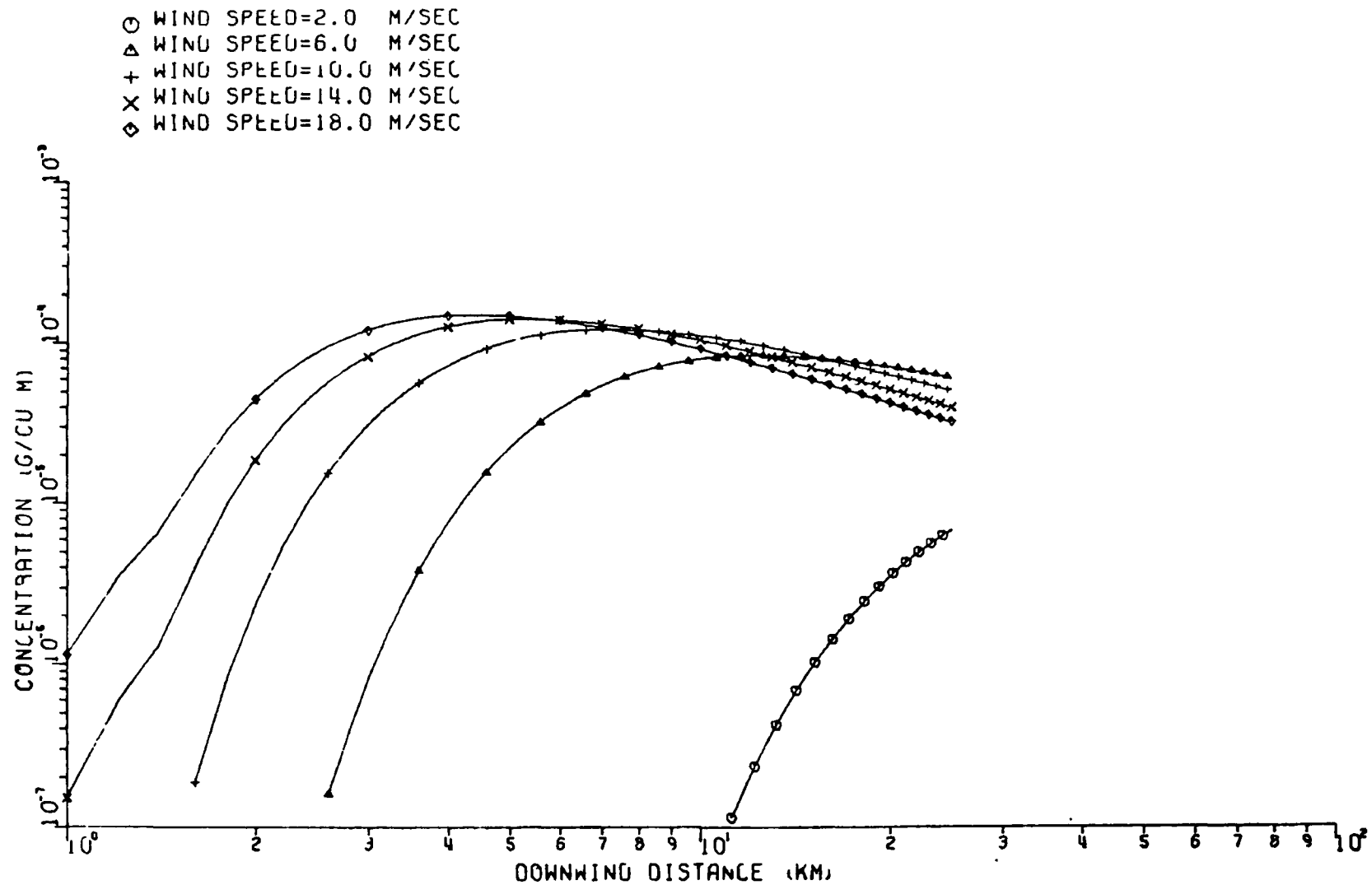


Figure C-4d. Plume centerline concentration versus downwind distance for stability Class D at the Canal Plant. F. B. Smith σ_z and Pasquill-Turner σ_y dispersion curves used. Flat terrain assumed. Wind speeds are at stack top

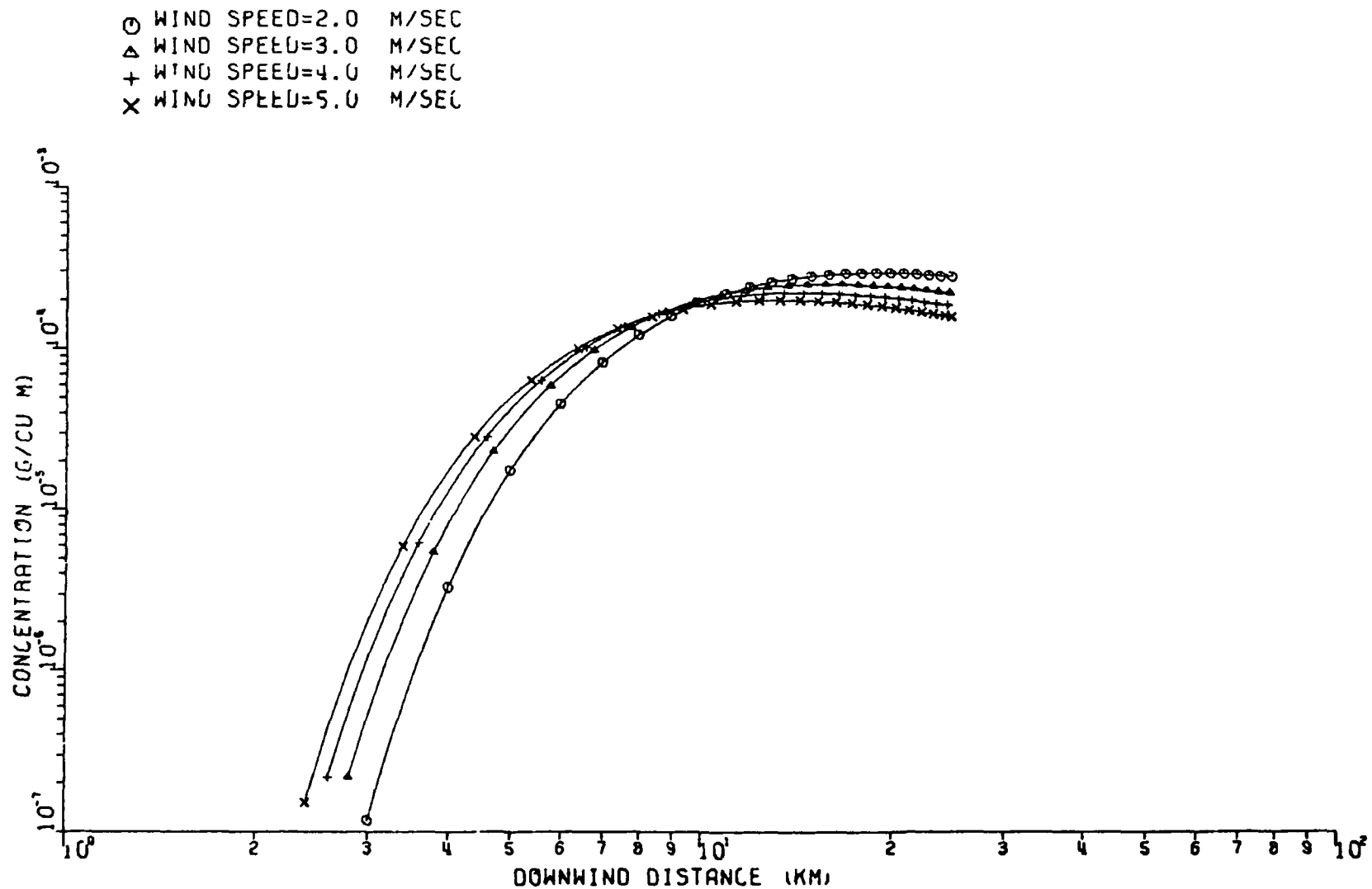


Figure C-4e. Plume centerline concentration versus downwind distance for stability Class E at the Canal Plant. F. B. Smith σ_z and Pasquill-Turner σ_y dispersion curves used. Flat terrain assumed. Wind speeds are at stack top

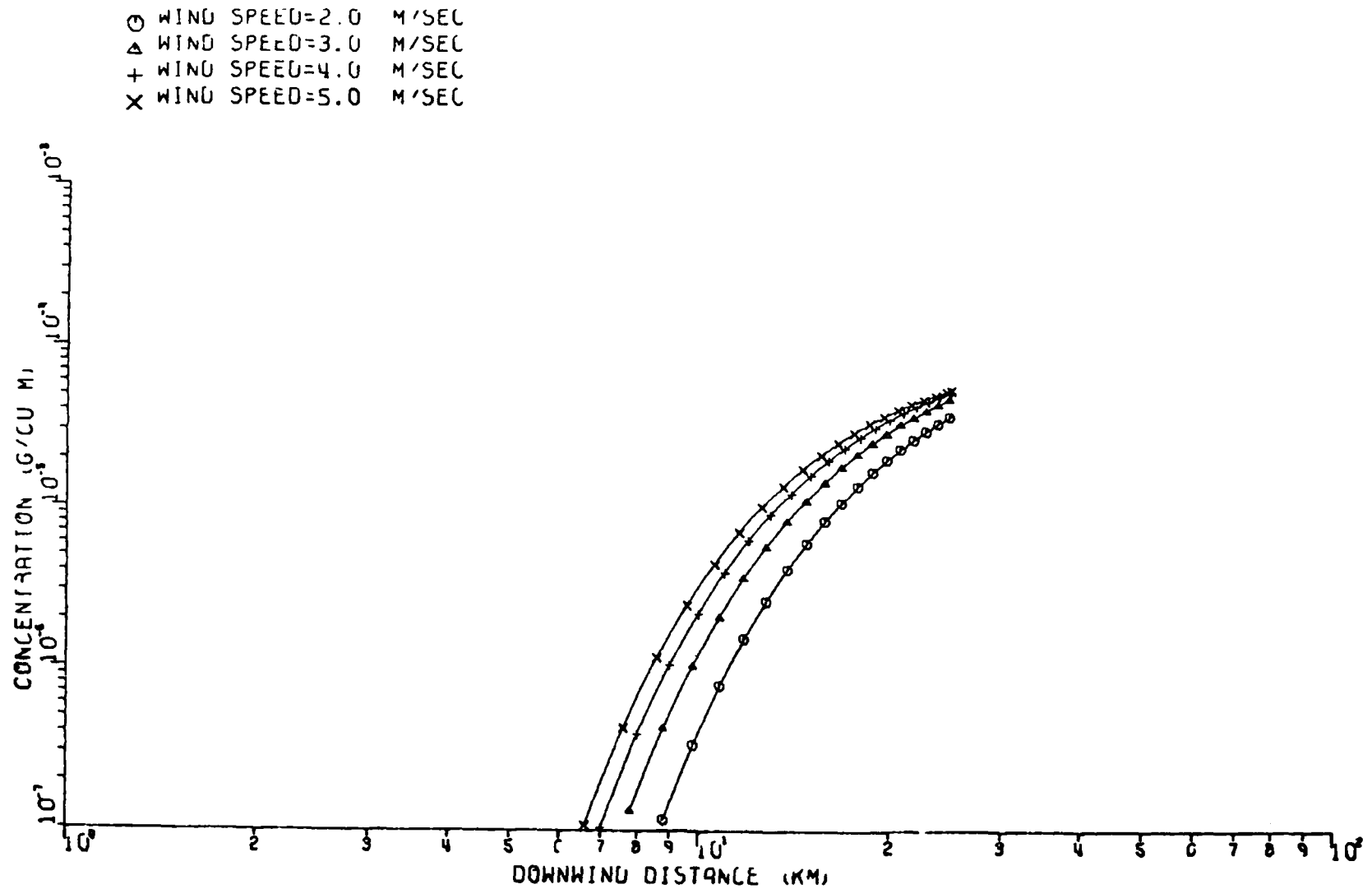


Figure C-4f. Plume centerline concentration versus downwind distance for stability Class F at the Canal Plant. F. B. Smith σ_z and Pasquill-Turner σ_y dispersion curves used. Flat terrain assumed. Wind speeds are at stack top

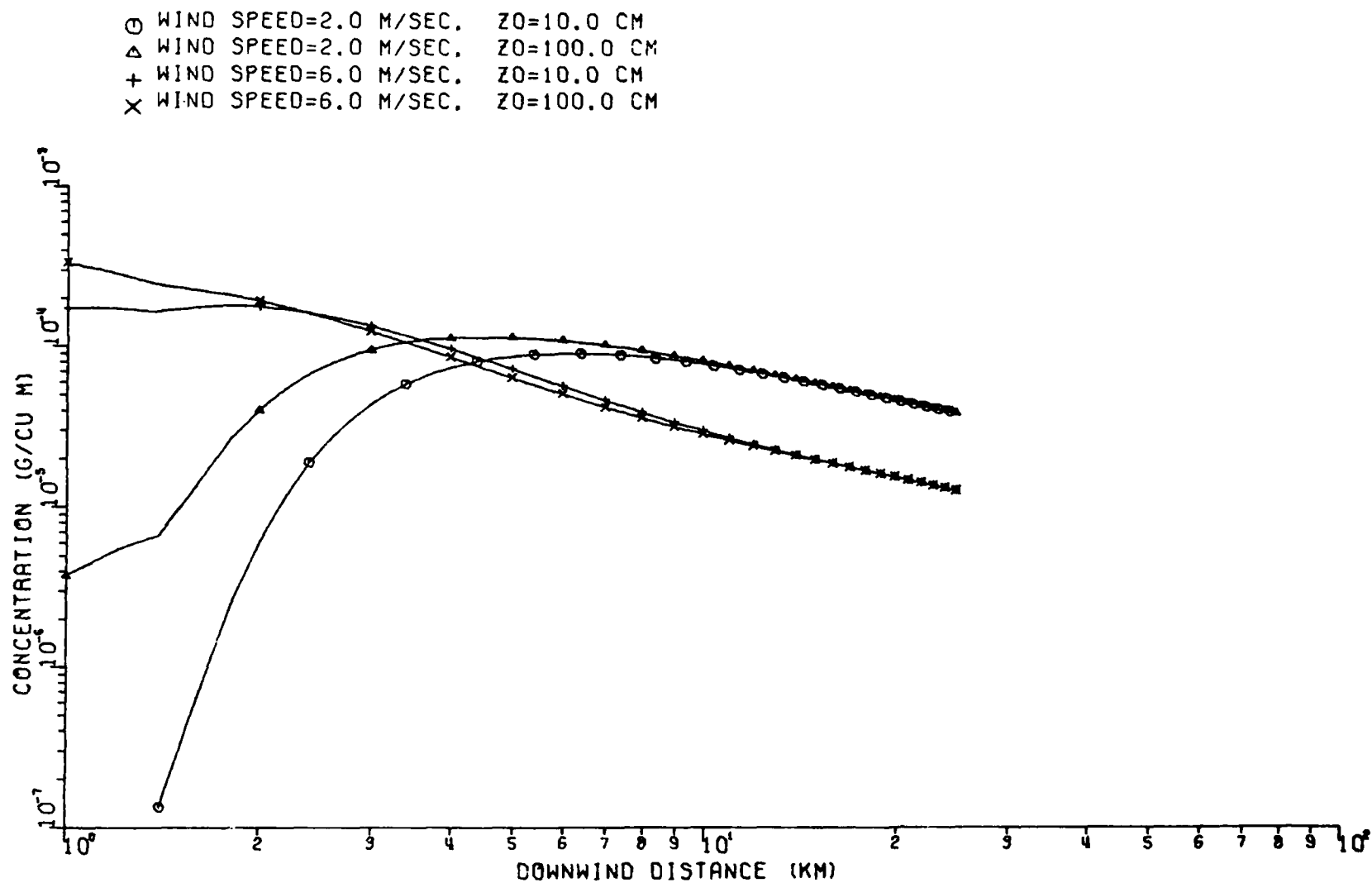


Figure C-5a. Effect of surface roughness upon ground level air concentrations for stability Class A at the Canal Plant. F. B. Smith σ_z and Pasquill-Turner σ_y curves used. Flat terrain assumed

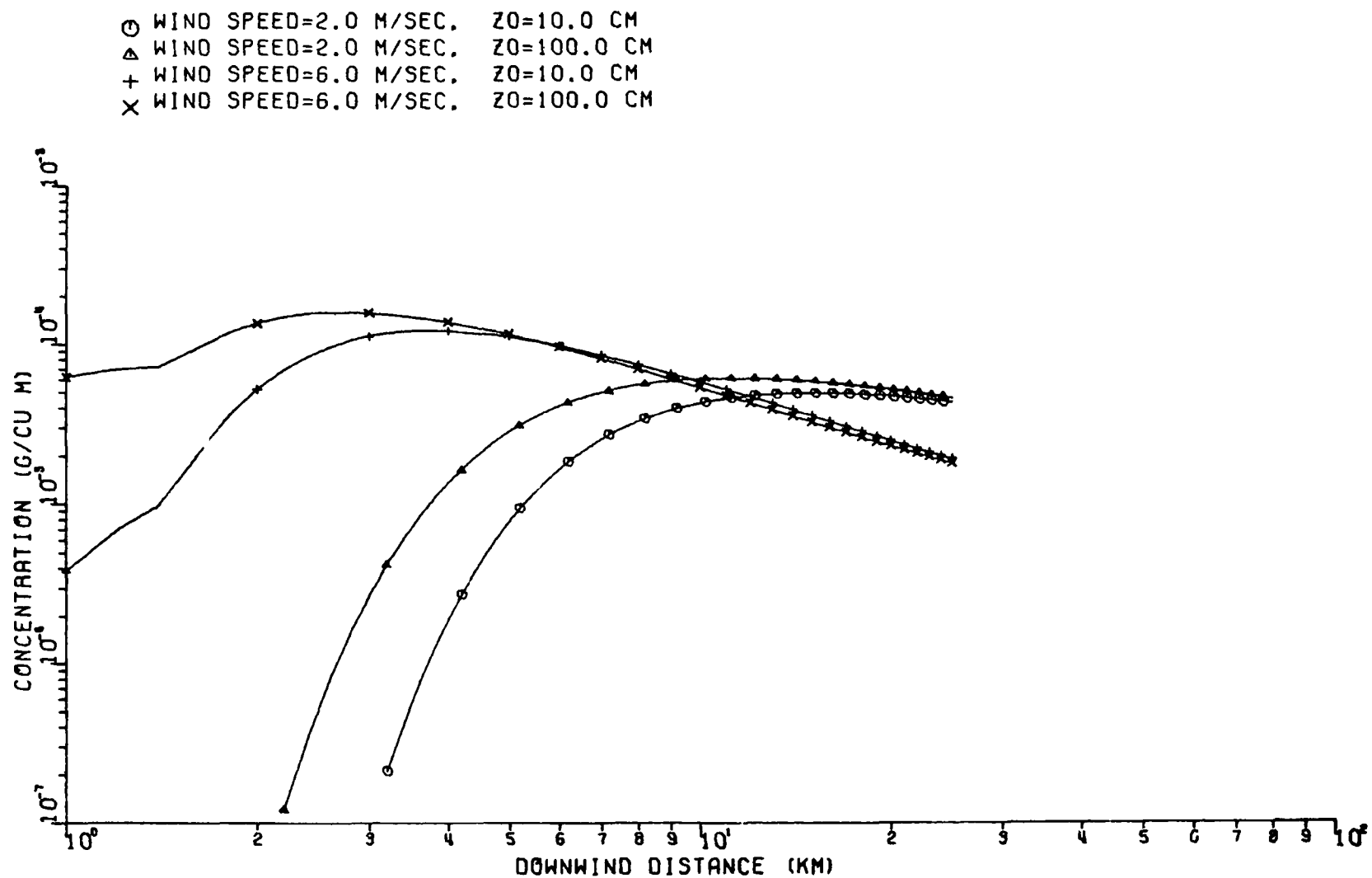


Figure C-5b. Effect of surface roughness upon ground level air concentrations for stability Class B at the Canal Plant. F. B. Smith σ_z and Pasquill-Turner σ_y curves used. Flat terrain assumed

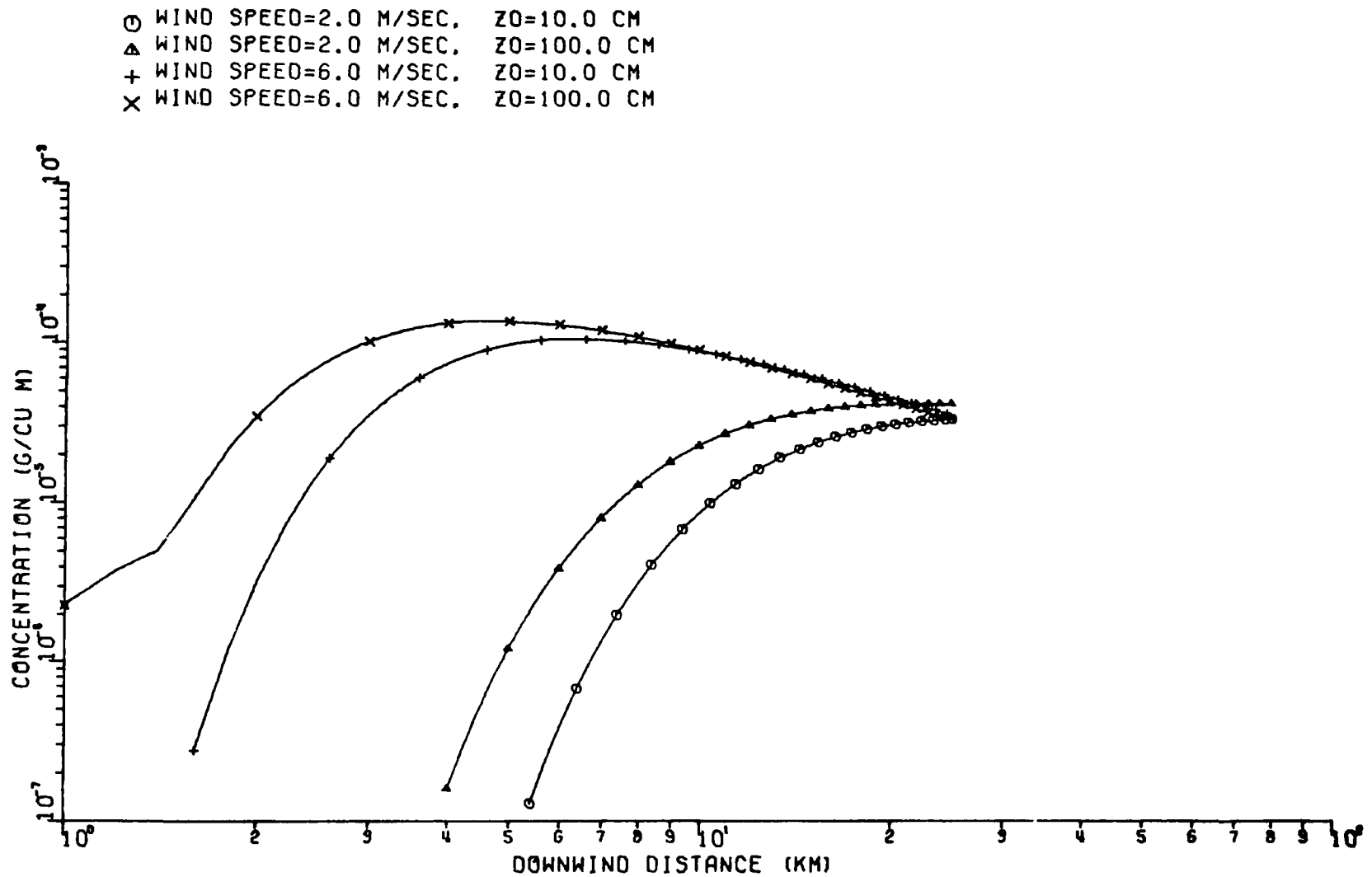


Figure C-5c. Effect of surface roughness upon ground level air concentrations for stability Class C at the Canal Plant. F. B. Smith σ_z and Pasquill-Turner σ_y curves used. Flat terrain assumed

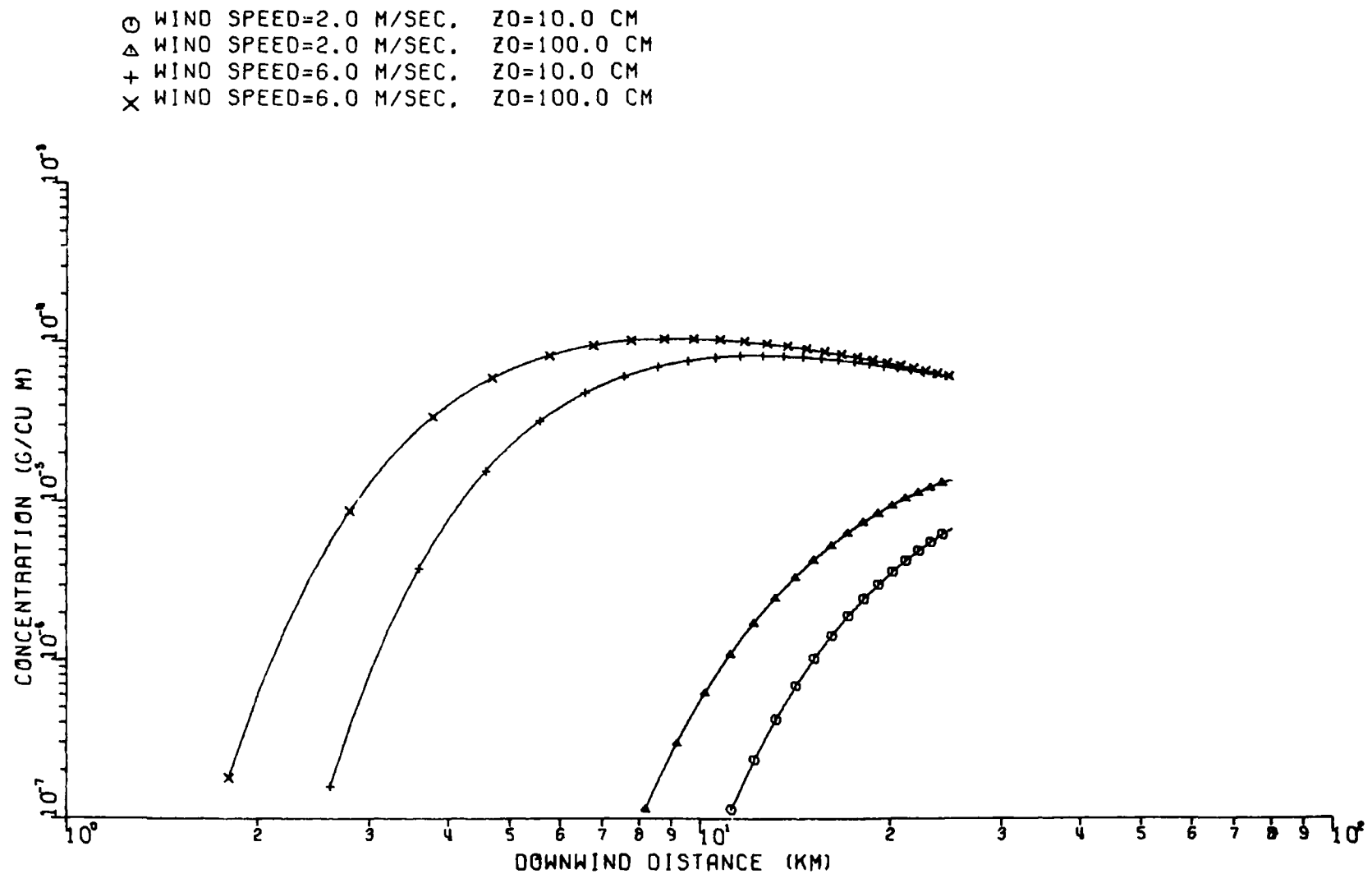


Figure C-5d. Effect of surface roughness upon ground level air concentrations for stability Class D at the Canal Plant. F. B. Smith σ_z and Pasquill-Turner σ_y curves used. Flat terrain assumed

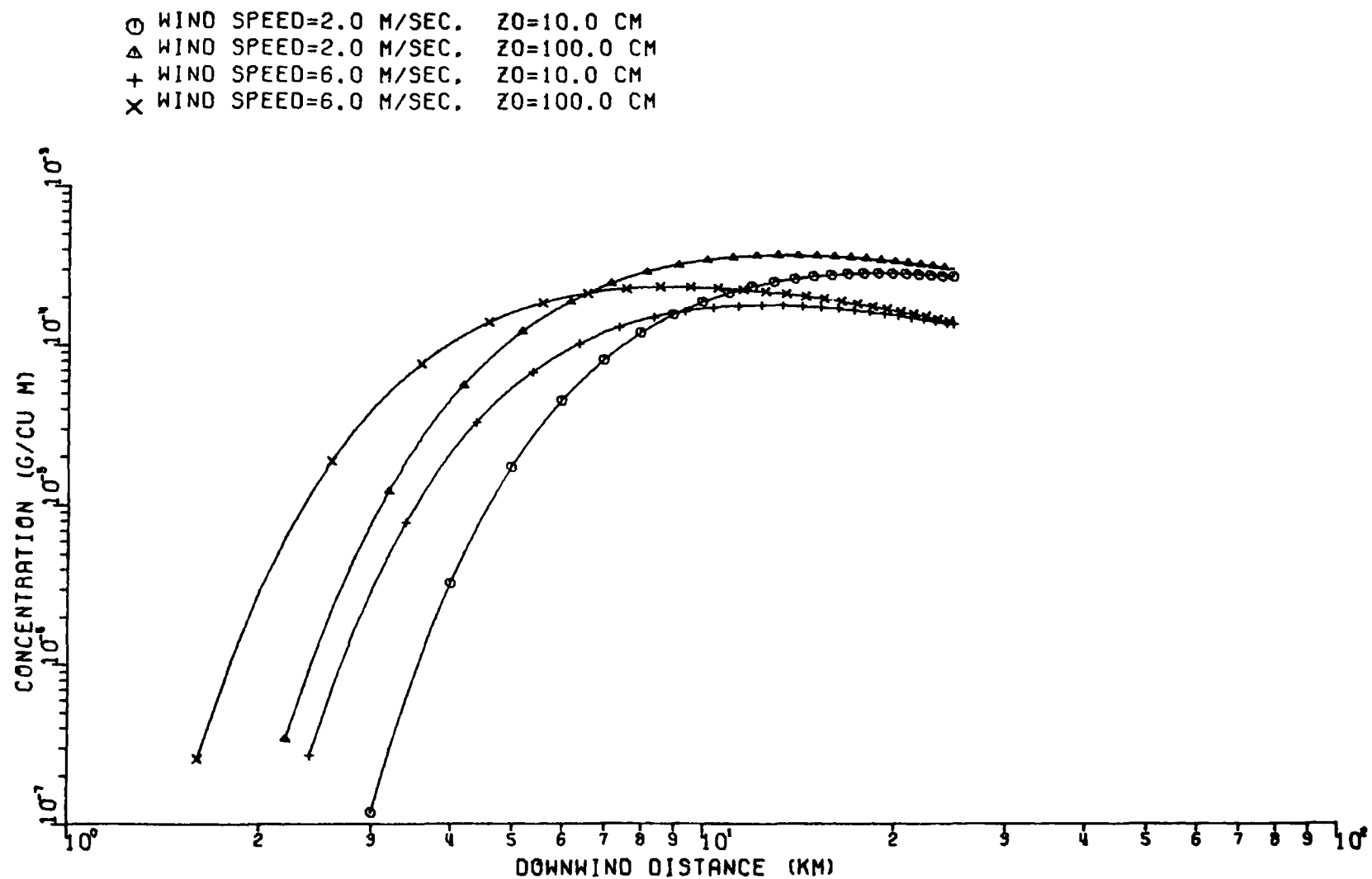


Figure C-5e. Effect of surface roughness upon ground level air concentrations for stability Class F at the Canal Plant. F. B. Smith σ_z and Pasquill-Turner σ_y curves used. Flat terrain assumed

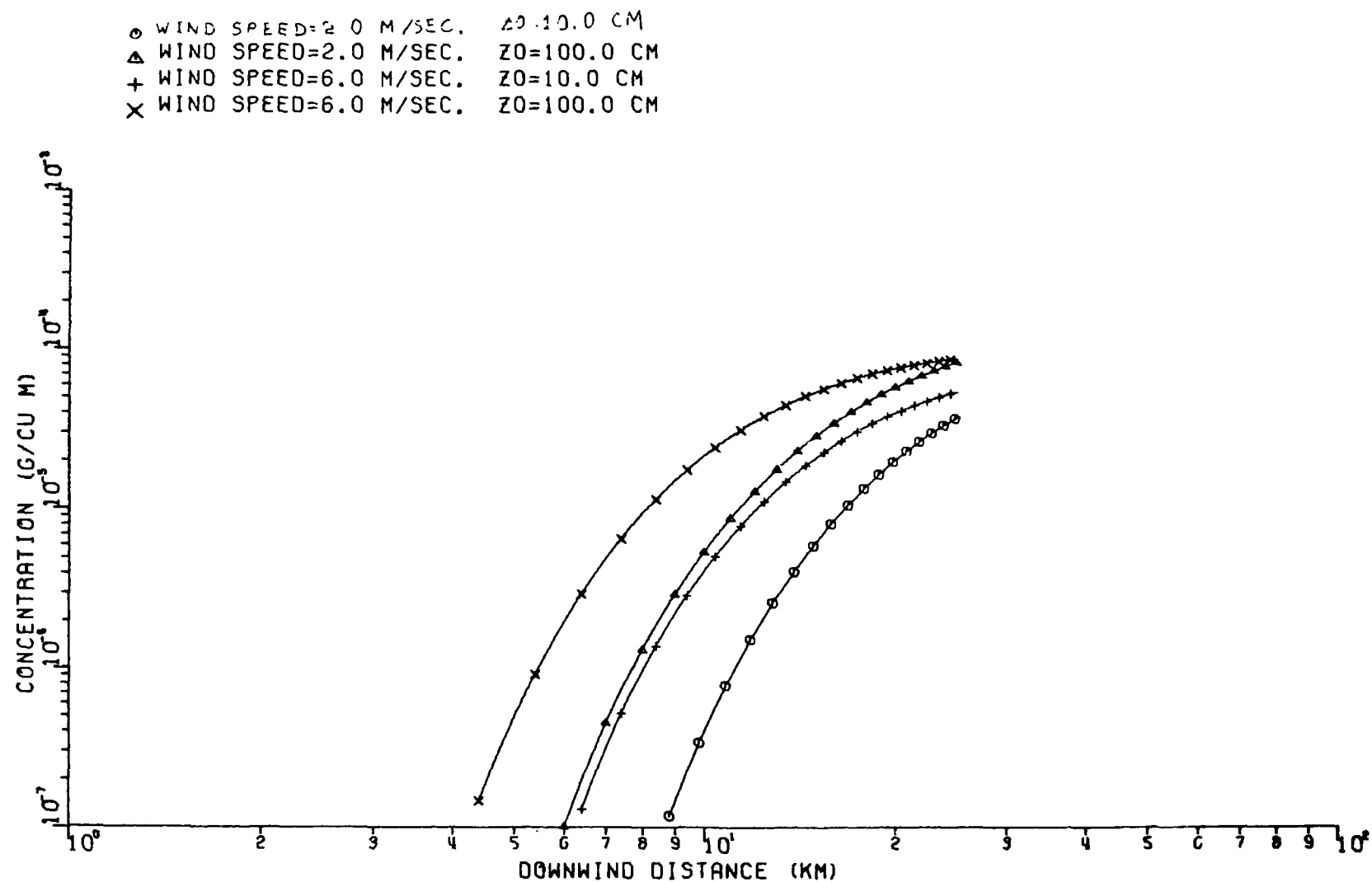


Figure C-5f. Effect of surface roughness upon ground level air concentrations for stability Class F at the Canal Plant. F. B. Smith σ_z and Pasquill-Turner σ_z curves used. Flat terrain assumed

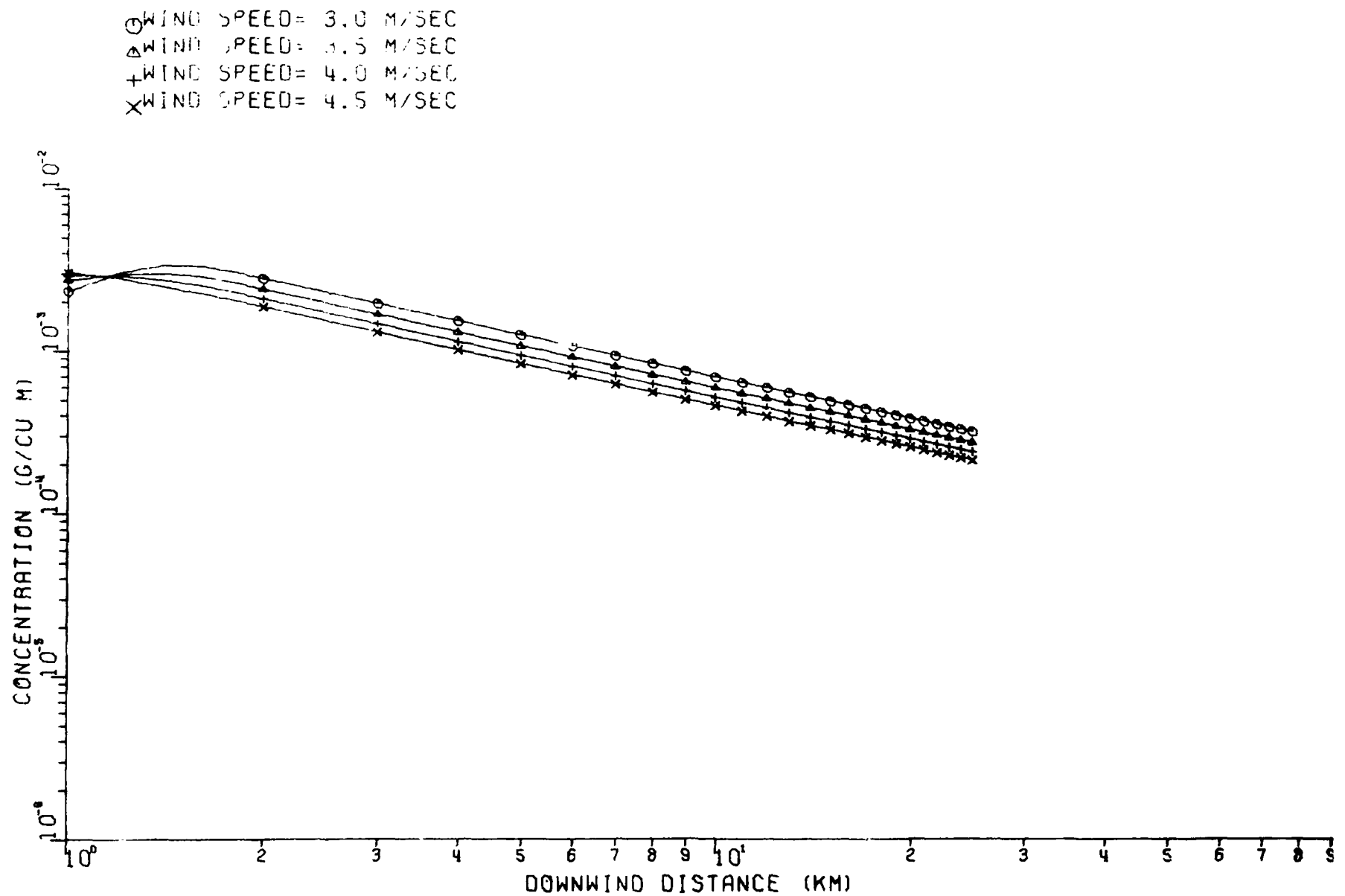


Figure C-6a. Plume centerline concentration versus downwind distance for stability Class A at the Muskingum Plant. Pasquill-Turner dispersion curves used. Flat terrain assumed. Wind speeds are at stack top

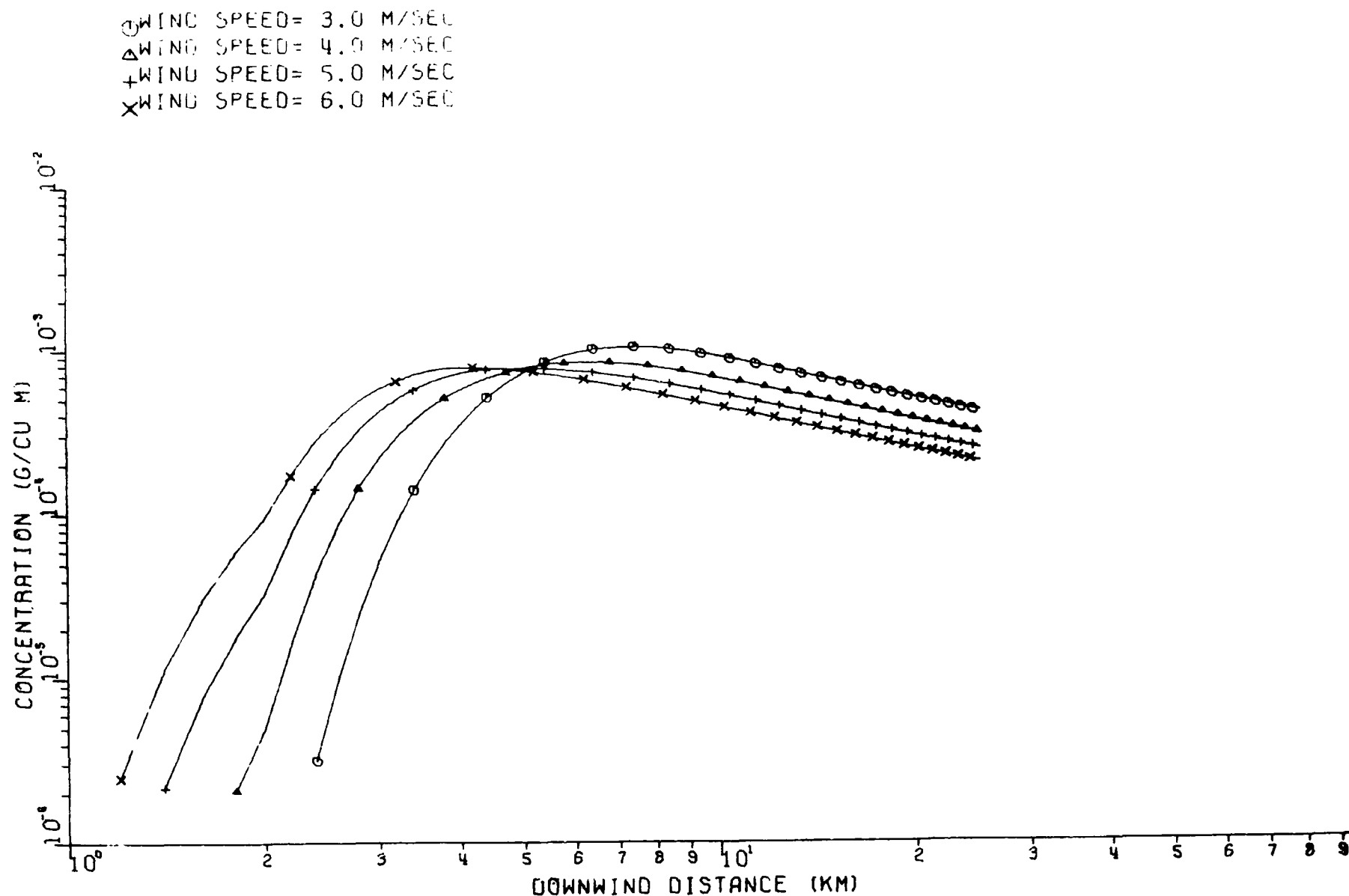


Figure C-6b. Plume centerline concentration versus downwind distance for stability Class B at the Muskingum Plant. Pasquill-Turner dispersion curves used. Flat terrain assumed. Wind speeds are at stack top

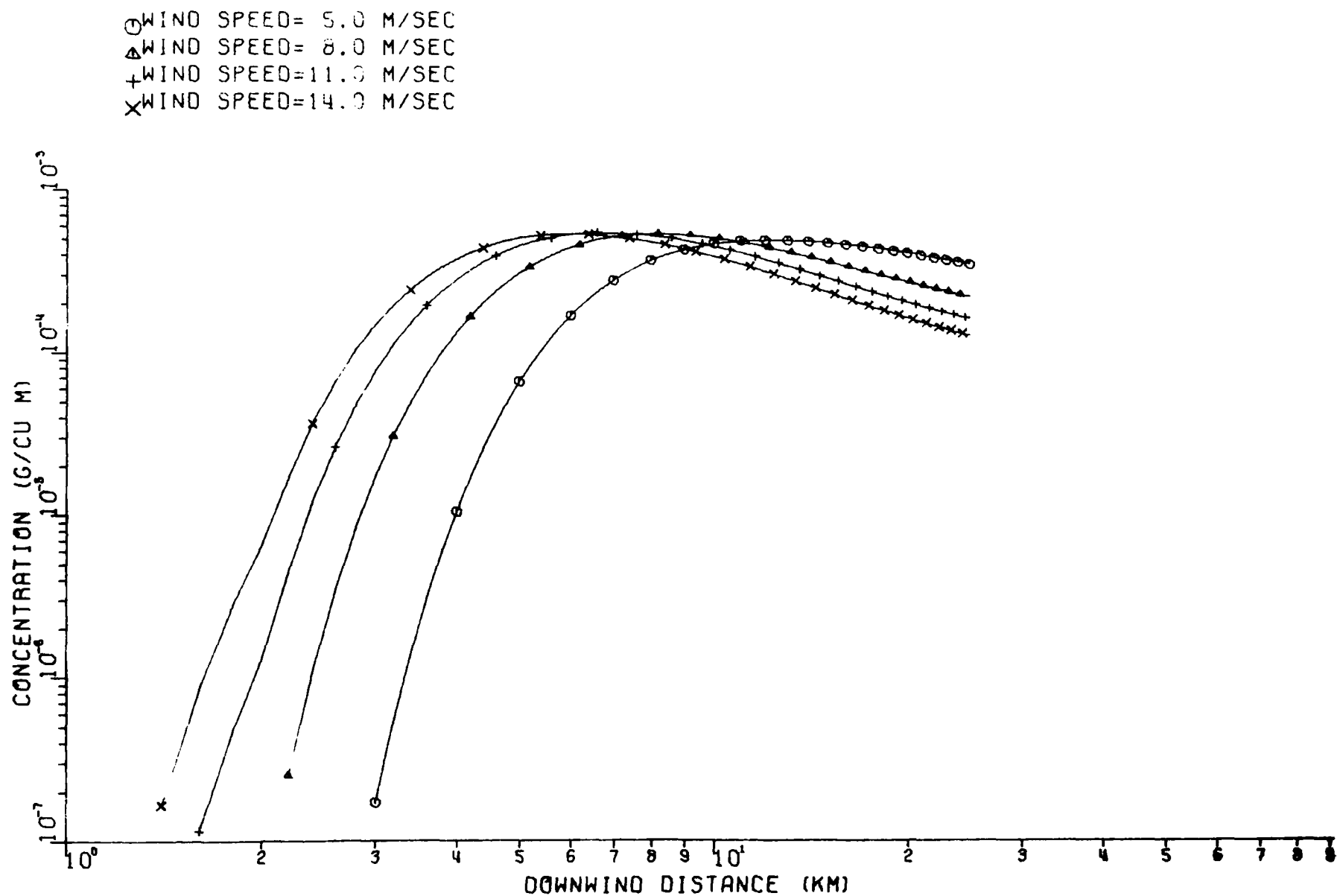


Figure C-6c. Plume centerline concentration versus downwind distance for stability Class C at the Muskingum Plant. Pasquill-Turner dispersion curves used. Flat terrain assumed. Wind speeds are at stack top

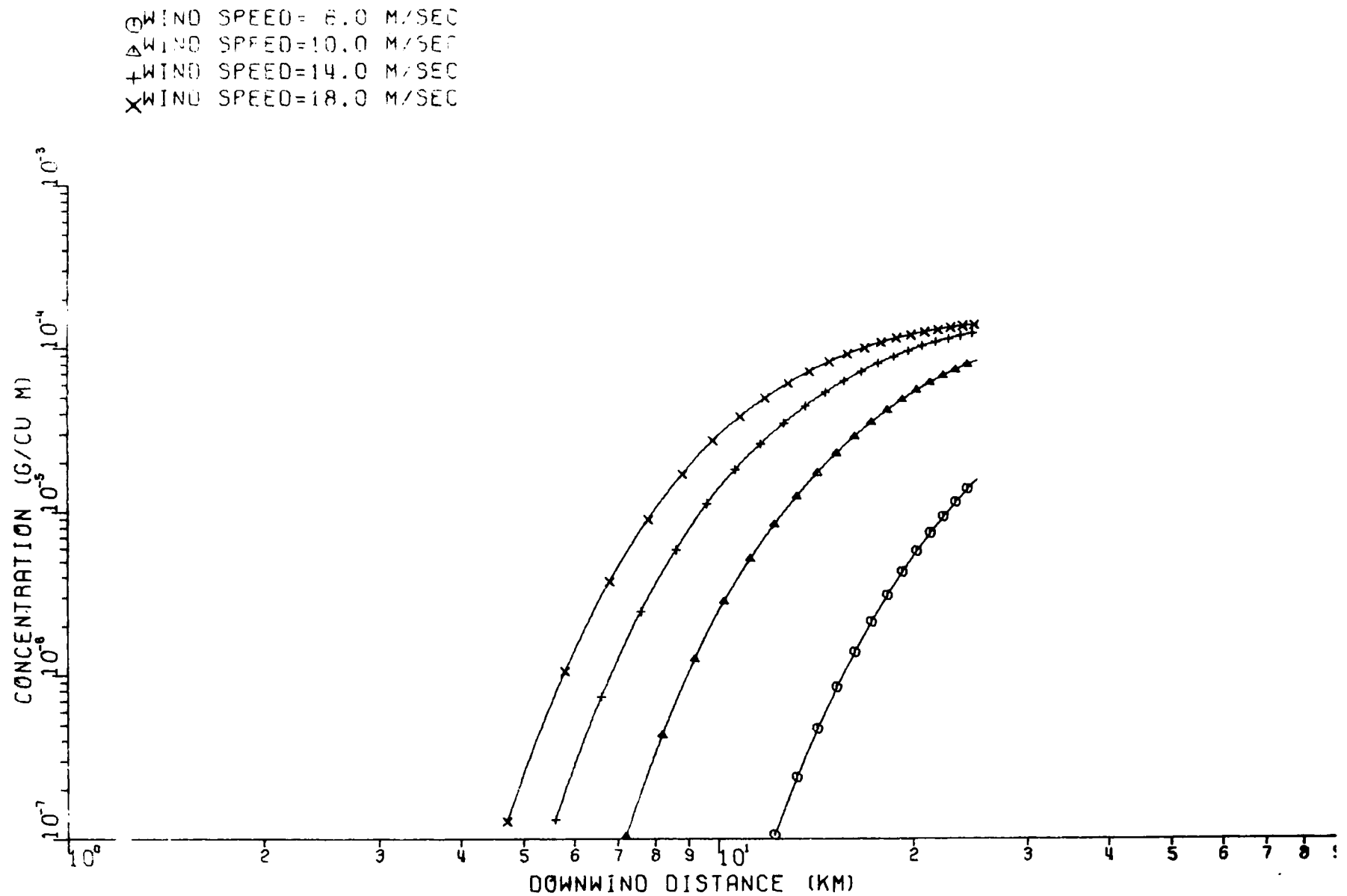


Figure C-6d. Plume centerline concentration versus downwind distance for stability Class D at the Muskingum Plant. Pasquill-Turner dispersion curves used. Flat terrain assumed. Wind speeds are at stack top

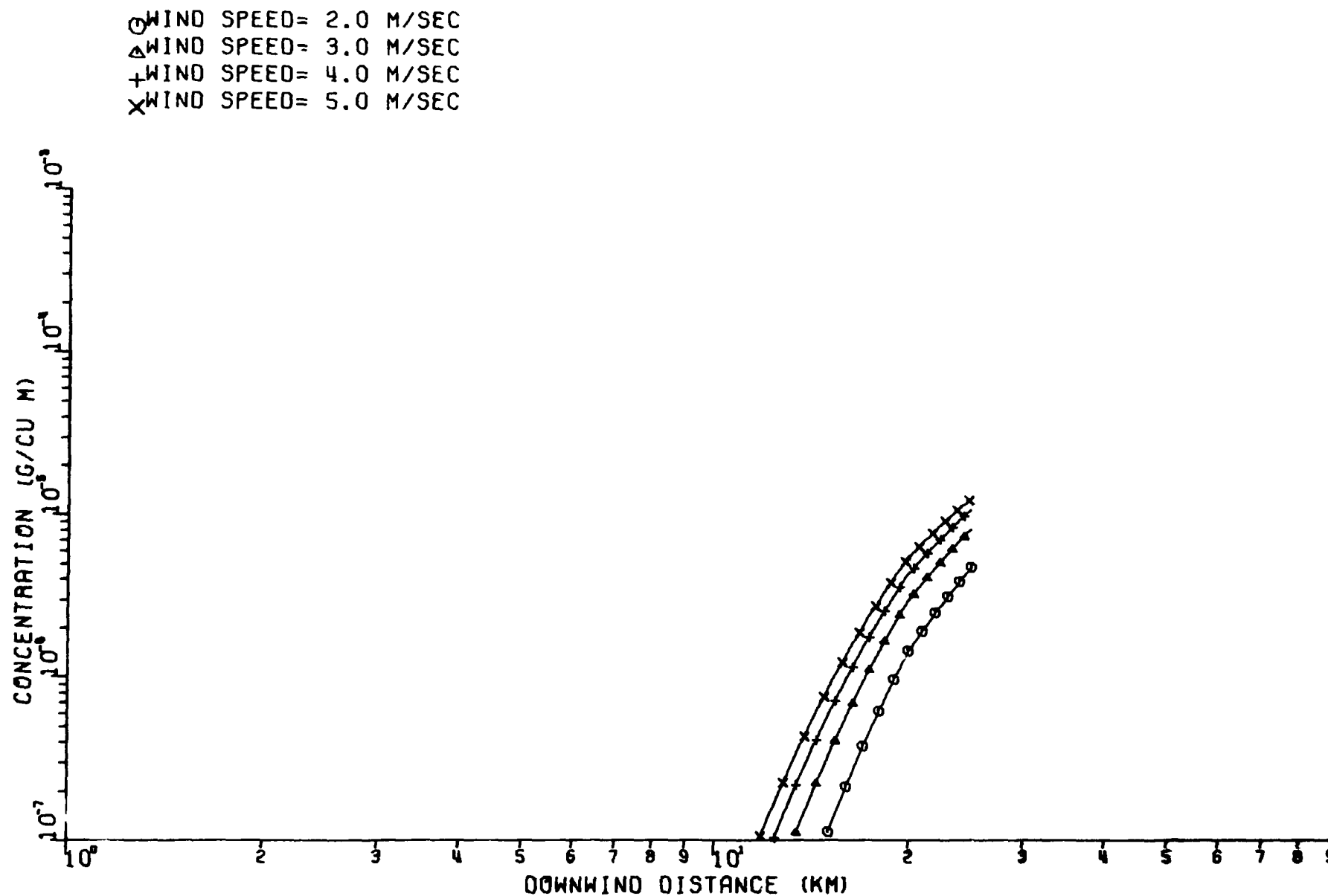


Figure C-6e. Plume centerline concentration versus downwind distance for stability Class E at the Muskingum Plant. Pasquill-Turner dispersion curves used. Flat terrain assumed. Wind speeds are at stack top

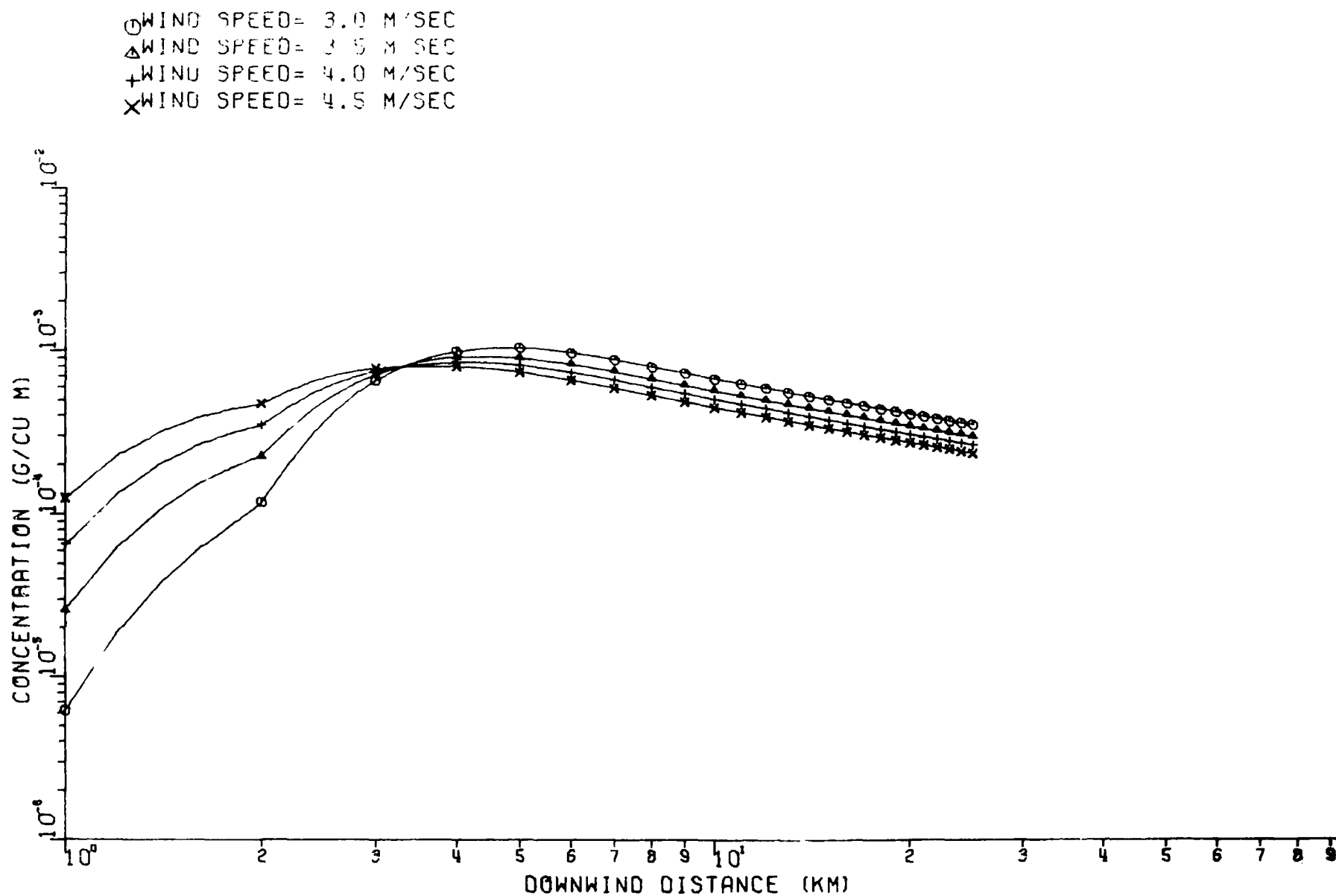


Figure C-7a. Plume centerline concentration versus downwind distance for stability Class A at the Muskingum Plant. Gifford-Briggs dispersion curves used. Flat terrain assumed. Wind speeds are at stack top

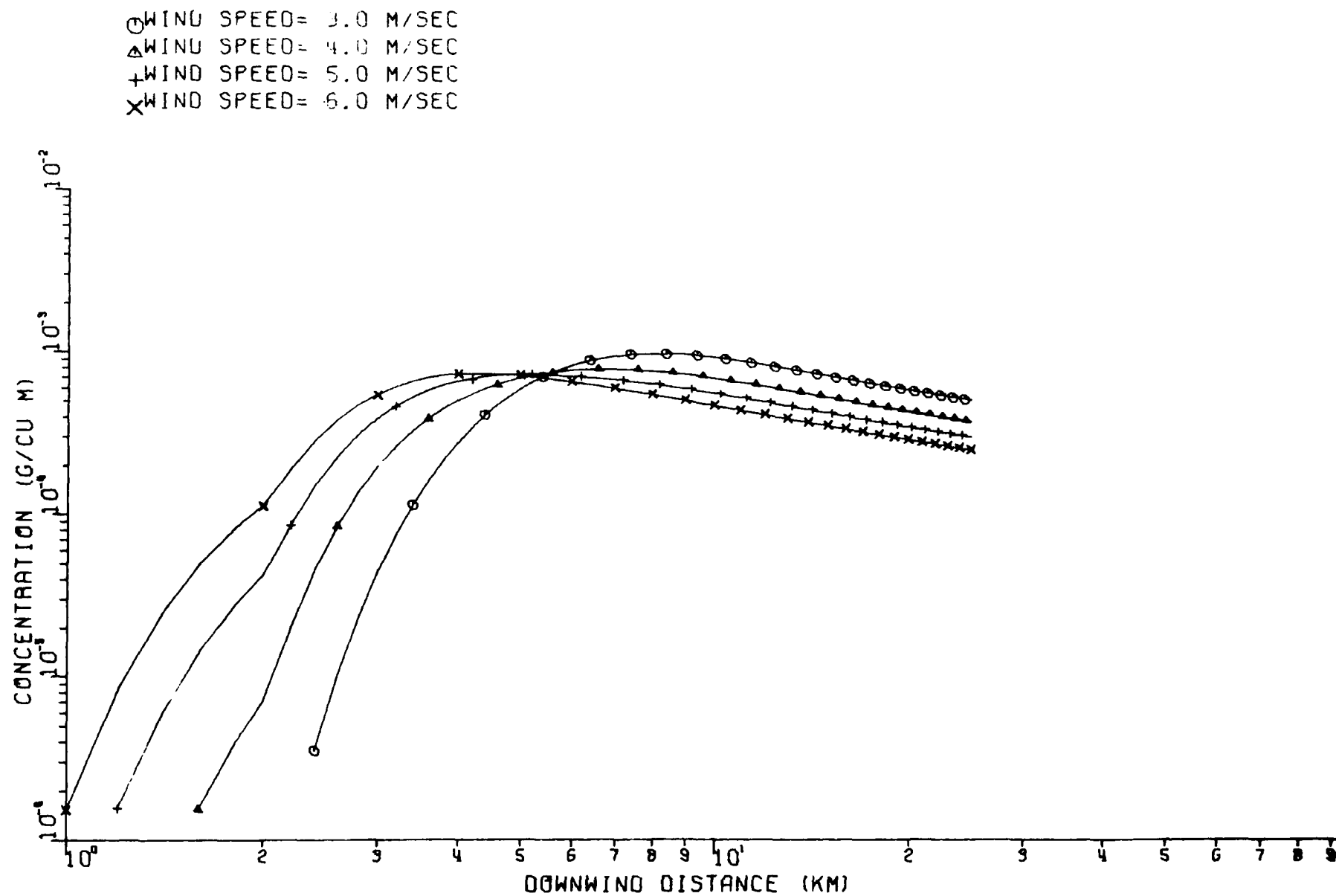


Figure C-7b. Plume centerline concentration versus downwind distance for stability Class B at the Muskingum Plant. Gifford-Briggs dispersion curves used. Flat terrain assumed. Wind speeds are at stack top

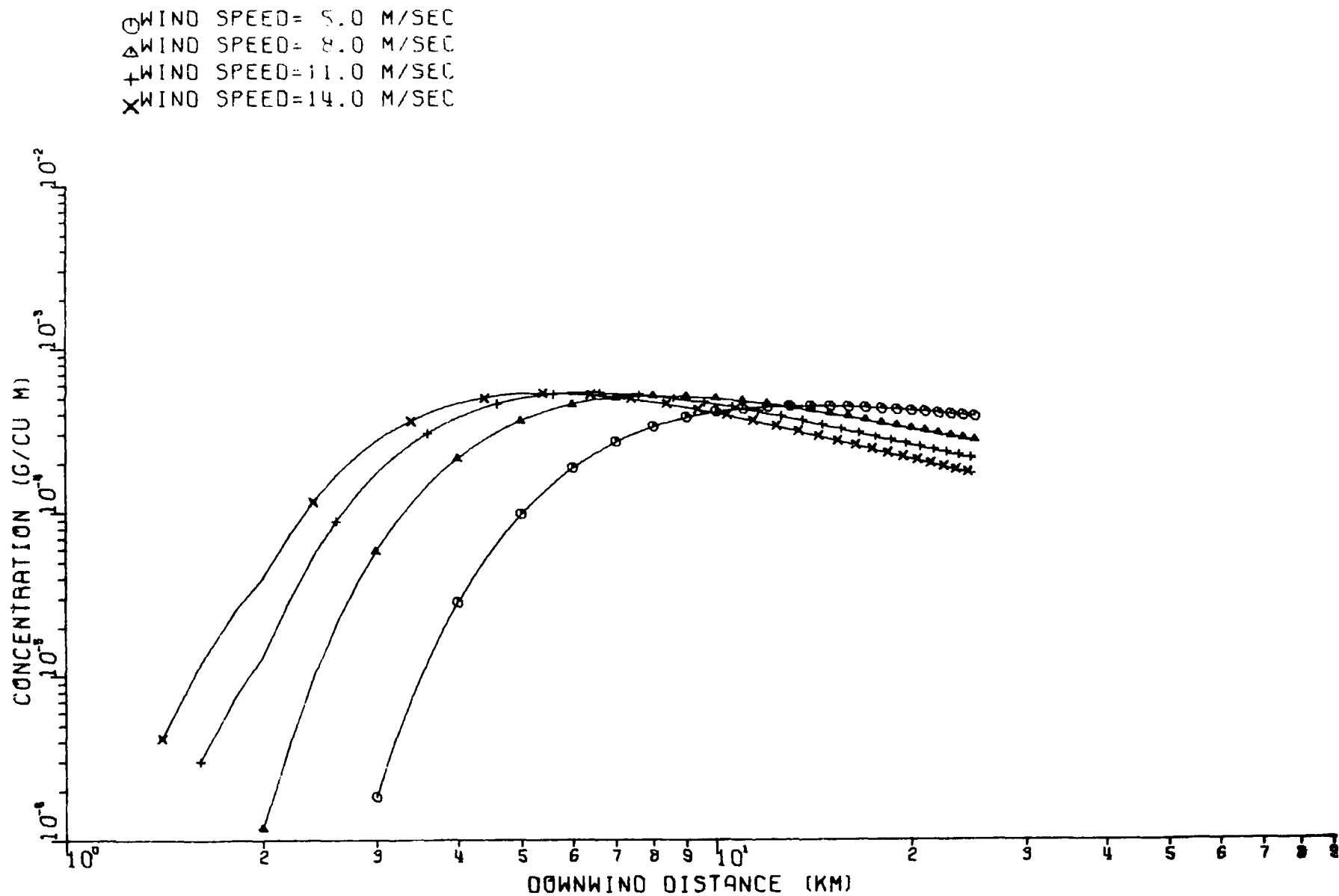


Figure C-7c. Plume centerline concentration versus downwind distance for stability Class C at the Muskingum Plant. Gifford-Briggs dispersion curves used. Flat terrain assumed. Wind speeds are at stack top

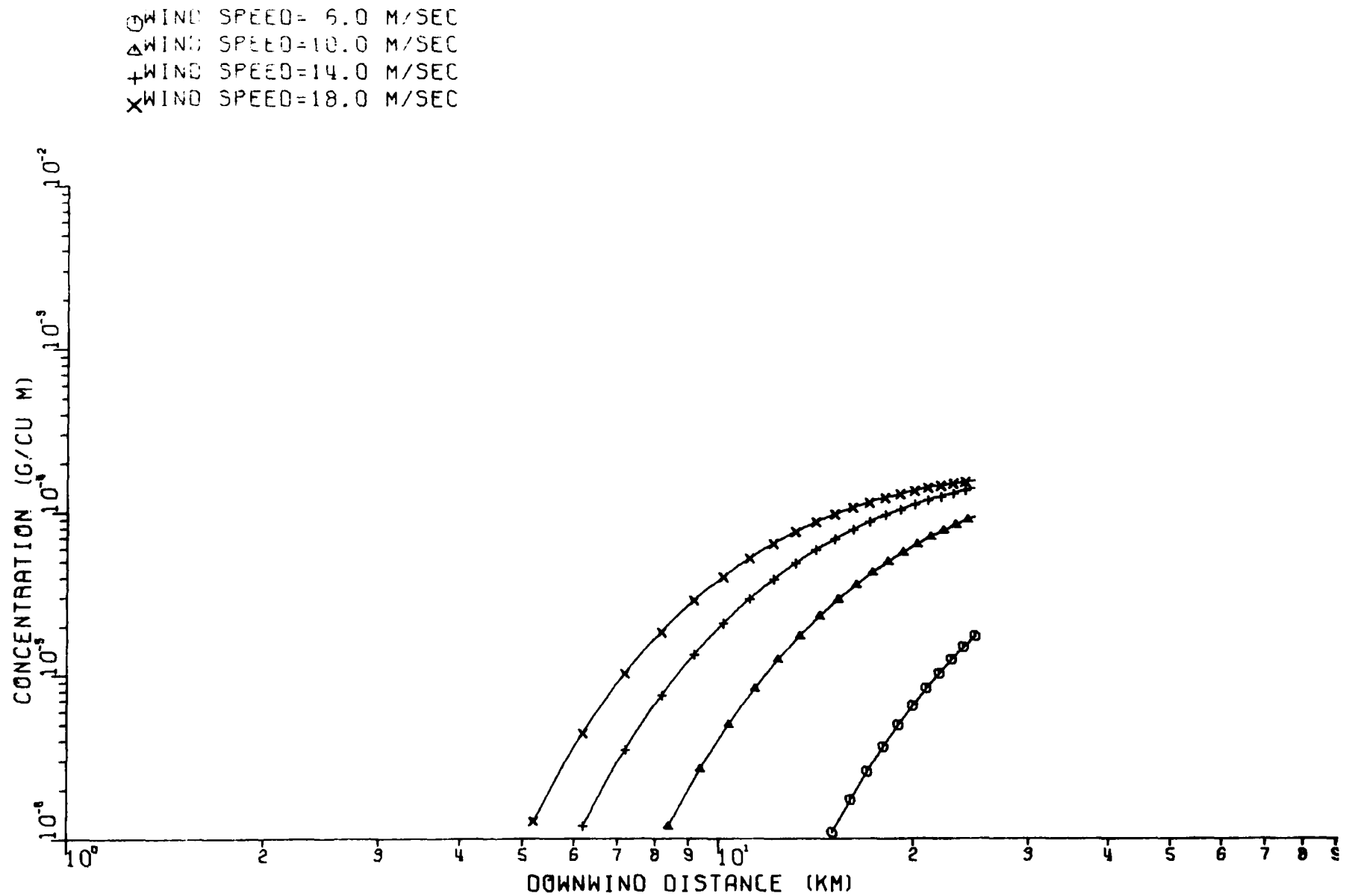


Figure C-7d. Plume centerline concentration versus downwind distance for stability Class D at the Muskingum Plant. Gifford-Briggs dispersion curves used. Flat terrain assumed. Wind speeds are at stack top

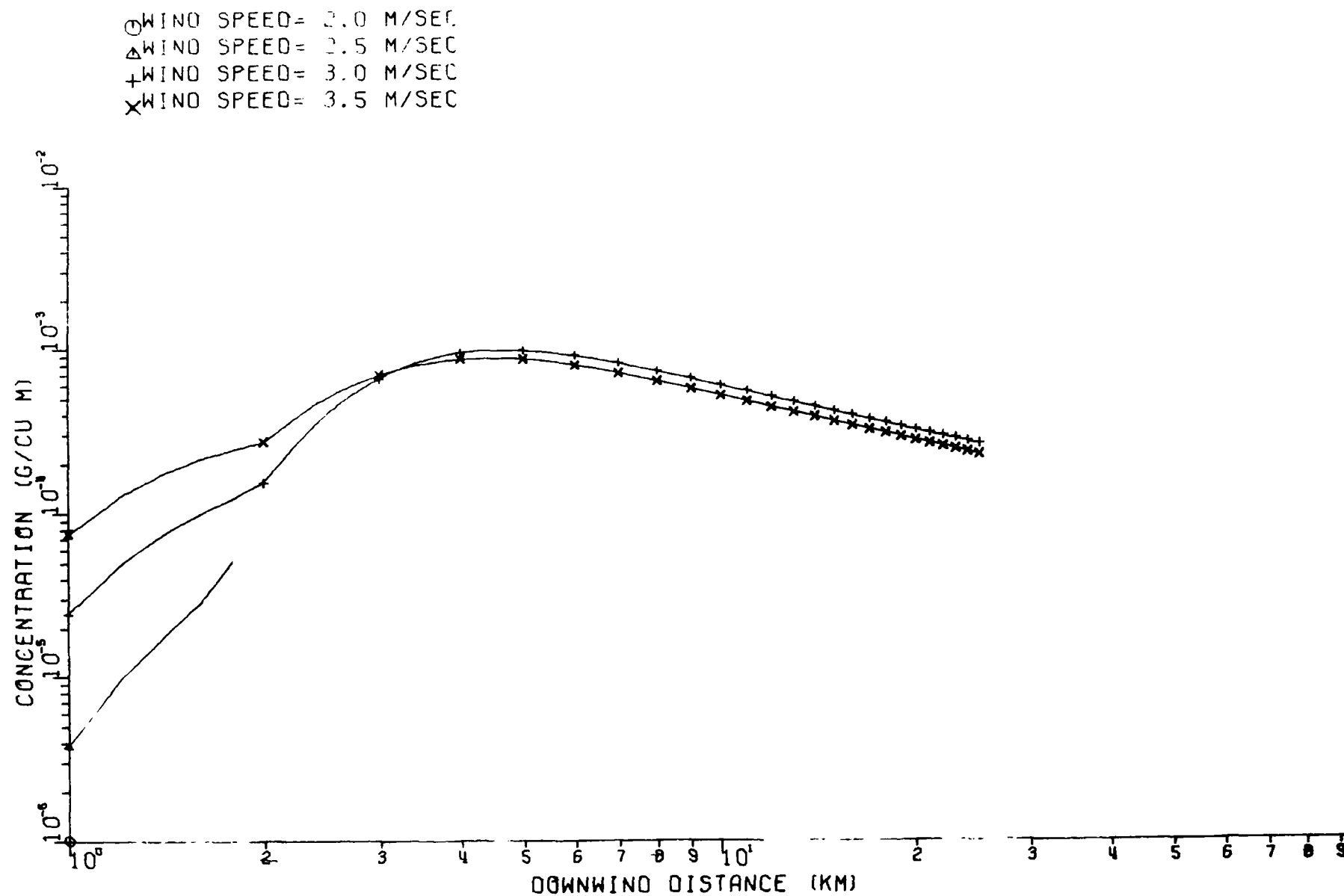


Figure C-8a. Plume centerline concentration versus downwind distance for stability Class B2 at the Muskingum Plant. Smith-Singer dispersion curves used. Flat terrain assumed. Wind speeds are at stack top

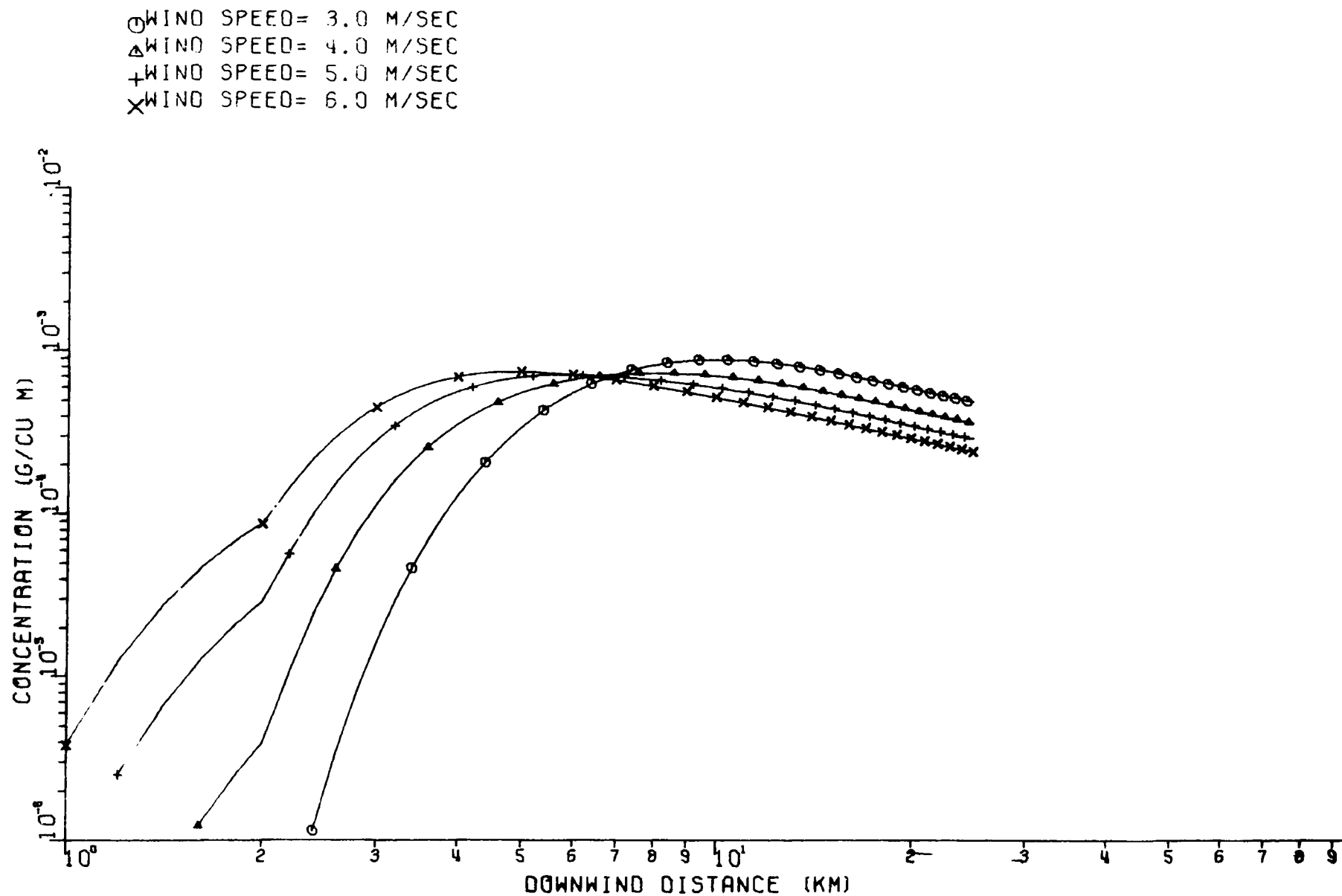


Figure C-8b. Plume centerline concentration versus downwind distance for stability Class B1 at the Muskingum Plant. Smith-Singer dispersion curves used. Flat terrain assumed. Wind speeds are at stack top

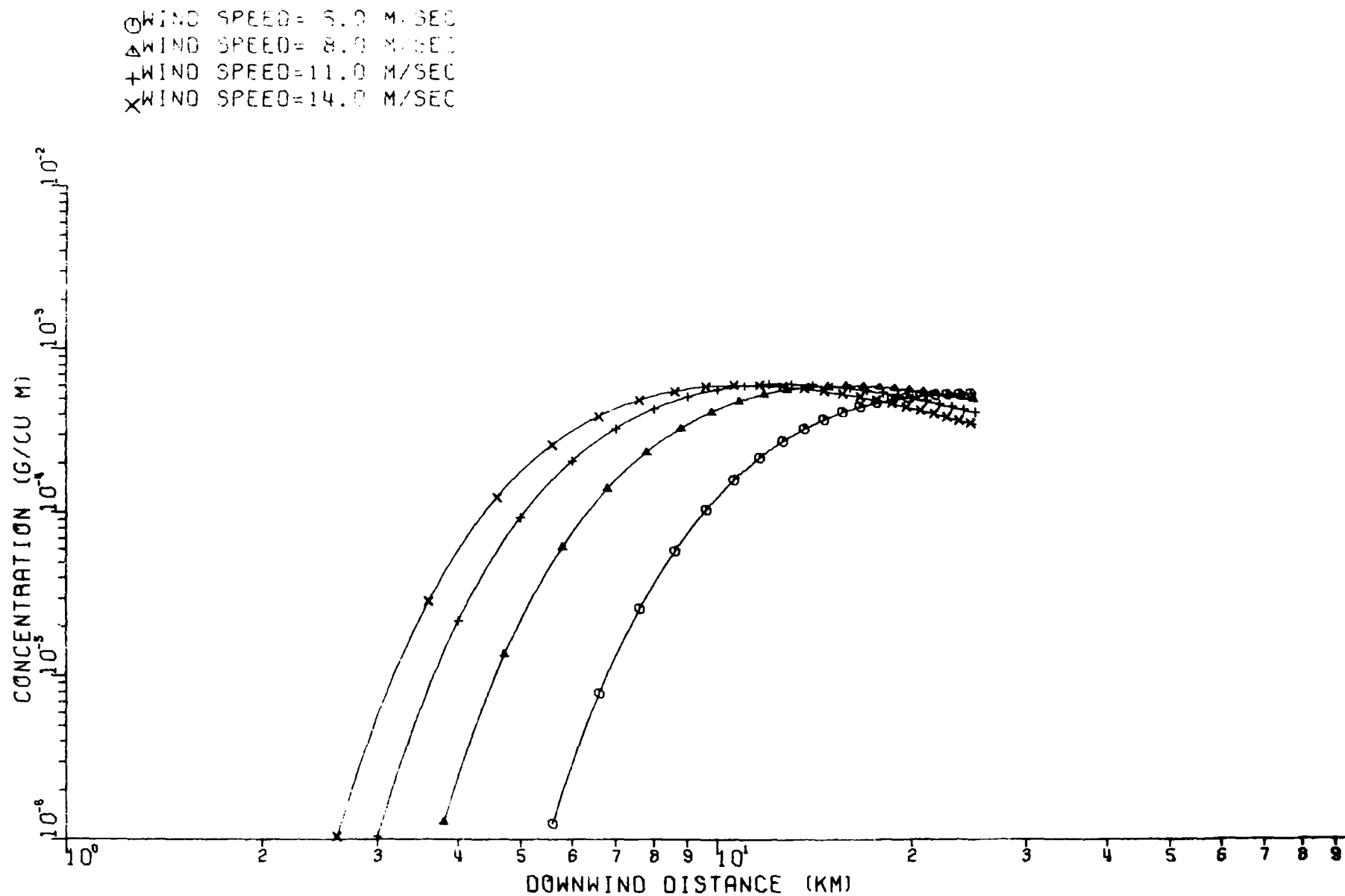


Figure C-8c. Plume centerline concentration versus downwind distance for stability Class C at the Muskingum Plant. Smith-Singer dispersion curves used. Flat terrain assumed. Wind speeds are at stack top

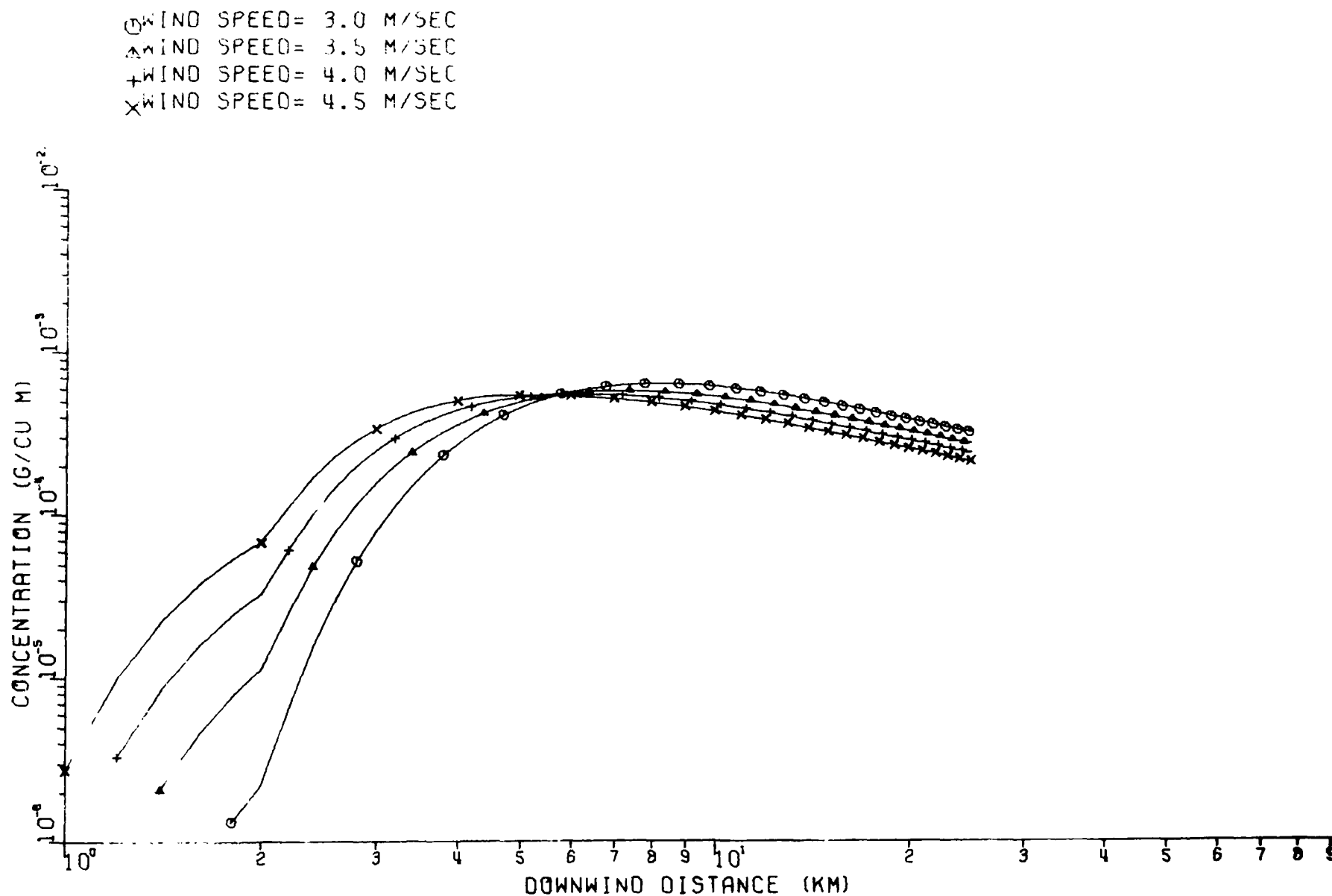


Figure C-9a. Plume centerline concentration versus downwind distance for stability Class A at the Muskingum Plant. F. B. Smith σ_z and Pasquill-Turner σ_y dispersion curves used. Flat terrain assumed. Wind speeds are at stack top

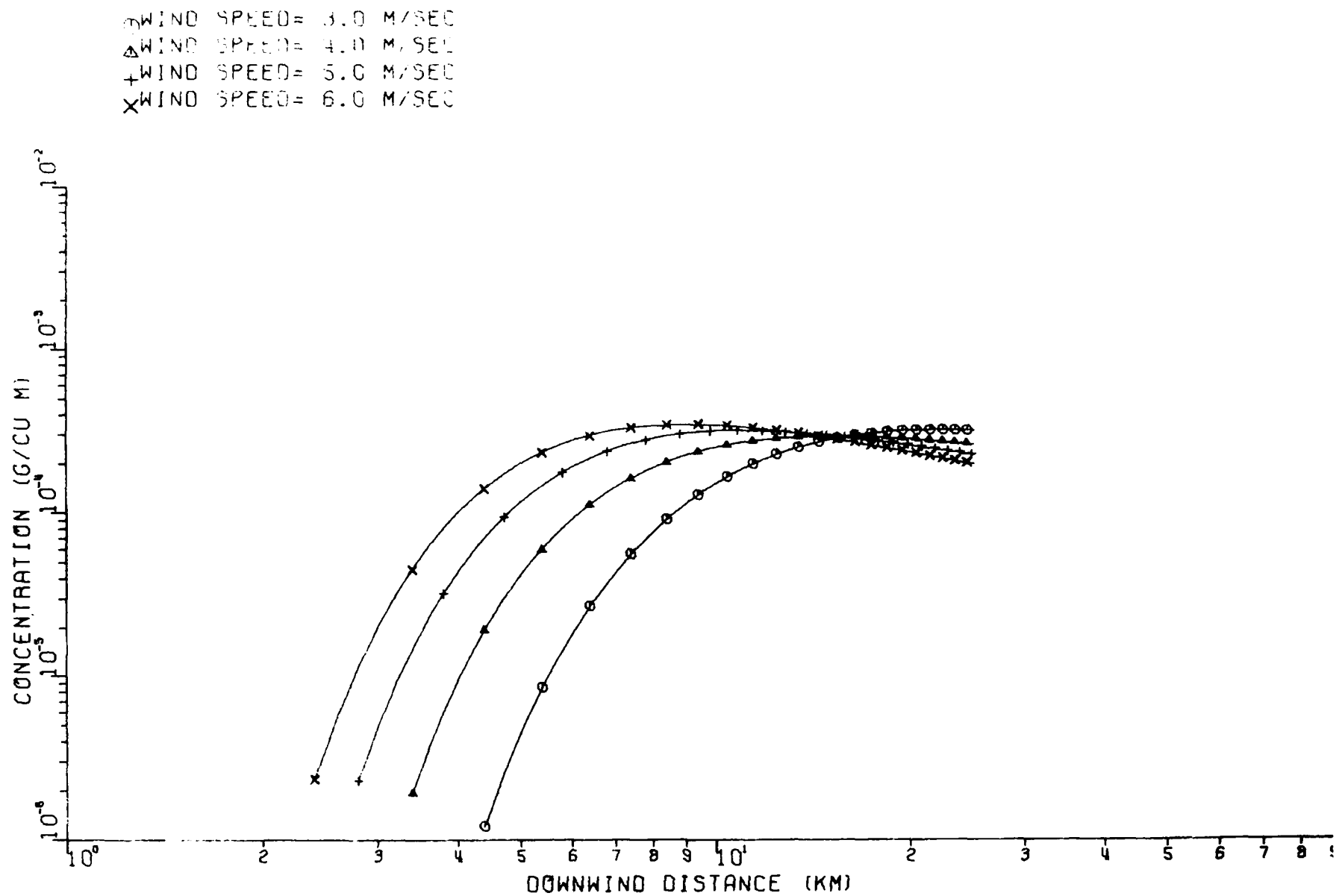


Figure C-9b. Plume centerline concentration versus downwind distance for stability Class B at the Muskingum Plant. F. B. Smith σ_z and Pasquill-Turner σ_y dispersion curves used. Flat terrain assumed. Wind speeds are at stack top

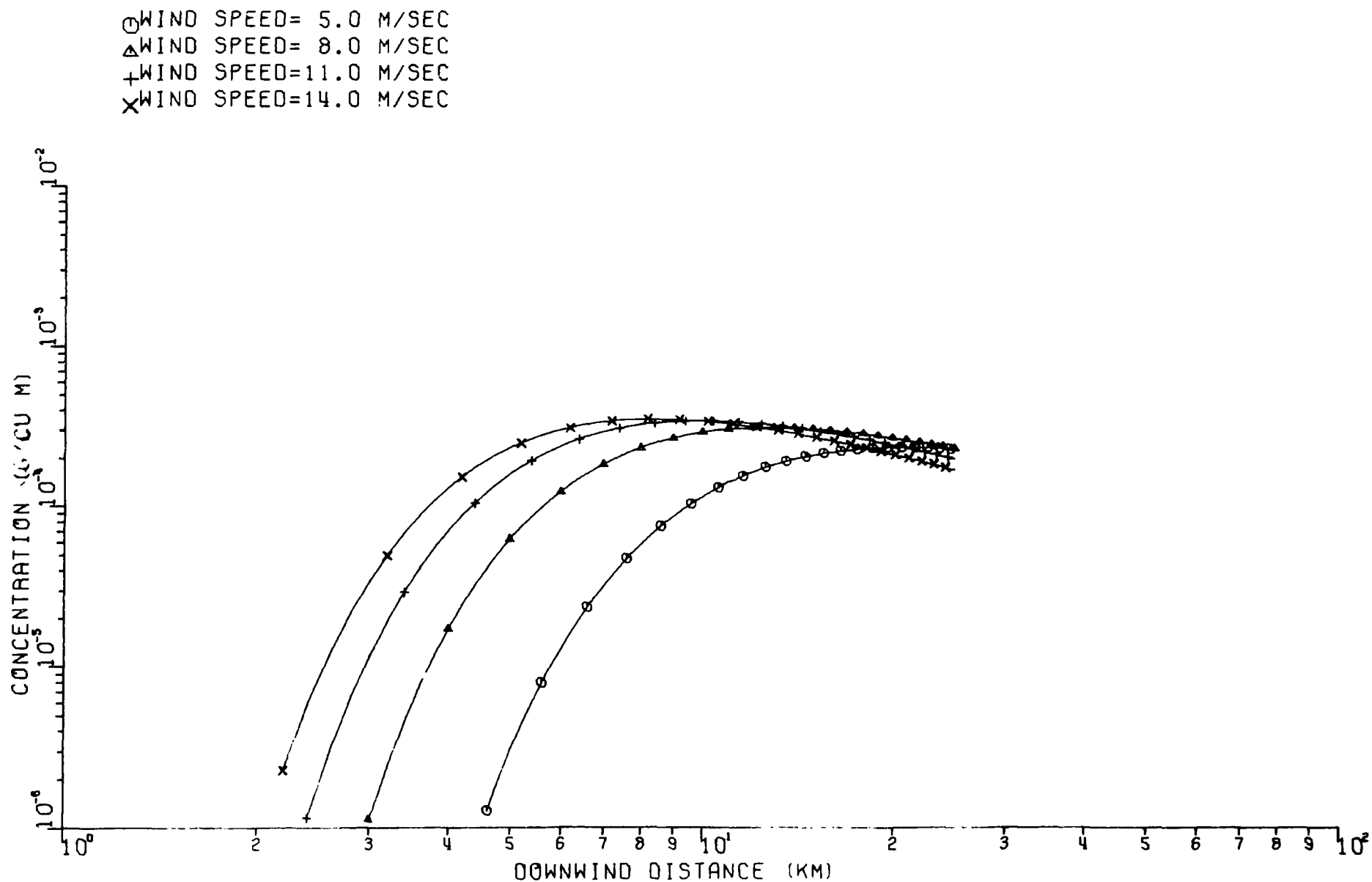


Figure C-9c. Plume centerline concentration versus downwind distance for stability Class C at the Muskingum Plant. F. B. Smith σ_z and Pasquill-Turner σ_y dispersion curves used. Flat terrain assumed. Wind speeds are at stack top

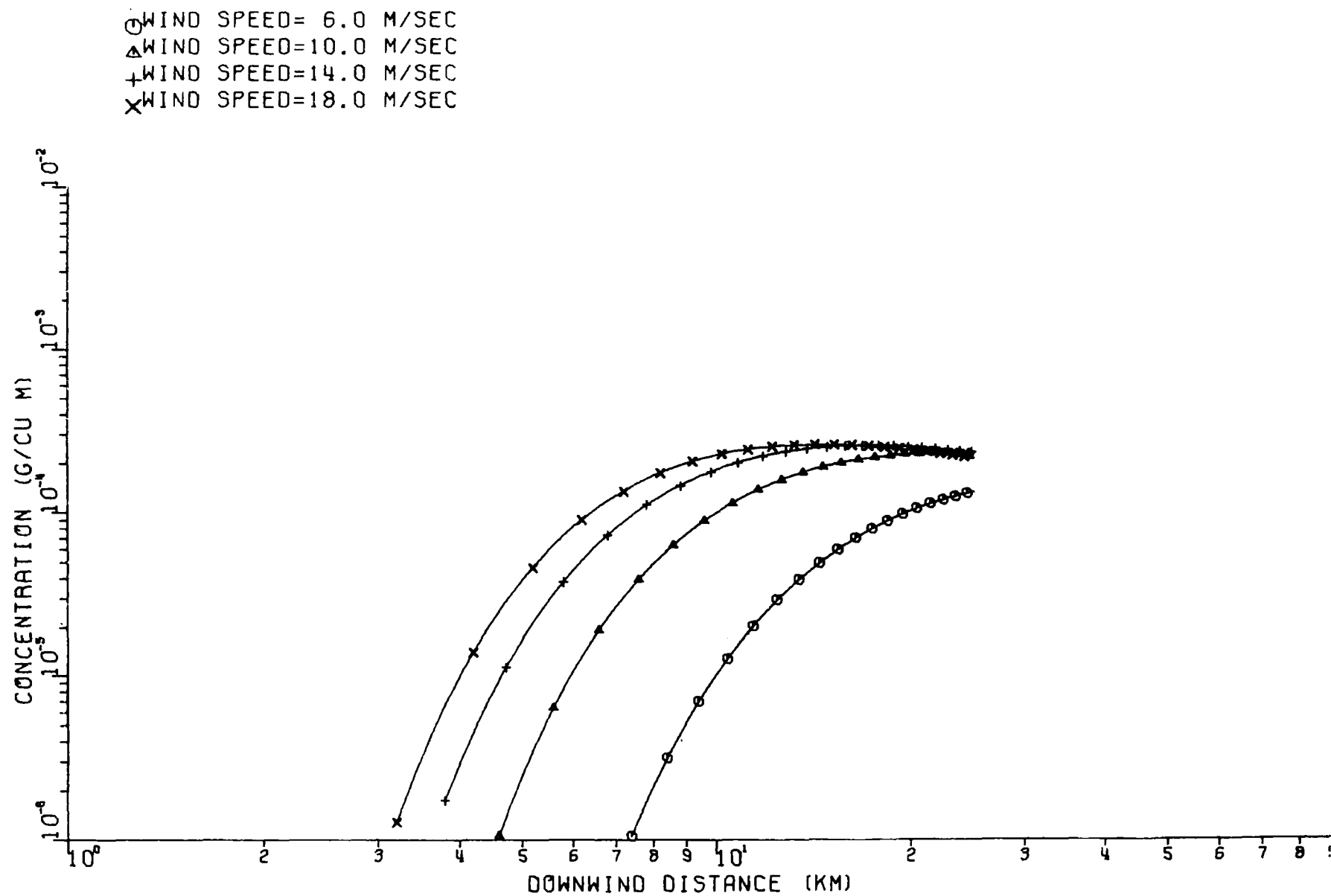


Figure C-9d. Plume centerline concentration versus downwind distance for stability Class D at the Muskingum Plant. F. B. Smith σ_z and Pasquill-Turner σ_y dispersion curves used. Flat terrain assumed. Wind speeds are at stack top

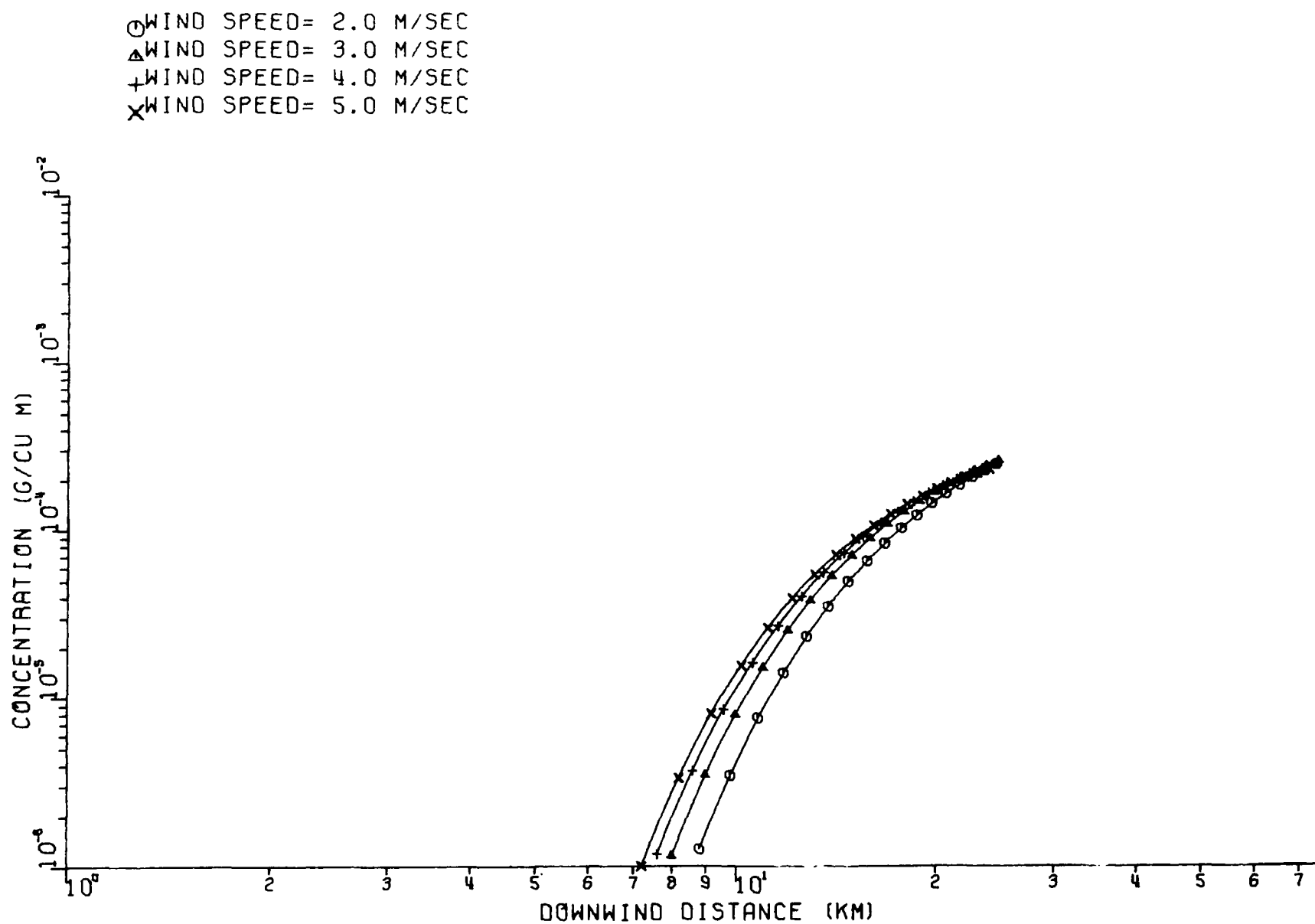


Figure C-9e. Plume centerline concentration versus downwind distance for stability Class E at the Muskingum Plant. F. B. Smith σ_z and Pasquill-Turner σ_y dispersion curves used. Flat terrain assumed. Wind speeds are at stack top

TECHNICAL REPORT DATA
(Please read Instructions on the reverse before completing)

1. REPORT NO. EPA-450/3-77-003b		2.		3. RECIPIENT'S ACCESSION NO.	
4. TITLE AND SUBTITLE IMPROVEMENTS TO THE SINGLE SOURCE MODEL, Volume II—Testing and Evaluation of Model Improvements				5. REPORT DATE January 1977	
				6. PERFORMING ORGANIZATION CODE	
7. AUTHOR(S) Michael T. Mills, Roger W. Stern, Linda M. Vincent				8. PERFORMING ORGANIZATION REPORT NO. GCA-TR-76-6-G(2)	
9. PERFORMING ORGANIZATION NAME AND ADDRESS GCA Corporation GCA/Technology Division Burlington Road Bedford, Massachusetts 01730				10. PROGRAM ELEMENT NO.	
				11. CONTRACT/GRANT NO. 68-02-1376 Task Order No. 23	
12. SPONSORING AGENCY NAME AND ADDRESS U.S. Environmental Protection Agency Research Triangle Park North Carolina 27711				13. TYPE OF REPORT AND PERIOD COVERED Final Report	
				14. SPONSORING AGENCY CODE	
15. SUPPLEMENTARY NOTES					
16. ABSTRACT The main purpose of this study was to determine whether alternate methods for stability index assignment and dispersion calculation would yield better agreement between measured and calculated cumulation frequency distributions of 1-hour SO ₂ concentrations when used in the EPA Single Source Model. The following dispersion curves were tested: Pasquill-Turner, Gifford-Briggs, Smith-Singer and F. B. Smith. A fractional stability assignment technique based upon the work of F. B. Smith was also investigated. Based upon model validation results for the Canal Power Plant in Massachusetts and the Muskingum Power Plant in Ohio, the Pasquill-Turner dispersion curves and stability index assignment algorithm currently used in the model were found to give the best agreement with measured concentration distributions. During the course of the study the incorporation of a variable stack gas exit velocity was evaluated and found not to appreciably affect the model predictions.					
17. KEY WORDS AND DOCUMENT ANALYSIS					
a. DESCRIPTORS		b. IDENTIFIERS/OPEN ENDED TERMS		c. COSATI Field/Group	
18. DISTRIBUTION STATEMENT		19. SECURITY CLASS (This Report) UNCLASSIFIED		21. NO. OF PAGES 174	
		20. SECURITY CLASS (This page) UNCLASSIFIED		22. PRICE	